Synthesis and properties of helical polyisocyanopeptides

Erik Schwartz

Synthesis and properties of helical polyisocyanopeptides

Een wetenschappelijke proeve op het gebied van de
Natuurwetenschappen, Wiskunde en Informatica

Proefschrift

ter verkrijging van de graad van doctor
aan de Radboud Universiteit Nijmegen
op gezag van de rector magnificus prof. mr. S.C.J.J. Kortmann,
volgens besluit van het college van decanen
in het openbaar te verdedigen op maandag 25 januari 2010
om 15.30 uur precies

door

Erik Schwartz
geboren op 14 augustus 1980
te Wisch

Promotores:

Prof. dr. Roeland J. M. Nolte
Prof. dr. Alan E. Rowan
Prof. dr. Jeroen J. L. M. Cornelissen (Universiteit Twente)

Manuscriptcommissie:

Prof. dr. ir. Jan C.M. van Hest
Dr. ir. Richard Hoogenboom
Prof. dr. Dick. J. Broer (Technische Universiteit Eindhoven)

Paranimfen:

Leonie Waanders
Renoud Marijnissen

This research was financially supported by the Dutch Technology Foundation STW (project number NBC.6592).

De foto op de cover is gemaakt door Marta Comellas Aragonès. Vormgeving en layout door Laura Comellas.

Het gedicht op de cover van dit proefschrift is van Ramsey Nasr. Sinds januari 2009 is Nasr Dichter des Vaderlands. Het complot is afkomstig uit de bundel Tussen lelie en waterstofbom. The early years (2009) en werd overgenomen met toestemming van uitgeverij De Bezige Bij. Geniet ook van Het complot op internet: http://www.youtube.com/watch?v=mcZSC_D787A.

Druk: Ipskamp Drukkers BV, Enschede
ISBN: 978-90-9025000-7

De geschiedenis van de wetenschap is (ook) een geschiedenis van geloof, gissen en missen, passen en meten, geknutsel in laboratoria, kijken en nog eens kijken. Een cruciale fase in deze geschiedenis is de zogenaamde 'wetenschappelijke revolutie' van de zeventiende eeuw, de geboorte van de moderne wetenschap. Als wetenschapper in de postmoderne tijd ben ik het aan de revolutionairen verplicht, en aan de gemeenschap, om te allen tijde een kritische houding aan te nemen. Neem niets voor vanzelfsprekend aan, wees niet bang te vallen, maar sta weer op.

"Het verhaal gaat dat toen aan het einde van de achttiende eeuw de Franse wiskundige Laplace zijn grote samenvattende werk op dit gebied [van de theorie van het zonnestelsel], Mécanique céleste, aanbood aan keizer Napoleon, de laatste opmerkte dat God in het hele werk niet meer genoemd werd. Laplace zou daarop trots hebben geantwoord: Sire, die hypothese had ik niet meer nodig."

Rienk Vermij, 'De wetenschappelijke revolutie. Van Aristoteles naar Newton'

Table of contents

Preface

"What one can make, one can copy".[1] Without a doubt this axiom holds for the security paper and banknote industry. Since the appearance of the first banknotes many centuries ago people have been trying to counterfeit them. "Whosoever forges notes or circulates counterfeit notes shall be beheaded. Whosoever reports and apprehends a counterfeiter shall receive a reward of 250 silver tael and the counterfeiter's entire property" was the warning that appeared on Chinese currency notes of the early Ming dynasty.[2] In England, during the period 1697–1832, forgery was a hanging offense and approximately 600 counterfeiters were condemned to death, but even this threat did not eliminate counterfeiting.[3] Although the times and circumstances have dramatically changed since these threats, human behaviour remained the same; the levels of counterfeiting are nowadays still increasing. In Europe in the first months of 2009 over 413,000 falsified banknotes have been confiscated.[4] As a consequence, the anti-counterfeiting industry is continuously looking for new science and technologies to make new materials, which can be used as anti-counterfeit features. The necessity for new materials and methods is, due to the advanced level of photocopying and publishing techniques, essential for the economies in the world. Over the years the anti-counterfeiting methods have been upgraded continuously, for example fluorescent polymers, polarisation and metameric effects, electro-chromic compounds, water-marks, holograms, raised print, see-through register and gold stripes have been introduced into the notes. The effect of fluorescent fibres in a bank note can be seen in Figure 1. Three different levels of security measures can be defined: *i*) the 'holy grail': the detection of the feature by the naked eye; *ii*) detection by shops, banks and cash machines and *iii*) detection by the central bank.

Figure 1. A € 50 banknote under normal light (left) and under UV light showing the fluorescent fibres (right).

The research described in this thesis aims at developing helical chromophore appended polyisocyanides for future applications as safety markers in security paper. These polymers might be unique candidates for incorporation as anti-counterfeit components in paper since

polyisocyanides have distinct chiro-optical properties as a consequence of their well-defined helical architecture. Their distinct properties cannot be reproduced by using alternative systems. In addition, the polymer conformation is stable even at the elevated temperatures, which is required for the processing of paper. The polymers can be used either as a fluorescent fingerprint in the paper or can be incorporated into the ink. In this thesis, the first steps towards the development of polyisocyanide-based materials that can be used as security markers are described. The emphasis is on the synthesis and characterisation of the isocyanide building blocks and their subsequent conversion into polymers. Preliminary experiments on the application of the developed chromophoric polyisocyanides as markers are reported in the Appendix of this thesis. Polyisocyanides are prepared from isocyanide monomers, which result in a polymer that has a backbone consisting of imine groups. The driving force for this polymerisation reaction is the transformation of a formally divalent carbon atom in the monomer to a tetravalent carbon atom in the polymer (Figure 2). An unusual feature of these polymers is that every main chain carbon atom bears a substituent. Due to this fact, considerable steric hindrance and therefore restricted rotation around the main chain carbon atoms is introduced into the polymer backbone. To minimise the steric crowding, the C–C bonds twist and adopt a helical structure. Millich proposed a so-called four-over-one helix, denoted as 4_1, (i.e., 4 repeat units per helical turn) for the main carbon chain in polyisocyanides.[5]

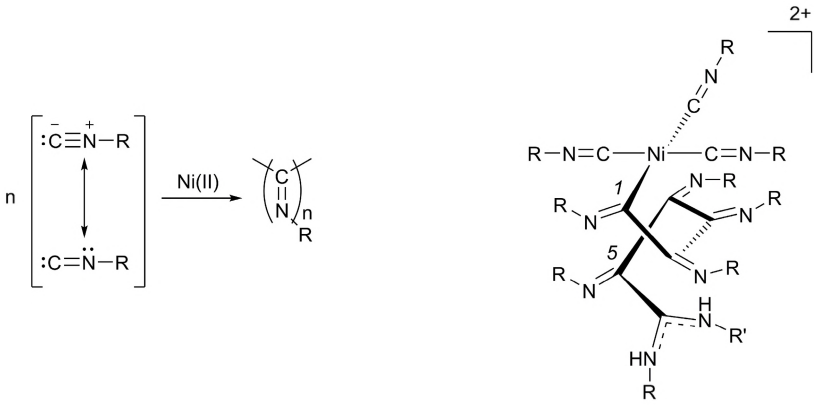

Figure 2. Nickel catalysed polymerisation of isocyanides (left) and structure of the growing helical polyisocyanide chain (right). R' (most often an alcohol) is the nucleophile that is required to start the polymerisation reaction.

The first catalyst for the polymerisation reaction of isocyanides was discovered by Millich who found that some isocyanides were polymerised by acid-coated glass.[5] Subsequently, Nolte studied the use of nickel ions and other transition metals as a catalyst for this purpose.[6] Based on kinetic measurements and experiments with optically active isocyanides the so-called "merry-go-round" mechanism for the Ni(II) catalysed polymerisation was

proposed.[7] The polymerisation is initiated by a nucleophile, (e.g., an amine or an alcohol) and, during the reaction, the isocyanide monomers coordinate to the nickel centre and are incorporated into the growing chain by a series of consecutive insertion reactions. This results in a helical polymeric backbone (Figure 2) in which the fifth side group is positioned more or less on top of the first one, the ninth on top of the fifth, etcetera. When achiral isocyanides are used, the intermediate, which is formed after attack of the nucleophile (R') on one of the coordinated isocyanide molecules, has no preference to attack either the left or the right neighbouring isocyanide. Consequently, for an achiral monomer and initiator, an equal amount of left- (*M*-) and right-handed (*P*-) helical polyisocyanides will be generated. Stereoselectivity (i.e., a preferred helical handedness) can be introduced when a chiral initiator or a chiral isocyanide is used.[8]

The helical conformation of polyisocyanides was confirmed by Nolte and co-workers[9] who resolved poly(*tert*-butyl isocyanide) into (+) and (–)-rotating fractions by using poly((*S*)-*sec*-butyl isocyanide) as a stationary phase during chromatographic purification. They also assigned the helical handedness of the resolved polymer on the basis of CD spectroscopy measurements.[10] The helical conformation of polyisocyanides has been the subject of intensive debates in the last decades. An overview of the reports dealing with the conformation of polyisocyanides can be found in reviews, book chapters and articles by Millich,[11] Nolte, [6,12] Hoffmann,[13] Salvadori,[14] Green,[15] Novak,[16] Takahashi,[17] Suginome[18] and Yashima.[19]

Following earlier work by Van Beijnen[20] and Van der Eijk,[21] Cornelissen and co-workers introduced di- and tripeptides as side groups in the polyisocyanides (Figure 3).

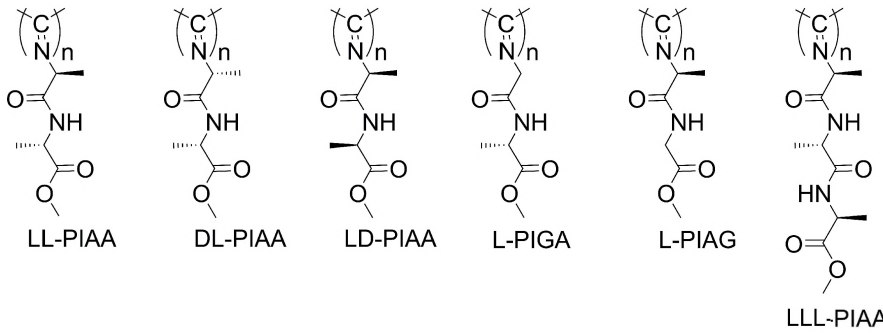

Figure 3. Chemical structures of some dipeptide and tripeptide derived polyisocyanides synthesised by Cornelissen and co-workers.

The polymerisation of peptide derived isocyanides led to macromolecules in which the helical backbone is stabilised by hydrogen bonds between the amide groups in parallel side chains, as could be demonstrated by detailed infrared and ^{1}H NMR spectroscopic

investigations. Each side chain can be regarded as an individual β-strand and the overall arrangement of the side chains leads to a helical β-sheet-like organisation.[22] By using the appropriate catalytic procedure (either acid or nickel(II)) control over the molecular weight of the resulting polymers with lengths ranging from 100 nm to 20 μm can be achieved.[23] Due to these properties, the polyisocyanopeptides have a well-defined architecture that makes them good candidates to precisely organise functional molecules. In addition, the criteria that are required for a material to be used in security paper, i.e., i) low costs; ii) easy and fast detection; and iii) stability towards chemical and physical processes, can be fulfilled. First, these materials are made from 'inexpensive' amino acid building blocks. Second, the novel architecture of the polymers can be readily detected by optical techniques such as Circular Dichroism (CD) and Fluorescence spectroscopies. Finally, the high rigidity of the polymers, as a result of the hydrogen bonding network between the side chains, offers stable polymers even at the elevated temperatures that are employed in the production of paper.

The general aim of the research presented in this thesis is, therefore, the construction of well-defined chromophoric helical arrays that possess unique properties that make them easy to detect but impossible to counterfeit. After the Preface, this thesis continues with an overview of the recent literature and focuses on chromophoric macromolecular ordering using rigid templates (Chapter 1). To gain more information on the helical nature of polyisocyanides, i.e., the handedness of the helices and the overall conformation, Vibrational Circular Dichroism (VCD) studies were performed (Chapter 2). The synthesis and studies of perylene and platinum porphyrin functionalised polyisocyanides is described in Chapter 3. In order to obtain a more uniform and modular platform for the construction of a wide variety of polyisocyanides, acetylene polyisocyanopeptides were synthesised (Chapter 4). It was found that depending on i) the stereochemistry of the constituting (alanine) amino acids; ii) the spacer length between the dipeptide and the acetylene moiety and iii) the presence of a trimethyl silyl protecting group distinct different polymer properties can be obtained. It was shown that these polymers can be readily post-modified with dodecyl azide using the copper catalysed Huisgen [3 +2] cycloaddition. This approach is extended in Chapter 5, where the post-functionalisation with chromophoric and water-soluble azides is presented. The use of two different chromophores, a coumarin and a perylene dye, results in random polymers in which absorption and emission from both polymers can be observed.
Chapter 6 describes the reverse post-modification strategy, i.e. based on azido appended polyisocyanopeptides. Water-soluble polymers were prepared by the random copolymerisation of azido isocyanopeptides with non-functionalised isocyanides derived from alanine followed by saponification of the compounds. The potential of the water-soluble polymers containing azide for derivatisation moieties by click chemistry was

successfully demonstrated by the reaction of these polymers with an acetylene functionalised rhodamine dye in aqueous solution.

In Chapter 7, the synthesis and characterisation of polyisocyanides with either a well-defined or a disrupted hydrogen-bonding network, is discussed. By using vibrational pump-probe spectroscopy, it was demonstrated that NH-stretch vibrational self-trapping can occur in the β-sheet helical polymers that posses an uninterrupted hydrogen-bonding array. Chapter 8 reports on the controlled surface-initiated polymerisation of isocyanide monomers, using different surfaces. Polymer brushes up to 250 nm in length could easily be obtained and the polymer growth was studied as a function of reaction time, monomer concentration and growth conditions with the help of atomic force microscopy (AFM), ellipsometry and various spectroscopic techniques.

References & Notes

(1) Hardwick, B.; Jackson, W.; Wilson, G.; Mau, A. W. H. *Adv. Mater.* **2001**, *13*, 980-984.

(2) Kranister, W. *The Moneymakers International*; Black Bear Publishing: Cambridge (UK), 1988.

(3) *National Materials Advisory Board (NMAB), Counterfeit Deterrent Features for the Next-Generation Currency Design*; National Academy Press: Washington, DC, 1993.

(4) Press release from the Euopean Central Bank on 13 July 2009.

(5) Millich, F. *Chem. Rev.* **1972**, *72*, 101-113.

(6) Nolte, R. J. M. *Chem. Soc. Rev.* **1994**, *23*, 11-19.

(7) Although the 'merry-go-round' mechanism allows many polymerisation characteristics and polymer properties to be explained, the actual mechanism of polymerisation is more complex as can be concluded from detailed mechanistic studies performed by Deming and Novak in the early 1990's.

(8) Drenth, W.; Nolte, R. J. M. *Acc. Chem. Res.* **1979**, *12*, 30-35; Kamer, P. C. J.; Cleij, M. C.; Nolte, R. J. M.; Harada, T.; Hezemans, A. M. F.; Drenth, W. *J. Am. Chem. Soc.* **1988**, *110*, 1581-1587.

(9) Nolte, R. J. M.; Van Beijnen, A. J. M.; Drenth, W. *J. Am. Chem. Soc.* **1974**, *96*, 5932-5933.

(10) van Beijnen, A. J. M.; Nolte, R. J. M.; Drenth, W.; Hezemans, A. M. F. *Tetrahedron* **1976**, *32*, 2017-2019.

(11) Millich, F.; Baker, G. K. *Macromolecules* **1969**, *2*, 122-128.

(12) Cornelissen, J. J. L. M.; Rowan, A. E.; Nolte, R. J. M.; Sommerdijk, N. A. J. M. *Chem. Rev.* **2001**, *101*, 4039-4070; Otten, M. B. J.; Metselaar, G. A.; Cornelissen, J. J. L. M.; Rowan, A. E.; Nolte Roeland, J. M. In *Foldamers: Structure, Properties, and Applications*; Hecht, S., Huc, I., Eds.; Weinheim: Wiley-VCH: 2007.

(13) Kollmar, C.; Hoffmann, R. *J. Am. Chem. Soc.* **1990**, *112*, 8230-8238.

(14) Clericuzio, M.; Alagona, G.; Ghio, C.; Salvadori, P. *J. Am. Chem. Soc.* **1997**, *119*, 1059-1071.

(15) Green, M. M.; Gross, R. A.; Schilling, F. C.; Zero, K.; Crosby, C., III *Macromolecules* **1988**, *21*, 1839-46.

(16) Deming, T. J.; Novak, B. M. *J. Am. Chem. Soc.* **1993**, *115*, 9101-9111.

(17) Takei, F.; Onitsuka, K.; Takahashi, S. *Macromolecules* **2005**, *38*, 1513-1516.

(18) Suginome, M.; Ito, Y. *Adv. Polym. Sci.* **2004**, *171*, 77-136.

(19) Hase, Y.; Nagai, K.; Iida, H.; Maeda, K.; Ochi, N.; Sawabe, K.; Sakajiri, K.; Okoshi, K.; Yashima, E. *J. Am. Chem. Soc.* **2009**, *131*, 10719-10732.

(20) van Beijnen, A. J. M. PhD thesis, Helical configuration of poly(iminomethylenes), University of Utrecht, **1980**.

(21) van der Eijk, J. M. PhD thesis, Synthesis and catalytic behaviour of imidazole anchored to poly(iminomethylenes), University of Utrecht, **1980**.

(22) Cornelissen, J. J. L. M.; Donners, J. J. J. M.; de Gelder, R.; Graswinckel, W. S.; Metselaar, G. A.; Rowan, A. E.; Sommerdijk, N. A. J. M.; Nolte, R. J. M. *Science* **2001**, *293*, 676-680.

(23) Metselaar, G. A.; Cornelissen, J. J. L. M.; Rowan, A. E.; Nolte, R. J. M. *Angew. Chem., Int. Ed.* **2005**, *44*, 1990-1993.

1

Literature survey: macromolecular multi-chromophoric scaffolding

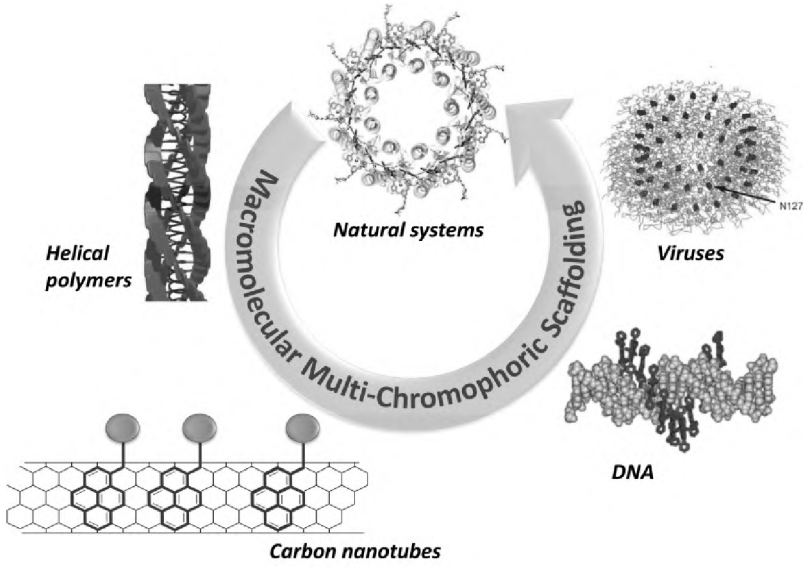

1.1 Introduction

Chromophores are of pivotal importance in nature and play a fundamental role in many aspects of life, such as photosynthesis and the processes within the circulatory system. They also act as dyes and pigments in a wide variety of technological applications. In many of these applications, the organisation of chromophores is of crucial importance for the performance of the assembly or device. To arrange the chromophores into functional architectures scientists have developed numerous approaches for the precise positioning of chromophoric building blocks and these have been applied extensively in the last years, in particular, in the field of the material sciences.[1] The aim of this aforementioned research is to control the electronic interactions between adjacent chromophoric units and thereby obtain materials with unique properties and potentially new applications.[2] Often the very elegant and essential chromophoric arrays that can be found in nature are used as a source of inspiration and sometimes as a blueprint for synthetic systems. A particular example is the photosynthetic system in which chlorophyll and bacteriochlorophyll chromophores are organised in such a way that the transfer of excitation energy and electrons occurs with a very high efficiency over large distances. This architecture–function relationship is also beautifully illustrated by the circular antenna complex of the purple bacteria LH2,[3] which displays an incredible efficiency towards the harvesting of sunlight. The precise organisation of the two ring-shaped arrays of chlorophylls allows for an efficient energy transfer from the outer- to the inner-ring and finally to the photosynthetic reaction centre where energy separation occurs.[4] The combination of the perfectly tuned energy gradient, the precisely interacting chromophores, the ability to store excess energy temporarily within the LH1 ring and the absorption of the solar light over a wide wavelength range makes this system extremely efficient (> 95 %) for absorbing photons (Figure 1).[5] The efficiency of this antenna is not only a result of the chromophores that are used but also relies on their precise orientation and positioning relative to one other. The positioning of the chromophores is controlled by the protein biomolecular scaffold; this has inspired many researchers over the last decades to create artificial systems in which chromophores are ordered and the unique properties of the structures are utilised. Several approaches to achieve high levels of chromophoric ordering within molecular systems, with the hope of creating efficient energetic interactions, have been attempted, based on for example, dendritic,[6] supramolecular, [7] or covalent systems.[8] Another approach, which combines the last two approaches, is to use rigid scaffolds that possess supramolecular features, which can be used to precisely organise the chromophores. The focus of this chapter is on the arrangement of chromophores by using rigid helical polymers, carbon nanotubes (CNTs), nucleic acids and viruses. The advantages and limitations of such approaches will be discussed.

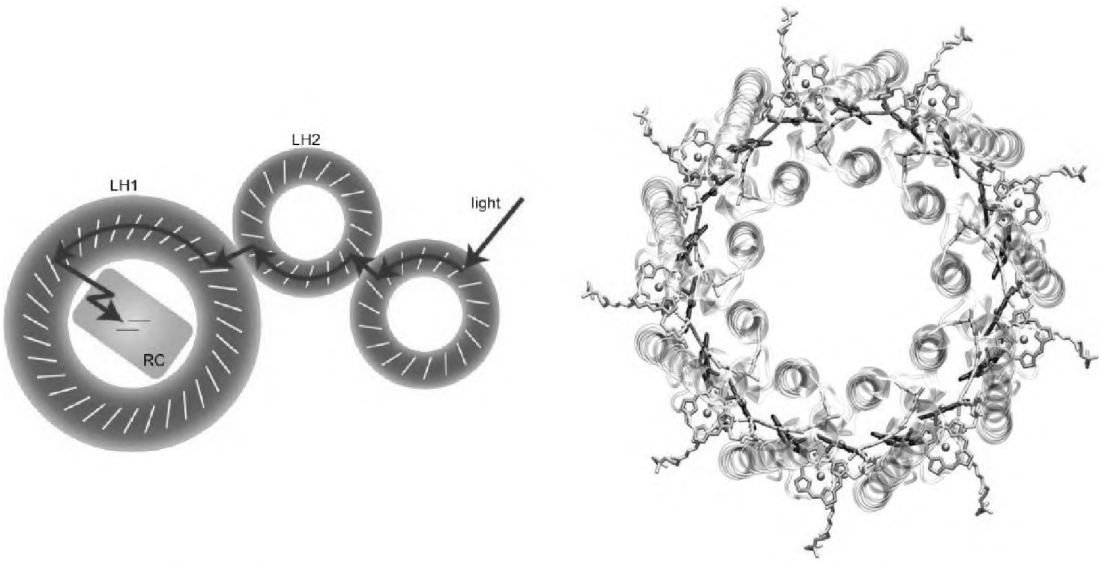

Figure 1. The transfer of a photon of light from the LH2 complexes through the LH1 complex and finally to the central photosynthetic reaction centre (Left). The crystal structure of the LH2 of purple bacteria *Rhodopseudomonas acidophilia,* which reveals a highly ordered array of chlorophyll molecules held in the required orientation by the peptidic alpha helices (Right). Three bacteriochlorophyll molecules are associated with each pair of helices.

1.2 Rigid helical polymers

One approach towards the ordering of chromophores is to make use of a synthetic polymer scaffold. Although linear polymers can be readily functionalised with dyes,[9] their overall architectural definition is often limited because they are flexible and can suffer from defects that may result in the formation of energy sinks. More attractive candidates for the arrangement of chromophores in well-defined arrays are rigid polymers, which are often helical.[10,11] The helix is one of the most important and basic structural motifs found in nature. The biological activities of biomacromolecules, such as proteins and nucleic acids, often depend on the presence of helical conformations. Also the function and physical properties of synthetic helical polymers are strongly correlated with the conformation of their macromolecular chains. Over the last 60 years, after the first discovery of a synthetic helical polymer by Natta in 1955,[12] a variety of helical polymers have been developed. In this chapter the emphasis will be on helical polymers that have been used as scaffolds for the organisation of chromophores into well-defined architectures. Although a host of helical polyacetylenes have been prepared, this class of polymers will not be discussed since they are rather flexible in contrast to other classes of helical polymers, such as polyisocyanates, polyisocyanides, polysilanes or polyguanidines. For an excellent overview on work conducted with polyacetylenes see the reviews by Tang[13] and Yashima.[14,15] The basic characteristics of the polymers that are described in this section have been discussed in the literature,[10,14] therefore only a brief description of the polymers is given here.

One class of helical polymers are the polyisocyanates,[16] which are characterised by an *N*-substituted amide repeat unit and a 8_3 helical conformation (Chart 1). These polymers have a low helix inversion barrier and are therefore dynamic in nature. The majority of investigated polyisocyanates are not functionalised and consist mainly of alkyl or aryl derivatives. The lack of functionalised polyisocyanates is ascribed to the harsh conditions required for the preparation of the monomer and to the anionic nature of the polymerisation reactions, which are not compatible with many functional groups. To overcome these problems, an azo-chromophore dye was introduced in the polymer chain by a trans-esterification reaction involving the methyl ester of the polymer.[17] The resulting polymer **1** (Chart 1) had a functionalisation degree of 30% and displayed a tenfold increase in the optical rotation value. This indicates that the chromophores attached to the polyisocyanate are in a helical environment. Unfortunately, no further photophysical studies were undertaken to obtain a more detailed picture of the arrangement of the chromophores. In related work, chiral azo dyes were introduced into the polymeric system by the copolymerisation of an azo dye derivatized isocyanate with hexylisocyanate (Chart 1), and the change in the helical conformation of the polyisocyanate backbone when triggered by the photoinduced isomerisation of the side chains was studied. For example, the chiroptical properties and the correlation between the helicity of the main chain and the photoisomerization of the side groups were studied by Circular Dichroism (CD) measurements.[18] It was apparent that at low concentrations of the chiral azo side groups a linear relationship was present between the ratio of cis and trans isomers and the preference for one particular helical conformation. At higher concentrations of the chiral azo side groups the stronger inducing species (i.e. the cis isomer) dictated the helical conformation, in agreement with the sergeant and soldier principle found by Green and co-workers in polyisocyanates.[16,19] Polysilanes possess a unique Si σ-conjugated backbone and like the polyisocyanates also belong to the class of dynamic helical polymers (Chart 1).[20] They are generally synthesised by simple Wurtz coupling reactions. The type of side chains in the polysilane has a dramatic influence on the rigidity, stability and optical properties of the polymer. A feature of polysilanes, shared with polyisocyanates, is the difficulty of synthesising derivatives with a wide variety of functionalities. The rigorous reaction conditions allow only alkyl or aryl substituents as side chains. To overcome this problem Qin and co-workers partially replaced the Si–alkyl group of the polymer backbone by Si–Cl groups. Subsequent etherification with diphenyl azo dyes (Chart 1) resulted in the highly chromophore-loaded (>50 %) polymer **2** (Chart 1), which showed a photoconductivity of 1.7 pS cm^{-1}, three orders of magnitude higher than the dark conductivity of simple polysilanes.[21] Another class of helical polymers are the polyguanidines, which have been extensively explored by the group of Novak (Chart 1).[22-24] These polymers adopt a 6_1 helical

conformation and are usually prepared by the (chiral) titanium catalysed polymerisation of carbodiimides. Stable helices with length up to 3 μm can be obtained by the incorporation of sterically demanding anthracene units, which can also act as UV-Vis chromophores allowing the close investigation of the polymer conformations.[24] Polymer **3** (Chart 1) exhibited a reversible, temperature and solvent-induced chiroptical switching behaviour due to a cooperative effect between the anthracene units (Figure 2), as visualised by a blue/red shift in the UV-Vis absorption peaks (at 25 °C λ_{max} = 384.4 nm and ε = 5400 M^{-1}; at 60 °C λ_{max} = 382.4 nm and ε = 4700 M^{-1}) and in the CD bands (at 25 °C λ = 382.0 nm Δε + 2.0 M^{-1} cm^{-1}; at 60 °C λ = 382.0 nm Δε –2.6 M^{-1} cm^{-1}), and opens a way to use these polymeric 'nanoshutters' as components in display technology.[23] In the reversible cooperative switching process the helix sense, imine configuration and helical pitch of the polymer does not change. By using Vibrational Circular Dichroism (VCD) and theoretical modelling the authors could assign the helicity and clarify to some extent the spatial arrangement of the anthracene units (Figure 2).

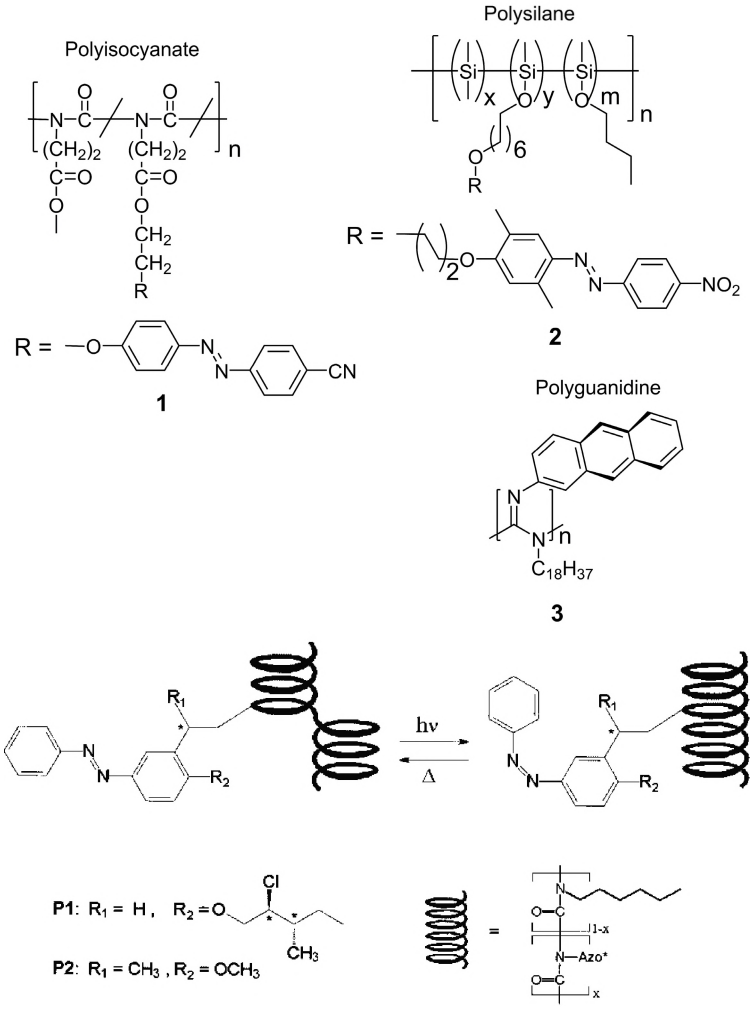

Chart 1. Chemical structures of the azo-benzene and anthracene based dynamic polymers **1**–**3** and the switching process in the chiral photochromic polyisocyanate copolymer.

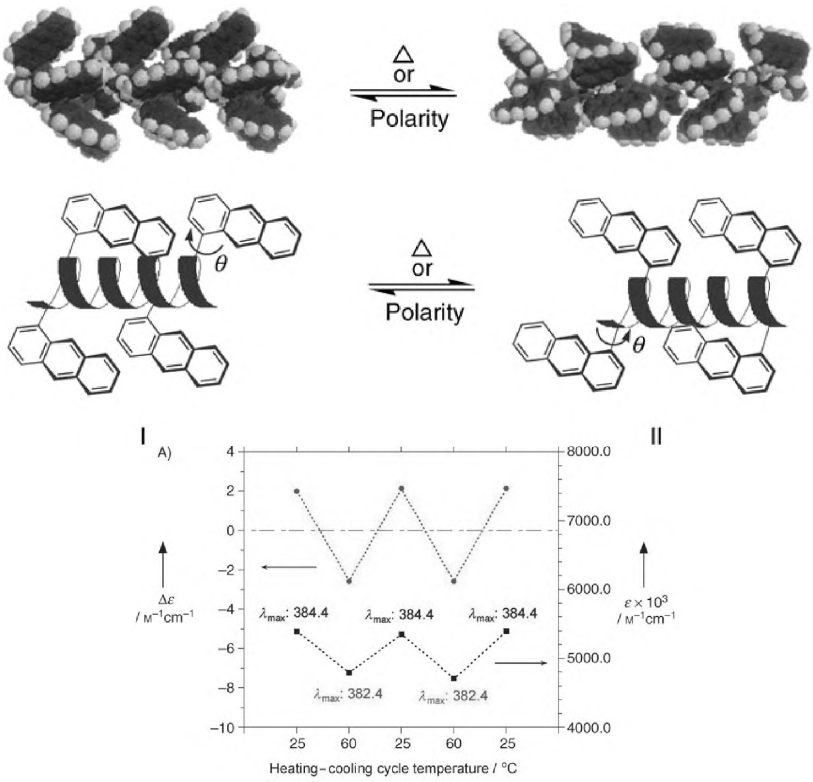

Figure 2. Theoretical models of the two states that result from the shutter-like motions of the anthracene units of **3** upon the application of heat or solvophobic driving forces (top). Heating–cooling thermal cycles of **3** in toluene (bottom).

In the polymers described above, the introduction of chromophoric units is often difficult due to the demanding reactions conditions required to synthesise these polymers. As a consequence the attachment of chromophores that are able to carry out electron or energy transfer is virtually unexplored. The chromophoric units are mainly used to study interesting phenomena of the polymers themselves, such as the sergeant and soldier effect, the dynamic nature of the helix, helical induction, liquid crystalline behaviour, memory effects and inversion barriers. Potential applications of these helical polymers could be their use as enantioselective catalysts or adsorbents.[25] In order to create systems in which the chromophores are in well-defined positions to generate efficient energy and electron transfer, such as required for photovoltaic devices or field effect transistors, an easy route to prepare such systems is needed. This can be achieved by using polyisocyanides; a class of polymers that have been explored by Nolte, Deming, Clericuzio, Yashima, Takhashi, Amabilino and others over the last thirty years. Polyisocyanides were the first polymers to be reported to possess a stable helical conformation.[26] The relatively easy preparation of the monomers, the very mild polymerisation conditions and the well-defined structural properties of the resulting polymers have made them very attractive scaffolds on which chromophores can be ordered.[27] Due to the specific 4_1 helical nature of these polymers, the

side groups are all placed at exact distances and precise positions with respect to one other (Chart 2). This ordering may allow for strong excitonic interactions between the chromophores over large distances, thus enabling the principle of chromophoric scaffolding to be realised. This principle was first successfully demonstrated by Hong and Fox who incorporated aromatic donor and acceptor side arms into homo, di- and tri-block copolymers to create a stiff polymer array for unidirectional electron and energy transfer.[28] With the help of fluorescence spectroscopy it was shown that the rigid polyisocyanide backbone was able to spatially define the chromophores and to inhibit the formation of excimers, which is rather surprising since the connection between the polymeric backbone and the aromatic side chains consisted of flexible ethyl linkers. In the block copolymers **4** and **5** (Chart 2) a singlet energy migration was observed at the donor-acceptor interface, which resulted in exciplex formation in the case of **4** and electron transfer at the block interface in the case of **5**. To suppress the formation of exciplexes a tri-block copolymer was developed that contained an intervening pentamethylphenyl block between the respective donor and acceptor blocks of polymer **6** (Chart 2).

Transient absorption spectroscopy of the anthracene functionalised polyisocyanide **5** revealed the formation of a radical ion pair with a long-lived lifetime of 1.1 μs. Analogous to the related helical polyisocyanate polymers, polyisocyanides were also decorated with azo dyes (polymer **7**), which acted as non-linear optically (NLO) active groups.[29-31] In solution a first hyperpolarizability exceeding 5000×10^{-30} electrostatic units was measured. Electric field-induced second-harmonic generation studies were conducted and these revealed that the non-linear response of polymer **7** was larger than that of the monomer.[31] When the polymer was studied at the air–water interface by using Langmuir-Blodgett films, a stable second harmonic generation, without the need of poling, was observed.[29,32] This NLO effect is a consequence of the highly defined orientation of the side arm chromophores on the scaffold, which cannot be achieved by the simple assembly of the monomers at the air–water interface.

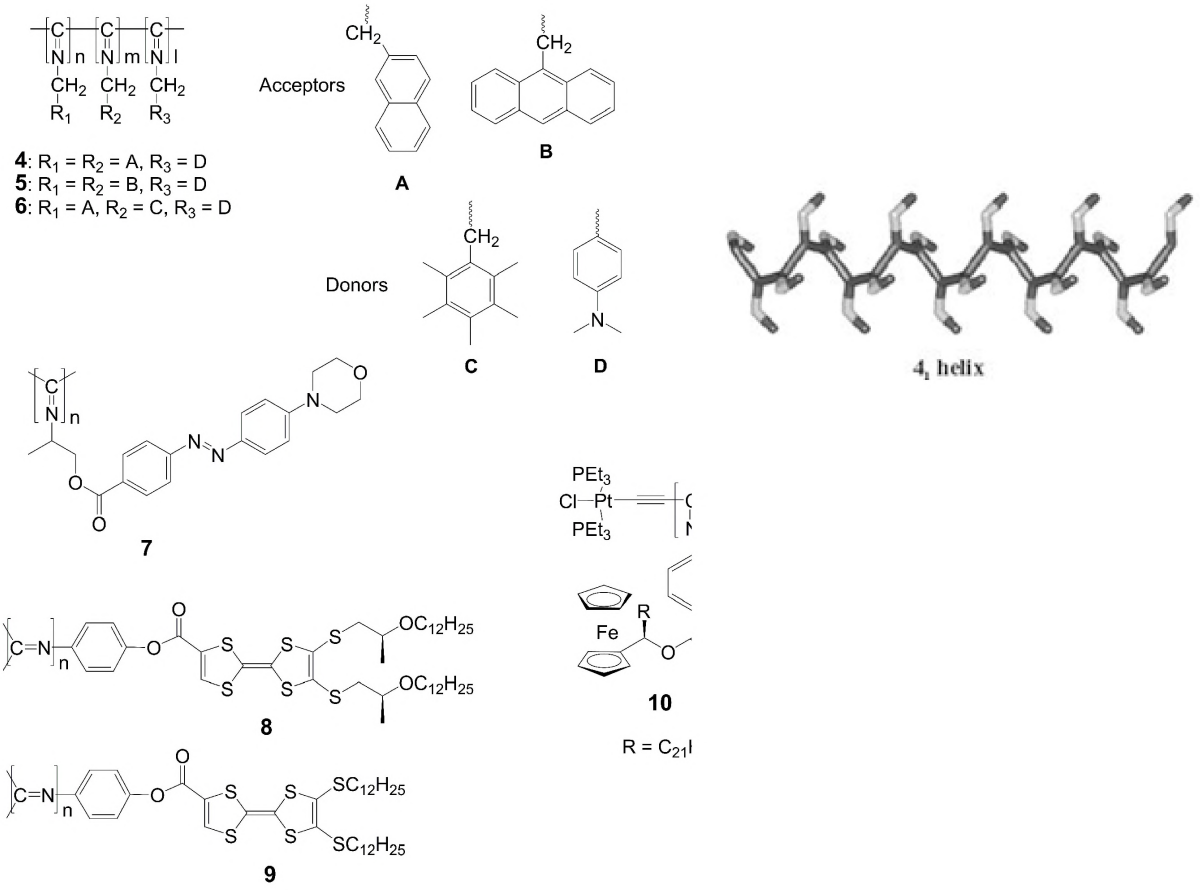

Chart 2. Chemical structures of polymers **4**–**10** and schematic representation of the 4_1 helical conformation of polyisocyanides.

The group of Amabilino synthesised the challenging (chiral) electroactive polyisocyanides bearing tetrathiafulvalene (TTF) derivatives.[33,34] One such polymer (**8**; Chart 2) was found to possess three extreme univalent states (UVSs) and two very wide mixed-valence states (MVSs), which are fully interconvertible as a result of fully reversible redox processes (Figure 3). It was shown by CD spectroscopy that the polymer had very different chiroptical properties, in comparison to the monomer, which are induced by the stereocenter located more than ~18 Å away from the polyimine backbone. The different redox states of the polymer were investigated by both cyclic voltammetry (CV) and UV-Vis spectroscopy and these studies showed that, by using a rigid scaffold, redox systems can be incorporated in a well-defined manner and hence allow these polymers to be used as multistate redox-switchable organic materials in molecular devices.[34] More recently, the same group has synthesised a related TTF derivatised polyisocyanide **9** (Chart 2) and, based on various spectroscopic techniques, concluded that, due to the precise arrangement of the π-electron-rich units, a charge transfer between the TTF moieties is observed upon oxidation.[33]

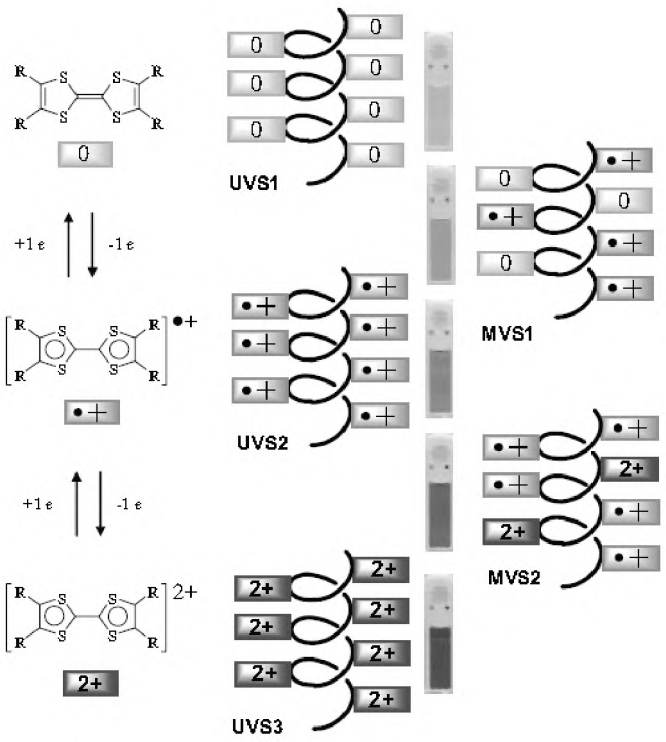

Figure 3. Schematic representation of the redox properties of the TTF units in the TTF functionalised polyisocyanide showing three univalent states (UVSs) and the two mixed-valence states (MVSs).

Redox active polyisocyanides have also been reported by Takahashi and co-workers,[35] who synthesised a chiral ferrocenyl isocyanide (monomer of **10**, Chart 2) and polymerised this monomer by using a Pd-Pt μ-ethynediyl dinuclear catalyst, which is especially active for aryl isocyanides.[36] The recorded redox cycles of the polymer **10** were completely reversible with a half-wave potential of approximately 0.6 V. The CD spectrum of the polymer exhibited a strong positive effect at λ = 360 nm, assigned to the n-π^* transition of the imine group, and a strong negative one at λ = 250 nm assigned to the π-π^* transition of the benzene rings. Upon electrochemical oxidation of the polymer at 1 or 1.5 V, the CD spectrum showed a decrease in the intensity of the positive Cotton effect at λ = 360 nm to 40% of the initial value and the disappearance of the negative Cotton effect at λ = 250 nm. In the UV-Vis spectrum new absorption bands at λ = 240–310 and 620 nm appeared upon oxidation, which were attributed to the ferrocenium chromophore. The CD signal could be restored to the original one by reduction of the polymer at 0.2 V. This switchable behaviour was also observed in the case of a the chemical oxidation with [NO][PF_6] and a reduction with [$(C_5Me_5)_2Fe$], suggesting that upon oxidation the helical backbone is transformed into a disordered structure by the electrostatic repulsion between the ferrocenium ions, yet refolds upon the reduction of these ions. This observation again highlights the advantage of a helical scaffold, which is able to restore high order upon oxidation or reduction.

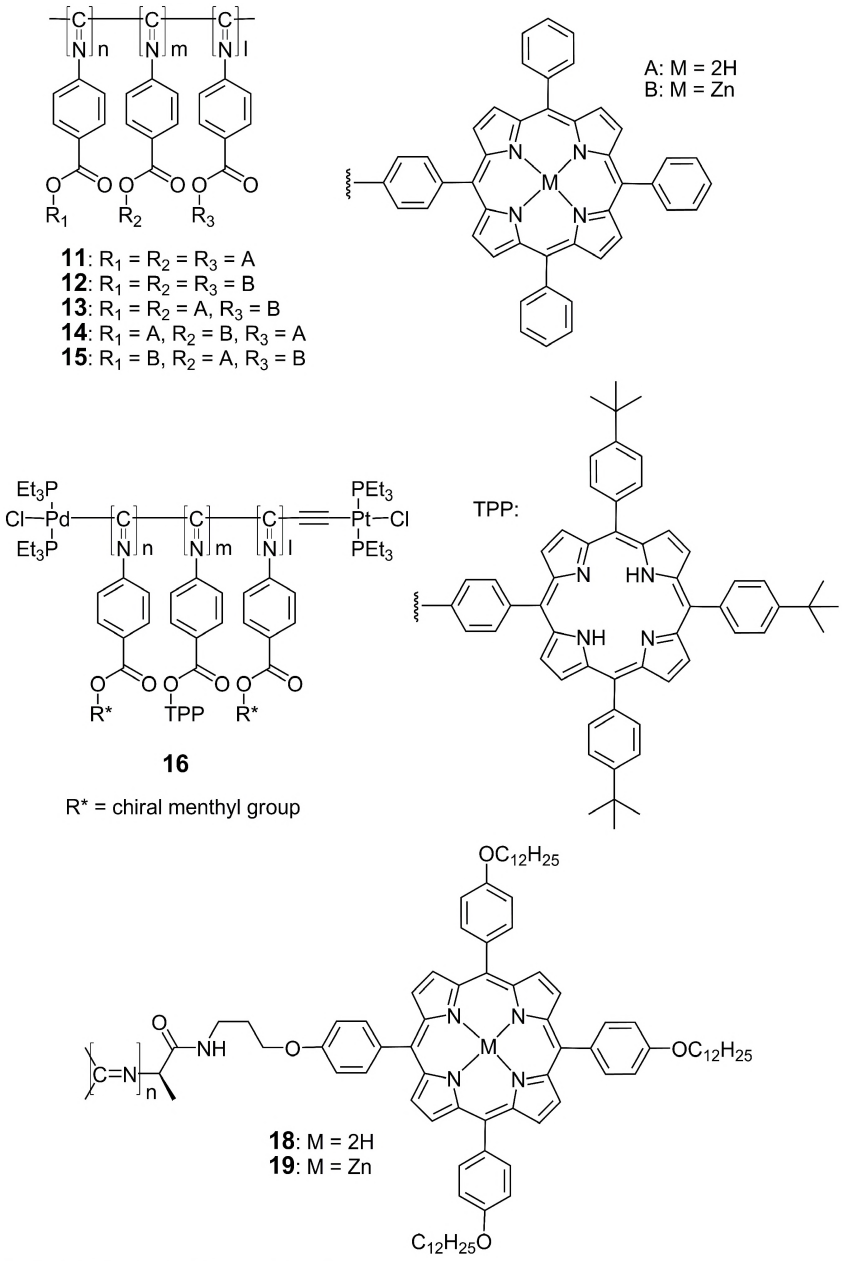

Chart 3. Chemical structures of polymers **11**–**19**.

Due to their versatility and their unique optical properties, numerous synthetic multi-porphyrin arrays have been developed by both covalent or non-covalent procedures[37] to generate materials with a broad range of potential applications.[38] The family of chromophoric polyisocyanides has been extended by the construction of porphyrin appended polyisocyanides, initially reported by the groups of Takahashi[39-41] and Nolte (Chart 3).[42,43] By using a Pd–Pt μ-ethynediyl dinuclear catalyst, the living polymerisation of various porphyrin pendant isocyanides was induced, which resulted in polymers **11**–**15** with precisely controlled molecular weights (see Figure 4 for a calculated model of polymer **11**).[39-41] In this way, for instance, a polymer with ca. 100 attached porphyrins was obtained.

Changing the monomer to catalyst ratio allowed the degree of polymerisation to be varied from 2 to 200, which could be visualised by an increase of the intensity of the band at λ = 400 nm in the UV-Vis absorption spectra of the polymers.

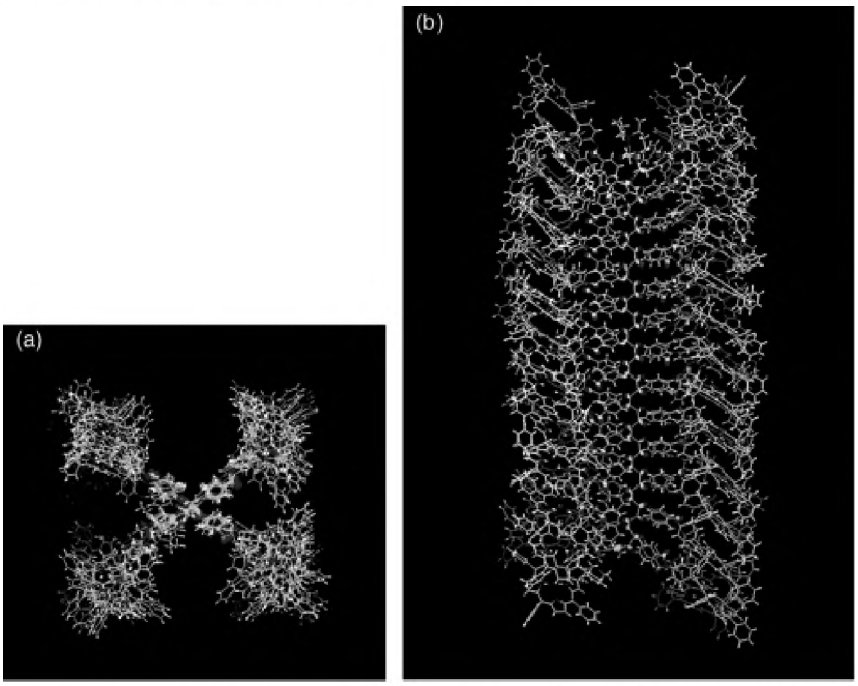

Figure 4. Top (a) and side view (b) of the energy-minimized structure of **11** (50 units) showing the stacks of porphyrins running parallel to the main chain of the polymer.

Photophysical studies revealed that the porphyrins in their stacks are excitonically coupled and arranged in a face-to-face manner. It was found that exciton–exciton annihilation rate constants were independent of the length of the polymer, which indicates a fast exciton migration through the stacks. Since the dinuclear metal catalyst also allows the possibility to construct block-copolymers, polymers of type **14** and **15** with various block lengths and with polydispersities of ~1.1 were prepared. The di- and tri-block copolymers contained both free base and zinc substituted porphyrins and displayed an energy transfer from the zinc to the free-base porphyrins with an efficiency of 35% in the case of **15**.[41] The rate constants for the excitation energy transfer process appeared to be the same for different block lengths of the free base and zinc porphyrins, again pointing to a fast exciton migration. In a novel approach Takahashi and co-workers also used the porphyrin as a spectator group in order to determine the screw sense of their polymers.[40] Incorporation of achiral porphyrin molecules as a central block in copolymer **16**, where the side blocks consisted of enantiopure menthyl side chains, resulted in a helical polymer with a preferred handedness in which the rigid helical conformation was maintained. Since the polyisocyanide architecture enforces an extremely short distance between the stacked porphyrin chromophores an exciton coupled bisignate Cotton effect was observed in the Soret band in the CD spectrum. From the sign of

this cotton effect the screw sense of the polymer could be determined using the exciton chirality method.[44] In a study published in 1985, Nolte and co-workers investigated the use of polyisocyanides as scaffolds for the grafting of porphyrins onto the polymer backbone to obtain catalytically active polymeric materials. This approach, however, resulted in incomplete coverage of the polymer chain with porphyrins and hence no complete homogenous stack of these molecules was obtained.[42] The discovery of the peptide based polyisocyanides, reported by the Nolte group in 2001,[45] opened a new way to use polyisocyanides as macromolecular scaffolds, since the peptide amide functionalities allowed the side groups to be aligned in one direction. This resulted in a hydrogen bonding network in the side chains of the polymers and hence a dramatic increase in rigidity of the overall structure, making it a better scaffold for the anchoring of chromophoric molecules (Figure 5).

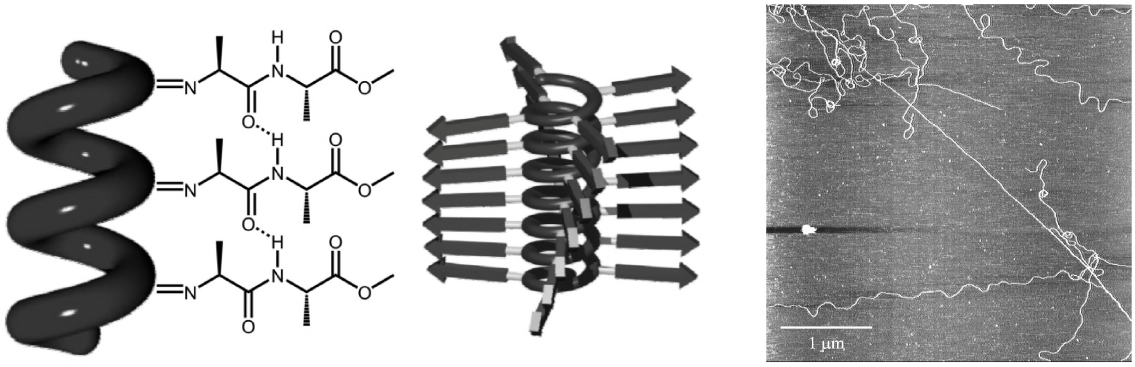

Figure 5. Schematic drawing of the hydrogen bonding network present in the side arms of a polyisocyanopeptide (left and middle) and an AFM image (right) showing the fibre like structures with lengths up to several micrometers. The arrows in are the peptide chains which form a β-sheet-like architecture running parallel to the polymer helix axis.

An additional benefit of these very rigid polymers (persistence length is ~76 nm) is that they can be synthesised with lengths ranging from hundreds of nanometres to several micrometers.[46] The helical porphyrin functionalised polyisocyanides **18** and **19** (Chart 3) were synthesised with average lengths of approximately 100 nm, as determined by Atomic Force Microscopy (AFM). This corresponds to a degree of polymerisation of ~830. The polydispersity of these polymers was ~1.3.[43] The UV-Vis absorption spectra (Figure 6) of the polymers showed a sharp Soret band at λ = 437 nm, indicative of porphyrin molecules arranged as J-aggregates. This band displayed a reversible change upon heating in organic solvents with the intensities of the CD bands of the chromophores decreasing upon warming and increasing upon subsequent cooling; this implies that the porphyrin architecture is a thermodynamic minimum. Resonance light scattering (RLS) experiments revealed that upon excitation the excited state is delocalized over at least 25 porphyrins in one stack, which corresponds to a delocalisation distance of ~100 Å. Depolarised RLS studies revealed that the

slip angle β between the first and the fifth porphyrin amounted to 30° (Figure 6), which results in a helical twist angle of 22° and an overall helical pitch of ~68–71 Å. Fluorescence anisotropy studies were performed to obtain additional information about the orientation of the porphyrins along the polymer scaffold. It was calculated from the anisotropy measurements that the porphyrin moieties are tilted by approximately 25° with respect to the helical axis of the polyisocyanide. The anisotropy measurements, in combination with the RLS studies, revealed an architecture in which the chromophores form a four-fold helter-skelter arrangement along the polymer backbone. The presence of a chiral interaction between monomer *n* and (*n*+4) in this slipped arrangement and between the neighbouring porphyrins *n* and (*n* +1) in the helix could be derived from CD spectroscopy. In the CD spectra intense CD bands were observed, which are reminiscent of the energy transfer process in the natural antenna systems and are ascribed to exciton delocalisation over large distances. Upon the addition of the bifunctional ligand 1,4-diazabicyclo[2.2.2]octane (DABCO) to the zinc porphyrin containing polymer **19** the CD spectrum changed to one that is indicative of a conformation in which the porphyrin stacks possess a helicity opposite to that of the DABCO free polymer. In line with this the infrared and CD spectra of the polyisocyanide backbone remained unaltered by the addition of DABCO.

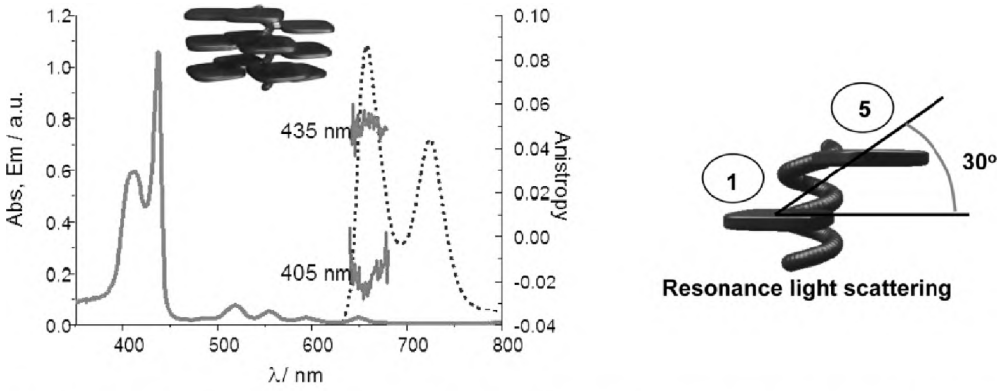

Figure 6. Absorption (black line), emission (dotted line) and fluorescence anisotropy spectra of **18** in toluene (left) and schematic illustration showing the orientation of the porphyrins 1 and 5 in the polymer with a slip angle of 30° (right).

To further explore the concept of organising pigments on rigid polymer scaffolds, polyisocyanides **20–22** possessing perylene-diimides (PDIs) (Chart 4), which are promising chromophores in organic electronic n-type materials, were explored (see also Chapter 3).[47-52] The combination of the hydrogen bonding arrays together with the additional π-π stacking interactions of the perylene side groups resulted in very stable helical polymers.[47,52] Fluorescence spectroscopic studies on **20** showed the presence of a broad, structureless, and red-shifted band in the emission spectrum of the polymer, indicative of an excimer-like

species. Fluorescence decay measurements revealed that species with a long lifetime of 19.9 ns were present, further supporting the idea that emission from these polymers occurred through an excimer species. By using a combination of confocal fluorescence microscopy and AFM it was possible to show that two species were formed in the polymerisation reaction, i.e. ill-defined oligomeric and well-defined polymeric species. The first species could not be visualised by AFM since they were too short and they displayed monomer-like fluorescence. The latter species had a more well-defined rigid structure and could be visualised as independent fibres by AFM. These longer fibres were found to primarily exhibit excimer emission. It could be concluded from a combination of confocal fluorescence spectroscopy and AFM upon excitation of these longer rods that the emission is moved along the isoelectronic perylene arrays and became quenched at perylene dimer sites, which resulted in excimer emission. These dimer sites can be fixed defects in the polymer or dynamic excimers that are formed throughout the polymer.

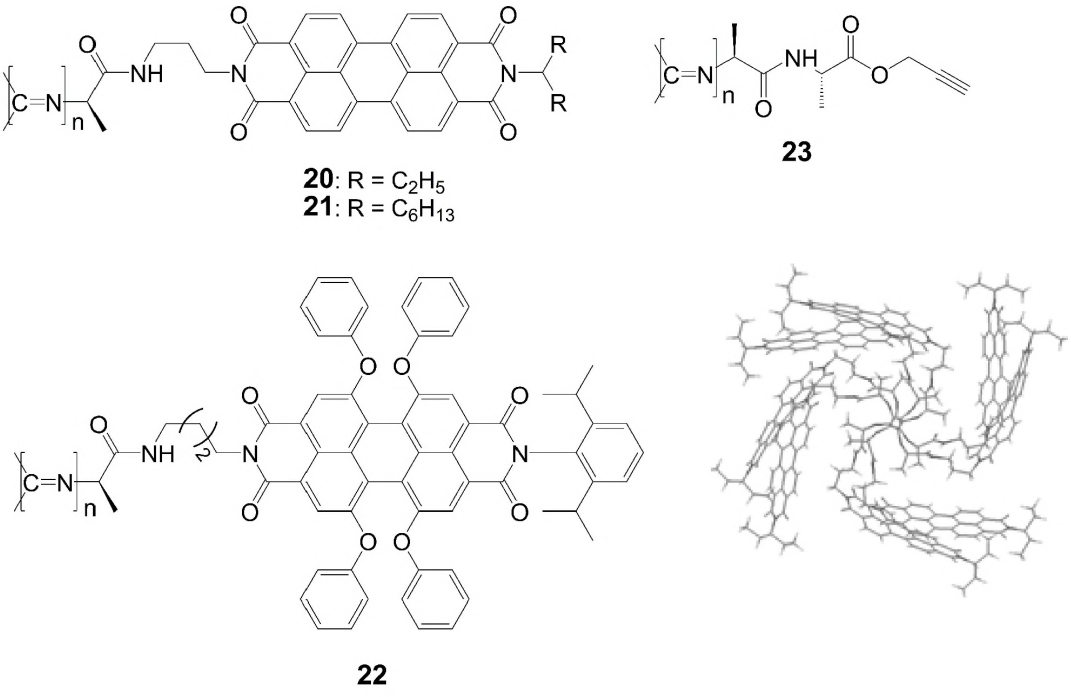

Chart 4. Chemical structures of polymers **20–23** and a top-view of the most probable conformation of the helix of **21** and the relative orientation of the perylene molecules.

Because polymer **20** was poorly soluble in organic solvents, polymer **21**, which contains long alkyl tails and hence improved solubility, was synthesised.[52] Extensive dynamic and molecular modelling studies, combined with spectroscopic studies, indicated that **21** is an ideal polymer system for electron and energy transport. This hypothesis was further strengthened by transient absorption spectroscopy studies, which indicated extremely rapid exciton migration rates and high charge densities in polymer **21**. The modelled structure as

depicted in Chart 4 shows the calculated PDI ordering, which accounts for all the observed physical properties (UV-Vis and CD) observed.

The electronic transport properties of the polymer stacks were examined in thin-film transistors and the experiments revealed carrier mobilities of the order of 10^{-3} cm^2 $V^{-1}s^{-1}$ at 350 K, which were found to be limited by inter-chain transport processes. This mobility value is intermediate between the values observed for amorphous spin-coated films of perylene and single-crystal perylenes.[50] Photovoltaic cells with an active layer of **21** as the electron acceptor and either P3HT[49,51] or PFB/F8BT[51] as electron donor were prepared and, although the overall efficiency was rather low (~0.2 %), a 20-fold improved power output compared to a cell with an active layer of a monomeric perylene homologue and P3HT was observed. In order to visualize the relationship between the architecture and the photovoltaic efficiency, AFM and Kelvin Probe Force Microscopy (KPFM) measurements were carried out on polymer films (Figure 7) by the group of Samori.[49] This allowed the direct visualization of the photovoltaic activity occurring in polymeric bundles of electron-accepting PDI wires and bundles of electron-donating P3HT chains with true nanoscale spatial resolution. It was evident from these AFM/KPFM and spectroscopic studies that the well-defined polyisocyanide chromophoric system has promising characteristics for applications; it enhances the lifetime of the separated state and is more efficient than monomeric perylene materials in a photovoltaic device.

The addition of bulky phenoxy substituents to the perylene bay area leads to a sterically hindered polyisocyanide (see **22**; Chart 4) and limited π-π stacking of the PDIs. The low quantum yield (3%) of the polymer is in line with H-aggregated PDI units. In contrast to the behaviour of **20** and **21**, the emission spectrum of **22** gave no evidence for the formation of excimers, which is consistent with the conclusion that the steric bulk seems to prevent the formation of excimeric pairs in **22**.

Although polymers **20–22** are promising candidates for electron transfer their synthesis are extremely demanding. A more modular approach to prepare such polymers, based on the post-modification of a well-defined polyisocyanide scaffold was therefore developed. Polymeric scaffold **23** (Chart 4), with side arms containing two alanine groups and a terminal acetylene functionality, was synthesised (see also Chapters 4 and 5). This compound can be easily modified by reacting it with azides using the well-established click-chemistry approach.[53] The wide variety of azides available allows one to access a vast array of functionalised polymers with varying properties.

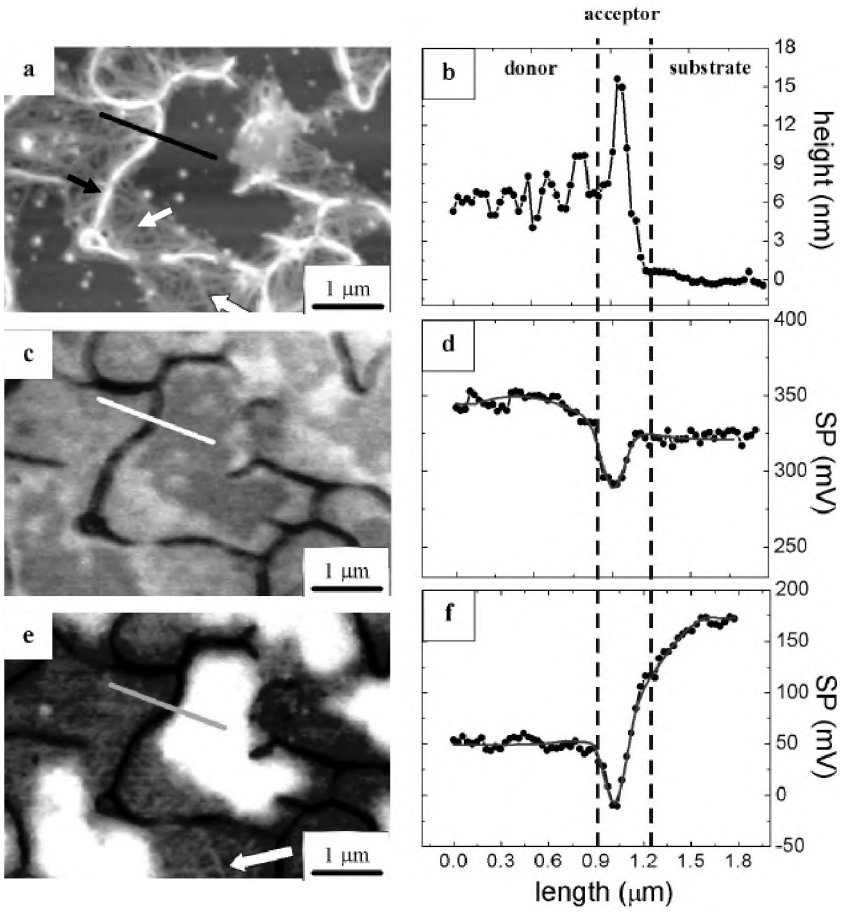

Figure 7. KPFM data of thin films of **21** and P3HT and (a) AFM image of an ultrathin blend of **21** and P3HT deposited on silicon. (c, e) Surface potential images of the same area as in (a), without (c) and with (e) illumination by white light (~60 mW cm^{-2}). An overall negative potential shift upon illumination is visible. (b, d, f) Measured (black lines) and simulated (red lines) profiles obtained by tracing the arbitrary lines ((a) black, (c) white and (e) light blue) in the corresponding images (a), (c) and (e).

The clicking of ethylene glycol azides to polymer scaffold **23** was found to result in the formation of water-soluble polymers. The co-clicking of the scaffold with the same azide in conjunction with a perylene azide gave, for the first time, chromophoric water-soluble polyisocyanopeptides, which exhibited the same CD spectrum in water as in dichloromethane. By the use of two chromophoric azides, a coumarin dye and a perylene dye, random copolymers were formed in which the absorption and emission from both chromophores were present. Furthermore, interaction between the chromophores was observed, evidenced by a quenched and blue-shifted emission of the coumarin molecules that are in close proximity to a perylene molecule. This shows that two different chromophores can now be readily incorporated into the polymers and opens the way to polymeric materials with a wide range of optical properties.

The above presented approach, in which a rigid polymer chain is used as a scaffold in order to control the position of dye molecules, is a very versatile one. The mechanical properties of the polymers, that is, their rigidity on the nanometre scale, the flexibility of the linker and

the stacking of the dye molecules can all be adjusted by chemical modification. The ability to orient chromophores in space into a more efficient energy and electron transfer geometry, which cannot so easily be achieved by self-assembly, offers considerable opportunities for materials with improved mechanical and opto-electronic properties.

1.3 Carbon nanotubes and related structures

An alternative way to arrange chromophores is to employ a carbon nanotube (CNT) as a scaffold to which chromophores can be attached. Since CNTs possess unique properties numerous modifications have been developed in order to improve their solubility and electronic properties. CNTs may also find applications for the transport of biological molecules.[54] The ability to attach chromophores to CNTs would allow for their visualization and possible tracking of the movement of biomacromolecules. The study of CNT in combination with chromophores has, however, been primarily focussed on the grafting of chromophores onto CNTs for photo-induced electron transfer. In general, two strategies have been employed, i.e. covalent and non-covalent (supramolecular) functionalisation of CNTs. It is important to note that, due to the method of preparation, CNTs have been randomly decorated and hence in a less controlled manner in contrast to, for example, viruses or polymers, which are built up from chromophoric monomers that are subsequently self-assembled or polymerised. The covalent approach to chromophoric functionalised CNTs was utilized by Sun and co-workers.[55] They synthesised porphyrin decorated single-walled CNTs (SWNT) with the porphyrin molecules covalently attached to the nanotubes with either a short (CH_2) or a long (C_6H_{12}) linker. From fluorescence studies it became evident that for the long linking species the fluorescence is suppressed, presumably due to the stacking of the porphyrin units because the spacer was flexible. The fluorescence of the compounds with a short spacer revealed that the photo excited state properties of the chromophores remained unaffected, that is, no quenching of the fluorescence was observed. In related work porphyrin molecules were directly linked to the CNT through an ester linkage (Figure 8).[56] By using thermogravimetric analysis (TGA) a grafting density ranging from 8–22% was found to be present. Upon excitation at λ_{exc} = 550 nm of the porphyrin-SWNT hybrid the emission was almost fully quenched with the energy being channelled into the SWNT. No intermolecular electron transfer between the porphyrins was reported.

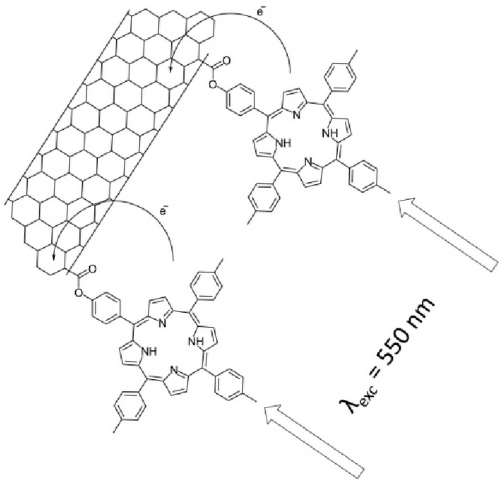

Figure 8. Porphyrins linked to CNTs through an ester linkage leading to almost complete photoinduced electron transfer from the porphyrin to the CNT.

The covalent attachment of phthalocyanines to CNTs resulted in stable assemblies for which steady-state and time resolved fluorescence spectroscopy studies indicated that a strong photophysical interaction was present between the chromophores and the CNTs.[57] Following on this success, novel phthalocyanine-CNT complexes were prepared utilising the click chemistry protocol.[58] These complexes were tested for their photovoltaic properties and internal photo conversion efficiencies (ICPE) up to 17.3% could be reached, which suggests a considerable potential for such systems.

Another class of chromophores that could serve as donor materials in CNT complexes are TTF molecules.[59] The SWNTs have been modified with carboxylic acid groups, followed by EDC coupling to an alcohol functionalised TTF to give the nano-hybrid materials. Spin-coated solutions on silicon wafers revealed thin bundles as well as aggregates of tubes. Furthermore, by changing the spacer between the TTF and the CNT or by extending the π-system of the TTF the charge separation and the charge recombination could be controlled.

Recently, also graphene, a very promising candidate in materials science, has been used as a support to arrange porphyrin molecules.[60] From detailed infrared (IR) and UV-Vis spectroscopy studies, as well as TEM studies, it could be concluded that the used amino porphyrins were covalently linked to the graphene oxide through an amide bond. It appeared that the fluorescence of the porphyrin molecules in these donor-acceptor nano-hybrids was quenched due to a possible electron-transfer process.

Although the covalent approach for the preparation of these materials is very versatile it may lead to a disruption of the π-system of the CNTs and hence in partial loss of electronic and structural properties. For this reason non-covalent procedures, which, in principle, are more simple to apply and rely upon Van der Waals, π-π stacking and/or Coulombic

interactions were also investigated. In general, four approaches have been used to create chromophoric carbon nanotubes in which the chromophores are non-covalently linked to the CNT (Figure 9). These are based on i) simple non-covalent interactions between the chromophore and the CNT (A), ii) a charged polymer that is covalently attached to the CNT allowing multiple coulombic interactions with an oppositely charged chromophore (most often a porphyrin) (B), iii) charged pyrene derivatives that have favourable π-π stacking interactions with the CNT and also interact through coulombic interactions with an oppositely charged chromophore (C) and iv) a chromophore that is directly attached to a pyrene molecule, which interacts with the CNT (D). In all cases supramolecular assemblies are created where the donor and the acceptor are in close contact leading to interesting properties. In these approaches there is, however, no direct control over the positioning of the chromophores in the hybrid since the attachment to the CNT occurs at random. It is of interest to note that the rigid structure of the CNT in most cases is not used as a template to increase communication between the chromophores but to realize strong interactions between these chromophores and the CNTs.

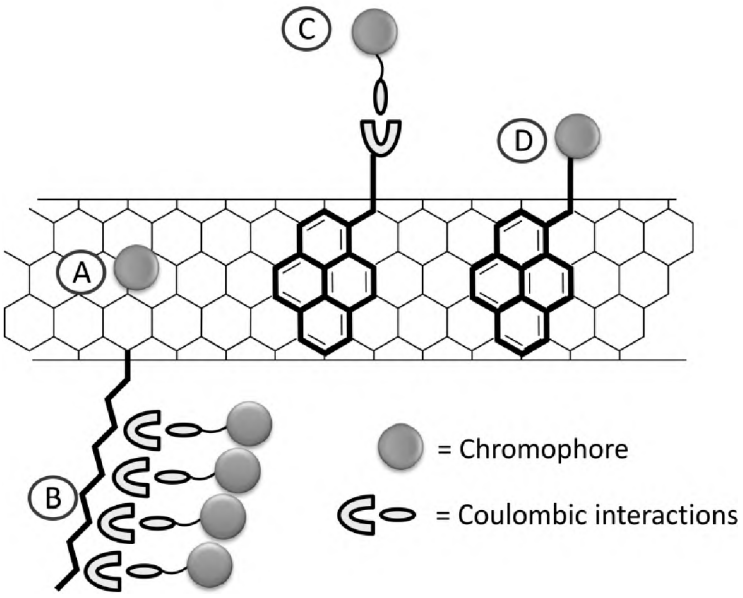

Figure 9. Schematic drawings of the four approaches developed to construct chromophoric CNT complexes.

Porphyrins[61-67] and phthalocyanines[68] are the most frequently used dyes to decorate CNTs (Approach A, Figure 9). Early work by Nakashima[61] and Sun[62] reported the generation of stable porphyrin–nanotube hybrids when there was an excess of porphyrin molecules in solution. Removal of the excess porphyrin resulted in precipitation of the nanotubes, which indicates that dissociation of the complex occurs rapidly. Without the complete removal of the excess porphyrin from the porphyrin-nanotube hybrid suspension, detailed photophysical studies could be carried out and these revealed charge transfer features that

are persistent on the time scale of hundreds of nanoseconds.[69] The interaction between the porphyrin and the CNT could be enhanced by using conjugated porphyrin polymers[63] or by applying polymer wrapping.[64] Kamat and co-workers used CNTs to order protonated porphyrins in the form of J- and H-aggregates.[65] It was demonstrated with the help of TEM that in the presence of a strong acid the hybrid complexes assembled into large rod-like structures (Figure 10a,b), in which the porphyrins were randomly distributed over the CNT. In the absence of a strong acid, the interaction was weaker and clusters of the protonated porphyrins were formed (Figure 10c). This striking difference is attributed to the strong intermolecular interactions that occur between porphyrin moieties and /or ordered aggregation effects in the protonated form.

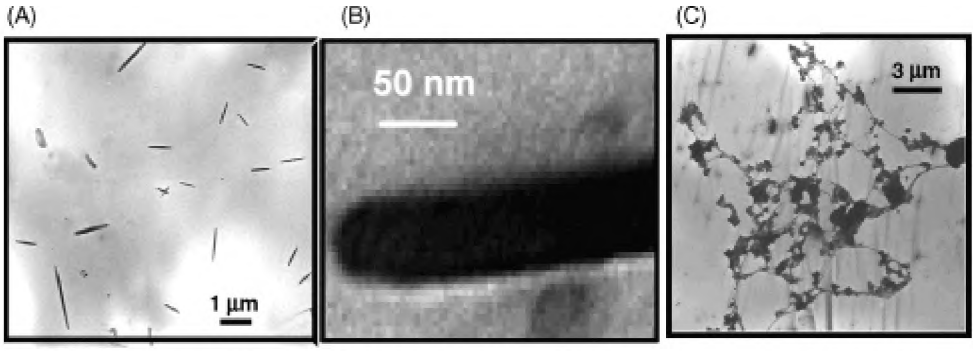

Figure 10. (a, b) TEM images of the rod-like CNT-porphyrin hybrid complexes that are formed in acidified THF. (c) TEM image of the CNT-porphyrin adducts formed in THF without acid present revealing no clear, assembled structures.

Water-soluble porphyrin-CNT complexes have also been developed, which allowed the alignment of nanotubes on polydimethylsiloxane (PDMS) surfaces and the subsequent transfer of these objects to silicon substrates by stamping. Despite the presence of large areas of aggregated porphyrins on the silicon substrate, multiple CNTs aligned parallel to each other were obtained.[70] An extensive study into the multiple and complex interactions that are present in non-covalently linked porphyrin-nanotube complexes[66,67,71,72] and in TTF-nanotube complexes[73,74] (as a complementary study to their earlier work in this area[59]) has been published by Guldi, Prato and co-workers.

A water soluble polymer, i.e. poly-[(vinylbenzyl)trimethylammonium chloride] ($PVBTA^{n+}$), has been used in combination with CNTs as a positively charged scaffold to align negatively charged porphyrin molecules through electrostatic interactions (Figure 9, approach B).[67] A similar approach based on negatively charged CNTs and positively charged porphyrin molecules has also been reported.[71] The hybrid complex was readily soluble in water and was found to be stable for months without any observable precipitation. Photoexcitation of the complex in solution resulted in the fast generation of radical ion pairs (i.e. 0.15 ns) that

had very long lifetimes (2.2 µs). Photocurrent measurements gave monochromatic internal photoconversion efficiencies (ICPE) up to 9.9%. Supramolecular pyrene-porphyrin CNT complexes were prepared by using a combination of electronic and π-π interactions (Figure 9, approach C). [91, 92] Detailed photophysical studies on these complexes revealed that long lived radical ion pairs were formed as a product of the rapid excited-state deactivation of the porphyrin. These studies have given an interesting insight into the processes involved, which is important for the application of these nano-hybrid materials in electronic devices. The same authors have also described a hybrid complex in which the chromophores were directly attached to the pyrene units (Figure 9, approach D). To this end, a TTF molecule was linked to a pyrene with a flexible linker allowing for optimised interactions with the outer surface of the CNT, leaving the latter structure intact. [91] A ratio of 1:750, i.e. a single pyrene-TTF unit per 750 carbon atoms of the CNT was estimated to be present in the final complex as concluded from Thermogravimetric Analysis (TGA). Due to the close distance between the TTF molecules and the CNT, very fast electron transfer (on the nanosecond scale) between these species was observed. Recently, these investigations have been extended to a series of single-walled and multi-walled CNTs.[92] From these studies it was apparent that stable charge-separated states are formed only in the case of multi-walled CNTs as compared to single-walled CNTs, where only short lifetimes were found. This might be explained by a stabilisation of the excited state species in the former cases as a result of the presence of a large number of tubes in the multi-walled CNTs.

Closely related to the family of CNTs are the carbon nanohorns (CNHs).[75] Carbon nanohorns are spherical aggregates typically composed of thousands of carbon nanotubes of about 2–5 nm in diameter and 30–50 nm in length. Their characteristic features include a conical end on one side of the tubular structure, a high porosity and a large (rough) surface area. The aggregation of CNHs leads to the formation of dahlia-flower-like superstructures. Although the use of CNHs as scaffolds for chromophores has not been investigated to the extent it is in the case of CNTs, some examples of porphyrin CNH nano-hybrids have been recently reported. Using approach C (Figure 9), Ito and co-workers were able to prepare TTF chromophoric nano-hybrids by exploiting the electronic and π-π interactions between the CNH, the positively charged pyrene molecules and the negatively charged TTFs.[76] A comprehensive spectroscopic characterisation, which offered a schematic overview of all the processes taking place in the hybrid, was carried out. These studies indicated an electron transfer process between the TTF units and the CNHs as also reported for the TTF-CNT hybrids.[91] As with CNTs, CNHs could also be decorated with porphyrins by three different routes. These included i) the simple attachment of the porphyrin to the CNH by direct π-π interactions,[77] ii) the covalent attachment of the porphyrin to the CNH with an amide bond (see for the molecular structure and a representative high-resolution TEM image Figure

11),[78] and iii) the use of ethylene glycol spacers that are covalently linked to the CNHs.[79] In all cases the CNH hybrids were analyzed in detail generating interesting information about the formation of charged separated states, electron transfer and hybrid stability. This information is required for further optimisation of the structures in the case of application in organic devices. Recently, a porphyrin CNH hybrid was used to fabricate a cancer phototherapy system, which highlights the fact that these chromophoric carbon nanostructures are very useful for practical applications.[80]

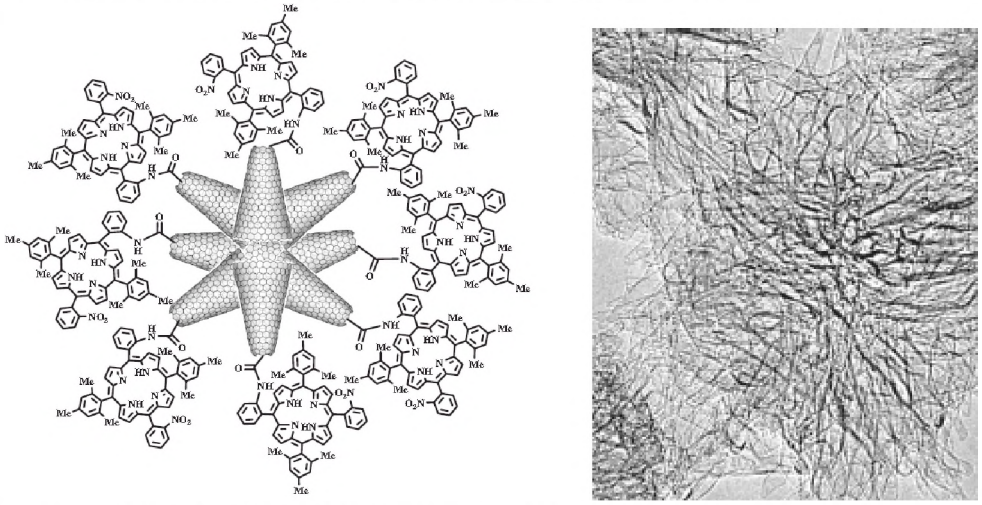

Figure 11. Schematic depiction (left) and a high-resolution TEM image (right) of the structure of a porphyrin CNH nano-hybrid.

In summary, CNTs, being one of the stiffest compounds known to date, are attractive scaffolds for the immobilisation of chromophores. Although a high level of molecular control is not always achieved, these nanotubes offer a versatile platform for the construction of interesting donor–acceptor materials. In recent years, the assembly and the structural and photophysical properties of the chromophore-CNT hybrids have been extensively studied and their unique properties will open the way for utilisation in future organic devices.[81]

1.4 Nucleic acid based architectures

DNA is used by nature to encode information needed for the construction of living organisms. For chemists, DNA constitutes a unique programmable scaffold that holds great promise in numerous areas of nanotechnology.[82] Its key characteristics are:

(i) the presence of two complementary strands that can be reversibly assembled and disassembled; ii) the fact that it is chiral (helical) and iii) very rigid (persistence length of ~50 nm), with an ideal distance between two base pairs for the stacking of chromophores (3.3 Å in the B-form); iv) the possibility to synthesise it by automated procedures, thereby allowing site specific modification; v) the possibility to assemble it into complex 3D nano-structures and into nano-devices.

Due to these attractive properties DNA has been receiving increased attention as a scaffold for the precise arrangement of chromophores. In this section, we will highlight recent examples of DNA based multi-chromophoric assemblies which display new properties arising from the electronic communication between chromophores.[83,84] The supramolecular organisation of chromophores as a result of intercalation between DNA base pairs, will not be reviewed here.

Two main approaches have been used to organise chromophores on DNA. They can be denoted as “internal stacking” and “outside stacking” (Figure 12). In the first approach, the Watson–Crick base pairing is partly suppressed since either the base or the sugar part is substituted by the chromophore (Figure 12, left). The stability of the duplex is then provided by the base pairing at the unmodified sites and the contribution by the internal stacking of the introduced hydrophobic chromophores. In some cases, this internal arrangement constitutes a recognition motif that, in some way, can be viewed as an artificial base pairing (*vide infra*). In the second approach, the full Watson–Crick base pairing of the functionalised nucleotides is maintained, while also the base or the sugar is modified (Figure 12, right). The chromophores are thus tethered either to the 5 position of the pyrimidine ring or to the 7 position of the deazapurine ring of DNA, to maintain the *anti* conformation of the modified nucleoside. Another possibility to generate arrays of chromophores is to use a RNA scaffold, since the 2' position of the sugar can be readily derivatised without modifying the base or to use Lock Nucleic Acids (LNA) by taking advantage of the 2'-4' bridging unit as an anchoring site for a chromophore. This second approach has led to an "outside stacking" of the chromophores (Figure 12), which can further interact with the hydrophobic grooves generated by the "intact" internal stacking of the base pairs. In both approaches, adjacent chromophores can be brought close to one other and the distance between two base pairs (and thus between two anchoring sites) is optimal for physical communication between the chromophores. In this section we will mainly focus on chromophoric scaffolding using DNA. Related work with RNA and LNA has been recently highlighted and will not be discussed here.[84]

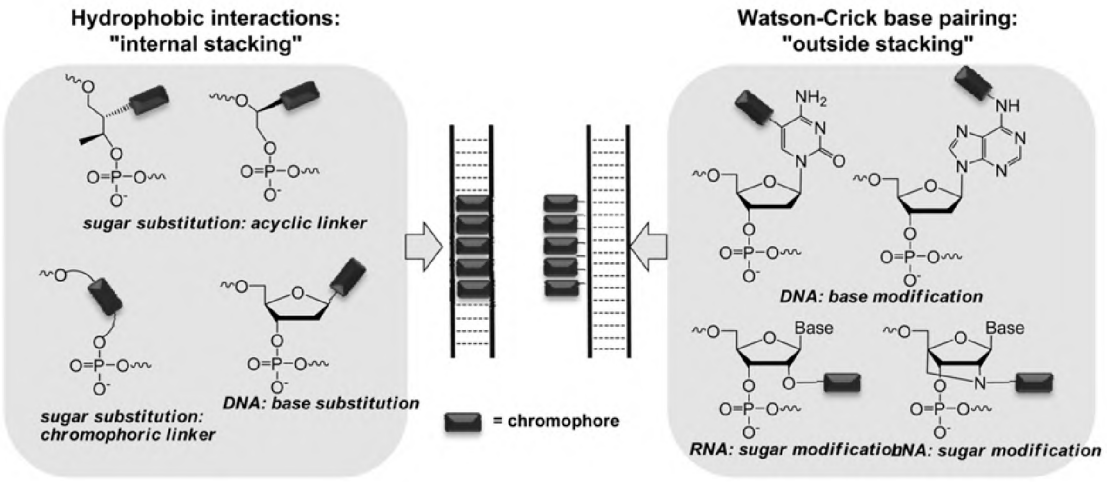

Figure 12. Strategies for the construction of chromophoric assemblies with the help of DNA based scaffolds.

First approach: internal stacking

Inspired by the structure of the DNA skeleton, the group of Kool has developed a new class of assembled fluorescent molecules, the so-called 'fluorosides'. They consist of short oligomers (generally tetramers) of C-nucleosides to which individual chromophores are grafted. The replacement of the DNA bases by flat aromatic (hydrophobic) molecules allows them to stack but also provides water solubility, thereby mimicking a single-stranded DNA. The close interaction of the chromophores is of interest for energy transfer and the possibility to easily tune the sequence of the chromophores (with a DNA synthesiser) allowed Kool and co-workers to synthesise libraries of oligo-fluorosides with unique properties.[85] As displayed in Figure 13a, a 256-member library composed of all combinations of fluorosides D, E, Y and Q was grown from PEG-polystyrene beads. The fluorescent properties of the fluorosides were found to be different from those of the individual chromophores, that is, large Stokes shifts and tuned absorption and emission properties were often observed. In addition, the emission was sequence dependent such that at least 50 different colours could be distinguished by the naked eye. A study conducted with fluorosides made of only two chromophores but with different sequences revealed the importance of the neighbouring interaction; the fluorophore sequence in such oligomers turned out to be as important as the fluorophore composition in determining the fluorescence properties.[86] The large Stokes shifts of the oligo fluorosides and their increasing brightness with increasing substitution make them particularly suited for biochemical and biophysical applications.[87] This work was extended to larger libraries (11^4 = 14 641 members) for the discovery by rapid combinatorial screening of sensors that change colour on light exposure.[88] From this library, three tetrafluorosides were selected and further studied. Upon light exposure a blue shift of the fluorescence was observed, probably caused by the selective reaction of one chromophore with oxygen (Figure 13b). This might result in the loss

of the initial excimer fluorescence and the emergence of monomer emission at shorter wavelengths. The clear separation of starting and final emission colours in these tetrafluorosides opens the possibility to measure light exposure over time.

The various oligomers could be simultaneously excited with a long wavelength UV light (i.e., 340–380 nm) to produce multiple emission colours. This is of particular interest in connection with the simultaneous tracking of more than one species by colour and maybe useful for the visualisation of species in moving systems where classical fluorophores fail. For instance, a set of 23 oligodeoxyfluorosides (ODFs) was prepared from a library with emission maxima ranging from 376 to 633 nm, thus yielding apparent colours from violet to red, all of which can be visualized directly (Figure 13c). Preliminary *in vitro* and *in vivo* experiments showed that the ODFs could penetrate the cellular membrane and tissues, were biostable and displayed no apparent toxicity in human tumor (HeLa) cells and live zebrafish embryos.[89] More importantly, multispectral imaging could be successfully carried out with a set of four dyes in real time in a dynamic system (living embryos) without the need of reconstructing of separated colour images (Figure 13d).

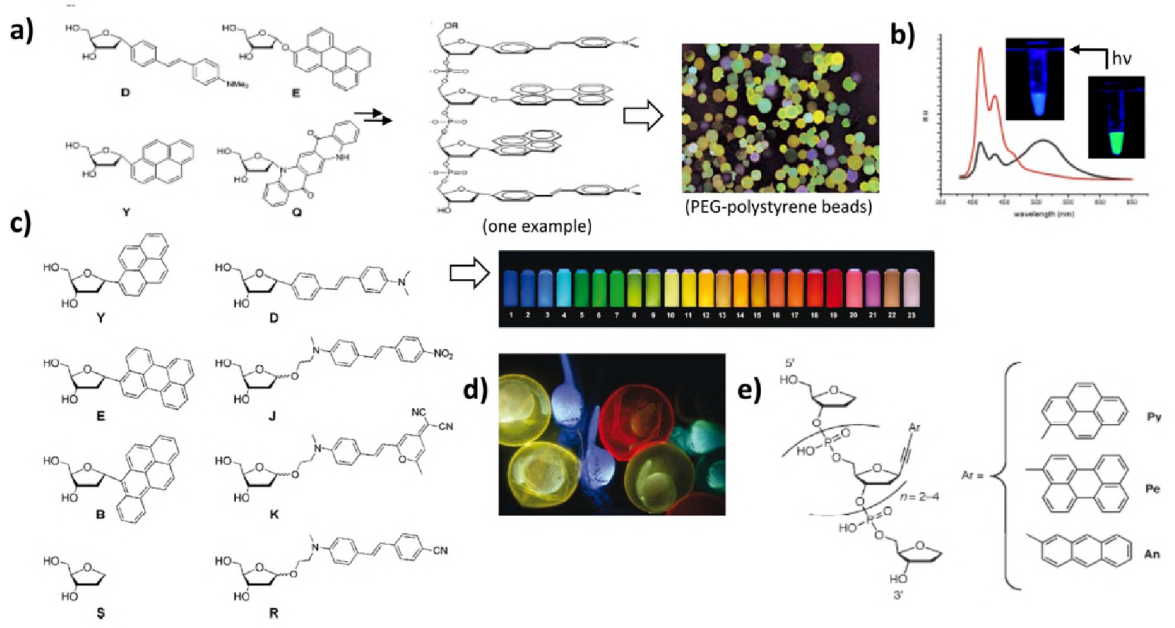

Figure 13. a) Construction of a 256-member library of tetrafluorosides from four different fluorosides leading to a wide range of colours at a single excitation wavelength; b) application to the development of a light sensitive sensor; c) various fluoroside monomers used for the selection of a set of 23 oligofluorosides displaying colours that cover the complete visible spectrum and (d) the use of four oligofluorosides (blue, cyan, yellow and red emitting) in the simultaneous observation of differently labelled live zebrafish embryos (the dyes were separately incubated with embryos; real image at 48 h post-fertilisation with excitation at 354 nm); e) related fluorescent oligomers based on alkynyl C-nucleosides developed by Inoue and co-workers.

In a similar approach, Inoue and co-workers synthesised analogous fluorosides starting from pyrene, perylene and anthracene residues connected to the furanoside through an acetylene linker. The anomeric configuration in these oligomers was exclusively β (Figure 13e).[90] This latter feature was required in order to investigate in detail the photophysical properties of these fluorescent oligomers. As in the Kool system, physical and electronic interactions were observed between the chromophores and the predominant excimer fluorescence was found to originate not only from homo-oligomers but also from hetero-oligomers.

In the search for non-natural, non-hydrogen bonded hydrophobic base pairs, which could be of potential interest in expanding the genetic alphabet, Leumann and co-workers connected biphenyl (Bph) and bipyridyl (Bpy) residues to C-nucleosides (Figure 14a). As a result of inter-strand stacking of their distal rings two Bpy C-nucleoside residues could recognise each other within a DNA duplex with an affinity equal to that of a G-C base pair.[91] When a number of these planar hydrophobic molecules were placed on both strands in the middle of a duplex oligodeoxynucleotide (ODN), they were found to form a zipper-like arrangement inside the duplex without altering the B-DNA conformation of the double helix (Figure 14a).[92] In the case of Bph homo-interactions, a stabilisation of 3.0–4.4 Kcal per additional Bph pair was measured. This artificial recognition motif opens interesting perspectives for instance in connection with the study of donor-acceptor systems (vide infra), the development of binary recognition codes and the realisation of charge transport.

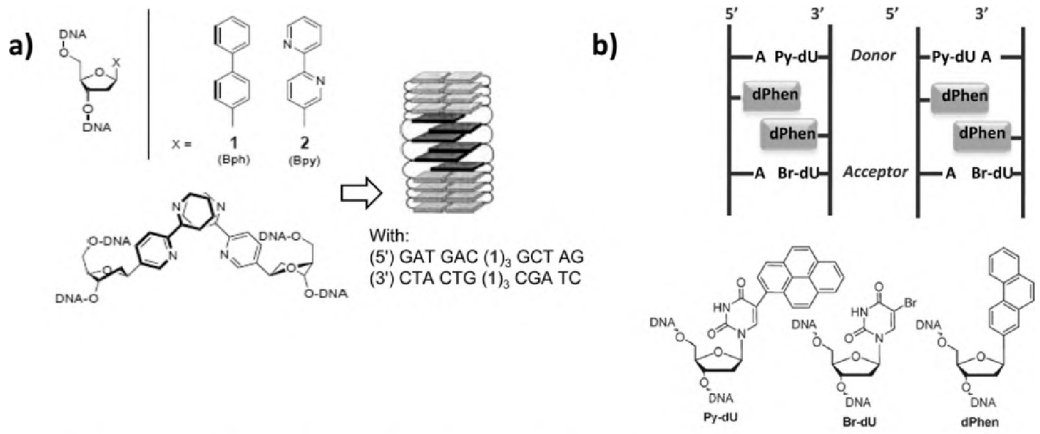

Figure 14. a) The two artificial hydrophobic base pairs studied by Leumann and their stacking mode (left) and the representation of the inter-strand zipper array when multiple Bph residues are introduced in the middle of a DNA duplex (right); b) the system used by Leumann to study electron transfer through an interstrand phenanthrenyl pair.

Using this artificial base pairing system, the group of Leumann has also investigated electron transfer through a stacked phenanthrenyl pair in DNA (Figure 14b).[93] Their system was made of 5-(pyren-1-yl)uridine as a photoinducible electron donor and 5-bromouridine as an electron acceptor, which also acts as a reporter molecule. The donor and acceptor molecules

were separated by an interstrand stack of two phenanthrenyl-C-nucleosides. The overall processes were monitored by quantifying strand cleavage at the level of 5-bromouridine upon illumination using polyacrylamide gel electrophoresis (PAGE) experiments. The authors concluded that electron transfer was effective through the phenanthrenyl stack, but seven times less efficient than in the situation where the phenanthrenes were absent. This was explained by assuming that the electron transfer from the excited pyrene to the phenanthrene was endergonic and proceeded by a superexchange mechanism, whereas electron transfer to a thymine was exergonic and followed the known hopping mechanism. This result, however, is only a proof of principle and further modifications of the phenanthrenyl stack might lead to an improvement of the efficiency.[94]

Another strategy based on sugar substitution, was investigated by the groups of Asanuma,[95-99] Wagenknecht[100,101] and Haner.[102-107] Asanuma and co-workers developed an acyclic linker based on D- or L-threoninol for the incorporation of dyes, such as Methyl Red and Naphthyl Red, into DNA (Figure 15a). In a first study, up to six dyes were introduced sequentially on a 18 mer strand (Figure 15bI).[95] In the single strand state, hypsochromicity with a narrowing of the absorption maximum, which increased with the number of incorporated dyes, was observed, indicating the formation of *H** aggregates. This cluster of dyes was, however, only stable in the single stranded form. Upon addition of the complementary strand incorporating an acyclic propanol derivative linker, a new type of aggregate was obtained, as evidenced by a red shift of the absorption maximum along with a broadening of the band. Interestingly, the reversible thermal denaturation/hybridisation of the duplex allowed the switching from one aggregate to the other. Since this strategy was not suited for the modification of a duplex DNA, the dyes were placed in alternating positions on both strands of the duplex, facing the acyclic linker.[96] UV-Vis and CD spectroscopy evidenced the formation of *H* aggregates with hetero- (Methyl Red/Naphtyl Red) and homo-combinations (Methyl Red/Methyl Red or Naphtyl Red/ Naphtyl Red) of dyes due to the interstrand stacking of the dyes in a face to face manner (Figure 15bII,III). It is noteworthy that the new absorption band in the case of the hetero *H* aggregates originated from exciton coupling among the chromophores, which is a rarely reported situation. NMR studies confirmed that the Methyl dyes of complementary strands were axially stacked and antiparallel to each other.[97] CD spectroscopy revealed that in the case of the D-threoninol linker the dyes were arranged in a right-handed helix as in the B-form of DNA whereas in the case of the L stereoisomer a less pronounced helix form was obtained. In addition, the duplex structure was found to be stabilised in the case of homo-clustering if no acyclic linker was facing the dyes (thus leading to pseudo base pairs, Figure 15bIV). This generated an unwound cluster of stacked chromophores resembling a ladder-like structure and with stronger exciton coupling interactions.[98] These differences in dye clustering nicely illustrate how a DNA-inspired

scaffold can be used to fine tune chromophore-chromophore interactions. In different work, the reversible photo-switching mode between the cis and trans form of a diazo dye was used to construct a photoresponsive molecular tweezer.[125]

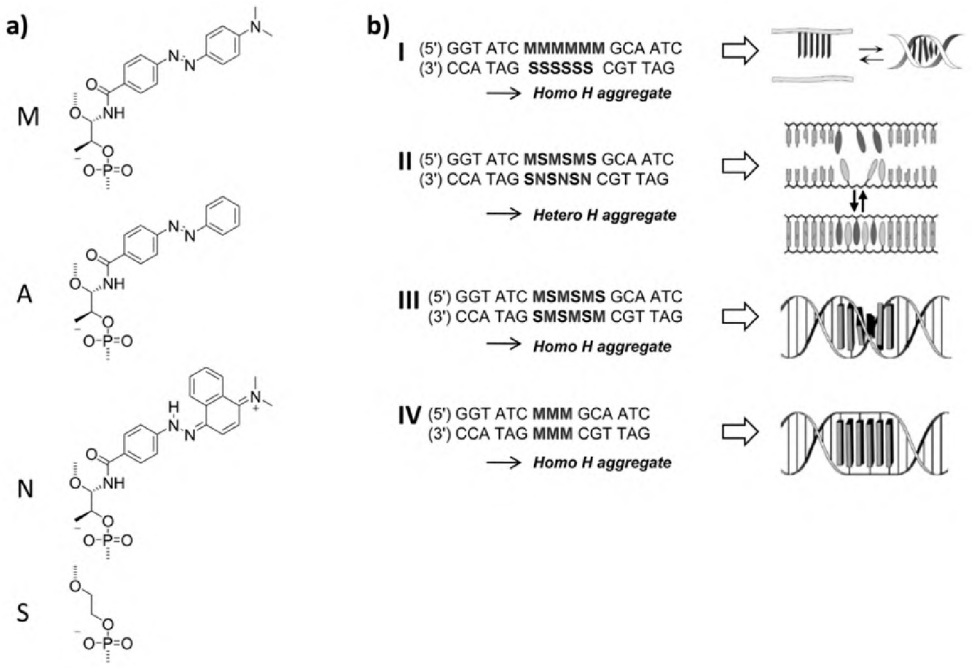

Figure 15. a) Structures of the diazo dyes based on an acyclic D-threoninol linker used by Asanuma; b) examples of duplexes modified with dyes and representation of their stacking modes.

Wagenknecht and co-workers used (*S*)-aminopropan-2,3-diol as an acyclic linker in the phosphodiester backbone to introduce perylene diimide units (PDI) into a DNA duplex (*P*, Figure 16a).[100] The (*S*) configuration of the linker was chosen in order to mimic the stereochemical situation at the 3'-position of the natural 2'-deoxyribofuranoside and the linker was tethered to one of the imide functions of the PDI. When placed on both complementary strands, an interstrand PDI dimer was found to stabilise the duplex by 2.4°C, which is rather unusual for such a modification with a flexible acyclic linker. The interstrand stacking of the PDIs, which can be seen as an artificial DNA base substitution, give rise to a typical excimer fluorescence signal and could be used as a readout for the pairing interaction. Interestingly, when two PDI chromophores were introduced on the same strand around a questionable site where a base mismatch or deletion could be present (Figure 16a), no excimer fluorescence was observed in the case of a correct base pairing. In contrast, almost exclusively excimer fluorescence was detected in the case of a wrong base pairing. This allowed the determination of the amount of matched counter strands in a mixture of counter strands that differ only in a single base, which is of obvious interest for diagnostic applications.

These studies were extended to systems with up to six chromophores.[101] Interstrand alternating sequences of PDI and thymine or abasic sites were designed to obtain a zipper like arrangement of the PDIs with characteristic excimer fluorescence (Figure 16b). The compounds displayed exciton coupled CD signals indicative of a helical arrangement of the stacked PDI units in the duplex. The helix sense was found to be directed by the DNA scaffold if no sterically demanding thymine groups were present (Figure 16b, X = S). In contrast, in the presence of thymine (Figure 16b, X = T) the PDI aggregates were forced to adopt a different stacking mode, with the angles between the chromophores being alternating 35–45° (left) and 85–95° (right) (see the model in Figure 16b). This work again highlights the flexibility of the "DNA approach" in respect to tune chromophoric interactions.

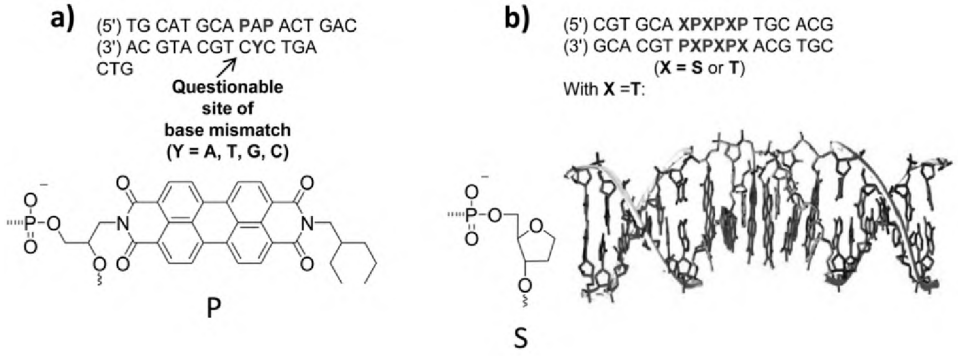

Figure 16. The use of a PDI in combination with an acyclic linker for the detection of a single base mismatch (a) or to obtain a zipper-like recognition motif (b).

A different approach was followed by the group of Haner, who prepared compounds in which the chromophore itself, i.e. phenanthrenyl group, was the linker between two phosphodiester functions (Figure 17a). The introduction of up to 14 of these residues, in the middle and on both strands of a duplex ODN, could be done successfully.[102] Apart from the stabilising effect of the flanking nucleobases, stabilisation also came from interstrand stacking interactions of the phenanthrenyl residues from opposite strands leading to only a slight decrease in stability of 1.2 °C per artificial base pair modification. Modelling of a hybrid with seven phenanthroline base pairs revealed a significant lengthening of the DNA duplex in comparison to the unmodified duplex, with the same overall number of residues. According to CD measurements the B-DNA structure was not destroyed (Figure 17a). It is noteworthy that the interstrand clustering of the non-nucleoside building blocks creates a foldamer structure that is stable in aqueous media.

Following the same strategy, multiple pyrene residues were embedded inside a DNA duplex in an interstrand stacking arrangement (Figure 17b).[103] A large stabilisation of the hybrid was observed if more than six artificial nucleosides were introduced (ΔTm = +23 °C in the case of seven modified base pairs). In addition to the interstrand stabilisation, intrastrand folding of

the single chain was found to facilitate the duplex formation, likely by reducing the entropy change. Interestingly, CD spectroscopy measurements revealed that the pyrenes within the stack were arranged in a right-handed helical conformation, which was further confirmed by molecular modelling. The twisting of the stacked pyrenes was caused by the flanking nucleobases and driven by hydrophobic interactions and probably relayed by inter-strand H-bonding of the amide units. The helical organisation was found to have a profound influence on the fluorescence properties of the duplex. In the case of 14 stacked pyrenes, excimer-type fluorescence was observed in both duplex and single strand, and an unexpected blue shift of the excimer fluorescence was found to occur when the temperature was decreased. This behaviour is likely the result of the switching from a sandwich type arrangement of the stacked pyrenes to a twisting arrangement of these dye molecules. These studies were extended to hetero-hybrid systems. For instance, mixing pyrene and PDI type of residues led to an alternating zipper like arrangement (SESE, see Figure 17b) within the duplex allowing for a quenching of the fluorescence of the PDI units by the adjacent pyrenes.[104] When the pyrene residues were mixed with TTF units (Figure 17b), a quenching of the pyrene fluorescence was observed. The later process is likely to proceed through a photo-induced electron transfer from the TTF to the pyrene residues in the stacked assembly.[105] Recently, also triazolylpyrenes[107] and alkynyl pyrenes,[106] have been including in these studies providing new scopes in the design of artificial double-stranded helices for applications in nanotechnology.

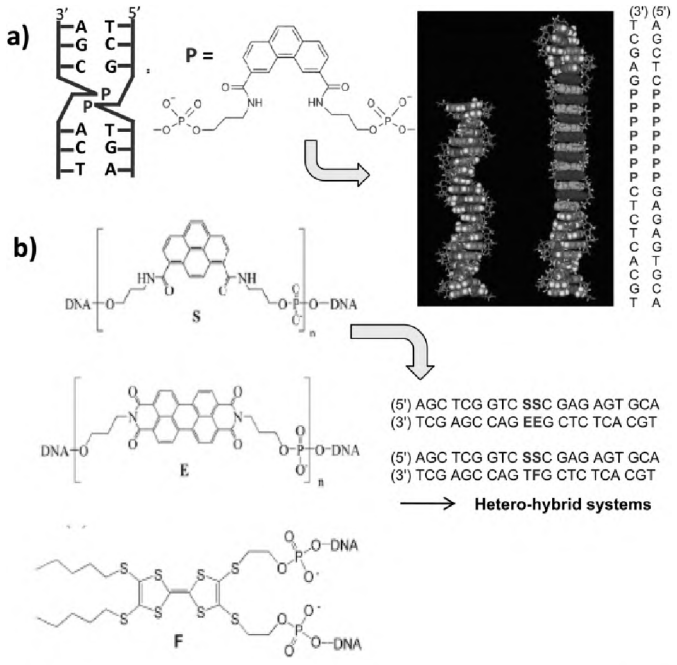

Figure 17. a) Phenanthrenyl linker used by Haner and schematic representation of the interstrand interaction between two of these linker molecules (left). Modelling of a 21-mer DNA duplex incorporating seven modified phenanthrene base pairs compared to the non-modified analogue (right). b) Structures of Haner's pyrene, PDI and TTF linkers for the construction of heterohybrid DNA systems.

Second approach: outside stacking

The organisation of chromophores using DNA based skeletons while keeping the Watson–Crick interactions intact has been studied by the groups of Wagenknecht (DNA),[108-110] Stulz (DNA),[111-113] Yamana (RNA)[114] and Wengel (LNA).[115] Wagenknecht and co-workers applied the DNA base modification strategy to obtain helical stacks that consisted of up to five adjacent pyrenes. The chromophores were linked covalently to the uridine units by a C–C bond allowing for a strong electronic coupling (Figure 18).[108] Melting temperature studies indicated that the incorporation of one pyrene unit destabilised the duplex but no additional destabilisation was observed in the case of five adjacent pyrenes. This showed that a certain amount of destabilisation was regained by the hydrophobic interaction between the chromophores. CD spectroscopy studies revealed an excitonic coupled CD signal in the wavelength range of the chromophore absorption band, which pointed to a right-handed helical arrangement of the pyrenes. The hybridisation of the modified DNA strand with its unmodified counter strand led to a strong enhancement in the fluorescence intensity, which was higher than the sum of the individual chromophores. In addition, a bathochromic shift of the emission maxima, which accounts for excitonic interactions in a regular and highly organised structure, was observed. The helical arrangement of the chromophores could tolerate the presence of one mismatch but was disrupted if two or more mismatches were present. A similar highly organised helical π-stacked arrangement of dyes along the major groove of duplex DNA was also obtained in the case of 1-ethynylpyrene, but only if more than three chromophores were synthetically incorporated adjacent to each other (deduced from CD measurements) (Figure 18).[109] When five chromophores were present the fluorescence intensity turned out to be very sensitive to the incorporation of a single mismatch. By using two different chromophores (i.e. 5-(pyren-1-yl) and 5-(10-methyl-phenothiazin-3-yl), PyU and PzU, respectively),[110] it was possible to modulate the absorption and fluorescence properties of the assemblies, i.e. by varying the sequence of the chromophores within the π-arrays. These sequence specific assemblies of chromophores are potentially useful for the construction of optical nanodevices and as nucleic acid sensors for molecular diagnostics.

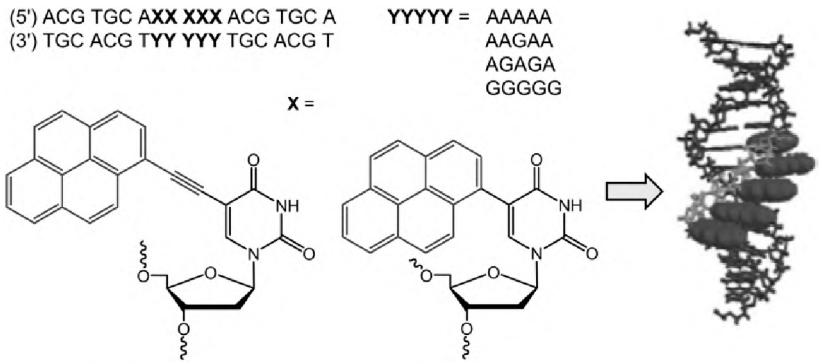

Figure 18. Pyrene and 1-ethynylpyrene modified uridines used by Wagenknecht et al.

In their quest for porphyrin arrays, Stulz and co-workers introduced up to eleven porphyrins in a DNA chain through acetylene linkers attached to the 5 position of the 2'-deoxyuridines. Two architectures were investigated, one in which all the porphyrins were tethered to the same single strand and one in which the porphyrins were placed on the two complementary strands in an alternating fashion, which led to very different features (Figure 19). In the first case,[111] the porphyrins were aligned along the major groove of the duplex and displayed electronic interaction in the ground and excited states as a result of their helical stacking (see modelling in Figure 19a). This was evidenced from a broadening of the porphyrin absorbance (Soret-band) and by the fact that the emission of the porphyrin arrays was quenched compared to the situation where the porphyrins were introduced non-adjacently. A strong destabilisation of the duplex by ΔTm ~5–7 °C per porphyrin modification was, however, observed as can be expected for such sterically demanding substituents. The situation was slightly improved when less bulky diphenylporphyrins were incorporated but destabilisation still occurred.[112]

Interestingly, the single strand itself adopted a helical elongated secondary structure, which was stable up to 55 °C in the case of eleven porphyrins. In this structure the porphyrins were also stacked as deduced from absorption and emission spectroscopy and from modelling studies (Figure 19a). Compared to its duplex form, the porphyrin absorbance was lower and the emission was more quenched, which pointed to a more efficient stacking of the porphyrins in a more hydrophilic environment. This behaviour is in contrast to the pyrene-DNA/RNA arrays, where such a helical secondary structure stabilised by the stacking of the chromophores was never observed with a single strand. This has an obvious interest for the construction of photonic nano-wires.

In a second study,[113] Stulz and co-workers used another strategy and introduced the porphyrins onto the two complementary strands of a duplex, in such a way that a shift of one base in their positioning was present (Figure 19b). This alternating arrangement led to a zipper-like assembly in which up to 11 porphyrins were aligned along the major groove and

stacked by pairs involving one porphyrin of each strand in a zigzag fashion. In this case, no destabilisation of the duplex was found to occur if more than four porphyrins were introduced, which is likely due to the inter-strand interaction of the chromophores. Broadening of the porphyrin Soret-band and a decrease of the fluorescence intensity when lowering the temperature indicated that the porphyrins interacted electronically when stacked in the zipper array. Interestingly, this approach allowed the authors to insert a metal (Zn) in one of the two strands, which led to an alternate stacking of metal free and metal incorporated porphyrins in the duplex without loss of thermal stability (Figure 19b). Energy transfer was effective in this system since, upon annealing of the free and metalated strands, fluorescence of the Zn-porphyrin was partially quenched whereas enhanced fluorescence of the free porphyrin was observed. These results highlight the potential of DNA as a scaffold to arrange metal ions on a nanometre scale, which obviously opens perspectives in the construction of nano-electronic and photonic wires.

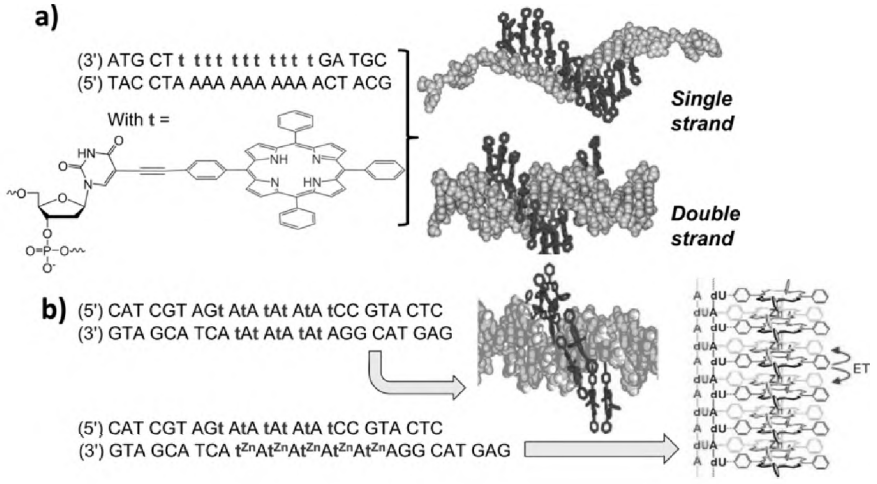

Figure 19. a) Structure of a porphyrin modified thymine nucleotide used for the construction of DNA helical arrays; b) alternate stacking of metal-free and Zn-porphyrins in a DNA strand displaying energy transfer.

Alternative strategies for the construction of DNA-based photonic wires: sequential chromophore arrays

In an alternative strategy, DNA molecules have been used as scaffolds to organise chromophores in the weakly coupled regime, the objective being the design of photonic wires. Donor and acceptor molecules are used to inject and release energy, and the transport of excited state energy is realised either by using a cascade of differently absorbing and emitting chromophores or by using similar chromophores as mediator units, which transport energy by hopping. Whereas the first strategy allows for unidirectional energy transport, it suffers from energy loss at each step of the process thereby limiting the length

of the photonic wire. On the other hand, the latter strategy does not allow unidirectional energy transfer, which leads to a decrease of the overall end-to-end efficiency.

In early work, Shchepinov and co-workers designed a flexible system for multiple fluorescence resonance energy transfer (FRET) processes (see Figure 20a).[116] The different chromophores (pyrene, perylene, fluorescein and tetramethyl-rhodamine) display overlapping absorption and emission spectra and sequential energy transfer across all four chromophores with high overall efficiency was observed. Interestingly, energy transfer was not detected when the propanediol linkers between each pair of fluorophores were absent, which suggested that a certain degree of freedom of the fluorophores was needed for the energy transfer to occur.

Improvement of this system can be realised by making use of a more rigid scaffold such as DNA. Sauer and co-workers investigated an energetic downhill cascade arrangement of five different chromophores that form an overlapping pathway for a unidirectional energy transfer (Figure 20b).[117] For this purpose, the chromophores were attached to short oligonucleotides that were sequentially hybridised to a single strand DNA backbone. The chromophores are thus separated by a distance of 10 base pairs (*c.a.* 3.4 nm), which does not allow the control of their relative orientation but prevents dimer formation, which is essential to avoid energy sinks (Figure 20b). Ensemble fluorescence measurements revealed an end-to-end energy transfer efficiency of ~0.15, which is much lower than the expected one based on theoretical considerations. To investigate the origin for the FRET efficiencies obtained in bulk measurements, single molecule fluorescence spectroscopy (SMFS) was used to probe, at the single molecular level, the sources of heterogeneity in the multistep energy transfer processes.[118] For this, the template DNA strand was grafted onto a glass surface. A subpopulation of ~10% of the immobilized photonic wires showed a predominantely red emission, which corresponded to a unidirectional, highly efficient (up to 90%), multistep energy transfer over a distance of 13.6 nm and a spectral range of ~200 nm. It was found that conformational freedom of the wire and partial DNA hybridisation led to multiple pathways for the photon emission. The use of DNA ligases to enhance the rigidity of the multi-chromophoric assemblies or the development of new labelling strategies to fix the conformation of the fluorophores might improve the efficiency of the energy transfer in these systems beyond five molecules.

Ohya and co-workers used the same strategy and introduced four chromophores with overlapping absorption and emission spectra, i.e. an eosine (Eo) molecule, one or two tetramethylrhodamine molecules and a Texas Red (TR) molecules as donor, mediator(s) and acceptor, respectively (Figure 20c).[119] Multistep FRET from Eo to TR through the mediator(s) was observed over a distance of ~10 nm with about 20% efficiency. Quake and co-workers

followed a related strategy to construct nanometre-scale optical waveguides based on a repeating fluorophore for energy transport (Figure 20d).[120]

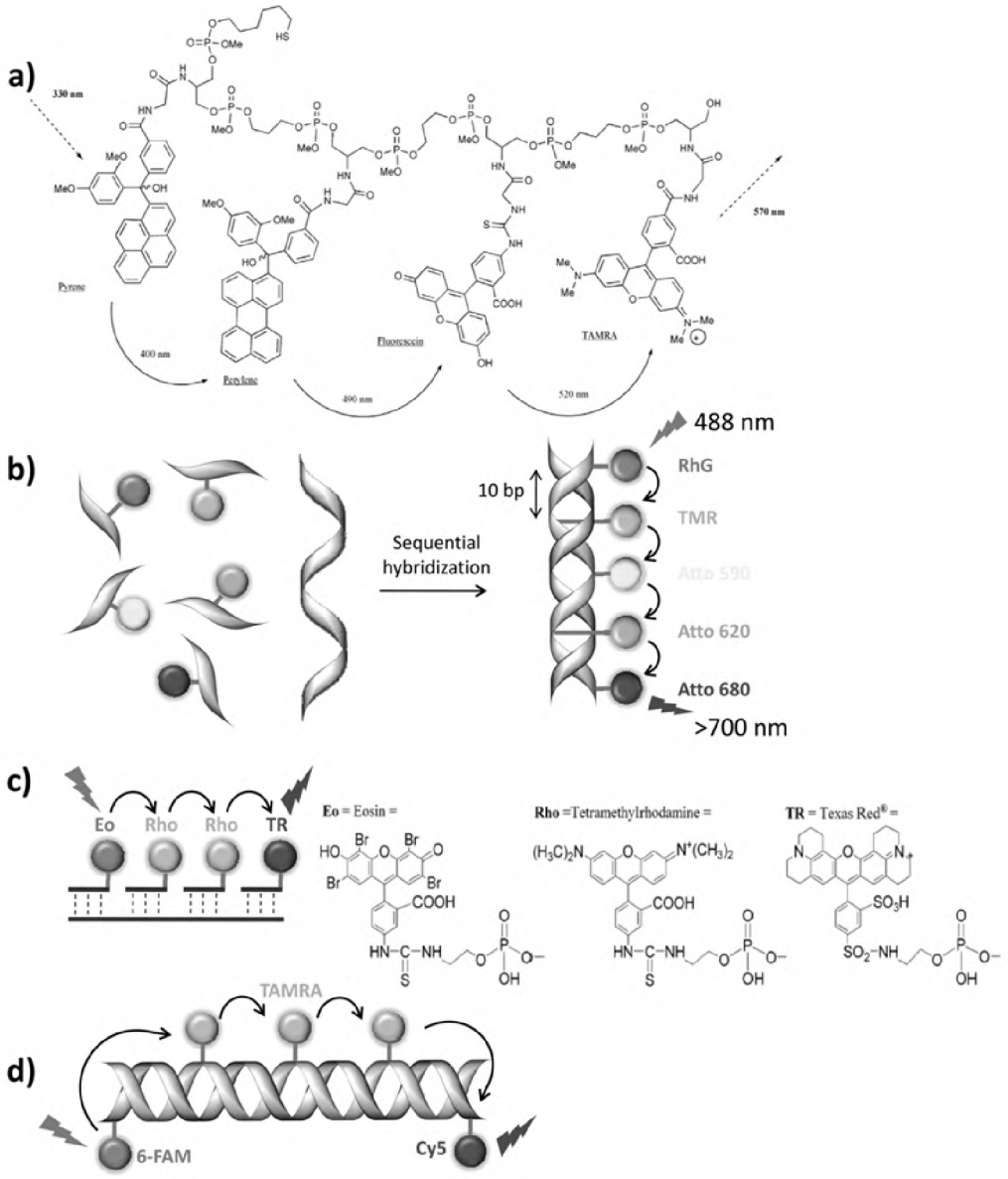

Figure 20. a) Sequential energy transfer across four chromophores tethered to a single-stranded acyclic backbone; b) unidirectional multistep FRET with five chromophores arranged in an energetic down-hill cascade; c) multistep FRET in sequential chromophore arrays assemblies; d) Quad-FRET assembly with 6-FAM, TAMRA and Cy5 as donor, repeating fluorophore and acceptor molecules, respectively.

Input (6-carboxyfluorescein, 6-FAM) and output (Cy5) molecules were tethered to the 3' and 5' end of a single DNA strand that was hybridised with the complementary strand bearing three mediator molecules (6-tetramethylrhodamine-5(6)-carboxamide, TAMRA). The five chromophores are thereby separated from one other by 10 base pairs; quad-FRET efficiency of about 20% over the five chromophores was obtained.

The use of DNA as scaffold for the construction of chromophoric assemblies is still an emerging field, but one can already glimpse prospective applications, such as new fluorescent labelling agents, photonic nanowires, artificial base pairing, new recognition codes and charge transfer systems. It is clear that the programmability of DNA and its self-assembled architectures are ideal for the construction of precisely defined chromophoric nano-objects with a high degree of modularity. Many exciting developments will without a doubt emerge from this approach.

1.5 Viruses

Viruses and virus-like particles (VLPs) have recently been receiving increased attention because of their tremendous potential in the field of materials science.[121] These programmable and easily modifiable biological building blocks can serve as ideal scaffolds for nanomaterial based devices. In recent years VLPs have also been used as a scaffold to arrange chromophoric molecules in a well-defined spatial relationship. This approach is still in its early stages, but without a doubt very promising for the construction of unique biohybrid materials. A considerable advantage of the use of viruses is that their architectures are very precise and monodisperse as can be concluded from crystal structure studies. In addition, due to the advances in the biosciences, viruses can be readily modified leading to site specific positioning of the chromophores and hence exact control over the architecture of the final system up to sub nanometre resolution. In 2005, Francis and co-workers were the first to demonstrate that chromophoric molecules can be selectively attached to a virus.[122] By using standard peptide coupling conditions, a rhodamine derivative could be coupled to both the outer and inner surface of the tobacco mosaic virus (TMV).

Very high levels of modification, ~2100 external and ~650 internal sites per 300 nm rod, could be achieved without perturbing the stability of the assembled capsids. This elegant proof of principle paved the way for the construction of linear arrays of chromophores arranged in a well-defined fashion using the precise architecture of the TMV as a scaffold. In addition, the assembly properties of the TMV can be controlled and finely tuned by genetic modification of the TMV coat protein (TMVCP) monomers. By using recombinant TMVCP monomers bearing reactive cysteine groups on the loop of the monomer, a series of chromophores, for example, pyrenes,[123] porphyrins (see for example Figure 21a)[124] and derivatized rhodamines,[125] could be introduced using 'maleimide chemistry'.

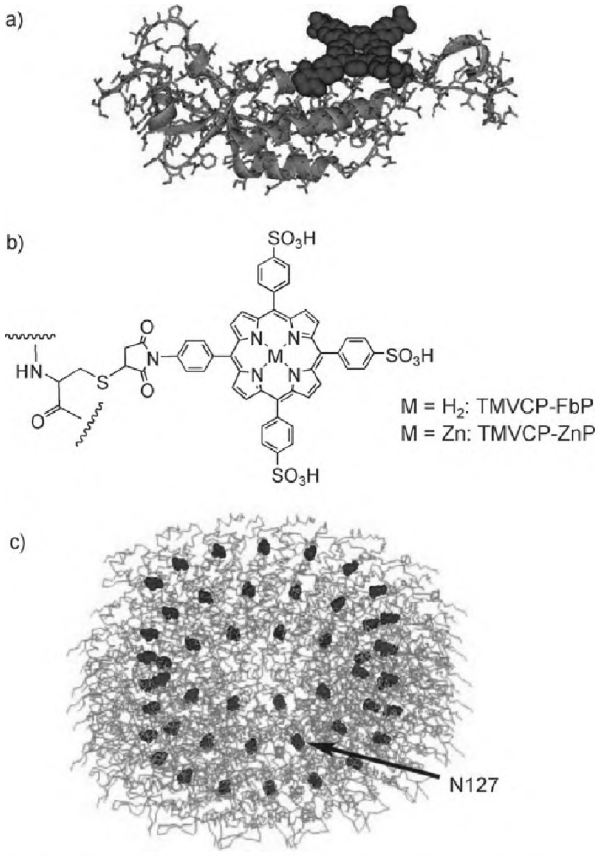

Figure 21. a) Structure of the TMVCP–porphyrin conjugated monomer; the porphyrin moiety was introduced at the amino acid position 127. b) Chemical structure of the porphyrin used in the study of Majima and co-workers. Porphyrin derivatives were introduced to the cysteine residue of a TMV monomer through maleimido–thiol coupling. c) Crystal structure of the TMV assembly with the amino acid N127 molecules shown in dark grey.

Depending on the pH of the system, zinc or free base porphyrin functionalised TMVCP building blocks could be assembled into double-layer disk-type assemblies or rod-type structures as analysed by AFM. To gain insight into the electronic properties of their system, different mixtures of the zinc (Zn) porphyrin TMVCP conjugates and free base (FB) porphyrin TMVCP conjugates were used to form a random mixture of chromophores in the TMV assembly (Figure 21). The energy transfer rates (from Zn to FB) amounted to $3.1–6.4 \times 10^9$ s^{-1}, as determined by time-resolved fluorescence spectroscopy.[124]

Based on the same cysteine strategy, donors **24** and **25** and acceptor **26** were incorporated randomly into the TMV assembly (Figure 22). The assemblies contained around ~700 chromophores per 100 nm rod with a spacing between the chromophores that is within the Förster radius for energy transfer between the dyes. The ability of the virus to precisely order the chromophores was illustrated by fluorescence measurements, which indicated that at least 20 donor chromophores can funnel energy into a single acceptor.[125] A more detailed understanding of the energy transfer processes in this system was obtained by

time-resolved fluorescence spectroscopy (for a TMV conjugates with a **24**:**26** ratio of 100:1.), which revealed that the energy transfer from **24** to **26** occurred in 187 ps with an efficiency of 36%. The three pathways for the dissipation of electronic energy from the excited state of the donor chromophore included donor emission, donor-to-donor transfer and donor-to-acceptor transfer.[126] The energy transfer values might be lower than those found in nature, yet as a first example they are comparable to other synthetic analogues and the optimisation in the structural arrangement of the chromophores within the bioconjugates can be expected to lead to significant improvements in the future.

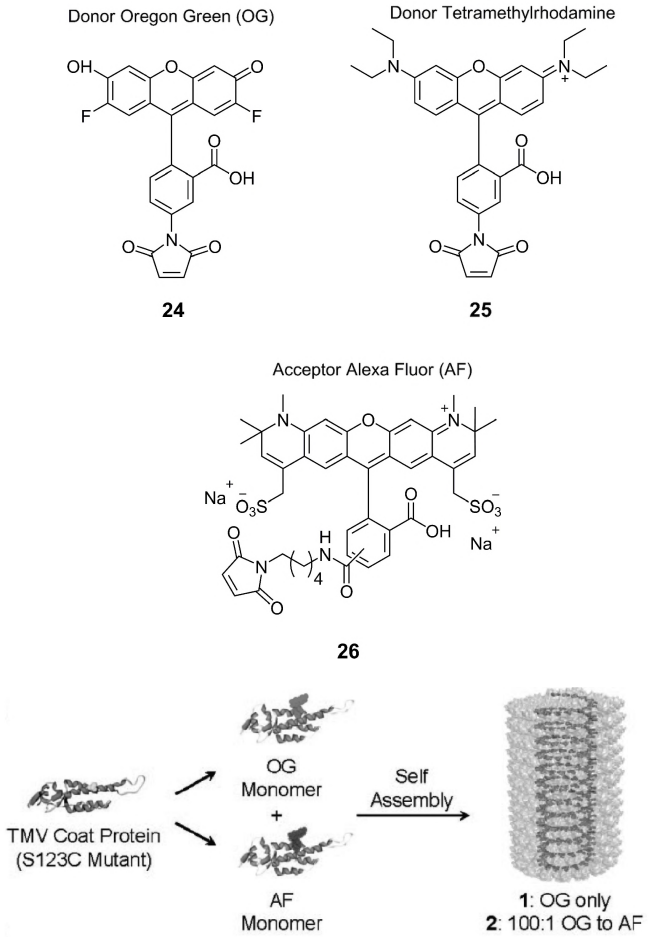

Figure 22. Chemical structures of the donor (**24** and **25**) and acceptor (**26**) molecules used for the construction of chromophoric TMV conjugates. TMVP monomers labelled with either OG (**24**) or AF (**26**) were combined in a 100:1 ratio to form the rod-shaped assemblies.

A non-covalent approach, in which cationic porphyrins were bound to the outer surface of a bacteriophage in a similar fashion to that reported for CNTs, was also recently reported.[127] Interestingly, a FRET from the external tryptophan residues of the phage to the interacting porphyrin molecules was clearly observed. A Förster radius of about 30 Å was calculated, which allows efficient transfer of excitation energy and is in agreement with a tryptophan residue being present in the N-terminal region of the phage. Bearing in mind that the ratio of

tryptophan to porphyrin residues is roughly only 250:1, a careful design of the porphyrin–phage bioconjugate could further increase the efficiency as an antenna system. In this respect site directed mutagenesis and recombinant cloning techniques are efficient tools to realise this.

1.6 Conclusion & Outlook

In this chapter four interesting macromolecular scaffolds to arrange chromophores into functional architectures have been described. They differ in structure, size, shape and physical properties and thus offer chemists and physicists a wide range of tools to play with. Inspired by the light harvesting systems in nature various helical polymer scaffolds have been developed over the last years. Due to the versatility of the available synthetic procedures the polymers can be readily adjusted to meet the required specifications. The ordering of chromophores in space with the help of polymer scaffolds offers unique possibilities to prepare materials with new electronic and mechanical properties. For example, in the case of polyisocyanides the helical nature of the polymer in combination with the fact that functional side-arms can be precisely positioned along the polymer backbone, results in unique molecules that can act as nanowires along which excitons can rapidly migrate. In the coming years, the incorporation of chromophores in a specific fashion, for example, to create a downhill energy path will be an interesting challenge.

The attachment of chromophores to CNTs has recently become a topic of increased research activity. Initially, the focus was more on the covalent attachment of the chromophores to the CNTs, but since this approach can lead to disruption of the π-system of the CNTs and hence in partial loss of electronic and structural properties, activities have been more directed towards non-covalent interactions. Elegant systems based on coulombic, van der Waals, and/or π-π interactions have emerged in recent years. Comprehensive photophysical studies of the chromophore–CNT hybrids have given more insights in the physical processes that take place offering interesting possibilities for materials with new and promising electronic properties. The synthetic work together with the detailed spectroscopic characterisations have paved the way for applying these hybrids in organic electronic devices in the coming years.

Natural systems are currently receiving great interest as scaffolds for chromophoric molecules. It is evident that DNA, with its programmable architecture, offers unique possibilities for this purpose, but this field is still in its early stages and many scouting studies are still needed. Like DNA, viruses also offer a programmable and easily modifiable building block for the creation of nanomaterials. Although in its early stages, significant progress has already been made by various groups and it can be expected that further optimisation of the

virus-chromophore constructs will lead to significant improvements and hence interesting applications in the near future.

1.7 References & Notes

(1) Lehn, J. M. *Science* **2002**, *295*, 2400-2403; Whitesides, G. M.; Mathias, J. P.; Seto, C. T. *Science* **1991**, *254*, 1312-1319.

(2) Kasha, M. *Spectrochim Acta* **1958**, *12*, 386-386; Mcrae, E. G.; Kasha, M. *J. Chem. Phys.* **1958**, *28*, 721-722.

(3) Mcdermott, G.; Prince, S. M.; Freer, A. A.; Hawthornthwaitelawless, A. M.; Papiz, M. Z.; Cogdell, R. J.; Isaacs, N. W. *Nature* **1995**, *374*, 517-521.

(4) v. Grondelle, R.; Dekker, J. P.; Gillbro, T.; Sundstrom, V. *Biochimica Et Biophysica Acta-Bioenergetics* **1994**, *1187*, 1-65.

(5) Bahatyrova, S.; Frese, R. N.; van der Werf, K. O.; Otto, C.; Hunter, C. N.; Olsen, J. D. *J Biol Chem* **2004**, *279*, 21327-21333; Fleming, G. R.; vanGrondelle, R. *Current Opinion in Structural Biology* **1997**, *7*, 738-748; Linnanto, J.; Korppi-Tommola, J. E. I. *Phys. Chem. Chem. Phys.* **2002**, *4*, 3453-3460; Pullerits, T.; Sundstrom, V. *Acc. Chem. Res.* **1996**, *29*, 381-389; Scheuring, S.; Seguin, J.; Marco, S.; Levy, D.; Robert, B.; Rigaud, J. L. *Proceedings of the National Academy of Sciences of the United States of America* **2003**, *100*, 1690-1693.

(6) Bosman, A. W.; Janssen, H. M.; Meijer, E. W. *Chem. Rev.* **1999**, *99*, 1665-1688; De Schryver, F. C.; Vosch, T.; Cotlet, M.; Van der Auweraer, M.; Mullen, K.; Hofkens, J. *Acc. Chem. Res.* **2005**, *38*, 514-522.

(7) Schenning, A. P. H. J.; Meijer, E. W. *Chem. Commun.* **2005**, 3245-3258.

(8) Hoeben, F. J. M.; Jonkheijm, P.; Meijer, E. W.; Schenning, A. *Chem. Rev.* **2005**, *105*, 1491-1546.

(9) Schultze, X.; Serin, J.; Adronov, A.; Frechet, J. M. J. *Chem. Commun.* **2001**, 1160-1161; Redl, F. X.; Lutz, M.; Daub, J. *Chem. Eur. J.* **2001**, *7*, 5350-5358.

(10) Cornelissen, J.; Rowan, A. E.; Nolte, R. J. M.; Sommerdijk, N. *Chem. Rev.* **2001**, *101*, 4039-4070.

(11) Nakano, T.; Okamoto, Y. *Chem. Rev.* **2001**, *101*, 4013-4038.

(12) Natta, G.; Pino, P.; Corradini, P.; Danusso, F.; Mantica, E.; Mazzanti, G.; Moraglio, G. *J. Am. Chem. Soc.* **1955**, *77*, 1708-1710.

(13) Lam, J. W. Y.; Tang, B. Z. *Acc. Chem. Res.* **2005**, *38*, 745-754.

(14) Yashima, E.; Maeda, K. In *Foldamers: Structure, Properties, and Applications*; Hecht, S., Huc, I., Eds.; Wiley-VCH: Weinheim, 2007, p 331-366.

(15) Yashima, E.; Maeda, K.; Furusho, Y. *Acc. Chem. Res.* **2008**, *41*, 1166-1180.

(16) Green, M. M.; Peterson, N. C.; Sato, T.; Teramoto, A.; Cook, R.; Lifson, S. *Science* **1995**, *268*, 1860-1866.

(17) Koeckelberghs, G.; Van Beylen, M.; Samyn, C. *Mat Sci Eng C-Bio S* **2001**, *18*, 15-20.

(18) Mayer, S.; Maxein, G.; Zentel, R. *Macromolecules* **1998**, *31*, 8522-8525; Mayer, S.; Zentel, R. *Macromol. Chem. Physic.* **1998**, *199*, 1675-1682.

(19) Green, M. M.; Garetz, B. A.; Munoz, B.; Chang, H. P.; Hoke, S.; Cooks, R. G. *J. Am. Chem. Soc.* **1995**, *117*, 4181-4182.

(20) Fujiki, M. *Macromol. Rapid. Comm.* **2001**, *22*, 539-563.

(21) Tang, H. D.; Liu, Y. Y.; Huang, B.; Qin, J. G.; Fuentes-Hernandez, C.; Kippelen, B.; Li, S. J.; Ye, C. *J. Mater. Chem.* **2005**, *15*, 778-784.

(22) Goodwin, A.; Novak, B. M. *Macromolecules* **1994**, *27*, 5520-2; Tang, H. Z.; Garland, E. R.; Novak, B. M.; He, J. T.; Polavarapu, P. L.; Sun, F. C.; Sheiko, S. S. *Macromolecules* **2007**, *40*, 3575-3580; Tang, H. Z.; Boyle, P. D.; Novak, B. M. *J. Am. Chem. Soc.* **2005**, *127*, 2136-2142; Tian, G. L.; Lu, Y. J.; Novak, B. M. *J. Am. Chem. Soc.* **2004**, *126*, 4082-4083.

(23) Tang, H. Z.; Novak, B. M.; He, J. T.; Polavarapu, P. L. *Angew. Chem., Int. Ed.* **2005**, *44*, 7298-7301.

(24) Tang, H. Z.; Lu, Y. J.; Tian, G. L.; Capracotta, M. D.; Novak, B. M. *J. Am. Chem. Soc.* **2004**, *126*, 3722-3723.

(25) Okamoto, Y.; Nakano, T. *Chem. Rev.* **1994**, *94*, 349-372.
(26) Nolte, R. J. M.; Van Beijnen, A. J. M.; Drenth, W. *J. Am. Chem. Soc.* **1974**, *96*, 5932-3.
(27) Nolte, R. J. M. *Chem. Soc. Rev.* **1994**, *23*, 11-19; Suginome, M.; Ito, Y. *Adv. Polym. Sci.* **2004**, *171*, 77-136.
(28) Hong, B.; Fox, M. A. *Macromolecules* **1994**, *27*, 5311-5317; Hong, B.; Fox, M. A. *Can. J. Chem.* **1995**, *73*, 2101-2110.
(29) Teerenstra, M. N.; Hagting, J. G.; Schouten, A. J.; Nolte, R. J. M.; Kauranen, M.; Verbiest, T.; Persoons, A. *Macromolecules* **1996**, *29*, 4876-4879.
(30) Kauranen, M.; Verbiest, T.; Meijer, E. W.; Havinga, E. E.; Teerenstra, M. N.; Schouten, A. J.; Nolte, R. J. M.; Persoons, A. *Adv. Mater.* **1995**, *7*, 641-4.
(31) Kauranen, M.; Verbiest, T.; Boutton, C.; Teerenstra, M. N.; Clays, K.; Schouten, A. J.; Nolte, R. J. M.; Persoons, A. *Science* **1995**, *270*, 966-969.
(32) Teerenstra, M. N.; Klap, R. D.; Bijl, M. J.; Schouten, A. J.; Nolte, R. J. M.; Verbiest, T.; Persoons, A. *Macromolecules* **1996**, *29*, 4871-4875.
(33) Gomar-Nadal, E.; Mugica, L.; Vidal-Gancedo, J.; Casado, J.; Navarrete, J. T. L.; Veciana, J.; Rovira, C.; Amabilino, D. B. *Macromolecules* **2007**, *40*, 7521-7531.
(34) Gomar-Nadal, E.; Veciana, J.; Rovira, C.; Amabilino, D. B. *Adv. Mater.* **2005**, *17*, 2095-2098.
(35) Hida, N.; Takei, F.; Onitsuka, K.; Shiga, K.; Asaoka, S.; Iyoda, T.; Takahashi, S. *Angew. Chem., Int. Ed.* **2003**, *42*, 4349-4352.
(36) Onitsuka, K.; Joh, T.; Takahashi, S. *Angew. Chem., Int. Ed.* **1992**, *104*, 851-852.
(37) Elemans, J. A. A. W.; Van Hameren, R.; Nolte, R. J. M.; Rowan, A. E. *Adv. Mater.* **2006**, *18*, 1251-1266.
(38) Chou, J. H.; Kosal, M. E.; Nalwa, H. S.; Rakow, N. A.; Suslick, K. S. *The Porphyrin Handbook, Vol. 6*; Academic Press: New York, 2000; Vol. 6.
(39) Takei, F.; Onitsuka, K.; Kobayashi, N.; Takahashi, S. *Chem. Lett.* **2000**, 914-915; Takei, F.; Nakamura, S.; Onitsuka, K.; Ishida, A.; Tojo, S.; Majima, T.; Takahashi, S. *Chem. Lett.* **2003**, *32*, 506-507; Takei, F.; Kodama, D.; Nakamura, S.; Onitsuka, K.; Takahashi, S. *J. Polym. Sci., Part A: Polym. Chem.* **2005**, *44*, 585-595.
(40) Takei, F.; Hayashi, H.; Onitsuka, K.; Kobayashi, N.; Takahashi, S. *Angew. Chem., Int. Ed.* **2001**, *40*, 4092-4094.
(41) Fujitsuka, M.; Okada, A.; Tojo, S.; Takei, F.; Onitsuka, K.; Takahashi, S.; Majima, T. *J. Phys. Chem. B* **2004**, *108*, 11935-11941.
(42) Razenberg, J. A. S. J.; Vandermade, A. W.; Smeets, J. W. H.; Nolte, R. J. M. *J. Mol. Catal.* **1985**, *31*, 271-287.
(43) de Witte, P. A. J.; Castriciano, M.; Cornelissen, J. J. L. M.; Scolaro, L. M.; Nolte, R. J. M.; Rowan, A. E. *Chem. Eur. J.* **2003**, *9*, 1775-1781.
(44) Matile, S.; Berova, N.; Nakanishi, K.; Novkova, S.; Philipova, I.; Blagoev, B. *J. Am. Chem. Soc.* **1995**, *117*, 7021-7022; Matile, S.; Berova, N.; Nakanishi, K.; Fleischhauer, J.; Woody, R. W. *J. Am. Chem. Soc.* **1996**, *118*, 5198-5206; Berova, N.; Nakanishi, K.; Woody, R. W. *Circular Dichroism:Principles and Applications*; 2nd ed.; Wiley-VCH: New-York, 2000.
(45) Cornelissen, J. J. L. M.; Donners, J. J. J. M.; de Gelder, R.; Graswinckel, W. S.; Metselaar, G. A.; Rowan, A. E.; Sommerdijk, N. A.; Nolte, R. J. M. *Science* **2001**, *293*, 676-80.
(46) Samori, P.; Ecker, C.; Goessl, I.; de Witte, P. A. J.; Cornelissen, J. J. L. M.; Metselaar, G. A.; Otten, M. B. J.; Rowan, A. E.; Nolte, R. J. M.; Rabe, J. P. *Macromolecules* **2002**, *35*, 5290-5294.
(47) de Witte, P. A. J.; Hernando, J.; Neuteboom, E. E.; van Dijk, E. M. H. P.; Meskers, S. C. J.; Janssen, R. A. J.; van Hulst, N. F.; Nolte, R. J. M.; Garcia-Parajo, M. F.; Rowan, A. E. *J. Phys. Chem. B* **2006**, *110*, 7803-7812.
(48) Hernando, J.; de Witte, P. A. J.; van Dijk, E. M. H. P.; Korterik, J.; Nolte, R. J. M.; Rowan, A. E.; Garcia-Parajo, M. F.; van Hulst, N. F. *Angew. Chem., Int. Ed.* **2004**, *43*, 4045-4049.

(49) Palermo, V.; Otten, M. B. J.; Liscio, A.; Schwartz, E.; de Witte, P. A. J.; Castriciano, M. A.; Wienk, M. M.; Nolde, F.; De Luca, G.; Cornelissen, J. J. L. M.; Janssen, R. A. J.; Mullen, K.; Rowan, A. E.; Nolte, R. J. M.; Samori, P. *J. Am. Chem. Soc.* **2008**, *130*, 14605-14614.

(50) Finlayson, C. E.; Friend, R. H.; Otten, M. B. J.; Schwartz, E.; Cornelissen, J.; Nolte, R. L. M.; Rowan, A. E.; Samori, P.; Palermo, V.; Liscio, A.; Peneva, K.; Mullen, K.; Trapani, S.; Beljonne, D. *Adv. Funct. Mater.* **2008**, *18*, 3947-3955.

(51) Foster, S.; Finlayson, C. E.; Keivanidis, P. E.; Huang, Y.-S.; Hwang, I.; Otten, M. B. J.; Lu, L. L.; Schwartz, E.; Nolte, R. J. M.; Rowan, A. E. *Macromolecules* **2009**.

(52) Schwartz, E.; Palermo, V.; Finlayson, C. E.; Huang, Y.-S.; Otten, M. B. J.; Liscio, A.; Trapani, S.; González-Valls, I.; Brocorens, P.; Cornelissen, J. J. L. M.; Peneva, K.; Müllen, K.; Spano, F.; Yartsev, A.; Westenhoff, S.; Friend, R. H.; Beljonne, D.; Nolte, R. J. M.; Samori, P.; Rowan, A. E. *Chem. Eur. J.* **2009**, *15*, 2536-2547.

(53) Kitto, H. J.; Schwartz, E.; Nijemeisland, M.; Koepf, M.; Cornelissen, J.; Rowan, A. E.; Nolte, R. J. M. *J. Mater. Chem.* **2008**, *18*, 5615-5624; Schwartz, E.; Kitto, H. J.; de Gelder, R.; Nolte, R. J. M.; Rowan, A. E.; Cornelissen, J. J. L. M. *J. Mater. Chem.* **2007**, *17*, 1876-1884.

(54) Martin, C. R.; Kohli, P. *Nature Reviews Drug Discovery* **2003**, *2*, 29-37; Bianco, A.; Kostarelos, K.; Prato, M. *Current Opinion in Chemical Biology* **2005**, *9*, 674-679; Prato, M.; Kostarelos, K.; Bianco, A. *Acc. Chem. Res.* **2008**, *41*, 60-68; Lacerda, L.; Bianco, A.; Prato, M.; Kostarelos, K. *Adv. Drug Deliver Rev.* **2006**, *58*, 1460-1470.

(55) Li, H. P.; Martin, R. B.; Harruff, B. A.; Carino, R. A.; Allard, L. F.; Sun, Y. P. *Adv. Mater.* **2004**, *16*, 896-900.

(56) Baskaran, D.; Mays, J. W.; Zhang, X. P.; Bratcher, M. S. *J. Am. Chem. Soc.* **2005**, *127*, 6916-6917.

(57) Ballesteros, B.; Campidelli, S.; de la Torre, G.; Ehli, C.; Guldi, D. M.; Prato, M.; Torres, T. *Chem. Commun.* **2007**, 2950-2952.

(58) Campidelli, S.; Ballesteros, B.; Filoramo, A.; Diaz, D. D.; de la Torre, G.; Torres, T.; Rahman, G. M. A.; Ehli, C.; Kiessling, D.; Werner, F.; Sgobba, V.; Guldi, D. M.; Cioffi, C.; Prato, M.; Bourgoin, J. P. *J. Am. Chem. Soc.* **2008**, *130*, 11503-11509.

(59) Herranz, M. A.; Martin, N.; Campidelli, S. P.; Prato, M.; Brehm, G.; Guldi, D. M. *Angew. Chem., Int. Ed.* **2006**, *45*, 4478-4482.

(60) Xu, Y.; Liu, Z.; Zhang, X.; Wang, Y.; Tian, J.; Huang, Y.; Ma, Y.; Zhang, X.; Chen, Y. *Adv. Mater.* **2009**, *21*, 1-5.

(61) Murakami, H.; Nomura, T.; Nakashima, N. *Chem. Phys. Lett.* **2003**, *378*, 481-485.

(62) Li, H. P.; Zhou, B.; Lin, Y.; Gu, L. R.; Wang, W.; Fernando, K. A. S.; Kumar, S.; Allard, L. F.; Sun, Y. P. *J. Am. Chem. Soc.* **2004**, *126*, 1014-1015.

(63) Cheng, F. Y.; Adronov, A. *Chem. Eur. J.* **2006**, *12*, 5053-5059.

(64) Satake, A.; Miyajima, Y.; Kobuke, Y. *Chem. Mater.* **2005**, *17*, 716-724; Guldi, D. M.; Taieb, H.; Rahman, G. M. A.; Tagmatarchis, N.; Prato, M. *Adv. Mater.* **2005**, *17*, 871-875.

(65) Hasobe, T.; Fukuzumi, S.; Kamat, P. V. *J. Am. Chem. Soc.* **2005**, *127*, 11884-11885.

(66) Guldi, D. M.; Rahman, G. M. A.; Prato, M.; Jux, N.; Qin, S. H.; Ford, W. *Angew. Chem., Int. Ed.* **2005**, *44*, 2015-2018.

(67) Rahman, G. M. A.; Troeger, A.; Sgobba, V.; Guldi, D. M.; Jux, N.; Tchoul, M. N.; Ford, W. T.; Mateo-Alonso, A.; Prato, M. *Chem. Eur. J.* **2008**, *14*, 8837-8846.

(68) Wang, X. B.; Liu, Y. Q.; Qiu, W. F.; Zhu, D. B. *J. Mater. Chem.* **2002**, *12*, 1636-1639.

(69) Rahman, G. M. A.; Guldi, D. M.; Campidelli, S.; Prato, M. *J. Mater. Chem.* **2006**, *16*, 62-65.

(70) Chen, J. Y.; Collier, C. P. *J. Phys. Chem. B* **2005**, *109*, 7605-7609.

(71) Guldi, D. M.; Rahman, G. M. A.; Jux, N.; Tagmatarchis, N.; Prato, M. *Angew. Chem., Int. Ed.* **2004**, *43*, 5526-5530.

(72) Ehli, C.; Rahman, G. M. A.; Jux, N.; Balbinot, D.; Guldi, D. M.; Paolucci, F.; Marcaccio, M.; Paolucci, D.; Melle-Franco, M.; Zerbetto, F.; Campidelli, S.; Prato, M. *J. Am. Chem. Soc.* **2006**, *128*, 11222-11231.

(73) Ehli, C.; Guldi, D. M.; Herranz, M. A.; Martin, N.; Campidelli, S.; Prato, M. *J. Mater. Chem.* **2008**, *18*, 1498-1503.

(74) Herranz, M. A.; Ehli, C.; Campidelli, S.; Gutierrez, M.; Hug, G. L.; Ohkubo, K.; Fukuzumi, S.; Prato, M.; Martin, N.; Guldi, D. M. *J. Am. Chem. Soc.* **2008**, *130*, 66-73.

(75) Inagaki, M.; Kaneko, K.; Nishizawa, T. *Carbon* **2004**, *42*, 1401-1417.

(76) Pagona, G.; Sandanayaka, A. S. D.; Maigne, A.; Fan, J.; Papavassiliou, G. C.; Petsalakis, L. D.; Steele, B. R.; Yudasaka, M.; Iijima, S.; Tagmatarchis, N.; Ito, O. *Chem. Eur. J.* **2007**, *13*, 7600-7607.

(77) Pagona, G.; Sandanayaka, A. S. D.; Araki, Y.; Fan, J.; Tagmatarchis, N.; Yudasaka, M.; Iijima, S.; Ito, O. *J. Phys. Chem. B* **2006**, *110*, 20729-20732.

(78) Pagona, G.; Sandanayaka, A. S. D.; Hasobe, T.; Charalambidis, G.; Coutsolelos, A. G.; Yudasaka, M.; Iijima, S.; Tagmatarchis, N. *Journal of Physical Chemistry C* **2008**, *112*, 15735-15741; Pagona, G.; Sandanayaka, A. S. D.; Araki, Y.; Fan, J.; Tagmatarchis, N.; Charalambidis, G.; Coutsolelos, A. G.; Boitrel, B.; Yudasaka, M.; Iijima, S.; Ito, O. *Adv. Funct. Mater.* **2007**, *17*, 1705-1711.

(79) Cioffi, C.; Campidelli, S.; Sooambar, C.; Marcaccio, M.; Marcolongo, G.; Meneghetti, M.; Paolucci, D.; Paolucci, F.; Ehli, C.; Rahman, G. M. A.; Sgobba, V.; Guldi, D. M.; Prato, M. *J. Am. Chem. Soc.* **2007**, *129*, 3938-3945.

(80) Zhang, M.; Murakami, T.; Ajima, K.; Tsuchida, K.; Sandanayaka, A. S. D.; Ito, O.; Iijima, S.; Yudasaka, M. *Proceedings of the National Academy of Sciences of the United States of America* **2008**, *105*, 14773-14778.

(81) Guldi, D. M.; Rahman, G. M. A.; Zerbetto, F.; Prato, M. *Acc. Chem. Res.* **2005**, *38*, 871-878.

(82) Seeman, N. C. *Nature* **2003**, *421*, 427-431.

(83) Hans-Achim Wagenknecht *Angewandte Chemie International Edition* **2009**, *48*, 2838-2841.

(84) Varghese, R.; Wagenknecht, H.-A. *Chem. Commun.* **2009**, 2615-2624.

(85) Gao, J.; Strassler, C.; Tahmassebi, D.; Kool, E. T. *J. Am. Chem. Soc.* **2002**, *124*, 11590-11591.

(86) Wilson, J. N.; Gao, J. M.; Kool, E. T. *Tetrahedron* **2007**, *63*, 3427-3433; James N. Wilson, Y. C., Samuel Tan, Andrea Cuppoletti, Eric T. Kool *Chembiochem* **2008**, *9*, 279-285.

(87) Cuppoletti, A.; Cho, Y.; Park, J.-S.; Strassler, C.; Kool, E. T. *Bioconjugate Chem* **2005**, *16*, 528-534.

(88) Gao, J.; Watanabe, S.; Kool, E. T. *J. Am. Chem. Soc.* **2004**, *126*, 12748-12749.

(89) Teo, Y. N.; Wilson, J. N.; Kool, E. T. *J. Am. Chem. Soc.* **2009**, *131*, 3923-3933.

(90) Junya Chiba, S. T., Kikyo Mishima, Hajime Maeda, Yasuaki Nanai, Kazuhiko Mizuno, Masahiko Inouye, *Chem. Eur. J.* **2007**, *13*, 8124-8130.

(91) Brotschi, C.; Häberli, A.; Leumann, C. J. *Angew. Chem., Int. Ed.* **2001**, *40*, 3012-3014.

(92) Brotschi, C.; Leumann, C. J. *Angew. Chem., Int. Ed.* **2003**, *42*, 1655-1658.

(93) Grigorenko, N. A.; Leumann, C. J. *Chem. Commun.* **2008**, 5417-5419.

(94) Grigorenko, N. A.; Leumann, C. J. *Chem. Eur. J.* **2009**, *15*, 639-645.

(95) Asanuma, H.; Shirasuka, K.; Takarada, T.; Kashida, H.; Komiyama, M. *J. Am. Chem. Soc.* **2003**, *125*, 2217-2223.

(96) Kashida, H.; Asanuma, H.; Komiyama, M. *Angew. Chem., Int. Ed.* **2004**, *43*, 6522-6525.

(97) Kashida, H.; Tanaka, M.; Baba, S.; Sakamoto, T.; Kawai, G.; Asanuma, H.; Komiyama, M. *Chem. Eur. J.* **2006**, *12*, 777-784.

(98) Kashida, H.; Fujii, T.; Asanuma, H. *Organic & Biomolecular Chemistry* **2008**, *6*, 2892-2899.

(99) Asanuma, H.; Liang, X.; Nishioka, H.; Matsunaga, D.; Liu, M.; Komiyama, M. *Nat. Protocols* **2007**, *2*, 203-212; Liang, X. G.; Nishioka, H.; Takenaka, N.; Asanuma, H. *Chembiochem* **2008**, *9*, 702-705.

(100) Wagner, C.; Wagenknecht, H.-A. *Organic Letters* **2006**, *8*, 4191-4194; Baumstark, D.; Wagenknecht, H.-A. *Angew. Chem., Int. Ed.* **2008**, *47*, 2612-2614.

(101) Baumstark, D.; Wagenknecht, H. A. *Chem. Eur. J.* **2008**, *14*, 6640-6645.

(102) Langenegger, S. M.; Haner, R. *Chembiochem* **2005**, *6*, 2149-2152.

(103) Malinovskii, V. L.; Samain, F.; Haner, R. *Angew. Chem., Int. Ed.* **2007**, *46*, 4464-4467; Lindegaard, D.; Madsen, A. S.; Astakhova, I. V.; Malakhov, A. D.; Babu, B. R.; Korshun, V. A.; Wengel, J. *Bioorgan Med Chem* **2008**, *16*, 94-99.

(104) Bouquin, N.; Malinovskii, V. L.; Haner, R. *Chem. Commun.* **2008**, 1974-1976.

(105) Bouquin, N.; Malinovskii, V. L.; Guegano, X.; Liu, S. X.; Decurtins, S.; Haner, R. *Chem. Eur. J.* **2008**, *14*, 5732-5736.
(106) Bittermann, H.; Siegemund, D.; Malinovskii, V. L.; Haner, R. *J. Am. Chem. Soc.* **2008**, *130*, 15285-15287.
(107) Werder, S.; Malinovskii, V. L.; Haner, R. *Organic Letters* **2008**, *10*, 2011-2014.
(108) Mayer-Enthart, E.; Wagenknecht, H. A. *Angew. Chem., Int. Ed.* **2006**, *45*, 3372-3375.
(109) Barbaric, J.; Wagenknecht, H. A. *Organic & Biomolecular Chemistry* **2006**, *4*, 2088-2090.
(110) Mayer-Enthart, E.; Wagner, C.; Barbaric, J.; Wagenknecht, H. A. *Tetrahedron* **2007**, *63*, 3434-3439.
(111) Fendt, L. A.; Bouamaied, I.; Thoni, S.; Amiot, N.; Stulz, E. *J. Am. Chem. Soc.* **2007**, *129*, 15319-15329.
(112) Bouamaied, I.; Nguyen, T.; Ruhl, T.; Stulz, E. *Organic & Biomolecular Chemistry* **2008**, *6*, 3888-3891.
(113) Nguyen, T.; Brewer, A.; Stulz, E. *Angew. Chem., Int. Ed.* **2009**, *48*, 1974-1977.
(114) Nakamura, M.; Ohtoshi, Y.; Yamana, K. *Chem. Commun.* **2005**, 5163-5165; Nakamura, M.; Shimomura, Y.; Ohtoshi, Y.; Sasa, K.; Hayashi, H.; Nakano, H.; Yamana, K. *Organic & Biomolecular Chemistry* **2007**, *5*, 1945-1951; Nakamura, M.; Murakami, Y.; Sasa, K.; Hayashi, H.; Yamana, K. *J. Am. Chem. Soc.* **2008**, *130*, 6904-6905.
(115) Sorensen, M. D.; Petersen, M.; Wengel, J. *Chem. Commun.* **2003**, 2130-2131; Hrdlicka, P. J.; Babu, B. R.; Sorensen, M. D.; Wengel, J. *Chem. Commun.* **2004**, 1478-1479; Hrdlicka, P. J.; Babu, B. R.; Sorensen, M. D.; Harrit, N.; Wengel, J. *J. Am. Chem. Soc.* **2005**, *127*, 13293-13299; Kumar, T. S.; Madsen, A. S.; Ostergaard, M. E.; Wengel, J.; Hrdlicka, P. J. *J. Org. Chem.* **2008**, *73*, 7060-7066; Astakhova, I. V.; Korshun, V. A.; Jahn, K.; Kjems, J.; Wengel, J. *Bioconjugate Chem* **2008**, *19*, 1995-2007; Astakhova, I. V.; Korshun, V. A.; Wengel, J. *Chemistry - A European Journal* **2008**, *14*, 11010-11026.
(116) Shchepinov, M. S.; Korshun, V. A. *Nucleosides, Nucleotides and Nucleic Acids* **2001**, *20*, 369 - 374.
(117) Heilemann, M.; Tinnefeld, P.; Mosteiro, G. S.; Parajo, M. G.; Van Hulst, N. F.; Sauer, M. *J. Am. Chem. Soc.* **2004**, *126*, 6514-6515; Tinnefeld, P.; Heilemann, M.; Sauer, M. *Chemphyschem* **2005**, *6*, 217-222.
(118) Heilemann, M.; Kasper, R.; Tinnefeld, P.; Sauer, M. *J. Am. Chem. Soc.* **2006**, *128*, 16864-16875; Sanchez-Mosteiro, G.; van Dijk, E. M. H. P.; Hernando, J.; Heilemann, M.; Tinnefeld, P.; Sauer, M.; Koberlin, F.; Patting, M.; Wahl, M.; Erdmann, R.; van Hulst, N. F.; Garcia-Parajo, M. F. *The Journal of Physical Chemistry B* **2006**, *110*, 26349-26353.
(119) Ohya, Y.; Yabuki, K.; Hashimoto, M.; Nakajima, A.; Ouchi, T. *Bioconjugate Chem* **2003**, *14*, 1057-1066.
(120) Vyawahare, S.; Eyal, S.; Mathews, K. D.; Quake, S. R. *Nano Letters* **2004**, *4*, 1035-1039.
(121) Manchester, M.; Steinmetz, N. F. *Current Topics in Microbiology and Immunology, Vol. 327: Viruses and Nanotechnology*; Springer: Heidelberg, 2009; Vol. 327; Young, M.; Willits, D.; Uchida, M.; Douglas, T. *Annual Review of Phytopathology* **2008**, *46*, 361-384; Comellas-Aragones, M.; Engelkamp, H.; Claessen, V. I.; Sommerdijk, N. A. J. M.; Rowan, A. E.; Christianen, P. C. M.; Maan, J. C.; Verduin, B. J. M.; Cornelissen, J. J. L. M.; Nolte, R. J. M. *Nat. Nanotech.* **2007**, *2*, 635-639.
(122) Schlick, T. L.; Ding, Z. B.; Kovacs, E. W.; Francis, M. B. *J. Am. Chem. Soc.* **2005**, *127*, 3718-3723.
(123) Endo, M.; Wang, H. X.; Fujitsuka, M.; Majima, T. *Chem. Eur. J.* **2006**, *12*, 3735-3740.
(124) Endo, M.; Fujitsuka, M.; Majima, T. *Chem. Eur. J.* **2007**, *13*, 8660-8666.
(125) Miller, R. A.; Presley, A. D.; Francis, M. B. *J. Am. Chem. Soc.* **2007**, *129*, 3104-3109.
(126) Ma, Y. Z.; Miller, R. A.; Fleming, G. R.; Francis, M. B. *J. Phys. Chem. B* **2008**, *112*, 6887-6892.
(127) Scolaro, L. M.; Castriciano, M. A.; Romeo, A.; Micali, N.; Angelini, N.; Lo Passo, C.; Felici, F. *J. Am. Chem. Soc.* **2006**, *128*, 7446-7447.

2

Polyisocyanides investigated by vibrational circular dichroism

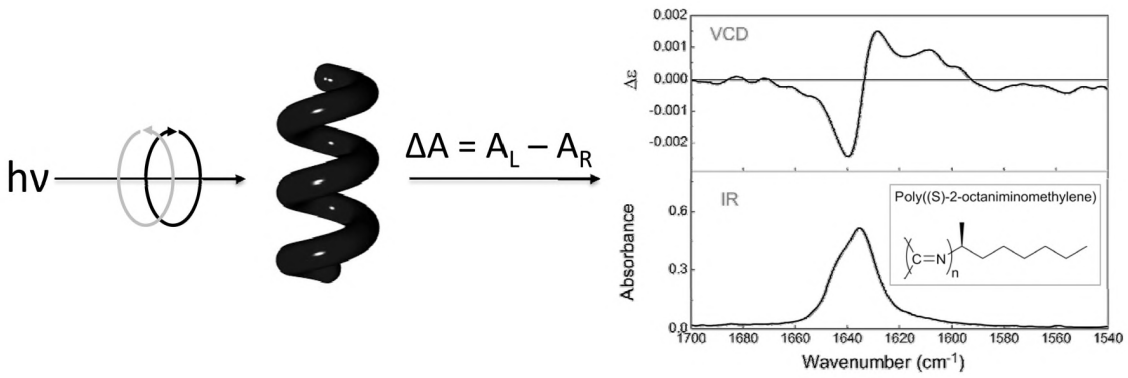

2.1 Introduction

The occurrence of only one form of a given chiral molecule in nature lies at the heart of the often totally different biological activity of the two forms of a chiral molecule. Chiral drugs, such as omeprazole, are of major importance for the pharmaceutical industry. Like many other drugs, the two enantiomers of omeprazole possess different pharmaceutical activity, which means the resolution of the enantiomers and the clinical testing of both is inevitable. The increasing importance of chiral drugs stimulated not only improved techniques for the resolution of racemic mixtures, but also led to the development of (new) methods for the characterisation of chiral molecules. A key factor towards understanding the pharmaceutical activity of a given chiral molecule is to determine the absolute configuration and conformation of the molecule. The two most common methods used to detect chirality and determine the optical activity of a chiral molecule are Optical Rotary Dispersion (ORD) and Circular Dichroism (CD).[1] An ORD spectroscopy reports on the difference in the refractive indices of left- and right-circular polarised light, whereas CD is the differential absorption of left- and right-circularly polarised light. In both techniques the spectra of the two mirror-image enantiomers of the chiral molecule are opposite in sign and as a consequence the absolute configuration (AC) of the chiral molecule can be determined using correlation rules, e.g., the 'Octant Rule'.[2] Unfortunately, these empirical methods sometimes result in incorrect assignment of the configuration. A more general method in which an optical activity measurement could be combined and correlated with the corresponding accurate *ab initio* quantum mechanical calculations to obtain the unequivocal AC determination of the chiral molecule is therefore desirable.[3] This desire led to the development, in the early to mid-1970s,[4] of Vibrational Circular Dichroism (VCD) spectroscopy , the extension of electronic CD spectroscopy into the infrared (IR) and near-IR regions of the spectrum, and in addition to the determination of the AC for moderately complex molecules. VCD spectroscopy is therefore a powerful tool to study conformational structures of chiral molecules.

In this chapter a short overview of the history of VCD spectroscopy and its applications in (polymer) chemistry is presented and the application of this technique to two different polyisocyanides is discussed.

2.2 Theoretical aspects

VCD spectroscopy is the extension of electronic CD spectroscopy to incorporate vibrational transitions and can be viewed as a combination of two spectral approaches; IR spectroscopy, which offers the frequency resolution (structural specificity) and CD spectroscopy, which gives bandshape variability (stereo-sensitivity). VCD spectroscopy has advantages over CD

spectroscopy since vibrational spectra are more informative and allow a more accurate comparison between theory and experiments. In addition, VCD spectroscopy determines properties of the ground electronic state of the molecule, whereas CD spectroscopy probes transitions and vibronic distributions in the excited states; this requires a computationally demanding calculation of the wavefunction of each excited state represented in the CD spectrum. In addition, there are only a few available bands in a CD spectrum and the molecule needs to have a chromophore, which absorbs in the UV/Visible range, which will report on the molecular stereochemistry. VCD spectroscopy is defined as the difference in absorbance (A) between the left and the right circularly polarised infrared radiation, $\Delta A = A_L - A_R$, or for a known pathlength and concentration in terms of molar absorptivity, $\Delta\varepsilon = \varepsilon_L - \varepsilon_R$. One disadvantage of VCD spectroscopy lies in the dimensionless anisotropy ratio $g = \Delta A/A = \Delta\varepsilon/\varepsilon$: the absorption band intensities are very small (five orders of magnitude less than their parent IR intensities) and typically the ratio g is in the order of ~10^{-3} to 10^{-4}, a factor of 10–100 smaller than those for CD spectroscopy.

The physical process associated with VCD spectroscopy can be illustrated by using a simple energy-level diagram, in which the vibrational transition is between the vibrational energy levels g^0 and g^1 of the ground electronic state. It can be seen that VCD spectroscopy is related to simple one-photon quantum transitions induced by left- or right-circularly polarised radiation.

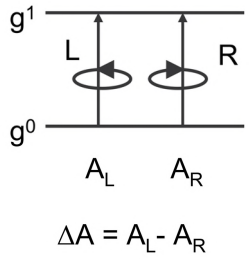

Figure 1. Energy-level diagram for VCD spectroscopy.

The formal theory for VCD spectroscopy, which is relatively complex because of the need to include non-Born–Oppenheimer coupling effects,[5] has been discussed extensively in the literature and will not be discussed in this chapter.[6,7] In short, VCD spectroscopy arises from the combined effect of linear (electric dipole) and circular (magnetic dipole) changes to the molecule due to the nuclear motion, whereas infrared absorption is only sensitive to the linear oscillation of charge.

2.3 Experimental setup

Historically, the first VCD spectrometers were based on dispersive scanning monochromators. In this way, a narrow range of vibrational frequencies and a good signal-

to-noise (S/N) ratio could be obtained, but the inefficiency of collecting data one wavelength at a time is significant compared to the Fourier Transform Infrared (FTIR) approach, from which a wide spectral range can be measured simultaneously.[6] Currently, most (commercial) VCD spectrometers are based on the latter design. A detailed picture of the modern version of the VCD setup is displayed in Figure 2.[8]

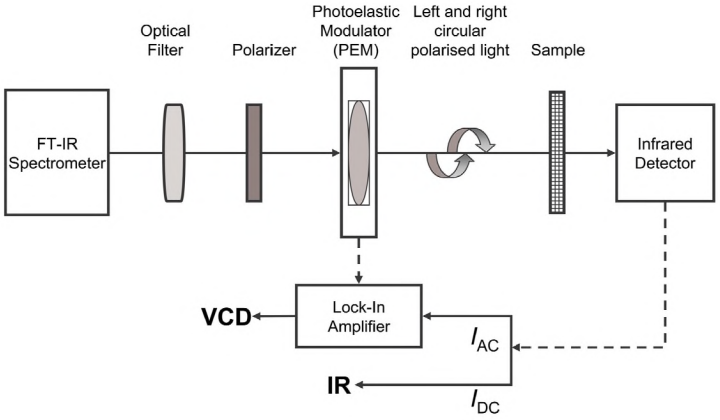

Figure 2. Block diagram of the optical-electronic layout of a FTIR-VCD spectrometer.

In this setup, IR radiation from either a thermal or an electrical source is first passed through an optical filter and is then followed by a polarizer and a photoelastic modulator (PEM),[9] which operates between 35 and 60 kHz. The latter combination creates left- (LCP) and right-circularly polarised right (RCP) and is the heart of the VCD setup. After the beam passes through the sample, it is focused on a liquid-nitrogen cooled MCT (mercury–cadmium–telluride) detector, which converts the IR beam intensity into an electric signal. This signal consists of two independent pathways, the average signal (dc), which contains information on the standard IR spectrum, and the differential signal (ac). This last pathway includes a lock-in amplifier tuned to the PEM frequency, which demodulates the signal at that frequency and leads to the VCD spectrum.[10]

The measurement of a VCD spectrum starts with the measurement of the corresponding IR spectrum. To obtain a good quality and reliable VCD spectrum the sampling conditions, including resolution, concentration, pathlength and solvent, should be adjusted in such a way that the absorbance is between ~0.4 and ~1.0 absorption units. As mentioned earlier, VCD intensities are intrinsically low and therefore they lead to non-trivial measurements as exemplified by polarisation, absorbance and birefringence artefacts, which lead to deviations of the baseline from true zero or to pseudo-VCD bands. Many measurement problems concerning artefacts associated with absorption bands can be resolved by the subtraction of the VCD spectrum of the opposite enantiomer or racemic mixture under identical sample conditions from that of the sample. Unfortunately, these sample are often

not readily accessible and, in the case of biological molecules, even unavailable. If the enantiomer or racemic mixture is not available a baseline can be obtained by measuring solely the solvent; this is, however, not ideal because absorbance artifacts are different for the solvent and the chiral molecule.[8] In the last decades, several approaches to tackle the severity of artifact measurements and to improve the setup of VCD spectroscopy have been published. Among various approaches and methods, the dual-PEM appears to be a potential breakthrough to cancel out artifacts, birefringence effects and improve the S/N ratio. Although the theory of this electro-optical setup is quite complex and will not be discussed here,[11] in effect the first PEM measures the VCD spectrum of the sample and the underlying birefringence baseline artifact, whereas the second PEM measures nearly the entire birefringence baseline artifact spectrum. The substraction of these two signals substantially removes artifacts from the VCD spectrum

Once the VCD spectrum of the molecule of interest is measured it is essential to compare the experimental VCD spectrum to a calculated VCD spectrum.[12] VCD spectra can be interpreted on an empirical level (a sophisticated analysis including a statistical approach) and through *ab initio* quantum-mechanical calculations. The first level was used in the early days and suffers from uncertainties in the approximations associated with both electronic modelling and vibrational analysis, which is typically empirical in nature. The expansion of computational capabilities along with density functional theory (DFT)[13] and improved algorithms such as Gaussian 03, makes the latter level of interpretation the most powerful analysis method used nowadays.

2.4 VCD spectroscopy on helical polymers

Since its discovery 40 years ago, VCD spectroscopy has passed many experimental and theoretical hurdles to become the mature technique of today. VCD spectroscopy can be applied to solve structural problems that arise from molecules containing amino acids, polypeptides, proteins and carbohydrates. Although additional progress is needed in some areas,[14] VCD spectroscopy has proven its value and due to the structure-rich information that can be gained from this technique it has the potential to play an important role as a complementary spectroscopic technique in the coming years. Historically, the majority of VCD studies involved the determination of the stereo-conformational features of a small chiral molecule,[3,8,15] but a growing area of applications involves larger molecular structures, such as (oligo)peptides,[16-18] DNA and proteins,[19-22] foldamers,[23] supramolecular assemblies,[24] nanoparticles and chiral (metal) complexes,[25] and polymers.[26-28] Since the topic of this thesis deals with (peptido)polymers this paragraph highlights the recent advances in VCD spectroscopy in the field of polymers.

The first polypeptide that was analysed by VCD spectroscopy was poly(benzyl-L-glutamate), a right-handed α-helical molecule.[29] The VCD spectrum was composed of a negative couplet for the NH-stretching vibration, a (strong) positive couplet in the amide I region (amide I´ if deuterated) and a less intense negative band in the amide II region. These bandshape patterns were shown to be characteristic for right-handed α-helices and distinctly different from the amide I signal in β-sheet and coil forms of polypeptides (Figure 3).[13] Although CD spectroscopy is an invaluable tool for the characterisation of α-helices, VCD spectroscopy has demonstrated to be a complementary tool to investigate various polypeptides structures,[18,30,31] which include different forms of helices (e.g., 3_{10}/α-helices)[13,17,32] and polypeptides containing a large fraction of aromatic residues[21,33] in which the π-π* transitions interfere with the amide signals making interpretation by means of CD spectroscopy very complicated.[34]

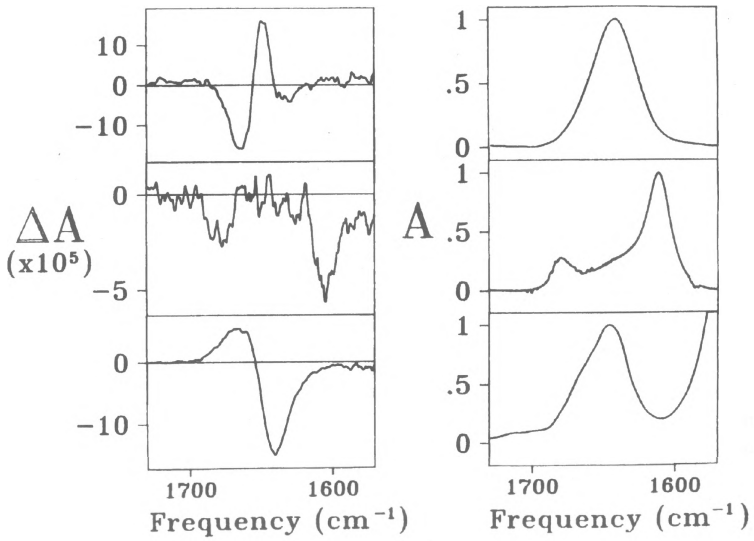

Figure 3. VCD (left) and IR (right) spectra of poly(L-Leu-L-Lys-L-Leu) in high salt concentration (α-helical form, top); poly-L-lysine at high pH (β-sheet form after heating, middle); and poly-L-glutamic acid at neutral pH (random coil form, bottom). Spectra were normalised to a peak absorbance of A_{max} = 1.0 for the amide I´ band.[13]

As for peptide polymers, the VCD spectra of proteins are straightforwardly studied in the Amide I region.[35] A range of proteins have been analysed by VCD spectroscopy and from these studies it became evident that there is a high variability of bandshapes. This can be explained by the contribution of all types of secondary structures that give rise to VCD signals of roughly the same intensity,[22,30,36] which is in contrast to CD spectroscopy, where, particularly in the lower energy UV region, the α-helical components dominate. This is illustrated in Figure 4, where a comparison between amide I´ VCD, IR and amide CD signals for three proteins: 1) haemoglobin with a high α-helix fraction; 2) concanavalin A, which has substantial β-sheet content with almost no helix; and 3) lysozyme, a protein with mixed α

and β structures, in D_2O is made. By comparison, the IR and CD spectra are roughly similar in shape, whereas the VCD spectra exhibit dramatic changes in the bandshapes, although the S/N ratio is significantly lower. The highly helical haemoglobin has a positive signal, in contrast to concanavalin A, which has a predominantly negative signature. This demonstrates that, at least on the qualitative level, VCD spectroscopy allows a better *structure versus spectra* relationship than CD spectroscopy.

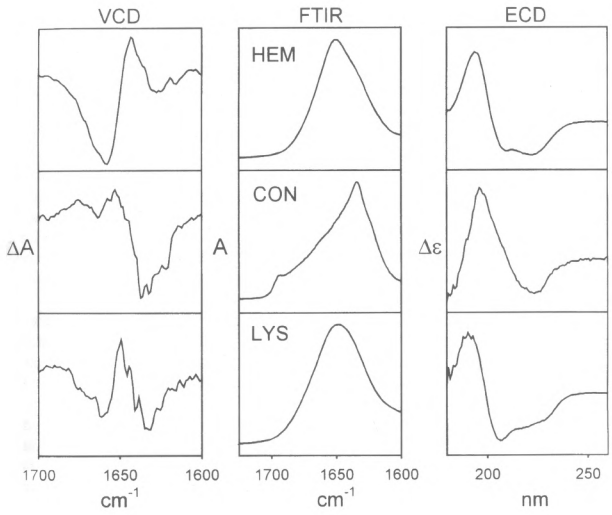

Figure 4. Comparison of the bandshapes of the amide I´ VCD (left), amide I´ FTIR (normalised to A_{max} = 1.0, middle), and ECD (electronic CD = CD) (right) signals for three globular proteins in D_2O solution: haemoglobin, high α-helix content (top); concanavalin A, high β-sheet content with little or no helix (middle); and lysozyme, a mixed α and β protein (bottom).[13]

A more recent example used to obtain structural information on proteins from VCD spectroscopy was reported by the group of Nafie and co-workers.[19] They studied the formation and dynamics of fibrils (which are of considerable interest because of its association with many neurodegenerative diseases[37]) of two proteins: hen egg white lysozyme and bovine insulin. The fibril formation was initiated by heating the protein solution at 60 °C in H_2O for two days for lysozyme and two hrs for insulin. The samples were then centrifuged and VCD spectra were taken from both the supernatant phase and gel phase. For both proteins an enormous and remarkably similar increase in VCD intensities compared to the native protein is observed. This behaviour is illustrated for lysozyme in Figure 5 (left), with the strong negative signal around 1625 cm^{-1} as a clear feature. Besides centrifugation, the process could also be followed by prolonged heating of the sample, which led to the same characteristic VCD signals (Figure 5, right).

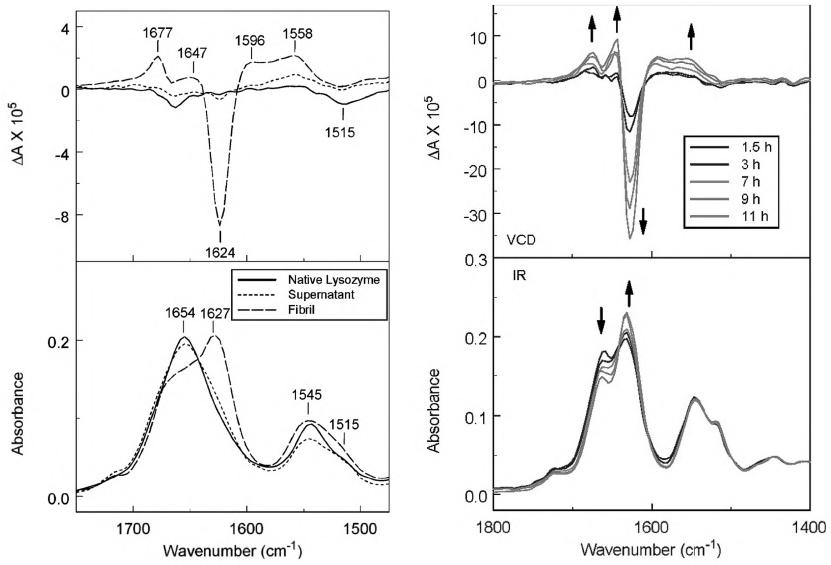

Figure 5. VCD (top) and IR (bottom) spectra of native lysozyme, centrifuged lysozyme supernatant and centrifuged lysozyme fibril gel (left) and VCD and IR progression of the fibril formation of insulin in H_2O at pH 2 and after heated 45 min at 65 °C (right).

VCD spectroscopy has only recently been of interest to the (synthetic) polymer community. After the exploratory work of Nafie, Keiderling and Stephens on poly(1-methylpropyl vinyl ether) and poly(4-methyl-1-hexene) this work was extended by Wieser and co-workers who examined chiral poly(vinyl ethers) and poly(acrylates) in the 90s.[28,38] To investigate the relationship between the structure and the properties of polythiophenes bearing chiral side chains, Polavarapu et al. examined the VCD spectra of monomeric and polymeric thiophenes.[27,39] By comparison of the VCD spectra the authors concluded that the repeating units in the polymers have the same configuration and conformation as those for the corresponding monomers.

Yashima and co-workers also exploited the VCD technique to study optically active poly(methylmethacrylate) (PMMA) stereocomplexes.[26] They obtained PMMA stereo-complexes[40] in a two step process. At first, an optically active syndiotactic (st)-PMMA/C_{60} was prepared by the addition of chiral alcohols and C_{60} molecules to st-PMMA that formed a peapod-like complex gel, in which the helicity was retained after complete removal of the chiral alcohols (Figure 6, top). Next, the C_{60} molecules, which are encapsulated within the helical st-PMMA cavity, were replaced by isotactic (it)-PMMA to form the first synthesised optically active stereocomplex.

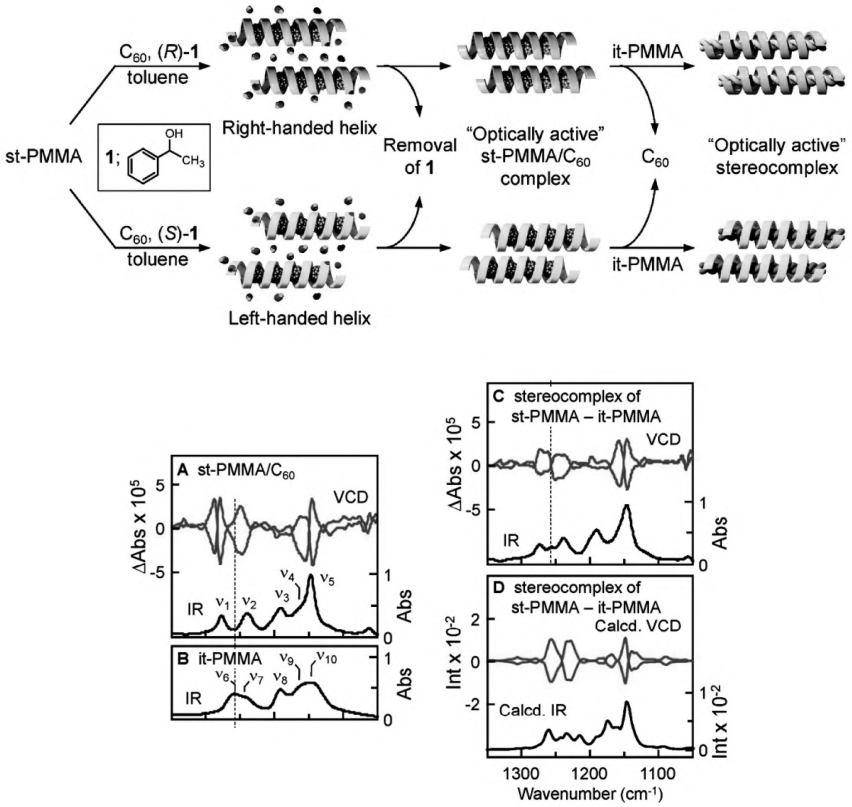

Figure 6. Schematic illustration of right- and left- handed stereocomplex formation with a triple-stranded helical structure (top) and observed VCD spectrum of complex gels (A) and stereocomplex st-PMMA/it-PMMA (C), IR (B) spectra of st-PMMA/C_{60} and calculated VCD spectra of st-PMMA/it-PMMA (D) (bottom).

By using (*R*)- or (*S*)-1-phenylethanol an excess of one-handedness of the st-PMMA/it-PMMA stereocomplex was achieved as was demonstrated by the mirror-image VCD bandshapes in the PMMA IR regions (Figure 6, bottom). The VCD signals are also significantly different compared to the VCD spectra of st-PMMA/C_{60}, in particular in the region around 1260 cm^{-1}, which correspond to the absorption bands of it-PMMA. Additional evidence for the preferred handedness of the stereocomplex was obtained from the experimental and calculated VCD spectra of the fully deuterated helical st-PMMA-*d8*.

Another elegant example, in which structural conformations of helical polymers were studied, was reported by Novak and co-workers. Like proteins and DNA, the function and physical properties of a (helical) polymer are strongly correlated with the conformation of the macromolecular chain. Of particular interest is the formation of helices as these structures to some extent allow the control of the organisation of macromolecules at various hierarchical levels. Over the last years the group of Novak prepared single screw sense, rigid helical polyguanidines that display attractive properties, such as the formation of birefringent, cholesteric mesophases or interesting optical switching phenomena.[41] In a recent contribution[42] a wide range of these chiral polymers are reported; two examples

(poly-I and poly-II, Figure 7) will be discussed here. Both polymers were obtained by the polymerisation of the achiral carbodiimide monomer *N*-(*n*-hexyl)-*N*-phenylguanidine using the chiral dialkoxy titanium(IV) catalysts **I** and **II** (Figure 7, right) and resulted in helical polyguanidines that were readily soluble in chloroform. To assign the screw sense of the helical polyguanidines their conformations were studied with VCD spectroscopy in combination with modelling calculations.[42] The VCD spectra of poly-I and poly-II are depicted in Figure 7 (left).

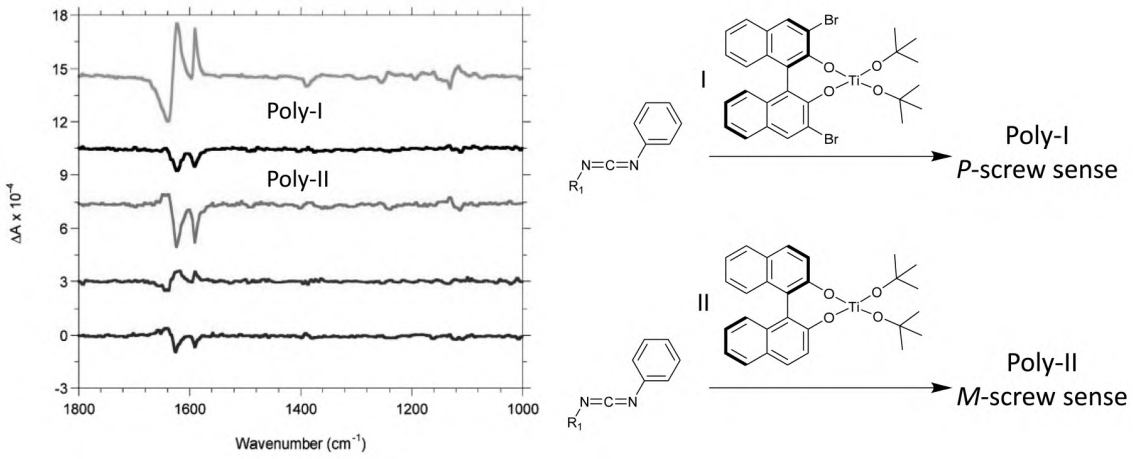

Figure 7. Experimental VCD spectra of helical polyguanidines in $CDCl_3$. The top two signals correspond to poly-I and poly-II, respectively (left) and polymerisation of the *N*-(*n*-hexyl)-*N*-phenylguanidine monomer using dialkoxy Ti(IV) catalysts I and II (right).

Poly I has a –1640, +1623 cm^{-1}, +1590 cm^{-1} pattern with a strong VCD intensity, which is opposite to the pattern of poly-II. This result is consistent with the positive optical rotation sign at the sodium D line found for poly-I and the negative $[\alpha]_D$ value of poly-II. To determine the handedness of the helical polyguanidines their experimental VCD spectra need to be compared with predicted VCD spectra. To this end, two model molecules A and B were built and their initial geometries which have a *P*-handedness, were optimised at the DFT level (Figure 8, left). The major difference in these two model molecules is the position of the benzene ring. The spectrum of model A compares well with the spectrum of poly-I (Figure 8, right) and therefore the authors believe that poly-I has a *P* screw sense and poly-II has an *M* crew sense. Unfortunately, the reason why the resulting polymers have opposite screw sense, despite the fact that the binapthyl ligand of the catalyst (Figure 8, right) possess the same *M*-handed configuration, remains unclear.

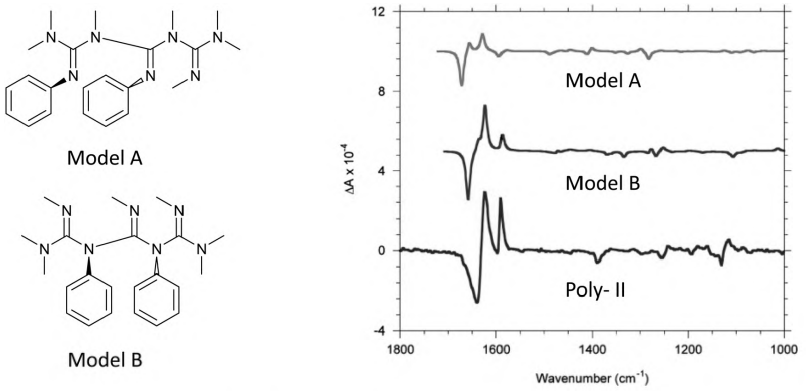

Figure 8. Structures of two model molecules used in the calculations (left) and comparison between the experimental VCD spectra of poly-I and the predicted spectra of model molecules A and B (right).

Another member of the class of helical polymers are polyisocyanides. Polyisocyanides are prepared by the nickel(II) induced polymerisation of isocyanide monomer units.[43] Restricted rotation around the single bonds that connect the main-chain carbon atoms of the polymer gives rise to the formation of a stable helix, provided that the isocyanide-substituents are sufficiently bulky. After the first evidence for the helical conformation[44] a vast amount of polyisocyanides have been prepared by us and others.[45] The determination of the screw sense of these helical polymers has been the subject of intense research efforts in the past and could only be determined using "indirect" methods with the help of chromophoric side groups (see below).[46-49] Recently, Yashima and co-workers investigated the structural changes of optically inactive poly(4-carboxyphenyl isocyanides), which could be transferred into one-handed helical structures upon the addition of chiral amines.[50] They prepared a series of isotopically labelled compounds and were able to assign the major peaks in the vibrational spectra (Figure 9), which, together with numerous other techniques, allowed the gathering of detailed information on the mechanism of helix induction in aromatic polyisocyanides.

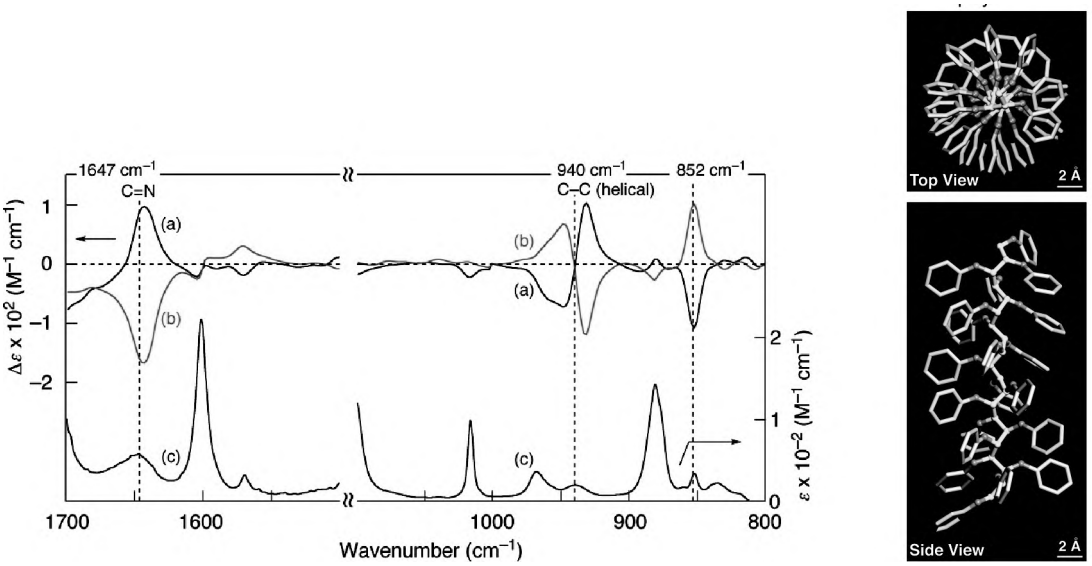

Figure 9. VCD (a,b) and IR (c) spectra of helical induced poly(4-phenylcarboxylate isocyanide) with an (*R*) (a,c) and an (*S*) (b) chiral amine (left). Top and side view of the same polymer with a 10_3 helical structure. The methyl ester groups and hydrogen atoms are omitted for clarity (right).

From above it is clear that VCD has emerged as a powerful tool to investigate molecular conformation. In this chapter we use the semi-quantitative coupled-oscillator approach in a preliminary analysis of the VCD spectrum of the CN-stretching mode of polyisocyanides.

2.5 Results and Discussion

Since the polyisocyanide polymers have a high persistence length we model them as infinitely long helices. To describe the vibrational absorption and the VCD spectrum of an infinite helical array of C=N groups in the coupled-oscillator approximation, one can use the theory developed recently[51-53] for the absorption and circular dichroism of helical aggregates of coupled, identical chromophores, each chromophore having a single, well-defined transition-dipole moment.[54] Taking the helix to be aligned along the *z*-axis, the positions and directions of the transition-dipole moments can be written as[51,52]

$$\begin{pmatrix} x_j \\ z_j \\ y_j \end{pmatrix} = \begin{pmatrix} R\cos j\gamma \\ R\sin j\gamma \\ hj \end{pmatrix} \quad \text{and} \quad \begin{pmatrix} \mu_j^x \\ \mu_j^y \\ \mu_j^z \end{pmatrix} = \mu \begin{pmatrix} \sin\theta\cos(j\gamma+\phi) \\ \sin\theta\sin(j\gamma+\phi R\sin j\gamma) \\ \cos\theta \end{pmatrix} \qquad (1)$$

respectively, with $j \in Z$, R the radius of the helix, γ the angle (relative to the helical axis) which separates consecutive units, h their vertical separation, θ the angle of the transition-dipole moment with the helical axis, and ϕ the angle that the projection of μ_j on the *xy* plane makes with the radius.[55] The above expressions are for a right-handed helix if $\gamma > 0$,

and for a left-handed helix if γ < 0. Since there is interaction between the transition dipoles, the energy eigenstates of the coupled-oscillator system are delocalised (vibrational excitons). It can be shown from group theoretical considerations[56,57] that only two eigenstates have IR activity: the completely symmetric *A* state with wavefunction $\left|\Psi_A\right\rangle = \sum_n \left|\upsilon_n = 1\right\rangle$, and the doubly-degenerate *E* state (also called the 'helical exciton state')[51] with wave functions $\left|\Psi_{E1}\right\rangle = \sum_n \sin n\gamma \left|\upsilon_n = 1\right\rangle$ and $\left|\Psi_{E2}\right\rangle = \sum_n \cos j\gamma \left|\upsilon_j = 1\right\rangle$ where $\left|\upsilon_j = 1\right\rangle$ denotes the state in which the *n*th vibrational chromophore is in the first vibrationally excited level. The frequencies of these two states are determined by the interactions between the chromophores in the helix:[51,57]

$$E_A = \omega_0 + \sum_n {}' J_n \tag{2}$$

$$E_E = \omega_0 + \sum_n {}' J_n \cos(n\gamma) \tag{3}$$

where ω_0 denotes the frequency of an isolated C=N group, and J_n the interaction energy between the 0th and *n*th C=N group (and the prime indicates that *n* = 0 has to be excluded from the summation). The absorption spectrum is hence given by[51]

$$A(\omega) = \frac{N\mu^2}{3}\left[\cos^2\theta F(\omega - E_A) + \sin^2\theta F(\omega - E_E)\right] \tag{4}$$

where *N* is the total number of chromophores, μ the transition-dipole moment of the $\upsilon = 0 \rightarrow 1$ transition of an isolated chromophore and $F(\omega)$ the normalized lineshape function.

It can be shown that the CD of the helix, defined as $R(\omega) = A_L(\omega) - A_R(\omega)$, is given by[51-53]

$$R(\omega) = \frac{N\mu^2\pi}{3}\left\{\begin{array}{l} \frac{R}{2\lambda}\sin 2\theta \sin\phi\left[F(\omega - E_A) - F(\omega - E_E)\right] \\ + \frac{h}{2\lambda}\sin^2\theta F'(\omega - E_E)\sum_n n\sin(n\gamma)J_n \end{array}\right\}, \tag{5}$$

where $F(\omega)$ is again the lineshape of the A and E absorption bands, $F'(\omega)$ the first derivative of the lineshape with respect to w, and J_n is the interaction energy between the *m*th and (*m*+*n*)th transition dipole moment (which is independent of *m* because of the

helical symmetry). The last term in this equation is sometimes referred to as 'helical circular dichroism'.[51,53]

Polyisocyanides represent a special, simple case of the above equations. In polyisocyanides, the C=N bonds all point radially outwards (the projection of the C=N bond on the *xy* plane is perpendicular to the helical axis), so $\theta = 0^0$. Consequently, the first term in Eq. (5) vanishes, so that the VCD spectrum should consist only of a single couplet, which is the derivative of the *E* absorption band. To establish the relation between the screw sense and the sign of the VCD couplet, we use the fact that nearest-neighbour interaction dominates, so that $J_n = \delta_{n,1} + \delta_{n,-1}$ and the summation in eq. (5) reduces to $2J_1 \sin\gamma$, where J_1 is the nearest-neighbour interaction energy. Consequently the CD of the helix is,

$$R(\omega) = \frac{N\mu^2 \pi h}{3\lambda} \sin^2\theta F'(\omega - E_E) J_1 \sin\gamma \qquad (6)$$

Since in polyisocyanides the nearest-neighbour C=N transition dipoles have charges with the same sign approaching each other, we have $J_1 > 0$. The VCD spectrum of a right-handed polyisocyanide ($\gamma = 90^0$, so $\sin\gamma = 1$ in Eq. (6)) should look like the derivative of the *E* absorption band, whereas the VCD spectrum of a left-handed polyisocyanide ($\gamma = -90^0$) should look like the derivative of the *E* absorption band multiplied by −1. There is therefore a direct relation between the screw sense of a polyisocyanide and its C=N-stretch VCD spectrum. An even stronger simplification can be obtained if we assume that the C=N bonds are perpendicular to the helical axis (that is, they are in the *xy* plane), hence $\theta = 90^0$. This reduces the first term in Eq. (4) to zero, so that the absorption spectrum should consist of one band (the *E* band) only,

$$A(\omega) = \frac{N\mu^2}{3} F(\omega - E_E) \qquad (7)$$

In case the C=N bonds are not exactly perpendicular to the helical axis, a weak *A*-band will still be present in the absorption spectrum. To verify the relation between the polyisocyanide screw sense and the C=N-stretch VCD spectrum, we have synthesised the helical poly-2-methylheptylisocyanides **1** (Figure 10) and determined their screw sense independently using CD.

The polymers poly(*R*)-2-methylheptylisocyanide **1a** and poly(*S*)-2-methylheptylisocyanide **1b** were obtained in three steps from the optically active amine starting material. Treatment of

the amine with an excess of ethyl formate afforded the *N*-formyl derivatives in quantitative yield. The isocyanides were obtained, as liquids with a rather piercing odour, by dehydration of the corresponding formamide with diphosgene and *N*-methylmorpholine (NMM) at low temperatures. The infrared absorption spectra showed the characteristic isocyanide stretching vibration at 2138 cm^{-1}. At the sodium-D-line (578 nm) the *R* isocyanide monomer had a negative optical rotation of $[\alpha]_D$ = –48°; for the *S* enantiomer $[\alpha]_D$ = +47°. The monomers were polymerised without solvent at room temperature by the addition of 3% $Ni(ClO_4)_2 \cdot 6H_2O$ to yield cream coloured solids in >80% yield.

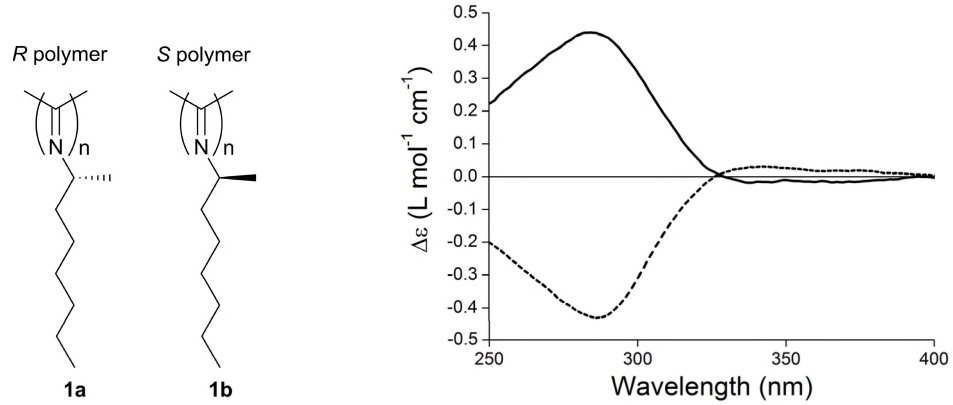

Figure 10. Chemical structure of the polyisocyanides **1** used in this study (left) and CD spectrum of **1a** (dotted line) and **1b** (solid line) in heptane (right).

Although optical rotation values can be used to obtain information about the conformations of the polymer, in this case the rigid environment of the polymer $(RN=C)_n$ might affect the conformation of the *R* substituent and thus its contribution to the optical rotation. We therefore studied the (helical) structure of these polyisocyanides by CD and VCD spectroscopies to get more detailed information. In the CD spectrum the n–π^* transition of the backbone imine functions can be monitored. The CD spectrum of **1** in heptane in the region λ = 250–400 nm, depicted in Figure 10, corresponds to this transition. In the polymer, both the chiral centre in the side chain as well as the helical structure of the main chain will induce rotational power in the N=C group.[58] The large negative band of **1a** (positive band for **1b**) with a maximum Δε at λ = 285 nm is attributed to the contribution of the chiral side chain. In theory, the helicity (screw sense) of the polymer can be derived from the sign sequence of the so-called "exciton couplet" by a comparison with a model compound, for example, poly(tert-butyliminomethylene), from which the screw sense was obtained by a resolution process.[46] In Figure 10 this couplet is not clearly visible because of the overlap with the band that arises from the chiral side chain, but the asymmetry of the curve is a first indication. On careful inspection of the curves a positive band at λ = 320 nm, as part of the "positive couplet" evident for the helicity, can be observed.[59] Such a couplet was also

observed for (*M*)-poly(*tert*-butyliminomethylene) and thus, by looking at the similarity of the couplets, it can be tentatively concluded that polymer **1a** is predominantly in the *M*-helical conformation. In this way, however, the screw sense is determined by an indirect method and the assignment of the exciton couplet can be hampered by side chain contributions to the Cotton effect originating from the backbone $n–\pi^*$ transitions.

The IR spectrum of these polyisocyanides, shown in Figure 11 (left), contains a C=N-stretch band with a shoulder on the high-frequency side. Based on the considerations above, we assign the main peak in the spectrum to the *E* transition, and the weaker shoulder to the *A* transition. The latter observation might indicate that the C=N bonds are not exactly perpendicular to the helical axis. By least-squares fitting two lorentzian line shapes to the spectrum, we obtain centre frequencies for the *E* and *A* transitions of 1635 and 1643 cm^{-1}, respectively.

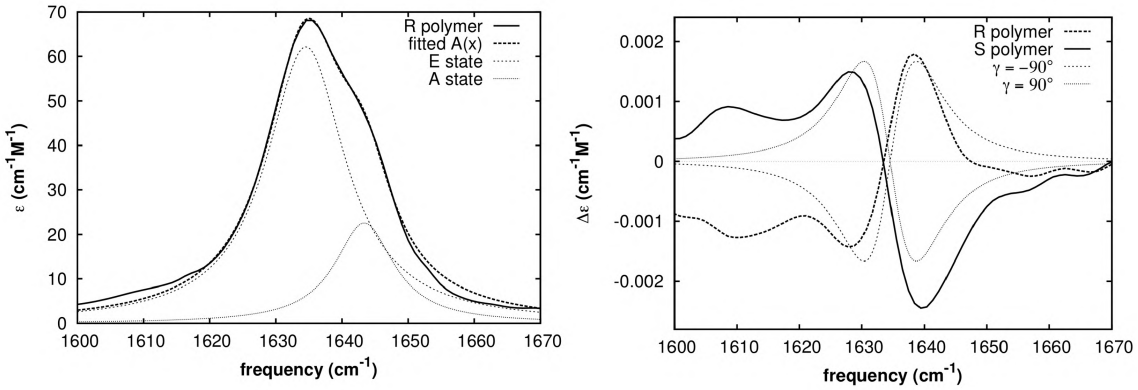

Figure 11. IR absorption spectrum of **1a** (*R*-polymer), together with a least-squares fit of two lorentzian lineshapes (left) and VCD spectra of **1a** (*R*-polymer) and **1b** (*S*-polymer) in heptane (0.15 M), together with Eq.(6) for γ = + 90 ° (right-handed helix) and γ = – 90 ° (left-handed helix) (right). The racemic polymer mixtures were subtracted from the spectra. The path length is 0.5 mm.

The VCD spectra of **1** in the C=N-stretching region are shown in Figure 11 (right). These spectra indeed contain a couplet centred at the frequency of the main (*E*) absorption band, as predicted. They also contain a singlet feature at lower frequency (around 1610 cm^{-1}), which is difficult to assign, since no corresponding band is present in the absorption spectrum (Figure 10). In the C=N-stretch region, the VCD spectra of the *R* and *S*-polymers indeed correspond to the VCD spectra predicted for a left- and right-handed helix.

The chiroptical properties of the dialanine derived helical polyisocyanides (See Preface) were also investigated. Induced by the optically pure alanine units in the side chain, the polyisocyanides **2** (Figure 12) adopt a helical conformation and hence CD and VCD spectroscopic measurements can be carried out to obtain structural information. The CD spectra of **2** have been discussed previously in detail[49,60] and it is tentatively believed that the well-defined arrangement of the amide groups, as a result of the hydrogen bonding, has

a major contribution to the Cotton effect at λ = 310 nm observed in the CD spectra (Figure 12).

VCD spectroscopy has been used to study the secondary structure of proteins and peptides; with amide I and amide II as the most fruitful regions and this is also the main focus of the VCD investigations of polymers **2**. The observed VCD spectra of enantiomers **2a** and **2b** are shown in Figure 13. Some interesting features regarding the VCD spectra can be noted. First, the VCD intensity is large. Second, instead of expected doublets for the amide I and amide II vibrations on the basis of helical symmetry, singlet bands are observed. These observations are non-traditional and require more elaborate modelling (DFT) studies, which are currently undertaken in the group of Prof. Nafie at the Department of Chemistry at Syracuse University, New York.

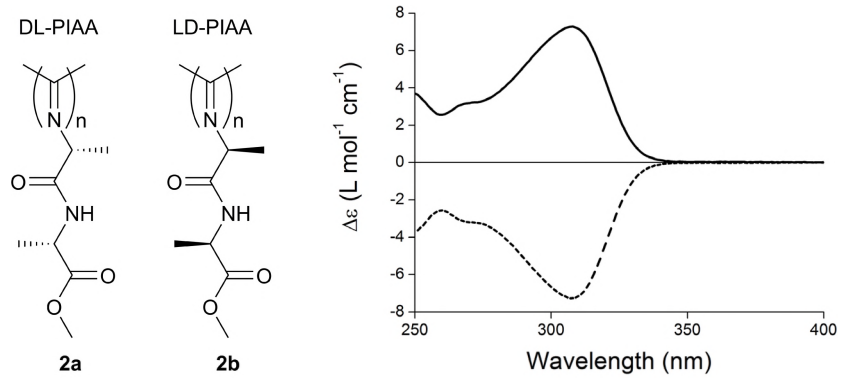

Figure 12. Molecular structure of polyisocyanides **2** derived from dialanine (left) and CD spectrum of **2a** (dotted line) and **2b** (solid line) in chloroform (right).

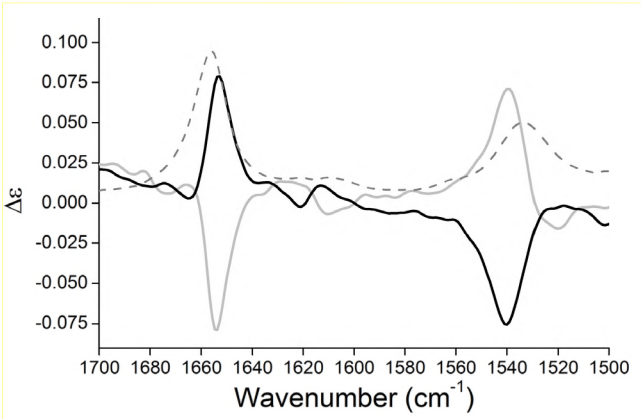

Figure 13. VCD spectra of **2a** (grey line) and **2b** (black line) and absorbance (ε/ 8000, dashed line) of **2a** in heptane (0.08 M). The racemic polymer mixtures were subtracted from the spectra. The path length is 0.1 mm.

2.6 Conclusion

In this chapter an overview of the use of VCD as a tool to investigate molecular conformations is described. A previously established theory, which allows the prediction of the vibrational circular dichroism (VCD) spectrum of an infinite helix in the coupled-oscillator

approximation, was applied to the VCD spectrum of the C=N-stretching mode of helical poly-2-methylheptylisocyanides. It was shown that if the C=N groups point radially outward from the helical axis, the CN-stretch VCD spectrum of a polyisocyanide should consist of a single couplet, the sign of which is directly related to the screw sense of the helix. In this way, we were able to verify the helical handedness of poly(*R*)-2-methylheptylisocyanide **1a** and poly(*S*)-2-methylheptylisocyanide **1b** and confirmed that the *R* polymer is a left-handed helix and that the *S* polymer is a right-handed helix.

2.7 Experimental

General

All solvents were distilled prior to use. All other chemicals were commercials products and used as received. Column chromatography was performed using silica gel (40–60 μm) purchased from Merck. TLC-analyses were carried out on silica 60 F_{254} coated glass from Merck and the compounds were visualised using Ninhydrine, $KMnO_4$, or $Ni(ClO_4)_2{\cdot}6H_2O$ in EtOH. ^{1}H NMR and ^{13}C NMR spectra were recorded on a Bruker AC-300 MHz instrument operating at 300 MHz and 75 MHz, respectively, unless otherwise stated. FT-infrared spectra were recorded on a ThermoMattson IR300 spectrometer equipped with a Harrick ATR unit; compounds were measured as solids or oils. Mass spectrometry measurements were performed on a JEOL Accutof instrument (ESI). Optical rotations were measured on a Perkin Elmer 241 Polarimeter at room temperature and are reported in 10^{-1} deg cm^2 g^{-1}. CD spectra were recorded on a Jasco 810 instrument equipped with a Peltier temperature control unit.

The infrared and VCD spectra were recorded with a Bruker PMA 50 TENSOR FT-IR spectrometer. The light beam was collimated to a sample while passing an optical filter (1800-600 cm^{-1}), a wired-grid polarizer and a ZnSe 50 kHz photoelastic modulator (PEM) (Hinds instruments). The light was then focused by a ZnSe (10 cm focal length) onto a HgCdTe detector (Model - D313/6) with BaF_2 windows. The PEM was adjusted for a maximum absorption at 1630 cm^{-1}. Calibration spectra were recorded using a CdS multiple wavelength plate and a second polarizer. VCD spectra were recorded at a resolution of 4cm^{-1}, by co-adding scan times of 3 × 10 minutes, 30 minutes and 2 × 60 minutes (total of 3 hours) for **1** and 2 × 10 minutes and 40 minutes (total 1 hour) for **2**, respectively. The samples were held in a fixed path length (0.5 mm for **1**, 0.1 mm for **2**, respectively) between CaF_2 windows. The spectra were corrected by subtracting the VCD spectra of the racemic mixtures. Calculations of the VCD spectrum were performed with the VisualBasic PMA50 software, using Blackman-Harris 4-term apodisation, Mertz phase correction and a zero-filling factor of four.

Synthesis

DL-PIAA (**2a**),[61] LD-PIAA (**2b**), [62] and poly(*R*)-2-methylheptylisocyanide (**1a**)[48] were synthesised according to literature procedures.

(*S*)-*N*-(2-methylheptyl)formamide

This compound was obtained in quantitative yield from the (*S*)-amine and from a 25% excess of ethyl formate according to a standard procedure.[63]

$[\alpha]_D$ (CH_2Cl_2 , *c* 1.7) = –7° . ^{1}H NMR (δ ppm, $CDCl_3$, 300 MHz, rotamers): 8.09 and 8.05 (rotameric s, 1H, HCO), 5.80 and 5.64 (rotameric br s, 1H, NH), 4.02 and 3.44 (rotameric sept., 1H, J = 6.6 Hz, CH), 1.42–1.24 (m, 10H,

CH_2), 1.19 and 1.12 (rotameric d, 3H, J = 6.6 Hz, $CHCH_3$), 0.84 (t, 3H, J = 7.1 Hz, CH_3). ^{13}C NMR (δ ppm, $CDCl_3$, 75 MHz, rotamers): 163.9 and 160.6 (rotameric C=O), 48.6 and 44.2 (rotameric CH), 37.9, 36.9, 31.8, 29.0, 26.0 (CH_2), 22.6 and 21.0 (rotameric, CH_3). FT-IR (cm^{-1}, ATR): 3264 (NH), 2957, 2925, 2854 (CH & CH_2 & CH_3), 1655 (amide I), 1539 (amide II), 1455, 1379 (CH_2 and CH_3). MS-ESI: m/z = 157 $[M+Na]^+$. HRMS for $C_9H_{19}NONa$: Calcd 180.1359. Found: 180.1364.

(*S*)-2-methylheptylisocyanide

The formamide (1.12 g, 7.1 mmol) was dissolved in CH_2Cl_2 (200 mL) under an N_2 atmosphere and *N*-methyl morpholine (1.97 mL, 17.8 mmol, 2.5 equiv.) was added. The resulting solution was cooled to –30 °C (acetone/CO_2) and diphosgene (0.43 mL, 3.6 mmol, 0.5 equiv.) in $CHCl_3$ (10 mL) was added dropwise over a period of 30 minutes, while the temperature was maintained at –30 °C. After complete addition of diphosgene, the yellow solution was warmed to 0 °C and an ice-cold saturated aqueous sodium bicarbonate solution (50 mL) was added and stirred vigorously for 10 minutes. The product was extracted with $CHCl_3$ (100 mL) and subsequently washed with an aqueous 10% (w/w) sodium bicarbonate solution and water (50 mL). The organic layer was dried (Na_2SO_4) and evaporated *in vacuo* resulting in a yellow liquid. The product was purified using column chromatography (1% MeOH in $CHCl_3$) to yield **(*S*)-2-methylheptylisocyanide**in 81% as a colourless liquid. $[\alpha]_D$ (CH_2Cl_2, *c* 1.0) = 47°. ^1H NMR (δ ppm, $CDCl_3$, 300 MHz): 3.44 (m, 1H, CH), 1.62–1.29 (m, 13H, CH_2 and $CHCH_3$), 0.88 (t, J = 6.9 Hz, CH_3H). ^{13}C NMR (δ ppm, $CDCl_3$, 75 MHz): 154.3 (t, J = 5.2 Hz, CN), 50.4 (t, J = 5.4 Hz, CH), 36.9, 31.8, 28.7, 25.8, 22.6 (CH_2), 21.8 ($CHCH_3$). FT-IR (cm^{-1}, ATR): 2958, 2920, 2863 (CH, CH_2 and CH_3), 2138 (CN). Anal. Calcd for $C_9H_{14}O_4N_3$: liquid too volatile for measurements.

The monomer (*R*)-2-methylheptylisocyanide had similar spectroscopic properties and $[\alpha]_D$ ($CHCl_3$, *c* 1.9) = -47.6°.[48]

Poly(*S*)-2-methylheptylisocyanide 1b

The polymerisation was achieved by the following standard procedure:[64] to a stirred solution of $Ni(ClO_4)_2{\cdot}6H_2O$ (5.24 mg) in MeOH (2 mL) was added at ambient temperature of (*S*)-2-isocyanooctane (1.1 mL). Immediately, an orange–red colour appeared and a cream coloured solid precipitated. After 5 hrs, the solvent was evaporated, the polymer was taken up in a minimal amount of $CHCl_3$ and the polymer was precipitated out by dropping this solution into MeOH/H_2O (100 mL (4:1 v/v)) with vigorous stirring. The product was filtered off and washed extensively with MeOH. Drying at 50 °C *in vacuo* gave the polymer as a cream solid in 93 % yield. $[\alpha]_D$ (C_6H_{14}, *c* 0.1) = –36°. ^1H NMR (δ ppm, $CDCl_3$, 300 MHz): 3.65–3.10 (br, 1H, CH), 1.95–1.20 (br, 13H, CH_2 and $CHCH_3$), 1.0–0.7 (br, 3H). IR (cm^{-1}, KBR): 2962, 2929, 2858 (CH, CH_2 and CH_3), 1635 (C=N), 1468, 1373 (CH_2 and CH_3). Anal. Calcd. for $C_9H_{17}N$: C, 77.63; H, 12.31; N, 10.06. Found: C, 77.84; H, 12.23; N, 9.94. Polymer **1a** had similar spectroscopic properties and $[\alpha]_D$ (C_6H_{14}, *c* 0.8) = 34°. Due to the rod-like nature of polyisocyanides determination of the molecular weights by GPC was not possible.

2.8 References & Notes

(1) Two other very powerful techniques readily available to chemist, X-ray crystallography and NMR spectroscopy have some drawbacks. X-ray crystallography needs a (high) quality crystal and to determine the AC the 'Bijvoet' method requires a heavy atom (e.g., sulphur). NMR spectra are not enantiomerically sensitive and need chiral shift reagents.

(2) Lightner, D. A. In *Circular Dichroism: Principles and Applications*; 2nd ed.; Berova, N., Nakanishi, K., Woody, R. W., Eds.; Whiley-VCH: New York, 2000.

(3) Stephens, P. J.; Devlin, F. J.; Pan, J. J. *Chirality* **2008**, *20*, 643-663.

(4) Barron, L. D.; Bogaard, M. P.; Buckingh.Ad *J. Am. Chem. Soc.* **1973**, *95*, 603-605; Holzwart, G.; Hsu, E. C.; Mosher, H. S.; Faulkner, T. R.; Moscowit, A. *J. Am. Chem. Soc.* **1974**, *96*, 251-252; Nafie, L. A.; Cheng, J. C.; Stephens, P. J. *J. Am. Chem. Soc.* **1975**, *97*, 3842-3843; Hug, W.; Kint, S.; Bailey, G. F.; Scherer, J. R. *J. Am. Chem. Soc.* **1975**, *97*, 5589-5590.

(5) Nafie, L. A.; Freedman, T. B. *J. Chem. Phys.* **1983**, *78*, 7108-7116.

(6) Nafie, L. A.; Freedman, T. B. In *Circular Dichroism: Principles and Applications*; 2nd ed.; Berova, N., Nakanishi, K., Woody, R. W., Eds.; Whiley-VCH: New York, 2000.

(7) Stephens, P. J. *J. Phys. Chem.* **1985**, *89*, 748-752.

(8) Freedman, T. B.; Cao, X. L.; Dukor, R. K.; Nafie, L. A. *Chirality* **2003**, *15*, 743-758.

(9) Hipps, K. W.; Crosby, G. A. *J. Phys. Chem.* **1979**, *83*, 555-562.

(10) Nafie, L. A. In *Advances in applied FTIR Spectroscopy*; Mackenzie, M. W., Ed.; Wiley & Sons: New York, 1988, p 67-104; Polavarapu, P. L. *Applied Spectroscopy* **1989**, *43*, 1295-1297; Keiderling, T. A. In *Practical Fourier Transform Infrared Spectroscopy. Industrial and Laboratory Chemical Analysis*; Ferraro, J. R., Krishnan, K., Eds.; Academic Press: San Diego, 1990, p 203-284.

(11) Nafie, L. A. *Applied Spectroscopy* **2000**, *54*, 1634-1645; Nafie, L. A. United States, 2002; Vol. US Patent #6480277.

(12) Stephens, P. J.; Lowe, M. A. *Annu. Rev. Phys. Chem.* **1985**, *36*, 213-241; Stephens, P. J.; Devlin, F. J. *Chirality* **2000**, *12*, 172-179.

(13) Keiderling, T. A. In *Circular Dichroism: Principles and Applications*; 2nd ed.; Berova, N., Nakanishi, K., Woody, R. W., Eds.; Whiley-VCH: New York, 2000.

(14) In the area of instrumentation for example an automatic baseline correction during the measurement is required. In the area of theoretical analysis *ab initio* calculations for large (bio)molecules are still beyond present capabilities because of the size of the basis set needed to obtain the most accurate level of calculations. The modelling of solvent effects needs also further improvement.

(15) Stephens, P. J.; Devlin, F. J.; Schurch, S.; Hulliger, J. *Theoretical Chemistry Accounts* **2008**, *119*, 19-28; Monde, K.; Miura, N.; Hashimoto, M.; Taniguchi, T.; Inabe, T. *J. Am. Chem. Soc.* **2006**, *128*, 6000-6001; Tarczay, G.; Magyarfalvi, G.; Vass, E. *Angew. Chem., Int. Ed.* **2006**, *45*, 1775-1777; Dunmire, D.; Freedman, T. B.; Nafie, A. A.; Aeschlimann, C.; Gerber, J. G.; Gal, J. *Chirality* **2005**, *17*, S101-S108.

(16) Deplazes, E.; van Bronswijk, W.; Zhu, F.; Barron, L. D.; Ma, S.; Nafie, L. A.; Jalkanen, K. J. *Theoretical Chemistry Accounts* **2008**, *119*, 155-176; Jalkanen, K. J.; Degtyarenko, I. M.; Nieminen, R. M.; Cao, X.; Nafie, L. A.; Zhu, F.; Barron, L. D. *Theoretical Chemistry Accounts* **2008**, *119*, 191-210; Lee, K. K.; Oh, K. I.; Lee, H.; Joo, C.; Han, H.; Cho, M. *Chemphyschem* **2007**, *8*, 2218-2226; Yoder, G.; Keiderling, T. A.; Formaggio, F.; Crisma, M.; Toniolo, C.; Kamphuis, J. *Tetrahedron-Asymmetry* **1995**, *6*, 687-690.

(17) Moretto, A.; Formaggio, F.; Kaptein, B.; Broxterman, Q. B.; Wu, L.; Keiderling, T. A.; Toniolo, C. *Biopolymers* **2008**, *90*, 567-574.

(18) Keiderling, T. A.; Silva, R. A. G. D.; Yoder, G.; Dukor, R. K. *Bioorgan Med Chem* **1999**, *7*, 133-141; Bour, P.; Keiderling, T. A. *J. Am. Chem. Soc.* **1993**, *115*, 9602-9607.

(19) Ma, S. L.; Cao, X. L.; Mak, M.; Sadik, A.; Walkner, C.; Freedman, T. B.; Lednev, I. K.; Dukor, R. K.; Nafie, L. A. *J. Am. Chem. Soc.* **2007**, *129*, 12364-12365.

(20) Krummel, A. T.; Zanni, M. T. *J. Phys. Chem. B* **2006**, *110*, 24720-24727; Tsankov, D.; Kalisch, B.; Van de Sande, J. H.; Wieser, H. *Biopolymers* **2003**, *72*, 490-499.

(21) Shanmugam, G.; Polavarapu, P. L. *J. Am. Chem. Soc.* **2004**, *126*, 10292-10295.

(22) Keiderling, T. A. *Current Opinion in Chemical Biology* **2002**, *6*, 682-688.

(23) Buffeteau, T.; Ducasse, L.; Poniman, L.; Delsuc, N.; Huc, I. *Chem. Commun.* **2006**, 2714-2716; Ducasse, L.; Castet, F.; Fritsch, A.; Huc, I.; Buffeteau, T. *J. Phys. Chem. A* **2007**, *111*, 5092-5098.

(24) Smulders, M. M. J.; Buffeteau, T.; Cavagnat, D.; Wolffs, M.; Schenning, A. P. H. J.; Meijer, E. W. *Chirality* **2008**, *20*, 1016-1022; Izumi, H.; Ogata, A.; Nafie, L. A.; Dukor, R. K. *J. Org. Chem.* **2008**, *73*, 2367-2372; Urbanova, M.; Setnicka, V.; Devlin, F. J.; Stephens, P. J. *J. Am. Chem. Soc.* **2005**, *127*, 6700-6711.

(25) Gautier, C.; Burgi, T. *J. Am. Chem. Soc.* **2006**, *128*, 11079-11087; Johannessen, C.; Thulstrup, P. W. *Dalton Transactions* **2007**, 1028-1033; Brotin, T.; Cavagnat, D.; Dutasta, J. P.; Buffeteau, T. *J. Am. Chem. Soc.* **2006**, *128*, 5533-5540; Petrovic, A. G.; Polavarapu, P. L. *J. Phys. Chem. A* **2007**, *111*, 10938-10943.

(26) Kawauchi, T.; Kitaura, A.; Kumaki, J.; Kusanagi, H.; Yashima, E. *J. Am. Chem. Soc.* **2008**, *130*, 11889-11891.

(27) Wang, F.; Polavarapu, P. L.; Lebon, F.; Longhi, G.; Abbate, S.; Catellani, M. *J. Phys. Chem. A* **2002**, *106*, 5918-5923.

(28) Andrushchenko, V.; McCann, J. L.; van de Sande, J. H.; Wieser, H. *Vibrational Spectroscopy* **2000**, *22*, 101-109.

(29) Singh, R. D.; Keiderling, T. A. *Biopolymers* **1981**, *20*, 237-240.

(30) Baumruk, V.; Keiderling, T. A. *J. Am. Chem. Soc.* **1993**, *115*, 6939-6942.

(31) Yasui, S. C.; Keiderling, T. A.; Sisido, M. *Macromolecules* **1987**, *20*, 2403-2406.

(32) Yoder, G.; Polese, A.; Silva, R. A. G. D.; Formaggio, F.; Crisma, M.; Broxterman, Q. B.; Kamphuis, J.; Toniolo, C.; Keiderling, T. A. *J. Am. Chem. Soc.* **1997**, *119*, 10278-10285.

(33) Yasui, S. C.; Keiderling, T. A. *Biopolymers* **1986**, *25*, 5-15.

(34) Woody, R. W.; Dunker, A. K. In *Circular Dichroism and the Conformational Analysis of Biomolecules*; Fasman, G. D., Ed.; Plenum Press: New-York, 1996, p 109-157.

(35) Proteins are usually deuterium exchanged by dissolution in D_2O followed by lyophilisation, before sample preparation at 2-5 mg / 100 µmL in D_2O. The VCD spectra obtained on proteins dissolved in D_2O without previous exchange are similar in form but of lower quality.

(36) Pancoska, P.; Baumruk, V.; Keiderling, T. A. *Biophysical Journal* **1994**, *66*, A393-A393; Pancoska, P.; Yasui, S. C.; Keiderling, T. A. *Biochemistry* **1991**, *30*, 5089-5103; Keiderling, T. A.; Yasui, S. C. *Biophysical Journal* **1986**, *49*, A64-A64.

(37) Ellis, R. J.; Pinheiro, T. J. T. *Nature* **2002**, *416*, 483-484.

(38) McCann, J. L.; Schulte, B.; Tsankov, D.; Wieser, H. *Mikrochim Acta* **1997**, 809-810; McCann, J. L.; Rauk, A.; Wieser, H. *Journal of Molecular Structure* **1997**, *408*, 417-420; Mccann, J.; Tsankov, D.; Hu, N.; Liu, G.; Wieser, H. *Journal of Molecular Structure* **1995**, *349*, 309-312.

(39) Lebon, F.; Longhi, G.; Abbate, S.; Catellani, M.; Zhao, C.; Polavarapu, P. L. *Synthetic. Met.* **2001**, *119*, 75-76.

(40) The stereocomplex of poly(methyl methacrylate) (PMMA) is a unique polymer based supramolecule composed of complementary isotactic (it)- and syndiotactic (st)-PMMAs with an it/st stoichiometry of 1:2. For a recent review see: Hatada, K.; Kitayama, T. *Polymer. Int.* **2000**, *49*, 11-47.

(41) Tang, H. Z.; Boyle, P. D.; Novak, B. M. *J. Am. Chem. Soc.* **2005**, *127*, 2136-2142; Tang, H. Z.; Lu, Y. J.; Tian, G. L.; Capracotta, M. D.; Novak, B. M. *J. Am. Chem. Soc.* **2004**, *126*, 3722-3723.

(42) Tang, H. Z.; Garland, E. R.; Novak, B. M.; He, J. T.; Polavarapu, P. L.; Sun, F. C.; Sheiko, S. S. *Macromolecules* **2007**, *40*, 3575-3580.

(43) Nolte, R. J. M. *Chem. Soc. Rev.* **1994**, *23*, 11-19; Suginome, M.; Ito, Y. *Adv. Polym. Sci.* **2004**, *171*, 77-136; Otten, M. B. J.; Metselaar, G. A.; Cornelissen, J. J. L. M.; Rowan, A. E.; Nolte Roeland, J. M. In *Foldamers: Structure, Properties, and Applications*; Hecht, S., Huc, I., Eds.; Weinheim: Wiley-VCH: 2007; Cornelissen, J. J. L. M.; Rowan, A. E.; Nolte, R. J. M.; Sommerdijk, N. A. J. M. *Chem. Rev.* **2001**, *101*, 4039-4070; Cornelissen, J. J. L. M.; Donners, J. J. J. M.; de Gelder, R.; Graswinckel, W. S.; Metselaar, G. A.; Rowan, A. E.; Sommerdijk, N. A. J. M.; Nolte, R. J. M. *Science* **2001**, *293*, 676-680.

(44) Nolte, R. J. M.; Van Beijnen, A. J. M.; Drenth, W. *J. Am. Chem. Soc.* **1974**, *96*, 5932-5933.

(45) Miyabe, T.; Hase, Y.; Iida, H.; Maeda, K.; Yashima, E. *Chirality* **2009**, *21*, 44-50; Schwartz, E.; Palermo, V.; Finlayson, C. E.; Huang, Y.-S.; Otten, M. B. J.; Liscio, A.; Trapani, S.; González-Valls, I.; Brocorens, P.; Cornelissen, J. J. L. M.; Peneva, K.; Müllen, K.; Spano, F.; Yartsev, A.; Westenhoff, S.; Friend, R. H.; Beljonne, D.; Nolte, R. J. M.; Samori, P.; Rowan, A. E. *Chem. Eur. J.* **2009**, *15*, 2536-2547; Palermo, V.; Otten, M. B. J.; Liscio, A.; Schwartz, E.; de Witte, P. A. J.; Castriciano, M. A.; Wienk, M. M.; Nolde, F.; De Luca, G.; Cornelissen, J. J. L. M.; Janssen, R. A. J.; Mullen, K.; Rowan, A. E.; Nolte, R. J. M.; Samori, P. *J. Am. Chem. Soc.* **2008**, *130*, 14605-14614; Onouchi, H.; Okoshi, K.; Kajitani, T.; Sakurai, S. I.; Nagai, K.;

Kumaki, J.; Onitsuka, K.; Yashima, E. *J. Am. Chem. Soc.* **2008**, *130*, 229-236; Kajitani, T.; Okoshi, K.; Yashima, E. *Macromolecules* **2008**, *41*, 1601-1611; Onitsuka, K.; Mori, T.; Yamamoto, M.; Takei, F.; Takahashi, S. *Macromolecules* **2006**, *39*, 7224-7231; Amabilino, D. B.; Serrano, J. L.; Sierra, T.; Veciana, J. *J. Polym. Sci., Part A: Polym. Chem.* **2006**, *44*, 3161-3174; Fujitsuka, M.; Hara, M.; Tojo, S.; Okada, A.; Troiani, V.; Solladie, N.; Majima, T. *J. Phys. Chem. B* **2005**, *109*, 33-35; Takei, F.; Kodama, D.; Nakamura, S.; Onitsuka, K.; Takahashi, S. *Journal of Polymer Science, Part A: Polymer Chemistry* **2005**, *44*, 585-595.

(46) Van Beijnen, A. J. M.; Nolte, R. J. M.; Drenth, W.; Hezemans, A. M. F. *Tetrahedron* **1976**, *32*, 2017-19.

(47) Van Beijnen, A. J. M.; Nolte, R. J. M.; Zwikker, J. W.; Drenth, W. *J. Mol. Catal.* **1978**, *4*, 427-32; Van Beijnen, A. J. M.; Nolte, R. J. M.; Naaktgeboren, A. J.; Zwikker, J. W.; Drenth, W.; Hezemans, A. M. F. *Macromolecules* **1983**, *16*, 1679-89; Cornelissen, J. J. L. M.; Graswinckel, W. S.; Rowan, A. E.; Sommerdijk, N. A. J. M.; Nolte, R. J. M. *J. Polym. Sci., Part A: Polym. Chem.* **2003**, *41*, 1725-1736.

(48) Van Beijnen, A. J. M.; Nolte, R. J. M.; Drenth, W.; Hezemans, A. M. F.; Van de Coolwijk, P. J. F. M. *Macromolecules* **1980**, *13*, 1386-1391.

(49) Cornelissen, J. J. L. M.; Sommerdijk, N. A. J. M.; Nolte, R. J. M. *Macromol. Chem. Physic.* **2002**, *203*, 1625-1630.

(50) Hase, Y.; Nagai, K.; Iida, H.; Maeda, K.; Ochi, N.; Sawabe, K.; Sakajiri, K.; Okoshi, K.; Yashima, E. *J. Am. Chem. Soc.* **2009**, *131*, 10719-10732.

(51) Didraga, C.; Klugkist, J. A.; Knoester, J. *J. Phys. Chem. B* **2002**, *106*, 11474-11486.

(52) Eisfeld, A.; Kniprath, R.; Briggs, J. S. *J. Chem. Phys.* **2007**, *126*, 104904.

(53) Somsen, O. J. G.; vanGrondelle, R.; vanAmerongen, H. *Biophysical Journal* **1996**, *71*, 1934-1951.

(54) In the notation of Refs 51–53 the polyisocyanide helix is a special case in which $n_2 = 0$.

(55) In the notation of Ref 51, $\phi = 90° - \alpha$

(56) Higgs, P. W. *Proceedings of the Royal Society of London Series a-Mathematical and Physical Sciences* **1953**, *220*, 472-485.

(57) Miyazawa, T. *J. Chem. Phys.* **1960**, *32*, 1647-1652.

(58) Tinoco, I. *J Chim Phys Pcb* **1968**, *65*, 91-97.

(59) Schellman, J. A. *Acc. Chem. Res.* **1968**, *1*, 144-151.

(60) Cornelissen, J. J. L. M. *Pure. Appl. Chem.* **2002**, *74*, 2021-2030.

(61) Metselaar, G. A.; Cornelissen, J. J. L. M.; Rowan, A. E.; Nolte, R. J. M. *Angew. Chem., Int. Ed.* **2005**, *44*, 1990-1993.

(62) Cornelissen, J. J. L. M.; Donners, J. J. J. M.; de Gelder, R.; Graswinckel, W. S.; Metselaar, G. A.; Rowan, A. E.; Sommerdijk, N. A.; Nolte, R. J. M. *Science* **2001**, *293*, 676-80.

(63) Moffat, J.; Newton, M. V.; Papenmei.G.J. *J. Org. Chem.* **1962**, *27*, 4058.

(64) Nolte, R. J. M.; Van Beijnen, A. J. M.; Zwikker, J. W.; Drenth, W. *Macromolecular Syntheses* **1985**, *9*, 81-83.

3

Polyisocyanides with perylene and platinum-porphyrin side groups[§]

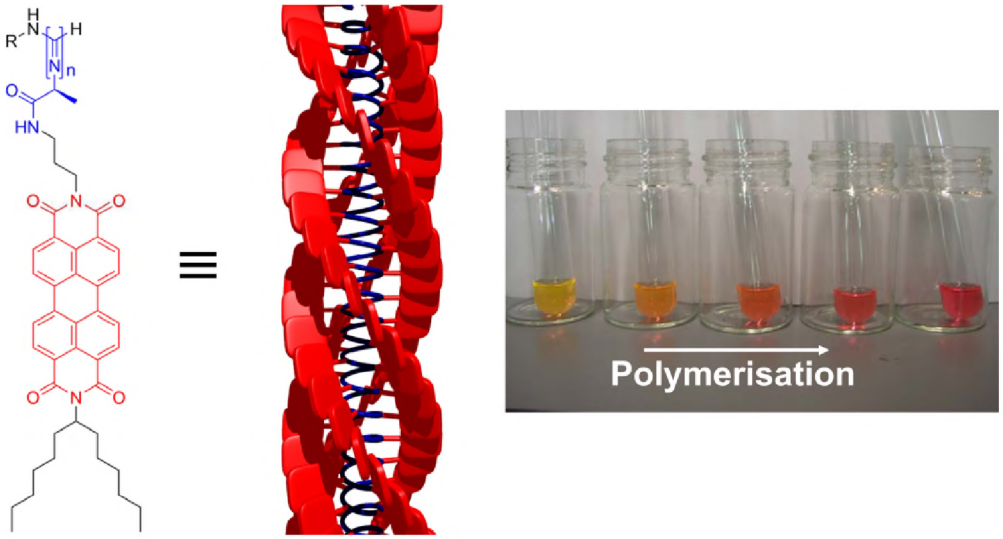

[§]Parts of this work have been published: Schwartz, E.; Palermo, V.; Finlayson, C. E.; Huang, Y.-S.; Otten, M. B. J.; Liscio, A.; Trapani, S.; González-Valls, I.; Brocorens, P.; Cornelissen, J. J. L. M.; Peneva, K.; Müllen, K.; Spano, F.; Yartsev, A.; Westenhoff, S.; Friend, R. H.; Beljonne, D.; Nolte, R. J. M.; Samori, P.; Rowan, A. E. *Chem. Eur. J.* **2009**, *15*, 2536–2547; Palermo, V.; Otten, M. B. J.; Liscio, A.; Schwartz, E.; de Witte, P. A. J.; Castriciano, M. A.; Wienk, M. M.; Nolde, F.; De Luca, G.; Cornelissen, J. J. L. M.; Janssen, R. A. J.; Mullen, K.; Rowan, A. E.; Nolte, R. J. M.; Samori, P. *J. Am. Chem. Soc.* **2008**, *130*, 14605–14614.; Finlayson, C. E.; Friend Richard, H.; Otten, M. B. J.; Schwartz, E.; Cornelissen, J. J. L. M.; Rowan, A. E.; Samori, P.; Palermo, V.; Liscio, A.; Peneva, K.; Mullen, K.; Trapani, S.; Beljonne, D. *Adv. Funct. Mater.* **2008**, *18*, 3947–3955.

3.1 Introduction

The synthesis of complex molecular systems in which chromophores are ordered in well-defined positions to achieve extremely high energy and electron transfer pathways represents a great challenge in chemistry and materials science. This goal lies at the foundation of various optoelectronic applications, such as photovoltaic devices and field effect transistors (FETs). Within the frame of (fundamental) research focussed on finding new systems for implementing these applications, the endeavour has been towards addressing the development of new structures that feature a cofacial arrangement of chromophores, such as polycyclic aromatic systems, to allow a high degree of π-orbital overlap and significant exciton coupling. High electron mobilities[1] and also fast exciton transport over large distances[2] have been measured in such cofacial systems. Several approaches to obtain well organised perylene-bis(dicarboximides) (PDIs) structures for application in solar cells and FETs are described in the literature including studies on perylene crystals,[3] aggregates[4-6] and liquid crystals.[7] Alongside the aggregation of monomeric PDIs units, several examples have also been reported in which face-to-face aggregation of PDIs is promoted by an oligomeric or polymeric architecture.[8,9] The investigations into the PDI structures have been mainly concentrated on flexible polymer architectures. We therefore decided to investigate the incorporation of PDI units onto the backbone of polyisocyanides, which are able to adopt a very stable, well-defined 4_1 helical conformation when the side chains contain a bulky group or bear additional stabilising interactions.[10,11] The introduction of peptide substituents orders the side groups into a precise architecture, resulting in an attractive scaffold onto which functional groups such as thiophenes,[12] porphyrins[13] and perylenes diimides,[14] can be arranged into well-defined arrays, thus creating new materials with potentially interesting properties. These polymers could therefore be ideal candidates for photovoltaic cells, although unfortunately they suffer from very poor solubility in organic solvents. [14] Moreover, the organisation of the perylenes makes the material interesting for applications as nanoscale or macroscopic wires and as field-effect transistors (FETs).

In this chapter, two methods to create perylene appended helical nanowires are described; namely, the formation of perylene pendant polyisocyanides and the formation of statistical copolymers containing perylene and platinum porphyrin groups. In addition, an attempt to construct a monomeric isocyanide provided with both a perylene and a porphyrin molecule, which are covalently linked, is described.

3.2 Helter-skelter-like perylene polyisocyanopepetides

In this paragraph the synthesis and characterisation of two new PDI-polyisocyanide systems both of which have an improved solubility in organic solvents, is briefly discussed. A more detailed overview on this subject can be found in the thesis of Matthijs Otten of our group.[15] We have designed polymer **P2**, which exposes sterically demanding phenoxy substituents in the bay area of the PDI, and polymer **P3**, which contains long alkyl tails in the side chains (Figure 1). The incentive for the preparation and study of **P2** was to determine whether the bulky phenoxy groups in the PDI bay area would hinder the well-known tendency of PDIs to stack through π-π interactions. Furthermore, the bulky character of the non-planar PDIs in **P2** may also inhibit the formation of excimers, which might be beneficial for exciton transportation, since excimer sites act as traps in which energy is lost as fluorescence. For the sake of comparison, polymer **P1**, which consists of a central PIC backbone exposing an alanine-alanine segment and terminal methoxy groups, was also prepared and studied.

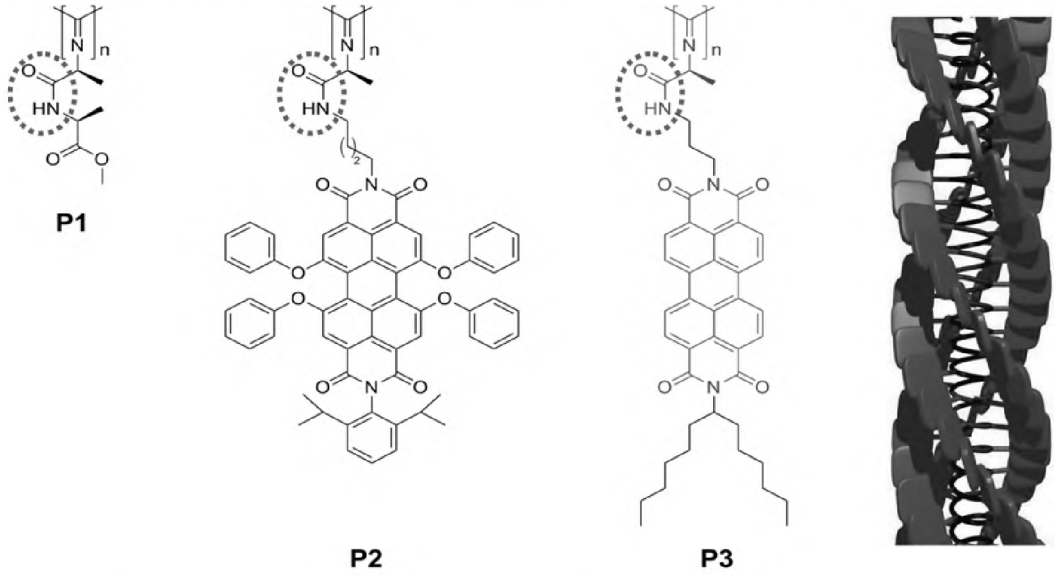

Figure 1. Molecular structures of the polymers **P1**–**P3**. The amide unit that is responsible for the stabilisation of the helical structure by forming a hydrogen bonding network is encircled. A schematic structure of **P3** is depicted on the right.

Synthesis

Polymers **P1**–**P3** were prepared by a nickel catalysed polymerisation reaction of the isocyanide monomers. The synthesis and characterisation of polymer **P1** has been described in detail in the literature and will not be discussed here.[16] The perylene-bis(dicarboximide) functionalised polymer **P3** was synthesised following a slightly modified strategy to that described for the synthesis of the PDI functionalised polyisocyanides with shorter alkyl tails.[14] In short, an amine functionalised asymmetric PDI, synthesised using the method reported by Langhals and co-workers,[17,18] was coupled to Boc-L-alanine. After removal of the

Boc protecting group, the amine was formylated and subsequently dehydrated using diphosgene and *N*-methylmorpholine.

Upon polymerisation of the isocyanide precursor, using a Ni(II) catalyst in CH_2Cl_2 at room temperature, of polymer **P3**, the reaction mixture turned from yellow to red, which is typical for the aggregation of PDIs and in this particular case indicative of the polymerisation leading to intramolecular aggregation of the PDI units. The polymer was purified by repetitive precipitation, first in methanol/water (1:1 v/v) and then in methanol until no monomer fluorescence was visible. The solubility of **P3** was found to be much larger than that of the perylene functionalised polyisocyanide described in previous work,[14] and therefore polymer **P3** is more easily studied and better processable. Polymer **P3** was soluble (to at least 10 mg ml^{-1}) in chlorinated solvents (CH_2Cl_2, $CHCl_3$, dichloroethane, tetrachloroethane) and solvents such as benzene, toluene and tetrahydrofuran. From IR spectroscopy it was concluded that upon polymerisation the absorptions at 3438 and 3391 cm^{-1}, attributed to the trans and cis amide N-H stretching vibrations, respectively,[19] shifted to 3294 cm^{-1}. This shift is indicative of hydrogen bond formation between the amides, exclusively in the trans configuration. It was determined from the disappearance of the isocyanide signal at 2140 cm^{-1} that the reaction was complete after ~1000 seconds.

In contrast to the fast polymerisation of the **P3** precursor isocyanide, seven days were required for the isocyanide monomer with the bulky phenoxy substituents in the bay area to be completely consumed, as concluded from TLC. This polymerisation occurs at a similar rate to that observed for the polymerisation of *tert*-butyl isocyanide[20]and can be attributed to the bulkiness of the PDI units. During the polymerisation of the bulky isocyanide the reaction mixture turned slightly darker, from purple to deep purple, but a clear colour change, as visible in the preparation of **P3**, was not observed. Polymer **P2** was purified by size exclusion chromatography and was found to be soluble in most organic solvents, including toluene and THF. Determination of the molecular weight (MW) of polymers **P2** and **P3** with the help of gel permeation chromatography (GPC) was difficult because the behaviour of a rod-like polymer in a gel is not straightforward. We, therefore, estimated the MW of these polymers by AFM using dilute solutions of the polyisocyanide (10^{-6} M in $CHCl_3$) spincoated onto freshly cleaved muscovite mica. This approach revealed single fibres and, due to their rigidity, the polymers were stretched out on the surface and their contour lengths could be accurately measured. This approach has been used by Prokhorova et al.[21] to determine the absolute molecular weight of polymethacrylates and polystyrenes with bulky substituents, and could also be applied to our polyisocyanopeptides.[22] According to the AFM images of **P3**, the average length of **P3** was 180 nm. From the analysis of AFM images of **P2** on muscovite mica, an average polymer chain length of 110 nm was determined. Assuming a 4_1 type helix with a helical pitch of 0.46 nm (measured by powder X-ray diffraction on **P1**,[22,23] 180 nm

corresponds to 1.2×10^3 repeat units and a M_n of 9×10^5 g mol^{-1}. For **P2** a value for M_n of 1.1×10^6 g mol^{-1} could be calculated.

UV-Visible spectroscopy

The absorption spectrum of **P3** in chloroform showed vibronic bands of the PDI S_0-S_1 optical transition between 400 and 600 nm (Figure 2). Compared to the spectrum of the isocyanide monomer, the absorption spectrum of the polymer revealed a blue shifted maximum and a relatively increased oscillator strength for the 0-1 and 0-2 vibrational transitions over the 0-0 transition; this can be quantified by the ratio of the absorptions $A^{0\rightarrow0}$/ $A^{0\rightarrow1}$, which has a value of 1.66 for the monomer and 0.66 for the polymer.[9] In addition, the maxima of all vibronic bands were red shifted by 2–6 nm and a broad absorption tail was found to be present at lower energy than the 0-0 transition of monomer **9**. These spectral changes observed upon polymerisation are reminiscent of weak exciton coupling interactions (strong exciton-phonon coupling) between the PDIs in H-type aggregates.[24]

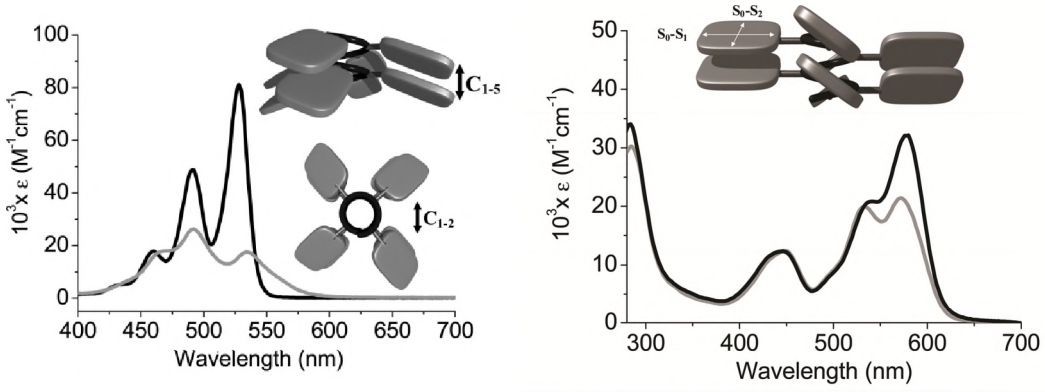

Figure 2. Absorption spectrum of **P3** (grey) and the isocyanide monomer precursor (black) ($CHCl_3$; 10^{-5} M). Inset: Illustration of the different interactions between the PDIs in polymer **P3** (left) and Absorption spectrum of **P2** (grey) and the isocyanide monomer (black). Inset: Illustration of the S_0-S_1 and S_0-S_2 transition dipoles ($CHCl_3$; 10^{-5} M) (right)

Circular Dichroism Spectroscopy

Since the polymers adopt a helical arrangement induced by the L-alanine unit in the side arms of the polymer, circular dichroism spectroscopy (CD) is a powerful tool to analyse the arrangement of the chromophores in the polyisocyanopeptides.[13,26] The CD spectrum of **P3** revealed strong positive and weaker negative signals for the exciton coupled S_0-S_1 vibronic transitions between 420 and 600 nm (Figure 3). No CD signal was detected for the monomer. The CD effect is unlike any other signals observed for chiral perylene bisimides stacks and can be rationalised by considering the multiple chiral interactions in which every perylene bisimide unit is involved.[6,27] In **P3** every chromophoric unit has chiral interactions with adjacent units within the same stack (C_{1-5}) and with units in adjacent stacks (C_{1-2}) (see Figure

2). Whereas the signal arising from interactions between two nearest PDIs in different stacks reflects the helicity of the polymer backbone, the signal between two perylenes within the same stack originates from the helicity of the S_0-S_1 transitions within the PDI stacks.[28] The positive signal at higher wavelength, most likely originating from a positive bisignate signal, would correspond to a right handed polymer helix.[29] This is in agreement with the smaller positive cotton effect at 317 nm originating from the helicity in the polyimine backbone. The latter signal is similar to that observed for right-handed helices of **P1** and also reflects the robustness of the isocyano-L-alanyl backbone, which is not influenced by the outer PDI substituents.[10,26,30] This robustness is also reflected by the identical CD spectra of polymer **P3** in different solvents, such as chloroform, tetrachloroethane and toluene.

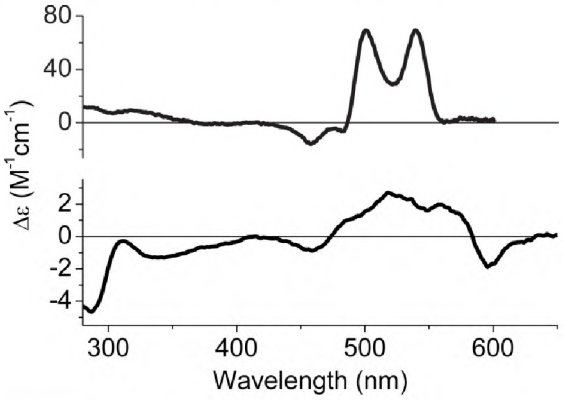

Figure 3. Circular Dichroism spectra of polymer **P3** (top) and polymer **P2** (bottom) ($CHCl_3$; 10^{-5} M).

The CD spectrum of **P2** displayed a signal for the perylene absorptions with a lower intensity (30 times) than that observed for **P3** (Figure 3). This suggests that the PDI units in the $C_{1\text{-}4}$ geometry (Figure 2) have either a very small twist angle with respect to each other or that this angle fluctuates between positive and negative values along the stack. It is possible that the weak CD effect originates not from exciton coupling, but from induced chirality in the perylene plane; for these phenoxy substituted PDIs an excess of an *M* or *P* twist is likely to be induced by the incorporation of these units into the helical polymer backbone. Such an effect has previously been observed for aggregates of similar PDIs for which a similar CD effect was observed.[27] A relatively strong signal for **P2** was visible at λ = 284 nm, preceded by a broad signal around λ = 338 nm. The signal located at 280 nm is most likely caused by chiral interactions between the phenoxy substituents, however, the imine backbone signal is also expected to be present in this region. It is therefore difficult to conclude from the CD signal in this region what the helical conformation of the polymers is.

Fluorescence spectroscopy

The fluorescence spectrum of **P3**, compared to that of monomer **9**, showed a broad structureless red shifted emission at λ = 625 nm with a fluorescence quantum yield of 3.7% (in $CHCl_3$ at ambient atmosphere[31]) upon excitation at the absorption maximum (λ = 492 nm; Figure 4). The low quantum yield and long fluorescence lifetime (≈24 ns as compared to the usual value of 3–4 ns in the perylene monomer[32]) of the emission are reminiscent of a parallel orientation of the transition dipoles and are in agreement with the absorption characteristics. The featureless emission of the polymer, which is red-shifted by more than 70 nm, together with the fact that the shift in the emission spectrum is much larger than the shift in the absorption spectrum, is indicative of the formation of an intramolecular excimer-like species, although the effect of aggregate states cannot be ruled out. Excimer species are only formed after excitation of monomeric species and therefore the emission, but not the absorption, is red-shifted. The chromophores in an excimer are typically 0.3–0.4 nm apart and can involve more than two chromophoric units in molecular aggregates.[14,33] The formation of excimers of aromatic hydrocarbons is restricted to a parallel cofacial conformation and confirms the hypothesis that the PDIs stack in an H-aggregated fashion.

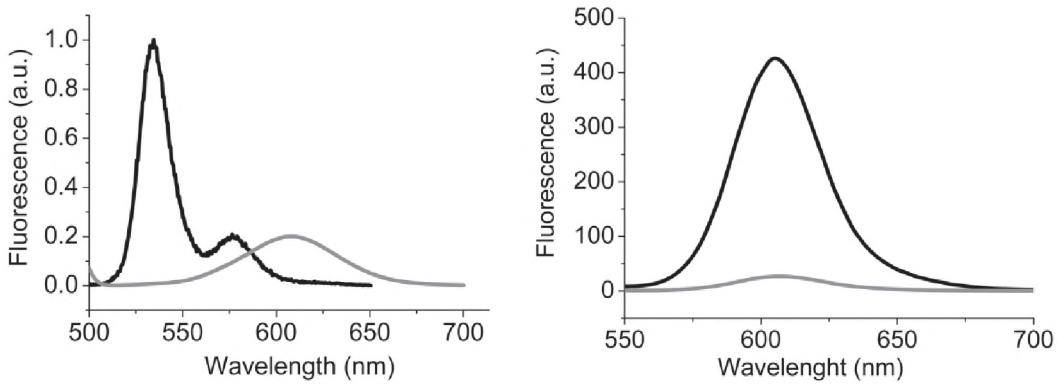

Figure 4. Solution fluorescence spectra of polymer **P3** (intensity ×5, grey) and the monomeric precursor (black) ($CHCl_3$; 10^{-6} M) (left) and solution fluorescence spectra of polymer **P2** (grey) and the monomeric precursor **12** (black) ($CHCl_3$; 10^{-6} M) (right).

The fluorescence spectrum of **P2** had a slightly red shifted emission at λ = 607 nm compared to λ = 605 nm observed for the monomer (Figure 4). This value is comparable to the shifts in the absorption spectrum (Figure 2). The fluorescence quantum yield of **P2** amounted to 3.0% with respect to the monomer. This low quantum yield is in line with H-aggregated PDIs, however, it can also be attributed to electron transfer between a PDI unit and a neighbouring phenoxy substituent. The emission spectra gave no evidence for the occurrence of excimer emission, as was observed for **P3**, which confirms that the steric bulk of the phenoxy groups of the PDI units in **P2** is able to prevent excimer formation.

Organic devices[15]

The photovoltaic efficiency of the n-type material **P3** with well-studied p-type polymers (P3HT,[34,35] PFB[35] and F8BT[35])[36] was investigated by bulk-heterojunction photovoltaic devices using indium tin oxide (ITO)/polyethylene-dioxythiophene:polystyrene sulphonate (PEDOT:PSS) as anode and aluminium as cathode. The devices had a modest overall efficiency of 0.2%, which is far from state-of-the-art for organic solar cells. It is noticeable, however, that there was at least one order of magnitude increase in maximum power efficiency as compared to the monomeric PDI analogue in the studies with P3HT and PFB. The blend system with F8BT showed no significant enhancement in performance, which might be due to the morphology (phase separation) and orientation of the perylene moieties with respect to the plane of the device substrate. To correlate this enhanced behaviour with respect to the polymeric architecture, AFM investigations on the mixtures were conducted.[34] These studies revealed that the two polymers form interpenetrated bundles having a nanophase segregated character and featuring a high density of contact points between the two different phases. To visualize the relationship between the architecture and the photovoltaic efficiency, Kelvin probe force microscopy (KPFM) measurements were carried out on submonolayer-thick films.

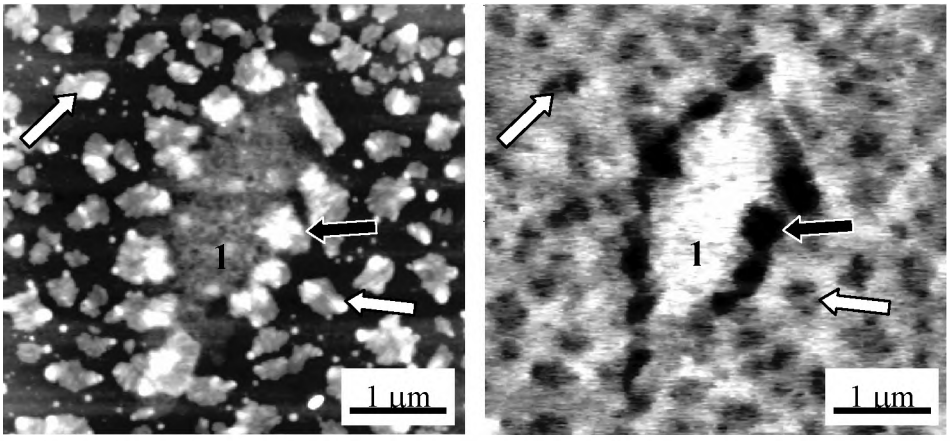

Figure 5. AFM (left) and KPFM (right) studies on monomeric PDI/P3HT blends on native silicon oxide. The potential image is recorded under white light (60 mW cm^{-2}) illumination. Monomeric PDI agglomerates are isolated (white arrows) or in contact (black arrows) with P3HT islands (marked with 1).

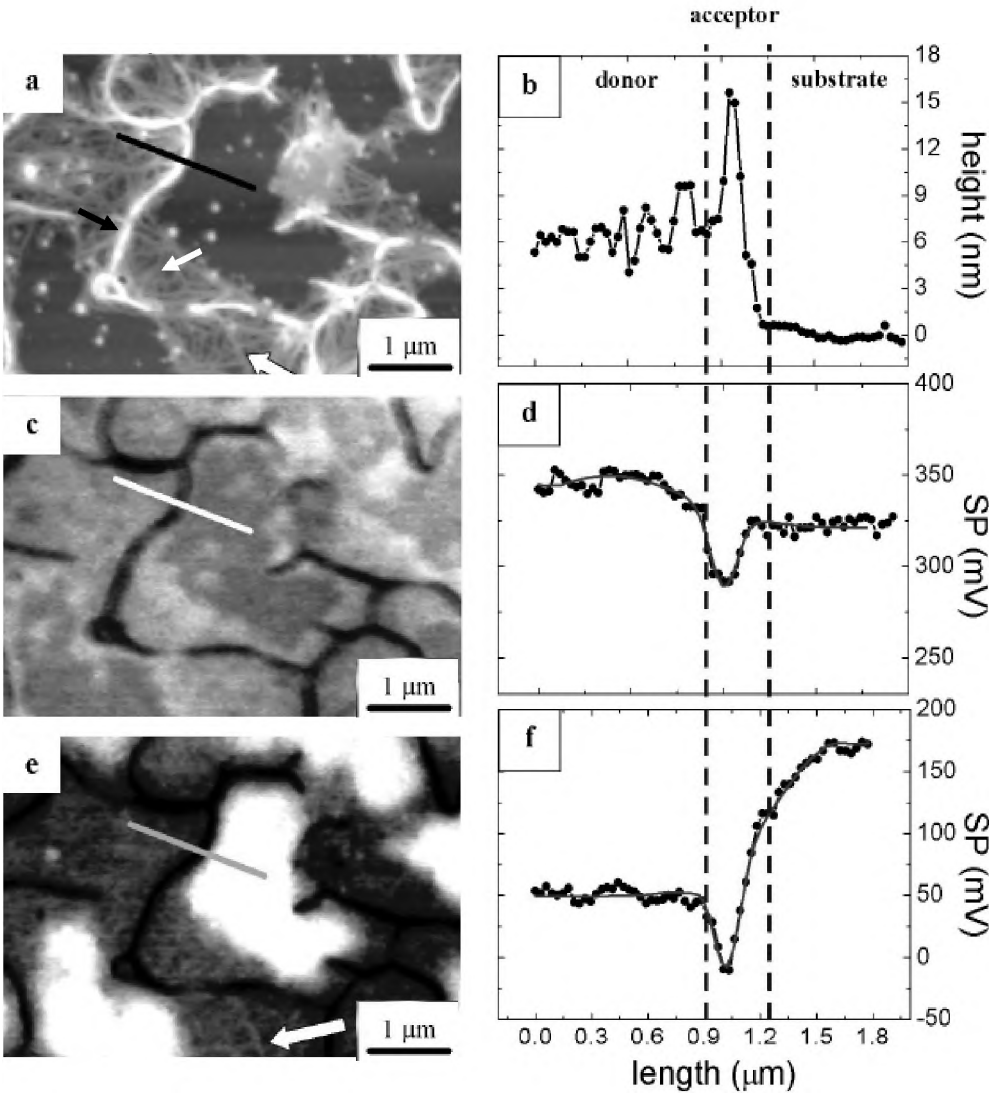

Figure 6. a) AFM topography image of a thin blend of **P3** and P3HT deposited on silicon. c) Surface potential (KPFM) image of the same area as in a), with no illumination and e) under white light (≈60 mW cm^{-2}) illumination. b), d) and f) Measured (black lines and circles) and simulated (red lines) profiles obtained tracing an arbitrary line in the corresponding images a), c) and e).

This technique allowed, for the first time, the direct visualisation of the photovoltaic activity occurring in such a nanoscale phase segregated thin film with true nanoscale spatial resolution, thus making possible a study of the correlation between function and architecture with nanoscale resolution. Significantly different results for the monomeric PDI-P3HT blend (Figure 5) were obtained compared to those obtained for the **P3**/P3HT blend (Figure 6). First, the observed potential difference between the two phases with the light off was much smaller in the **P3**/P3HT system than in the case of the monomeric PDI-P3HT blend. Second, the charging of the monomeric PDI clusters obtained upon light irradiation varied greatly. Figure 5 (right) displays the KPFM image corresponding to the topographic image shown on the left in Figure 5. In particular, upon light irradiation, the PDI clusters in contact

with the P3HT island (black arrows) became much more negatively charged (they appear darker in the KPFM image) than the clusters at a larger distance from any P3HT island (white arrows). The part of the cluster in connection with P3HT has a higher negative charge, whereas the other part of the same cluster, which is in contact with SiO_x, has a lower charge. This evidence indicates that the charges, which are generated at the monomeric PDI/P3HT interface are strongly localised and do not diffuse very far from the acceptor–donor interface, as could be seen for the **P3**/P3HT system.

The electronic transport properties of **P1–P3** were also studied in thin-film transistors (TFT). In TFT devices where the transistor channel lengths are somewhat greater than the average polymer chain length, carrier mobilities in the order of $10^{-5}/10^{-6}$ $cm^2 V^{-1} s^{-1}$ were found for **P3** (Figure 7), which are limited by inter-chain transport processes.

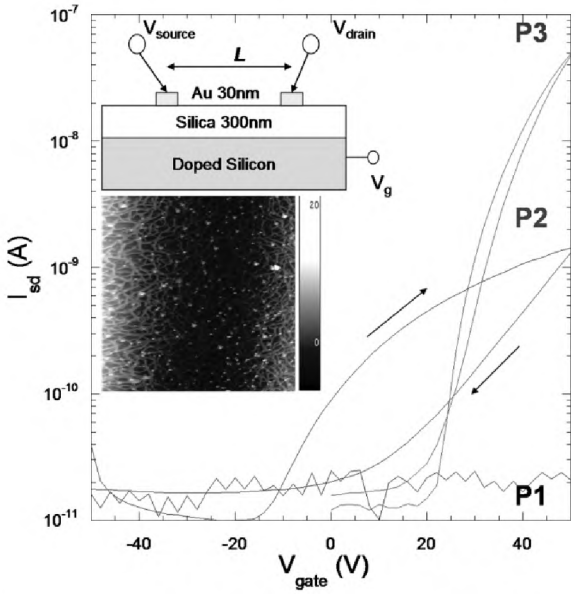

Figure 7. The top inset of this figure shows a schematic representation of the TFT device architecture. Channel lengths (L) varying between 2–20 µm were investigated and the devices were provided with inter-digitated electrodes, giving long device widths (W) of 10,000 µm and device capacitances of ~11nF cm^{-2}. The main figure shows the transfer characteristics of TFTs of **P1**, **P2** and **P3**, as indicated, with a source-drain bias of 20 V and L= 2 µm in each case. The gate-voltage sweep direction was from –50 V to +50 V and then back to –50 V, as indicated by the arrows. The lower inset shows a representative AFM image of a network of **P3** deposited into a transistor channel of length ~2 mm. The raised areas, toward the edges of the image, show where the material is deposited between the electrode and the channel. The micrograph has an area of 2 µm x 2 µm. The height scale (0–20 nm) is also shown.

Polymer **P1** did not show any semiconducting properties (no working transistor was obtained); **P2** gave working transistors but with very low n-type mobilities. The electron injection properties of the source and drain Au electrodes could be significantly improved by surface treatment with a chemisorbed alkanethiol self- assembled monolayer (SAM).[37] This approach gave a linear-regime mobility value (for **P3**) in the order of 10^{-4} cm^2 V^{-1} s^{-1}, an on-

off ratio of 10^5 and a sub-threshold swing of 5 V per decade, at room temperature.[38] Not surprisingly, we found carrier mobilities, which were intermediate in magnitude between the cases of amorphous spin-coated films of perylene and single crystal perylene transistors.[39]

These finding show that our perylene functionalised polymers can be used as materials in organic devices. With the help of the photophysical and morphological studies a greater understanding of the characteristics of the devices could be obtained.

3.3 Statistical copolymers with pendant perylene and platinum-porphyrin groups

In addition to perylenes, porphyrins and metallo porphyrins are also interesting compounds for the assembly of well-ordered materials. Over the last decades, numerous porphyrin complexes have been prepared and their photophysical properties, such as energy transfer, charge separation and recombination, have been thoroughly investigated. In our group a wide variety of porphyrin based materials have been synthesised, including porphyrin clips, boxes and porphyrin pendant polyisocyanides (see Chapter 1). Because both perylene and porphyrin isocyanides were available in our group, it was of interest to prepare statistical copolymers of these isocyanide compounds, with the aim to obtain a better understanding of the photophysical properties of the chromophoric polyisocyanides. In this section the synthesis and characterisation of the statistical copolymers is described and a brief summary of their complex photophysical characteristics is given. The photophysical studies were performed in the group of Prof. Sir Richard Friend at the Cavendish Laboratories in Cambridge.

Synthesis of monomer and polymers

Polymers **P4**–**P6** (Scheme 2 and Table 1) were prepared by a nickel-induced polymerisation reaction of the corresponding isocyanide monomers. The platinum porphyrin appended isocyanide **7** was synthesised according to a slightly modified strategy as described for the synthesis of the free base isocyano porphyrin reported by de Witte et al.[13] The mono hydroxy-porphyrin **1** was prepared by the Adler method (Scheme 1),[40] and converted into the platinum porphyrin **2**. To this end, **1** was treated with bis-benzonitrile-platinum(II) chloride in benzonitrile and the mixture was refluxed at 190 °C for 24 hrs. The metal insertion was accompanied by a colour change from purple to orange. The amino functionalised porphyrin **3** could be directly obtained from **2** by reaction with 3-bromopropylamine and NaOH as a base. Subsequently, compound **3** was functionalised with a Boc protected L-alanine by applying carbo diimide chemistry to yield **4**.

The Boc protecting group of **4** was removed with TFA and the product **5** was formylated with 2,4,5 trichlorophenyl formate to give **6**. The formamide was converted into the isocyanide **7**

using diphosgene as the dehydrating agent and *N*-methylmorpholine as a base. The perylene appended isocyanide **8** was synthesised as described in section 3.2. The polymerisation of each of the two chromophoric isocyanides resulted in the homopolymers **P3** (perylene) (see above) and **P4** (platinum-porphyrin), respectively (Scheme 2).

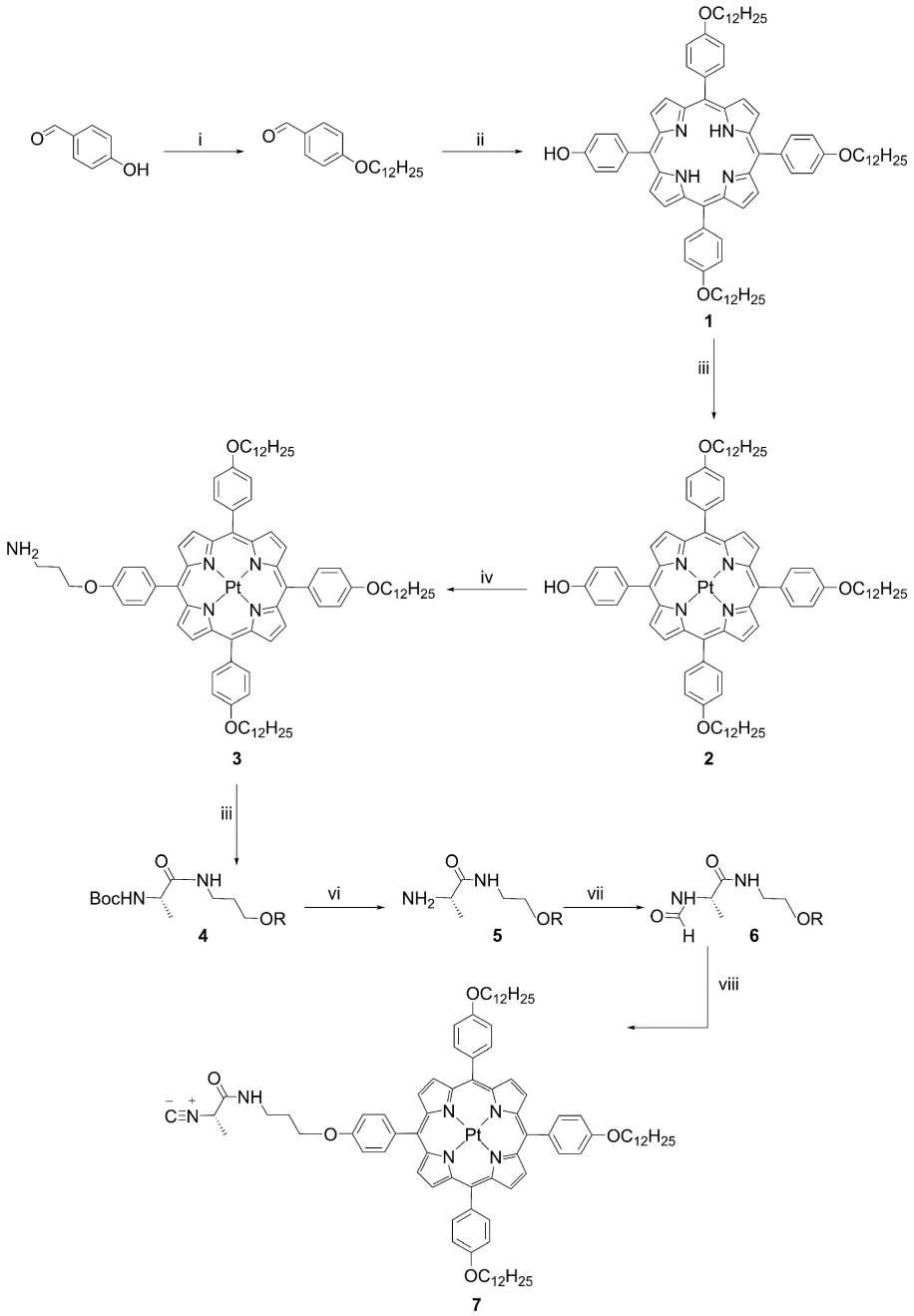

Scheme 1. Reagents and conditions for the synthesis of isocyanide monomer **7**. i) 1-bromo-dodecane, K_2CO_3, DMF, 40 hours; ii) 4-hydroxybenzenaldehyde, propionic acid, pyrrole, 140 °C; iii) $PtCl_2(PhCN)_2$, benzonitrile, 190 °C; iv) bromopropylamine hydrobromide, NaOH, DMF, toluene; v) Boc-L-alanine-OH, HOBt, DIPEA, EDC; vi) TFA, CH_2Cl_2; vii) 2,4,5-trichloro phenyl formate, CH_2Cl_2; viii) diphosgene, *N*-methylmorpholine, CH_2Cl_2, –30 °C. R = porphyrin in compounds **4**–**6**.

During the polymerisation of the platinum-porphyrin isocyanide **7** to form **P4** no clear colour change was observed. Polymers **P5** and **P6** were obtained by the statistical copolymerisation of monomers **7** and **8** using a feed ratio of 1:10 (for **P5**) and 1:1 (for **P6**), respectively (Scheme 2 and Table 1). The polymers were purified by repetitive precipitation in methanol/water and subsequently subjected to size-exclusion chromatography to remove non-reacted monomers from the solution.[41]

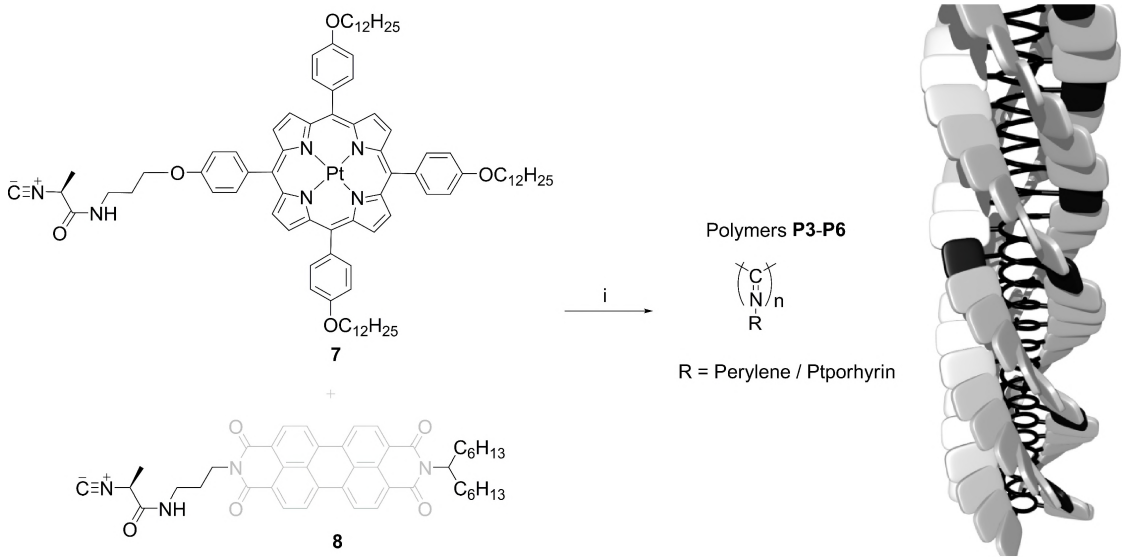

Scheme 2. Molecular structures of the isocyanide monomers **7** and **8** (left) and a schematic representation of the statistical copolymers obtained by the nickel-induced polymerisation of **7** and **8** with the backbone in black, the PDI groups in grey and the platinum-porphyrin groups in black (right). Reagents and conditions: i) 1/1000 equiv. $Ni(ClO_4)_2 \cdot 6H_2O$, CH_2Cl_2, rt.

Table 1 Polymers formed by the statistical copolymerisation of the isocyanide monomers **7** and **8**

Polymer	**P3**	**P4**	**P5**	**P6**
Ratio Perylene / Ptporphyrin	100/0	0/100	10/1	1/1

^{1}H NMR spectroscopy on the polymers **P4**–**P6** showed strong broadening of all the proton signals, which suggested the formation of polymers. In the IR spectrum, the signal of the isocyanide peak at ~2140 cm^{-1} had disappeared. Analogous to the related isocyanopeptides[13,22,42] the NH-stretch and the amide I vibrations had shifted indicating the presence of a hydrogen bonding network in the side chains of the polymers.

The L-alanine units in the side chains of the polymers can be expected to induce a helical conformation and therefore CD studies were conducted (Figure 8). The CD spectrum of **P3** displayed exciton coupled vibrations between 420 and 600 nm as described in section 3.2.[42]

The small cotton effect at 310 nm originates from the n-π^* transitions of the polyimine backbone and reflects the robustness of the poly(isocyano-L-alanine) system, which is not influenced by the chromophores. The CD spectrum of **P4** resembled the CD spectrum of the free-base porphyrin functionalised polyisocyanide.[13] The intense bisignate signal at 402 nm is, however, blue shifted compared to the free-base analogue (431 nm), which is ascribed to the insertion of the platinum metal. This bisignate signal stems from coupling interactions between the first and the fifth porphyrin molecule in the polymer backbone, which are located on top of each other. No CD signal was detected for either monomer **7** and **8**. For **P5** a similar spectrum was observed as for **P3**. The incorporation of the small amount of platinum-porphyrin apparently does not influence the helical arrangement of the perylenes and might indicates that the chirality is primarily expressed in homoblocks. The characteristic CD signals of both the perylene and platinum-porphyrin functions were observed in the CD spectrum **P6**, although the signals in the 350–450 nm regions were somewhat shifted and slightly modified with regard to shape.

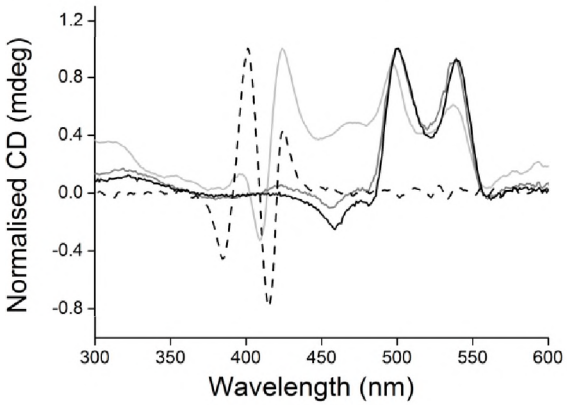

Figure 8. Normalised CD spectra of polymers **P3** (black line), **P4** (dotted line), **P5** (dark grey line) and **P6** (light grey) ($CHCl_3$; 10^{-5} M).

In collaboration with the group of Prof. Sir Richard Friend in Cambridge, photophysical studies were conducted on polymers **P3–P6**. Here only a brief description of the UV-Vis and the phosphorescence properties of these polymers are given; a more extensive and detailed description of the photophysical characteristics of the materials can be found elsewhere.[43]
The absorption and photoluminescence spectra of monomer **7** and polymer **P4** in $CHCl_3$ are shown in Figure 9. A sharp intense absorption band at λ = 405 nm accompanied with a weaker band at λ = 513 nm is observed in both monomer and polymer solutions. The first band is assigned to the S_0-S_2 transitions (Soret band), the latter band to the S_0-S_1 transition (Q band). A phosphorescence emission, induced by the strong orbit-coupling,[44] was detected at λ = 680 with a shoulder around λ = 745 nm. This shoulder might correlate to the formation of either a triplet dimer[45] or of aggregates.[46] The positions of the absorption and

emission bands are the same in the monomer and the polymer; slight changes in the band widths and relative intensities are, however, observed. Moreover, no splitting was observed in the Soret band.[25,47] If molecules are positioned in a parallel and stacked manner, the exciton model predicts that the coupling of the two transition dipoles will cause the lowest energy electronic transition of the dimer to split into two bands, with the higher energy band having all of the oscillator strength.[48] The lack of a significant band shift and/or splitting pattern thus suggests that the platinum-porphyrin polyisocyanide has a conformation or a relative distance between the porphyrins for which the exciton coupling is very weak between the porphyrin chromophores in the ground and excited states.

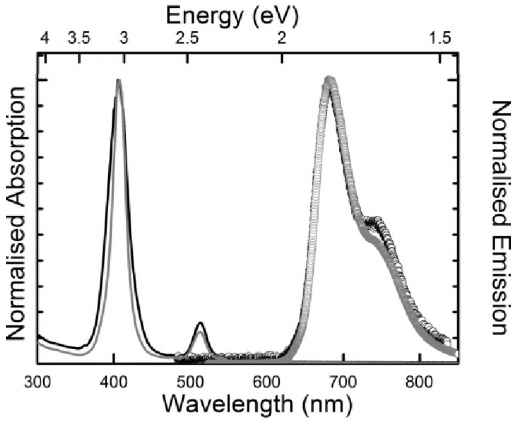

Figure 9. Normalised absorption (solid lines) and emission (circles) spectra of monomer **7** (grey lines) and polymer **P4** (black line) ($CHCl_3$, ~10^{-6} M).

The absorption and emission characteristics of monomers **7** and **8** and homopolymers **P3** and **P4** were used to analyse the properties of the statistical copolymers **P5** and **P6**. The absorption spectra of **P5** and **P6** combine the features of the Soret band from **P4** and the vibronic structures of **P3** (Figure 10). In both copolymers a substantial red shift of the Soret bands is observed. The Q band of **P4** is overlapping with the transition of the perylene polymer **P3**. In comparison with the λ = 405 nm Soret band in **P4**, a shift to 409 nm in **P6** and to 429 nm in **P5** (with a increasing weight percentage of perylene) is observed. The results indicate the presence of strong electronic couplings between the chromophores in their ground states, in particular between the perylene blocks and isolated platinum-porphyrin. The transition dipole moments of the perylene molecules are still maintained in a face-to-face manner in the copolymers as indicated by the intense band at λ = 492 nm.

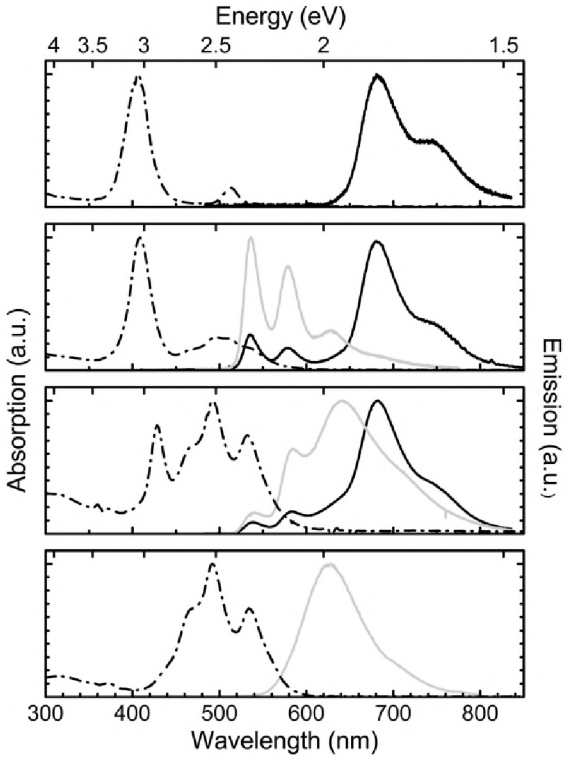

Figure 10. Absorption (dotted line) and emission (black line: λ_{exc} = 407 nm, grey line: λ_{exc} = 470 nm) for (a) **P4**, (b) **P6**, (c) **P5**, and (d) **P3** ($CHCl_3$, ~10^{-6} M).

From the above absorption spectra it can be seen that porphyrin molecules primarily absorb around λ = 405 nm and that the strong absorption of perylenes centres around λ = 490 nm. As such, we were able to selectively excite either the porphyrin or the perylene molecules, without perturbing the subsystem (unless charge or/and energy transfer occurs).

i) Excitation at 407 nm:

As shown by the blue lines in the emission spectra in Figure 10, both **P5** and **P6** in $CHCl_3$ have similar features as those observed for the homopolymer **P4**. Additional peaks at higher wavelengths (λ = 537 and λ = 578 nm) observed in the copolymers correspond to the aggregation of perylenes[49] and to monomeric perylene fluorescence. The positions and the intensities of the signals remain the same as those of the homopolymers, which suggests that electronic coupling between the platinum-porphyrin and the perylene in the excited state is weak when the excitation takes place preferentially at the platinum-porphyrin molecules.

ii) Excitation at 470 nm:

The perylene molecules in the polymer are preferentially excited at λ = 470 nm. In Figure 10 (green lines), the emission spectra of **P5** and **P6** in $CHCl_3$ are shown. For **P6** the emission

spectrum is characterised by a dominant monomer emission at λ = 537 and 580 nm and a smaller, broad band at and λ = 630 nm, which originates from the aggregation of perylenes. The main contributions to the emission spectrum of **P6** appear to originate from isolated chromophores and hence implies that the interactions between the perylene and porphyrin chromophores are rather weak. An additional shoulder is observed in the red region, which indicates the occurrence of porphyrin triplet states. The emission spectrum of **P5** consists of three peaks at λ = 541, 584 and 642 nm. The monomer-like emissions are red-shifted by 5 nm with respect to those in **P6**. In addition, the perylene aggregation band is the most prominent emission feature for **P5**. The presence of phosphorescence from the porphyrin chromophores upon direct excitation of the perylene may be either due to energy transfer from the perylene to the porphyrin molecules or to absorption by the isolated porphyrin molecules.

Further investigations, including temperature dependent studies, time-resolved photoluminescence, photoinduced absorption, transient absorption and anisotropy measurement offered a deeper insight into the complex photophysical processes taking place in the polymers.[43] An overview, summarizing these studies, of all the states found in the multi-chromophoric arrays is shown in Figure 11.

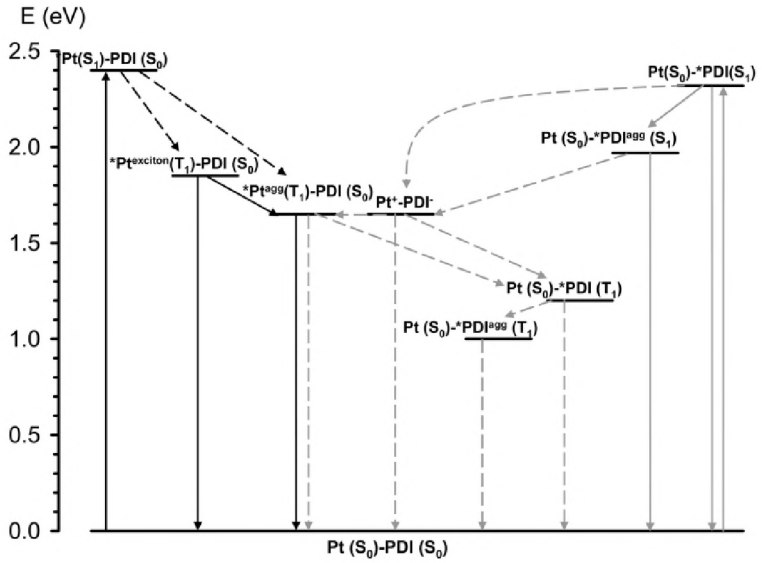

Figure 11. Photophysical pathways in **P5** or **P6** (black lines: λ_{exc} = 407 nm; direct excitation of platinum-porphyrin chromophores, grey lines: λ_{exc} = 470 or 492 nm; direct excitation of perylene chromophores).

3.4 Towards covalently linked perylene-porphyrin arrays

The photophysical properties of PDIs and porphyrins have been extensively studied over the last years and some deeper insight in the processes has been obtained.[5,50] The two chromophores are of interest as building blocks in organic electronic devices, since theoretically both electron and energy transfer between them is possible.[51,52] The first study on covalently linked porphyrins and perylene arrays was reported by Wasielewski and co-workers in 1992.[53] They created a molecular optical switch comprised of a PDI dye attached to two free-base porphyrins. Upon photo excitation of the porphyrin, electron transfer from the porphyrin to the PDI unit was observed. Lindsey and co-workers expanded this research and performed an extensive study on porphyrin-PDI dyads, which are covalently linked through alkynyl linkages (Chart 1).[51,54,55] The compounds have been studied in apolar and polar solvents to elucidate the different photophysical processes that take place. A variety of excited state processes were observed in the dyads, including energy transfer from the photo excited PDI to the porphyrin, electron transfer from the excited porphyrin to the perylene and charge recombination processes. Various substitution patterns on the chromophoric systems leading to various architectures (e.g., triads, stars, linear arrays) have been applied by the Würthner group,[56] the Wasielewski group[25,57] and the Johnston group (Chart 1).[58]

In this paragraph we present our work towards the construction of a covalently linked PDI-porphyrin array thereby expanding our investigations on PDI and porphyrin based polyisocyanides. To this end, a chromophoric dyad formed through a propyl linkage was designed; this dyad could subsequently be transformed into an isocyanoalanyl derivative suitable for the polymerisation with nickel ions.

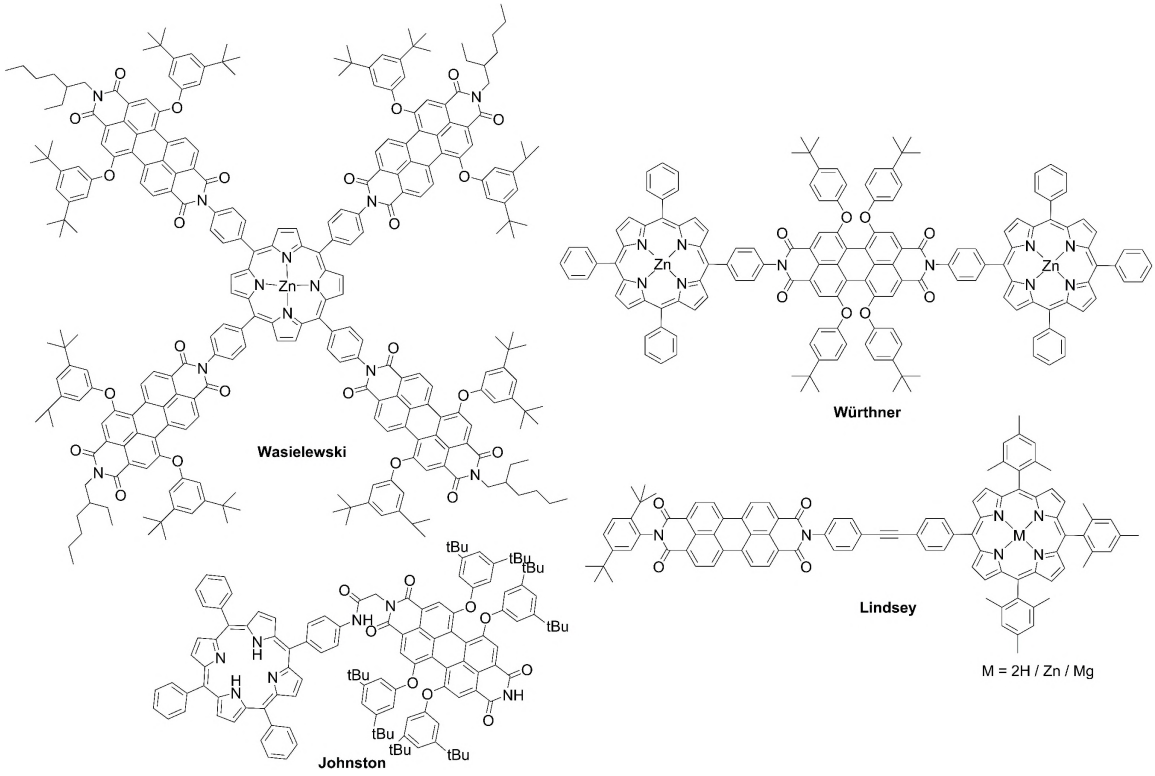

Chart 1. Various architectures of covalently linked PDI and porphyrin molecules.

Starting from 3,4:9,10-perylenetetracarboxydianhydride the perylene-porphyrin compound **13** was synthesised in three steps (Scheme 3). The first step involved the reaction of the perylene dianhydride **9** with potassium hydroxide in water, followed by the addition of acetic acid to generate the potassium salt **10**. This salt was treated with *N*-Boc-1,3-diaminopropane, which after stirring overnight and addition of potassium carbonate yielded the asymmetric perylene monoimide monoanhydride **11**. The porphyrin moiety was introduced by the reaction of the imide of **11** with the amine functionalised porphyrin **12** (obtained in a similar way as the platinum analogue **3**; Scheme 1), offering, after extensive column chromatography, the diimide **13**. After removal of the Boc-protecting group of **13**, the chromophoric amine was coupled to Boc-L-alanine under standard EDC coupling conditions to give **14**. Deprotection with acid and subsequent formylation with 2,4,5-trichlorophenyl formate led to the isolation of the formamide **15**, which was purified by column chromatography.

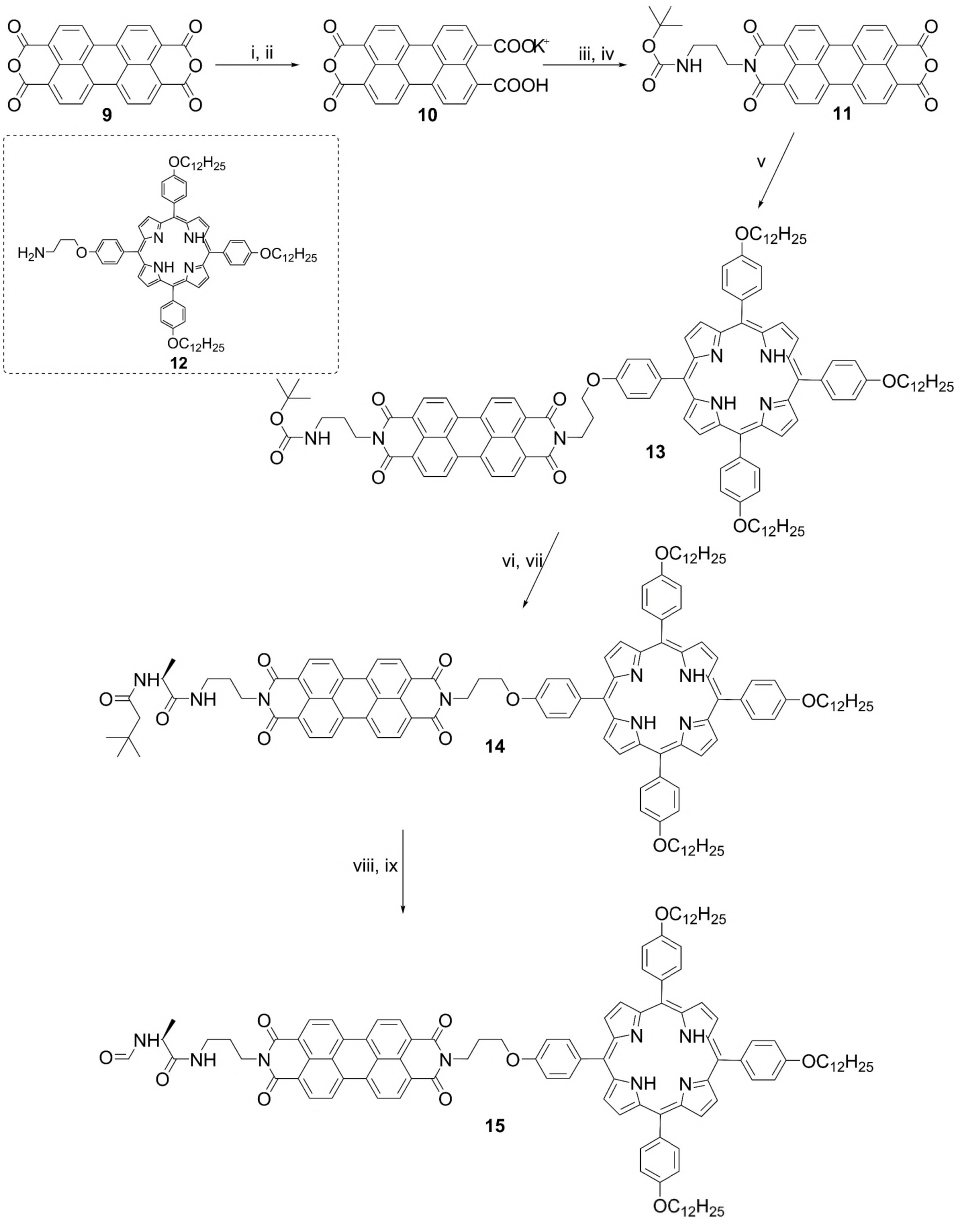

Scheme 3. Synthesis of PDI-porphyrin **15**; reagents and conditions. (i) KOH, H_2O, 90 °C, 2h; (ii) acetic acid, 90 °C, 40 min; (iii) 1-azido-3-aminopropane, H_2O, K_2CO_3, 90 °C, 48 h; (iv) 2M HCl; (v) **12**, imidazole, DMF, toluene, 97 °C; (vi) TFA, CH_2Cl_2; (vii) EDC, HOBt, DIPEA, Boc-L-Ala-OH, CH_2Cl_2; (viii) TFA, CH_2Cl_2; (ix) 2,4,5 trichlorophenyl formate, CH_2Cl_2. Inset shows the structure of the amine functionalised porphyrin **12**.

After purification of formamide **15**, several techniques were employed to enable its characterisation. In Figure 12 the ^{1}H NMR spectrum and the assignment of its proton resonances are shown. By performing gDQCOSY, gHSQC and ROESY NMR experiments all signals could be assigned. In the aromatic region, the β-pyrrole signals (15) of the porphyrin moiety appear at lowest field due to the anisotropic effect of the porphyrin ring current; the protons of the perylene (22 and 23) moiety are split into three sets of broader signals. The presence of the formamide group is confirmed by the proton signal at 8.23 ppm. Further

characterisation with soft ionisation mass spectroscopy (MALDI) verified the successful synthesis of compound **15** (Figure 13).

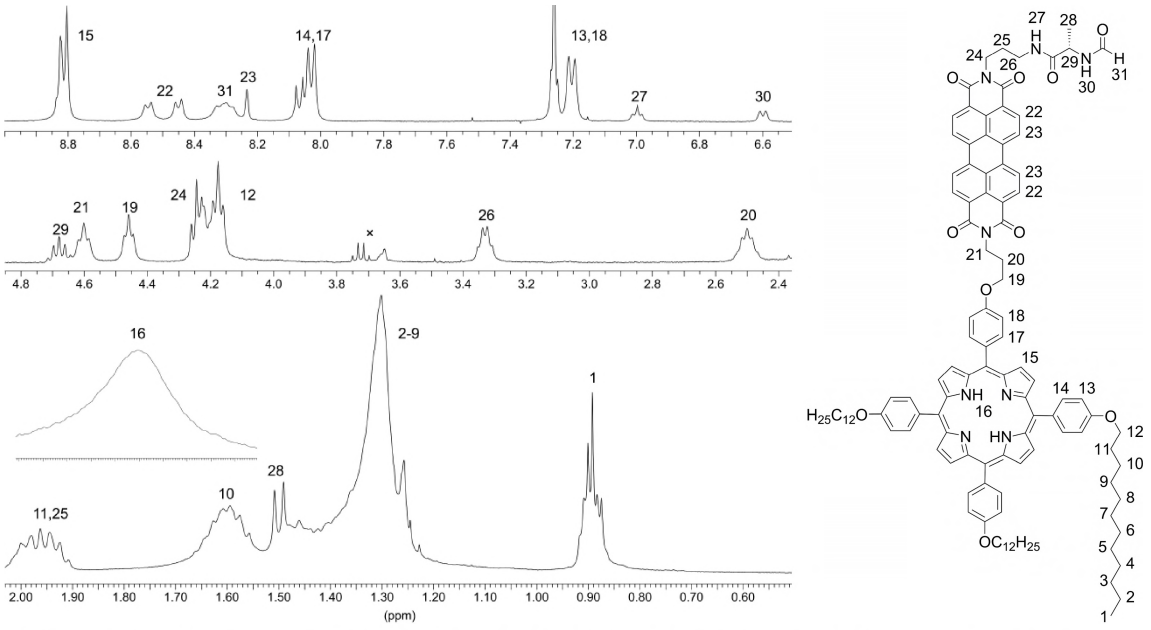

Figure 12. ^{1}H NMR spectrum of **15** in $CDCl_3$. Inset shows the inner protons of the porphyrin (16) at –2.8 ppm. For the assignment of the chemical shifts in the NMR spectrum, the protons are numbered according to molecular structure on the right; × denotes impurity.

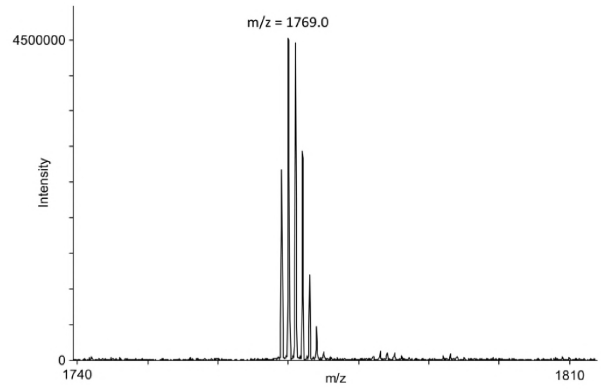

Figure 13. MALDI-TOF spectrum of **15**.

Free-base porphyrins, i.e., porphyrins with two hydrogen atoms in the centre, exhibit several characteristic absorption bands: four Q bands as a result of the different symmetry in the region, at λ = ~500 – 650 nm and an intense B band, also called Soret band at λ = ~380–420 nm.[59] Perylene imides are characterised by a vibronically structured strong absorption, S_0-S_1, in the visible region of the spectrum on the range λ = 450–550 nm.[60] The absorption spectrum of formamide **15** resembles the spectrum of a normal free-base porphyrin and of a normal perylene diimide (PDI) (Figure 14). The absorption of the porphyrin is much stronger

due its higher extinction coefficient (ε) compared to that of PDI. The formamide displays a Soret band at λ = 422 nm and Q bands at higher wavelength arising from the porphyrin. The signals at λ = 459, 489 and 526 nm stem from the 0-2, 0-1 and 0-0 vibronic transitions of the PDI, respectively. These bands belong to transitions in the long direction of the perylene, i.e., through the nitrogen atoms. The weak signal arising from the transition perpendicular to the transition in the long direction, S_0-S_2, appears at λ = 366 nm. In summary, when compared to absorption spectra of related porphyrins[59,61] or perylenes[62] described in the literature, the absorption spectrum of **15** is similar in shape and has comparable maxima and intensities, indicating a very weak perylene-porphyrin interaction. No detectable CD signal was found at ~10^{-6} M concentration.

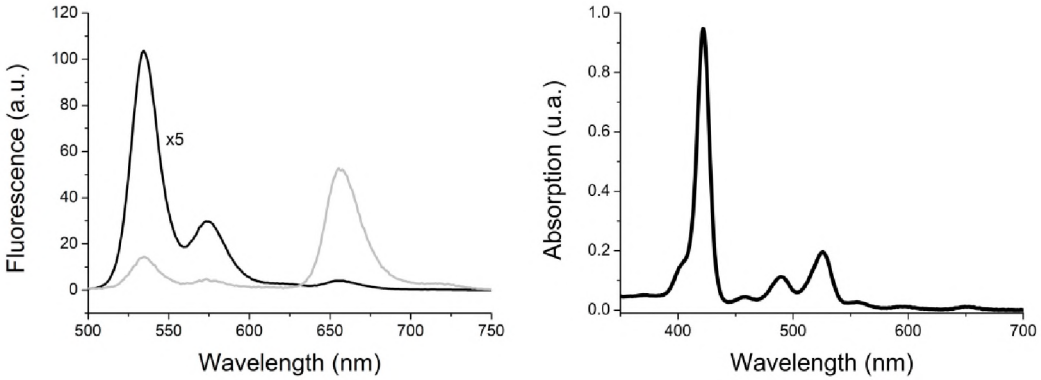

Figure 14. UV-Vis (left) and Fluorescence (right) spectra of **15** (~10^{-6}, $CHCl_3$). Black line: λ_{exc} = 492 nm; grey line λ_{exc} = 425 nm.

The fluorescence spectrum of formamide **15**, when photo excited at λ = 425 nm (i.e., photoexcitation of the porphyrin) showed a typical two-band profile of a free-base porphyrin with maxima at λ = 656 nm and λ = 718 nm (less pronounced), originating from the 0-1 and 0-0 vibronic transitions (Figure 14). A characteristic PDI emission spectrum was found when the formamide was photo excited at λ = 492 nm; a strong band at λ = 534 nm and a weaker band at λ = 575 nm were observed. As shown in Figure 14, the band-intensity for the PDI fluorescence is much stronger than for the porphyrin fluorescence and can be attributed to the difference in fluorescence quantum yield (Φ_f) of PDIs and porphyrins (~1 vs. ~0.1, respectively). On excitation of the PDI moiety the emission was found to almost exclusively occur from the PDI chromophore. This is in contrast to the work of Lindsey and co-workers,[55] who formed a PDI-porphyrin complex that has a conjugated spacer between the two chromophores, which allowed energy transfer to occur. Although in addition to these typical features a very low intensity emission from the second chromophore i.e., the chromophore that was not excited, occurs in our system, which might indicate energy transfer, the fluorescence spectra parallel the results obtained from the absorption studies

and support the hypothesis of very weak interchromophoric electronic interactions. Further photophysical studies are, however, required to obtain more information about the electronic and energy processes in these systems.

Unfortunately, attempts to convert the formamide into the isocyanide were unsuccessful. Several attempts were undertaken by using various dehydrating agents, various ratios of the dehydrating agents and various temperatures. In Table 2 an overview of the reactions conditions are shown. Only when a large excess of the dehydrating agents was used (entries 4 and 8) a reaction was found to occur, however, according to IR and ^{1}H NMR spectroscopy the obtained product was not the expected isocyanide. To prevent any possible intramolecular docking of the side arms or reaction of the inner core, the porphyrin **15** was converted into the corresponding Zn analogue. Conversion to the isocyanide was, however, still unsuccessful. It remains unclear why the isocyanide could not be formed, since the synthesis of mono-chromophoric PDI and porphyrin isocyanides is possible and formamide **15** is constructed from similar building blocks.

Table 2 Reaction conditions and results for the reaction of formamide **15** with dehydrating agents

Entry	Dehydrating agent & base	Equivalents[a]	Temperature	Conversion
1	Diphosgene & *N*-methylmorpholine[b]	0 - 3	–30°C	No
2	Diphosgene & *N*-methylmorpholine[b]	4 - 8	0°C - 25°C	No
3	Burgess reagent[c]	1.5 - 5	40°C	No
4	Burgess reagent[c]	4 - 10	40°C	Yes[d]
5	$POCl_3$ & Et_3N[e]	3	0°C - 25°C	No
6	$SOCl_2$ & Na_2CO_3[f]	6	–30°C - 25°C	No
7	Cyanuric chloride & Et_3N[g]	3	50°C[h]	No
8	Cyanuric chloride & Et_3N[g]	3 - 5	50°C - 100°C[h]	Yes[d]

[a]In entries 1–4 a range of equivalents was used. [b]In CH_2Cl_2/$CHCl_3$, Ugi method.[63] [c]Inner salt of *N*-(triethylammoniumsulfonyl) carbamate; the advantage of this reagent is that it can be used at higher temeperatures.[64] [d]On TLC the formamide was completely consumed, however, no isocyanide was formed according to IR and ^{1}H NMR spectroscopy (for entry 4: reaction carried out overnight in CH_2Cl_2/$CHCl_3$). [e]In CH_2Cl_2/$CHCl_3$, see for example: Ugi[65] or Böhme.[66] [f]In DMF/toluene, see for example Niznik[67] or Drenth.[68] [g]Originally developed by Wittman for the synthesis of aliphatic isocyanides,[69] recently applied by Porcheddu for the synthesis of aromatic isocyanides.[70] [h]By using the procedure developed by Porcheddu, **15**, Et_3N, CH_2Cl_2 and the cyanuric chloride were placed in a sealed tube and the reaction mixture was exposed to microwave irradiation (from 3–15 min).

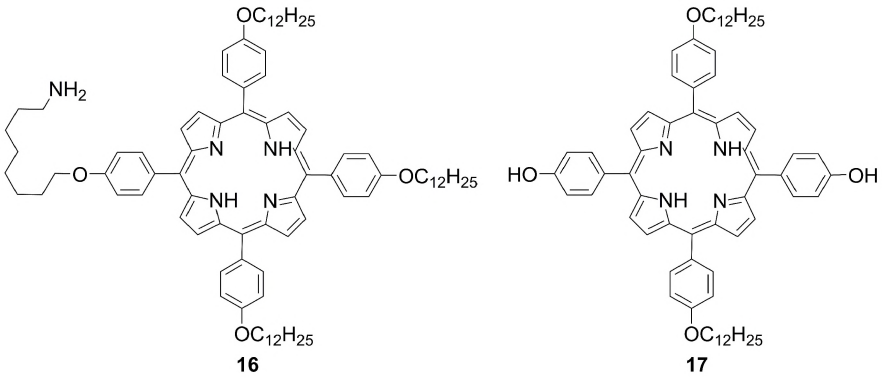

Chart 2. Alternative compounds **16** and **17** for the synthesis of di-chromophoric building blocks.

Alternative starting compounds for the synthesis of a di-chromophoric isocyanide with PDI and porphyrin building blocks are depicted in Chart 2. To test the effect of the spacer length between the PDI and the porphyrin moieties on the isocyanide conversion, a porphyrin with an increased alkyl tail (**16**) between the amine end group and the porphyrin (octyl instead of propyl as for **15**) was proposed (Chart 2). The intermediate Boc-L-alanyl appended di-chromophoric compound could, however, not be obtained with sufficient purity. In a different attempt, it was tried to prepare an isocyanide in which the chromophoric units are reversed as compared to **15**. To this end, a *p*-dodecylphenoxy dipyrromethene (2,2'-((4-(dodecyloxy)phenyl)methylene)bis-1H-pyrrole)) was synthesised, which can be reacted with 4-(dodecyloxy)benzaldehyde to yield the tetra *meso*-substituted porphyrin **17** (Chart 2). Selective protection of this porphyrin and subsequent coupling to a derivatised perylene would allow the preparation of the di-chromophoric building block. The synthesis of the desired porphyrin **17** was, however, hampered by a very high scrambling of the porphyrin substituents, which made the purification and isolation of **17** unsuccessful.[71] The partial alkylation of a tetra-hydroxyporphyrin towards the synthesis of **17** also failed. In summary, the synthesis of an alanine derived isocyanide built up from covalently attached PDI and porphyrin building blocks could not be achieved.

3.5 Conclusion

In this chapter, we have demonstrated that by using a well-defined polymeric scaffold, perylene and porphyrin molecules can be nicely arranged. As a polymeric scaffold we have selected a polyisocyanide, which was decorated with perylenes (**P2** and **P3**), with platinum porphyrins (**P4**) and mixtures of both chromophores (**P5** and **P6**). In the case of the perylene homopolymer **P3**, a thorough characterisation using various spectroscopic tools revealed a well-defined 4_1 helical architecture in which the perylene molecules form four 'helter-skelter-like' overlapping pathways along which excitons and electrons can rapidly migrate. The successful application of these polymeric materials in thin-film transistors (TFTs) and

photovoltaic devices was demonstrated, although the performances of the devices were somewhat disappointing. By using AFM and KPFM a deeper understanding of the characteristic features of the devices could be obtained. The statistical copolymers **P5** and **P6** were synthesised and spectroscopically characterised, revealing that complex photophysical processes occurred in these materials.

3.6 Experimental

General

All solvents were distilled prior to use. All other chemicals were commercials products and used as received. Silica gel (0.035–0.070 mm, pore diameter 6 mm) from Acros was used for column chromatography and silica 60 F_{254} coated glass plates (Merck) were used for TLC. ^{1}H NMR, ^{13}C NMR, gDQCOSY, gHSQC and ROESY spectra were recorded on a Bruker DMX-200 MHz, Bruker AC-300 MHz or Inova 400 MHz machines operating at room temperature. Chemical shift are reported in ppm. The following measurements were recorded at room temperature unless stated otherwise: FT-infrared on a ThermoMattson IR300 spectrometer equipped with a Harrick ATR unit; the compounds were measured as a solid; UV-Vis spectra on a Varian Cary 50 spectrometer; fluorescence spectra on a Perkin Elmer Luminescence spectrometer LS50B; CD spectra on a Jasco J600 CD spectrometer equipped with a Peltier temperature control unit. The infrared spectra in solutions were measured on a Bruker Tensor 27 instrument in a NaBr cell. FAB mass spectra were recorded on a VG-7070E mass spectrometer with 3-nitrobenzylalcohol as matrix. MALDI-TOF spectra were measured on a Bruker Biflex III spectrometer using dithranol as matrix. High resolution ESI mass spectra (HR-MS) were recorded on a JEOL AccuTOF spectrometer with polyethylene glycol as an internal reference. The sprayed solutions for HR-MS spectra of perylene bisimide compounds were prepared by dissolving ~1 mg PDI in 50–100 µl CH_2Cl_2 and subsequent dilution with MeOH to 1mL.

Synthesis

The mono-hydroxy porphyrin **1**,[13] the amine functionalised porphyrin **12**,[13] *N*-Boc-1,3-diaminopropane,[72] polymer **P1**,[16] *N,N'*-Bis(1-hexylheptyl)-3,4:9,10-perylenedicarboximide,[17] *N*-(1-hexylheptyl)perylene-3,4:9,10-tetracaboxylic-3,4-anhydride-9,10-imide,[18] *N*-(2,6-diisopropylphenyl)-1,6,7,12-tetraphenoxyperylene-3,4:9,10-tetracarboxy-9,10-monoanhydride-3,4-monoimide,[7] and the precursors for the isocyanide monomers of **P2** and **P3**[15] were synthesised according to literature procedures.

Isocyanide monomer for the synthesis of P3

Under Schlenk conditions, the corresponding perylene formamide (200 mg, 0.27 mmol) and *N*-methylmorpholine (NMM) (76 µl, 0.69 mmol, 2.5 equiv.) were dissolved in CH_2Cl_2 (50 mL) and the solution was cooled to –30°C using acetone/CO_2. A total amount of 180 µl NMM (1.64 mmol, 6 equiv.) and 39 µl diphosgene (0.32 mmol, 1.2 equiv.) were added in 3 steps; the reaction was followed by TLC. First 2.5 equiv. of NMM were added followed by dropwise addition (10 minutes) of 0.5 equiv. of diphosgene in CH_2Cl_2 (3 mL), always keeping the reaction temperature at –30°C. After a second addition of the same amounts of NMM and diphosgene, another 1 equiv. of NMM and 0.2 equiv. of diphosgene were needed to complete the reaction. During the reaction a colour change from red to orange was observed. The reaction mixture was brought to 0 °C and added to an ice-cold saturated aqueous sodium bicarbonate solution (100 mL) under vigorously stirring. After addition of $CHCl_3$ (100 mL), the organic layer was separated and washed with an aqueous 10% (w/w) sodium

carbonate solution. The solvent was evaporated *in vacuo* and the red solid was purified by column chromatography (1% MeOH, 1% Et_3N in $CHCl_3$) to yield 171 mg (88%) of the isocyanide. ^{1}H NMR (δ ppm, $CDCl_3$, 400 MHz): 8.58 (d, 4H, perylene H, $^3J_{HH}$ = 8.0 Hz), 8.48 (d, 2H, perylene H, $^3J_{HH}$ = 8.0 Hz), 8.44 (d, 2H, perylene H, $^3J_{HH}$ = 8.0 Hz), 7.51 (t, 1H, NH, $^3J_{HH}$ = 6.0 Hz), 5.18 (m, 1H, CH), 4.32 (m, 3H, NCH_2, CH ala), 3.38 (m, 2H, $NHCH_2$), 2.27 (m, 2H, $CHCH_2$), 2.05 (qn, 2H, $NHCH_2CH_2$, $^3J_{HH}$ = 6.2 Hz), 1.89 (m, 2H, $CHCH_2$), 1.73 (d, 3H, CH_3 ala, $^3J_{HH}$ = 7.0 Hz), 1.40-1.20 (br, 16H, CH_2), 0.84 (t, 6H, CH_3, $^3J_{HH}$ = 6.9 Hz). ^{13}C NMR (δ ppm, $CDCl_3$, 75 MHz): 166.0 (C=O), 163.4 (C=O, perylene), 160.8 (CN), 134.6, 133.7 131.4, 129.1, 129.0, 126.0, 125.9, 123.0, 122.6, 122.4 (aromatic perylene), 55.0 (CH), 53.7 (CH-ala), 37.7 (NCH_2), 36.8 ($NHCH_2$), 32.5 ($CHCH_2$), 31.9, 29.4, 27.2, 22.8 (CH_2), 28.0 ($NHCH_2CH_2$), 20.1 (CH_3-ala), 14.3 (CH_3). FT-IR (cm^{-1}, ATR): 3345 (NH), 2948, 2923, 2852 (C-H stretch), 2139 (C≡N), 1693, 1651 (O=CN, amide), 1593, 1577 (C=C aromatic), 1340 (C-N stretch), 810, 744 (CH aromatic). UV-Vis ($CHCl_3$): λ_{max} (ε) = 370 (4070), 433 (5340), 460 (18530), 491 (50780), 528 nm (84500 mol^{-1} L cm^{-1}). Fluorescence ($CHCl_3$, λ_{exc} = 492 nm): λ_{max} = 535, 575 nm. HR-MS (ESI) m/z: calculated for $C_{44}H_{46}N_4O_5Na$ 733.33659, found: 733.33620.

Isocyanide monomer for the synthesis of P2

This isocyanide was obtained in 93% from the formamide following the procedure as described for the synthesis of the isocyanide above. For the conversion a total of 15 equiv. of NMM and 3.2 equiv. of diphosgene were used these were added in 4 steps, starting with 2.5 equiv. of NMM and 0.5 equiv. of diphosgene. ^{1}H NMR (δ ppm, $CDCl_3$, 400 MHz): 8.24 (s, 2H, perylene H), 8.21 (s, 2H, perylene H), 7.42 (t, 1H, aromatic H para to N imide, $^3J_{HH}$ = 8.0 Hz), 7.27 (m, 10H, aromatic H meta to N imide, aromatic H meta to O perylene (bay area)), 7.11 (m, 4H, aromatic H para to O perylene (bay area)), 6.96 (d, 8H, aromatic H ortho to O perylene (bay area)), $^3J_{HH}$ = 8.0 Hz), 6.54 (br, 1H, NH), 4.21 (m, 1H, CH-ala), 4.16 (t, 2H, NCH_2, $^3J_{HH}$ = 7.2 Hz), 3.35 (m, 2H, $NHCH_2$, $^3J_{HH}$ = 6.8 Hz), 2.69 (sept, 2H, CH isopropyl, $^3J_{HH}$ = 5.6 Hz), 1.75 (m, 2H, $NHCH_2CH_2$), 1.63 (m, 2H, $NHCH_2CH_2$), 1.61 (d, 3H, CH_3 ala, $^3J_{HH}$ = 7.2 Hz), 1.05 (d, 12H, CH_3 isopropyl , $^3J_{HH}$ = 6.9 Hz). ^{13}C NMR (δ ppm, $CDCl_3$, 50 MHz): 166.0 (C=O), 163.3 (C=O perylene), 163.1 (CN), 155.8, 155.2 (C-O), 145.6, 133.0, 132.8, 130.5 (aromatic perylene), 130.0 (aromatic C meta to O perylene (bay area)), 129.4 (aromatic C para to N imide) 124.7, 124.6 (aromatic C para to O perylene (bay area)) 123.9 (aromatic C meta to N imide), 122.9, 122.5, 120.7, 120.6, 120.1, 119.6 (aromatic perylene), 120.3, (aromatic perylene), 119.9, 119.8 (aromatic H ortho to O perylene (bay area)), 53.5 (CH-ala), 39.4 (CH_2), 29.1 (CH isopropyl), 26.6 (CH_2), 25.2 (CH_2), 24.0 (CH_3 isopropyl), 19.7 (CH_3-ala). FT-IR (cm^{-1}, ATR): 3376 (NH), 3064, 2963, 2928, 2867 (C-H stretch), 2137 (CN), 1699, 1659 (O=CN, amide), 1587 (C=C aromatic), 1487, 1410 (C-H bend), 1338 (C-N stretch), 1309, 1285, 1202 (ether), 879 + 745 (C-H aromatic).UV-Vis ($CHCl_3$): λ_{max}(ε)= 266 (32040), 284 (34070), 446 (15020), 542 (20830), 580 (32160 mol^{-1} L cm^{-1}) nm.HR-MS (ESI) m/z: calculated for $C_{68}H_{54}N_4O_9Na$: 1093.37885, found: 1093.38105.

Polymer P3

To a stirred solution of the isocyanide monomer (138 mg, 0.194 mmol) in $CHCl_3$ (30 mL) was added 1/1000 equiv. of nickel (1 mL of a 0.19 mM solution of $Ni(ClO_4)_2$ in EtOH/$CHCl_3$). According to TLC, the isocyanide was completely consumed after 1 h. The polymer was concentrated to a smaller volume (~10 mL) and precipitated in 100 mL of methanol/water (1:1 v/v) under vigorous stirring. The solid was collected by centrifugation and subsequent decantation of the solvent. The material was then dissolved in chloroform (5 mL) and precipitated in methanol (~60 mL) after which the polymer was collected. The latter step was repeated several times until no monomer emission (λ_{max} = 535 nm) was observed for the solid dissolved in $CHCl_3$. Drying *in vacuo* gave the polymer as a red solid in 98% yield (135 mg). ^{1}H NMR (δ ppm, $CDCl_3$, 400 MHz): 8.68 (br, 8H, perylene H), 5.18 (br, 1H, CH), 4.28 (br, 3H, NCH_2, CH-ala), 3.34 (br, 2H, $NHCH_2$), 2.6–0.4 (br, 31H, CH_2, CH_3-ala, CH_3). FT-IR (cm^{-1},

ATR): 3291 (NH), 2946, 2924, 2855 (C-H stretch), 1695, 1654 (O=CN, amide), 1593, 1578 (C=C aromatic), 1342 (C-N stretch), 810, 747 (CH aromatic).UV-Vis ($CHCl_3$): λ_{max} = 372 (3500), 468 (17740), 492 (26180), 534 nm (17540 mol^{-1} L cm^{-1}). Fluorescence ($CHCl_3$, λ_{exc} = 492 nm): λ_{max} = 625 nm.

Polymer P2

To a stirred solution of the isocyanide monomer (20 mg, 0.019 mmol) in $CHCl_3$ (2 mL) a nickel solution was added (1/1000 equiv., 1 mL of a 0.019 mM solution of $Ni(ClO_4)_2$ in EtOH/$CHCl_3$). According to TLC, the isocyanide was completely consumed after 7 days. The polymer was purified by size exclusion chromatography (Bio-Beads) using CH_2Cl_2 as eluent and obtained as a red solid in 80% yield (16 mg). ^{1}H NMR (δ ppm, $CDCl_3$, 400 MHz): 8.40–7.60 (br, 4H, aromatic perylene), 7.60–5.80 (br, 24H, aromatic H NH), 3.64 (br, 3H, CH ala, CH_2) 2.55 (br, 2H, CH isopropyl), 1.80–0.80 (br, 19H, CH_2, CH_3 ala, CH_3 isopropyl). FT-IR (cm^{-1}, ATR): 3308 (NH), 3061, 2958, 2921, 2868, 2850 (C-H stretch), 1701, 1659 (O=CN, amide), 1587 (C=C aromatic), 1487, 1410 (C-H bend), 1341 (C-N stretch), 1310, 1286, 1200 (ether), 877 + 750 (C-H aromatic).UV-Vis ($CHCl_3$): λ_{max} (ε) = 266 (29410), 285 (30263), 448 (12381), 533 (19932), 572 nm (21373 mol^{-1} L cm^{-1}). Fluorescence ($CHCl_3$, λ_{exc} = 550 nm): λ_{max} = 606 nm.

Platinum-porphyrin 2

Under argon, monohydroxyporphyrin **1** (110 mg, 93 µmol) was dissolved in degassed benzonitrile (50 mL). To this solution two equiv. of bis-benzonitrile-platinum(II) chloride were added and the mixture was refluxed at 190 °C for 24 h. The solvent was then evaporated under vacuum and the product was purified by column chromatography (0.5% MeOH in $CHCl_3$) to yield orange **2** in quantitative yield. ^{1}H NMR (δ ppm, $CDCl_3$, 400 MHz): 8.77 (m, 8H, ß-pyrrole), 8.01 (m, 6H, ArH meta to $OC_{12}H_{25}$), 7.96 (m, 2H, ArH meta to *O*-aminopropyloxy), 7.23 (m, 6H, ArH ortho to $OC_{12}H_{25}$), 7.17 (d, 2H, ArH ortho to *O*-aminopropyloxy, J = 6.9 Hz), 5.03 (s, 1H, OH), 4.22 (t, 6H, OCH_2, J = 7.1 Hz), 1.97 (qn, 6H, OCH_2CH_2, J = 6.0 Hz), 1.60 (qn, 6H, $OCH_2CH_2CH_2$, J = 7.3 Hz), 1.48–1.22 (overlapping multiplets, 48H, aliphatic H), 0.90 (t, 3H, J = 7.0 Hz). ^{13}C NMR (δ ppm, $CDCl_3$, 75 MHz): 159.0 (ArC ipso to $OC_{12}H_{25}$), 155.5 (ArC ipso to OH), 141.2, 135.9, 135.4, 134.9, 133.5, 132.7 (ArC), 130.5 (br, ArC next to ArN), 117.0, 116.7, 114.7, 114.2, 113.7, 112.8 (ArC), 68.4 ($ArOCH_2$), 31.9 ($ArOCH_2CH_2$), 29.7-29.0 (CH_2), 26.2 ($CH_2CH_2CH_3$), 22.7 (CH_2CH_3), 14.1 (CH_3). FT-IR (cm^{-1}, ATR): 3430 (OH), 2922, 2851 (CH), 1241 (CO). MALDI-TOF m/z: calculated for $C_{80}H_{100}N_4O_4Pt$: 1374.8 (M^+), found: 1374.7.

Platinum-porphyrin 3

To a solution of **2** (467mg, 0. 34mmol) in DMF toluene (35 mL, 2:1 v/v) was added crushed NaOH (0.5 g, 0.4 mmol, 1.2 equiv.). After stirring for 1h at room temperature, 3-bromopropylamine hydrobromide (0.15 g, 0.68 mmol, 2 equiv.) was added and the mixture was stirred overnight, after which time another equivalent of 3-bromopropylamine was added. The suspension was stirred for 3h, poured into water and extracted with dichloromethane (2x). The combined organic layers were washed with water (2x), dried (Na_2SO_4) and evaporated. The solid was subjected to the column chromatography (0–5 % MeOH in $CHCl_3$) to yield **3** in 65 % yield.^{1}H NMR (δ ppm, $CDCl_3$, 400 MHz): 8.73 (m, 8H, ß-pyrrole), 8.02 (m, 6H, ArH meta to $OC_{12}H_{25}$), 7.95 (m, 2H, ArH meta to OCH_2), 7.19 (m, 2H, ArH ortho to OCH_2, J = 6.9 Hz), 7.07 (d, 3H, ArH ortho to $OC_{12}H_{25}$, J = 6.9 Hz), 7.00 (d, 3H, ArH ortho to $OC_{12}H_{25}$, J = 6.9 Hz), 4.09 (t, 2H, OCH_2, J = 6.4 Hz), 3.94 (t, 6H, OCH_2, J = 6.4 Hz), 2.43 (br, 2H, CH_2NH_2), 2.27 (br, 2H, NH_2), 1.85 (qn, 6H, OCH_2CH_2, J = 7.1 Hz), 1.81 (m, 2H, $CH_2CH_2NH_2$), 1.50 (qn, 6H, $OCH_2CH_2CH_2$, J = 7.2 Hz), 1.48–1.20 (overlapping multiplets, 48H, aliphatic H), 0.90 (t, 3H, J = 7.0 Hz). ^{13}C NMR (δ ppm, $CDCl_3$, 75 MHz): 158.8, 158.4 (ArC ipso to OR), 141.2, 141.1 134.8, 133.9, 133.4 (ArC), 130.5 (br, ArC next to ArN), 122.0, 121.8, 112.7, 112.6 (ArC), 68.2, 65.9 ($ArOCH_2$), 50.7 (CH_2NH_2), 31.9 ($ArOCH_2CH_2$), 29.7-29.4

(CH_2), 26.2, ($CH_2CH_2CH_3$), 26.1 ($CH_2CH_2NH_2$) 22.7 (CH_2CH_3), 14.1 (CH_3). FT-IR (cm^{-1}, ATR): 2921, 2850 (CH), 1240 (CO). MALDI-TOF: m/z = 1431.8 (M^+). Calcd for $C_{83}H_{107}N_5O_4Pt$: 1431.9.

Platinum-porphyrin 4

Platinum porphyrin **3** (323 mg, 0.22 mmol) was dissolved in CH_2Cl_2. Boc-L-alanine (46.8 mg, 0.25 mmol, 1.1 equiv.), HOBT (37.9 mg, 0.25 mmol, 1.1 equiv.), DIPEA (42.2 µL, 0.25 mmol, 1.1 equiv.) and EDC (47.4 mg, 0.25 mmol, 1.1 equiv.) were added to the solution and the reaction mixture was stirred overnight at room temperature. The solution was subsequently washed with an aqueous 10% (w/w) citric acid solution (2 × 200 mL), H_2O (200 mL), an aqueous 10% (w/w) sodium carbonate solution (2 × 200 mL) and H_2O (200 mL). The organic layer was dried (Na_2SO_4), concentrated and subjected to column chromatography (1% MeOH in CH_2Cl_2), yielding 91% of **4** as an orange solid. ^{1}H NMR (δ ppm, $CDCl_3$, 400 MHz): 8.72 (m, 8H, ß-pyrrole), 8.01 (dd, 8H, ArH meta to OR, J = 8.0 Hz), 7.21 (m, 8H, ArH meta to OR), 6.66 (t, 1H, NH, J = 6.3 Hz), 5.03 (br, 1H, NHBoc), 4.50 (q, 1H, CH Ala, J = 6.6 Hz), 4.24 (t, 2H, OCH_2, J = 5.6 Hz), 4.17 (t, 6H, OCH_2, J = 6.7 Hz), 3.62 (m, 2H, $NHCH_2$), 2.16 (qn, 2H, $NHCH_2CH_2$, J = 6.1 Hz), 1.95 (qn, 6H, OCH_2CH_2, J = 7.1 Hz), 1.59 (m, 6H, $OCH_2CH_2CH_2$), 1.44 (d, 3H, CH_3 Ala, J = 6.6 Hz), 1.40–1.25 (overlapping multiplets, 48H, aliphatic H), 0.91 (t, 3H, J = 6.6 Hz).. ^{13}C NMR (δ ppm, $CDCl_3$, 75 MHz): 173.0 (CO Ala), 158.8, 158.3 (ArC ipso to OR), 155.6 (CO Boc), 141.2, 141.1 134.6, 133.9, 133.4 (ArC), 130.6 (br, ArC next to ArN), 122.1, 122.0, 112.7 (br) (ArC), 79.9 ($C(CH_3)_3$), 68.1, 66.2 ($ArOCH_2$), 53.3 (CH Ala), 37.3 ($NHCH_2$), 31.9 ($ArOCH_2CH_2$), 29.7-29.3 (CH_2), 28.3 ($C(CH_3)_3$), 26.1 ($CH_2CH_2CH_3$), 26.1 ($CH_2CH_2NH_2$), 22.7 (CH_2CH_3), 18.3 (CH_3 Ala), 14.1 (CH_3). FT-IR (cm^{-1}, ATR): 3329 (NH), 2922, 2850 (CH), 1672 (Amide I), 1544 (amide II), 1239 (CO). MALDI-TOF m/z: calculated for $C_{91}H_{120}N_6O_7Pt$: 1603.1 (M^+), found: 1602.9

Platinum-porphyrin 6

To a solution of **4** (322 mg, 0.20 mmol) in CH_2Cl_2 (20 mL), trifluoro acetic acid (4 mL) was added and the mixture was stirred for 4 hrs. After evaporation of the solvent *in vacuo*, the product was dissolved again in CH_2Cl_2 (100 mL) and washed subsequently with an aqueous 10 % (w/w) sodium bicarbonate solution (2 × 100 mL) and brine (100 mL). The organic layer was dried (Na_2SO_4) and concentrated to *ca*. 25 mL after which an excess of 2,4,5-trichlorophenyl formate (200mg, 0.89 mmol, 5 equiv.) was added to a solution containing **5**. After stirring the mixture for 14 h the solution was washed with a saturated aqueous solution of sodium bicarbonate (2 × 100 mL) and brine (100 mL). The solvent was evaporated *in vacuo* and the solid was subjected to column chromatography (0–1.5 % MeOH in CH_2Cl_2) to give **6** (228 mg, 75%) as an orange solid.

^{1}H NMR (δ ppm, $CDCl_3$, 400 MHz): 8.78 (m, 8H, ß-pyrrole), 8.06 (s, 1H, HCO), 7.93 (m, 8H, ArH meta to OR), 7.09 (m, 6H, ArH meta to OR), 7.02 (d, 2H, ArH meta to OR, J = 8.6 Hz), 6.65 (t, 1H, NH, J = 5.4 Hz), 6.55 (d, 1H, NH, J = 7.3 Hz), 4.53 (q, 1H, CH Ala, J = 7.1 Hz), 4.02 (m, 8H, OCH_2), 3.44 (m, 2H, $NHCH_2$), 1.98 (br qn, 2H, $NHCH_2CH_2$, J = 5.1 Hz), 1.95 (m, 6H, OCH_2CH_2), 1.52 (m, 6H, $OCH_2CH_2CH_2$), 1.40–1.21 (overlapping multiplets, 51H, aliphatic H, CH_3 Ala,), 0.89 (t, 3H, J = 6.6 Hz).^{13}C NMR (δ ppm, $CDCl_3$, 75 MHz): 173.0 (CO Ala), 160.8 (HCO), 158.9, 158.3 (ArC ipso to OR), 141.1, 141.0 134.8, 134.0, 133.4 (ArC), 130.6 (br, ArC next to ArN), 122.1, 121.7, 112.6 (ArC), 68.1, 66.0 ($ArOCH_2$), 49.0 (CH Ala), 37.4 ($NHCH_2$), 31.9 ($ArOCH_2CH_2$), 29.7-28.9 (CH_2), 26.1 ($CH_2CH_2CH_3$, $CH_2CH_2NH_2$), 22.7 (CH_2CH_3), 18.5 (CH_3 Ala) 14.1 (CH_3). FT-IR (cm^{-1}, ATR): 3317 (NH), 2922, 2850 (CH), 1652 (Amide I), 1541 (amide II), 1239 (CO). MALDI-TOF: m/z = 1531.0 (M^+). Calcd for $C_{87}H_{112}N_6O_6Pt$: 1530.9.

Platinum-porphyrin 7

Under Schlenk conditions, formamide **6** (100 mg, 0.065 mmol) and N-methyl morpholine (NMM) (72 µl, 0.65 mmol, 10 equiv.) were dissolved in CH_2Cl_2 (50 mL) and the solution was cooled to –30°C using acetone/CO_2. Over a period of 30 min. diphosgene (8 µL, 0.065 mmol, 1 equiv.) in CH_2Cl_2 (3 mL) was added dropwise to the

reaction mixture, while the temperature was maintained at –30 °C. After complete addition of diphosgene, the reaction mixture was brought to 0 °C and added to an ice-cold saturated aqueous sodium bicarbonate solution (100 mL) under vigorously stirring. After addition of $CHCl_3$ (100 mL), the organic part was separated and washed with an aqueous 10 % (w/w) sodium carbonate solution. The solvent was evaporated *in vacuo* and the red solid was purified by column chromatography (1% MeOH in CH_2Cl_2) to yield 42 mg (43%) of **7**.

^{1}H NMR (δ ppm, $CDCl_3$, 300 MHz): 8.74 (m, 8H, ß-pyrrole), 7.97 (d, 6H, ArH meta to OR, J = 8.3 Hz), 7.94 (d, 2H, ArH meta to OR, J = 8.8 Hz), 7.13 (d, 6H, ArH meta to OR, J = 8.3 Hz), 7.09 (d, 2H, ArH meta to OR, J = 8.6 Hz), 6.98 (t, 1H, NH, J = 5.1 Hz), 4.22 (q, 1H, CH Ala, J = 7.1 Hz), 4.07 (m, 8H, OCH_2), 3.62 (q, 2H, NHCH_2, J = 5.6 Hz), 2.05 (qn, 2H, $NHCH_2CH_2$, J = 5.6 Hz), 1.89 (qn, 6H, OCH_2CH_2, J = 7.1 Hz), 1.67 (d, 3H, CH_3 Ala, J = 7.1 Hz), 1.55 (qn, 6H, $OCH_2CH_2CH_2$, J = 7.1 Hz), 1.43–1.25 (overlapping multiplets, 48H, aliphatic H), 0.90 (t, 3H, J = 6.6 Hz). ^{13}C NMR (δ ppm, $CDCl_3$, 75 MHz): 166.0 (CO Ala), 161.3 (CN), 158.9, 158.2 (ArC ipso to OR), 141.2, 141.0, 134.8, 134.2, 133.5, (ArC), 130.6 (br, ArC next to ArN), 122.1, 121.7, 112.7 (ArC), 68.2, 66.9 ($ArOCH_2$), 53.5 (CH Ala), 38.7 ($NHCH_2$), 31.9 ($ArOCH_2CH_2$), 29.7-29.4 (CH_2), 28.7 ($CH_2CH_2CH_3$), 26.2 ($CH_2CH_2NH_2$), 22.7 (CH_2CH_3), 19.9 (CH_3 Ala), 14.1 (CH_3). FT-IR (cm^{-1}, ATR): 3380 (NH), 2922, 2850 (CH), 2134 (CN), 1684 (Amide I), 1542 (amide II), 1239 (CO). MALDI-TOF: m/z = 1513.3 (M^+). Calcd for $C_{87}H_{110}N_6O_5Pt$: 1512.8.

Typical procedure for the statistical copolymerisation reactions

To a stirred solution of monomers **7** and **8** in CH_2Cl_2 (1 mL) was added 1/1000 equiv. of nickel catalyst (prepared from a solution of $Ni(ClO_4)_2{\cdot}6H_2O$ in 98 mL $CHCl_3$ and 2 mL ethanol) After complete consumption of the isocyanide according to TLC, the reaction mixture was precipitated in 10 mL of methanol/water (4:1 v/v) under vigorous stirring. The solid was collected by centrifugation and subsequent decantation of the solvent. Subsequently, the polymer was dissolved in chloroform (5 mL) again and precipitated in methanol (~60 mL) after which the solid was collected. The polymers were subjected to size exclusion chromatography to remove any unreacted isocyanide monomers. The ^{1}H NMR spectrum of the resulting polymers showed broad signals in the aromatic and the aliphatic regions. In the IR spectrum the isocyanide stretch was no longer evident. With AFM polymer fibers with length between 200 and 600 nm were visible.

3,4,9,10-Perylenetetracarboxy-3,4-anhydride potassium salt.

3,4:9,10-Perylenetetracarboxydianhydride (10.0 g, 25.5 mmol) was placed in a 3-necked round bottom flask and water (800 mL) was added. Potassium hydroxide (40.0 g, 0.71 mol) was added and the resulting mixture was stirred at 90 °C for 2 h, over which time the colour of the reaction mixture changed from red to green. Addition of acetic acid (50 mL) resulted in a colour change to brown and after stirring at 90 °C for 40 min the formed purple solid (11.0 g, 96%) was removed by filtration and washed thoroughly with methanol before the product was dried at 120 ºC. Due to the insolubility of this compound in all solvents, characterisation could not be performed.

***N*^{1}-(N-Boc-propyl)-3,4,9,10-Perylenetetracarboxy-3,4-anhydride-9,10-imide.**

3,4,9,10-Perylenetetracarboxy-3,4-anhydride potassium salt (0.58 g, 1.3 mmol) and N-*Boc*-1,3-diaminopropane (0.92 g, 5.3 mmol, 4.0 equiv.) were placed in a round bottom flask and water (60 mL) was added. The solution was stirred at 90 ºC for 4 h after which aqueous potassium carbonate (25%, 200 mL) was added. The solution was heated at 90 ºC for 3 h, over which time the colour changed from purple to green. The solid was filtered off and washed from the filter with a water (300 mL) and triethylamine (10 mL) mixture. The filtrate was diluted with a saturated citric acid solution in water (500 mL) and after waiting for one day the precipitated solid was

filtered off and washed with methanol. The product was obtained as a purple solid (0.65 g, 92%). Due to the insolubility of this compound, characterisation could not be performed.

For the assignment of the chemical shifts in the NMR spectra of the perylene-porphyrin compounds the protons are numbered as shown below:

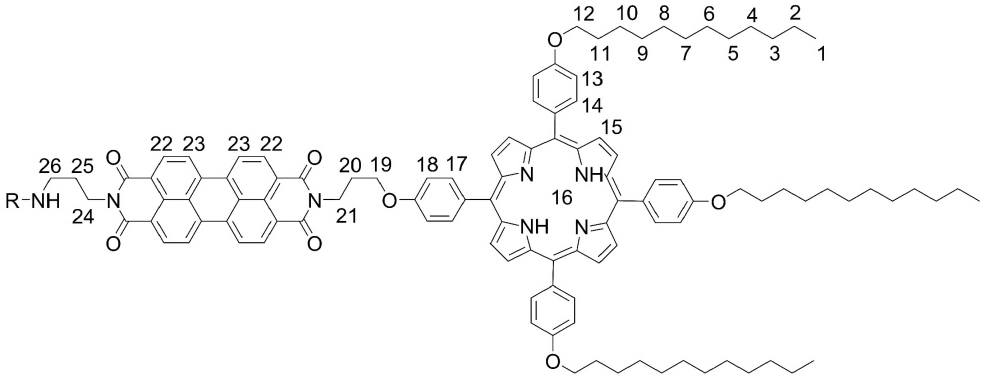

N-Boc-propyl-perylene-propyl-porphyrin 13

Under a N_2 atmosphere **12** (700 mg, 0.56 mmol), **11** (357 mg, 0.06 mmol) and imidazole (15.7 gr) were placed in a Schlenk vessel and DMF / Toluene (100 ml, 1:1 v/v) was added. The suspension was heated for 72 hrs at 97 ºC after which time the mixture was poured out in a saturated citric acid solution in water / ethanol (400 ml, 1:3 v/v). The solid was filtered off and washed with $CHCl_3$ and MeOH / $CHCl_3$ (1:9 v/v). The filtrate was subsequently washed with a 5% citric acid solution in water, dried (Na_2SO_4) and subjected to column chromatography (3 ×; 2% MeOH in $CHCl_3$, toluene and finally 0.25% MeOH in $CHCl_3$) to yield red-purple **13** in 44% yield. ^{1}H NMR (δ ppm, $CDCl_3$, 300 MHz): 8.76 (m, 8H, **15**), 7.99 (m, 12H, **22**, **14**, **17**), 7.40 (m, 4H, **23**), 7.22 (m, 8H, **13**, **18**), 5.35 (br, 1H, NH), 4.46 (br, 4H, **19**, **21**), 4.22 (tr, 2H, **24**, J = 5.5 Hz), 4.15 (tr, 6H, **12**, J = 6.4 Hz), 3.23 (br, 2H, **26**), 2.45 (br, 2H, **20**), 1.94 (m, 8H, **11**, **25**), 1.60 (m, 6H, **10**), 1.53 (s, 9H, $C(CH_3)_3$), 1.6–1.25 (m, 48H, **2**–**9**), 0.89 (m, 9H, **1**), –3.11 (s, 2H, **16**). MALDI-TOF: m/z = 1770.0 (M^+). Calcd for $C_{115}H_{131}N_7O_{10}$: 1770.0

Boc-L-ala-propyl-perylene-propyl-porphyrin 14

To a solution of **13** (80 mg, 0.05 mmol) in CH_2Cl_2 (20 mL), trifluoro acetic acid (2 mL) was added and the mixture was stirred for 4 h. After evaporation of the solvent *in vacuo*, the product was dissolved again in $CHCl_3$ (250 mL) and washed subsequently with an aqueous 10 % (w/w) sodium bicarbonate solution (100 mL) and brine (100 mL). The organic layer was dried (Na_2SO_4) and purified by column chromatography (3 % MeOH in $CHCl_3$). The product was used in the next step without further characterisation. For this reaction, the amine was dissolved in CH_2Cl_2 (50 mL) and to this solution were added Boc-L-alanine (15.5 mg, 0.08 mmol), HOBT (12.2 mg, 0.08 mmol) and EDC (18.1 mg, 0.09 mmol) and the reaction mixture was stirred overnight at room temperature. The solution was subsequently washed with an aqueous 10% (w/w) citric acid solution (2 × 200 mL), H_2O (200 mL), an aqueous 10 % (w/w) sodium carbonate solution (2 × 200 mL) and H_2O (200 mL). The organic layer was dried (Na_2SO_4), concentrated and subjected to column chromatography (1% MeOH in CH_2Cl_2), yielding 89% (74 mg) of **14** as a red-purple solid. ^{1}H NMR (δ ppm, $CDCl_3$, 400 MHz): 8.82 (m, 8H, **15**), 8.59 (d, 2H, **22**, J = 7.8 Hz), 8.52 (d, 2H, **22**, J = 7.8 Hz), 8.39 (m, 4H, **23**), 8.06 (m, 8H, **14**, **17**), 7.23 (m, 8H, **13**, **18**), 6.64 (d, 1H, NH), 5.55 (br, 2H, NH, CH Ala), 4.85 (br tr, 2H, **21**, J = 6.6 Hz), 4.46 (br tr, 2H, **19**, J = 5.9 Hz), 4.23 (m, 2H, **24**), 4.15 (tr, 6H, **12**, J = 6.1 Hz), 3.32 (m, 2H, **26**), 2.49 (m, 2H, **20**), 1.98 (m, 8H, **11**, **25**), 1.62 (m, 6H, **10**), 1.50 (d, 3H, CH_3 Ala, J = 5.1

Hz), 1.47 (s, 9H, $C(CH_3)_3$), 1.31–1.26 (m, 48H, **2–9**), 0.88 (m, 9H, **1**), –2.80 (s, 2H, **16**). MALDI-TOF: m/z = 1841.2 (M^+). Calcd for $C_{119}H_{138}N_8O_{10}$: 1848.1

N-formyl-L-ala-propyl-perylene-propyl-porphyrin 15

To a solution of **14** (30 mg, 0.02 mmol) in CH_2Cl_2 (20 mL), trifluoro acetic acid (4 mL) was added and the mixture was stirred for 4 h. After evaporation of the solvent *in vacuo*, the product was dissolved in CH_2Cl_2 (100 mL) and washed subsequently with an aqueous 10 % (w/w) sodium bicarbonate solution (2 × 100 mL) and brine (100 mL). The organic layer was dried (Na_2SO_4) and purified by column chromatography (4–6 % MeOH in $CHCl_3$). The product was used in the next step without further characterisation. For the formylation reaction, the amine was dissolved in CH_2Cl_2 (30 mL) and an excess of 2,4,5-trichlorophenyl formate (25 mg, 0.11mmol, 2.8 equiv.) was added. After stirring the mixture for 72 h the solution was washed with a saturated aqueous solution of sodium bicarbonate (2 × 100 mL) and brine (100 mL). The solvent was evaporated *in vacuo* and the solid was subjected to column chromatography (1.5 % MeOH in CH_2Cl_2) to give **15** (8.5 mg, 30%) as a red-purple solid. ^{1}H NMR (δ ppm, $CDCl_3$, 400 MHz): 8.80 (m, 8H, **15**), 8.46 (d, 2H, **22**, J = 6.8 Hz), 8.37 (d, 2H, **22**, J = 7.3 Hz), 8.23 (s, 1H, HCO), 8.17 (m, 4H, **23**), 8.03 (m, 8H, **14**, **17**), 7.20 (m, 8H, **13**, **18**), 7.03 (tr, 1H, CH_2NH, J = 5.7 Hz), 6.64 (d, 1H, CHNH, J = 6.4 Hz), 4.69 (qn, 1H, CH Ala, J = 6.9 Hz), 4.85 (br tr, 2H, **21**, J = 5.5 Hz), 4.46 (br tr, 2H, **19**, J = 5.3 Hz), 4.22 (m, 2H, **24**), 4.15 (tr, 6H, **12**, J = 6.1 Hz), 3.34 (br q, 2H, **26**, J = 5.9 Hz), 2.49 (br qn, 2H, **20**, J = 6.1 Hz), 1.96 (m, 8H, **11**, **25**), 1.60 (m, 6H, **10**), 1.50 (d, 3H, CH_3 Ala, J = 6.8 Hz), 1.30–1.25 (m, 48H, **2–9**), 0.89 (m, 9H, **1**), –2.89 (s, 2H, **16**). MALDI-TOF: m/z = 1769.0 (M^+). Calcd for $C_{114}H_{128}N_8O_{10}$: 1769.1. UV-Vis (CH_2Cl_2): λ_{max} (ε) = 422 (315449), 459 (14610), 489 (36525), 526 (66410) 555 (8965), 596 (3818), 651 (3685, mol^{-1} L cm^{-1}). Fluorescence (CH_2Cl_2) λ_{exc} = 425 nm: λ_{max} = 535, 574, 656 and 718; λ_{exc} = 492 nm: 535, 574 and 654.

3.7 References & Notes

(1) Dimitrakopoulos, C. D.; Malenfant, P. R. L. *Adv. Mater.* **2002**, *14*, 99-117; Struijk, C. W.; Sieval, A. B.; Dakhorst, J. E. J.; van Dijk, M.; Kimkes, P.; Koehorst, R. B. M.; Donker, H.; Schaafsma, T. J.; Picken, S. J.; van de Craats, A. M.; Warman, J. M.; Zuilhof, H.; Sudholter, E. J. R. *J. Am. Chem. Soc.* **2000**, *122*, 11057-11066.

(2) Gregg, B. A.; Sprague, J.; Peterson, M. W. *J. Phys. Chem. B* **1997**, *101*, 5362-5369.

(3) Chen, Z. J.; Debije, M. G.; Debaerdemaeker, T.; Osswald, P.; Wurthner, F. *Chemphyschem* **2004**, *5*, 137-140; Chesterfield, R. J.; McKeen, J. C.; Newman, C. R.; Ewbank, P. C.; da Silva, D. A.; Bredas, J. L.; Miller, L. L.; Mann, K. R.; Frisbie, C. D. *J. Phys. Chem. B* **2004**, *108*, 19281-19292; Malenfant, P. R. L.; Dimitrakopoulos, C. D.; Gelorme, J. D.; Kosbar, L. L.; Graham, T. O.; Curioni, A.; Andreoni, W. *Appl. Phys. Lett.* **2002**, *80*, 2517-2519.

(4) Ahrens, M. J.; Sinks, L. E.; Rybtchinski, B.; Liu, W. H.; Jones, B. A.; Giaimo, J. M.; Gusev, A. V.; Goshe, A. J.; Tiede, D. M.; Wasielewski, M. R. *J. Am. Chem. Soc.* **2004**, *126*, 8284-8294; Balakrishnan, K.; Datar, A.; Naddo, T.; Huang, J. L.; Oitker, R.; Yen, M.; Zhao, J. C.; Zang, L. *J. Am. Chem. Soc.* **2006**, *128*, 7390-7398; Franke, D.; Vos, M.; Antonietti, M.; Sommerdijk, N. A. J. M.; Faul, C. F. J. *Chem. Mater.* **2006**, *18*, 1839-1847; Guan, Y.; Zakrevskyy, Y.; Stumpe, J.; Antonietti, M.; Faul, C. F. J. *Chem. Commun.* **2003**, 894-895; Sugiyasu, K.; Fujita, N.; Shinkai, S. *Angew. Chem., Int. Ed.* **2004**, *43*, 1229-1233; Tauber, M. J.; Kelley, R. F.; Giaimo, J. M.; Rybtchinski, B.; Wasielewski, M. R. *J. Am. Chem. Soc.* **2006**, *128*, 1782-1783; Zakrevskyy, Y.; Faul, C. F. J.; Guan, Y.; Stumpe, J. *Adv. Funct. Mater.* **2004**, *14*, 835-841; Palermo, V.; Liscio, A.; Gentilini, D.; Nolde, F.; Mullen, K.; Samori, P. *Small* **2007**, *3*, 161-167; De Luca, G.; Liscio, A.; Maccagnani, P.; Nolde, F.; Palermo, V.; Mullen, K.; Samori, P. *Adv. Funct. Mater.* **2007**, *17*, 3791-3798; Liscio, A.; De Luca, G.; Nolde, F.; Palermo, V.; Muellen, K.; Samori, P. *J. Am. Chem. Soc.* **2008**, *130*, 780-781.

(5) Giaimo, J. M.; Gusev, A. V.; Wasielewski, M. R. *J. Am. Chem. Soc.* **2002**, *124*, 8530-8531.

(6) Thalacker, C.; Wurthner, F. *Adv. Funct. Mater.* **2002**, *12*, 209-218.

(7) Liu, S. G.; Sui, G. D.; Cormier, R. A.; Leblanc, R. M.; Gregg, B. A. *J. Phys. Chem. B* **2002**, *106*, 1307-1315; Wurthner, F.; Chen, Z. J.; Dehm, V.; Stepanenko, V. *Chem. Commun.* **2006**, 1188-1190; Wurthner, F.; Thalacker, C.; Diele, S.; Tschierske, C. *Chem. Eur. J.* **2001**, *7*, 2245-2253.

(8) Han, J. J.; Wang, W.; Li, A. D. Q. *J. Am. Chem. Soc.* **2006**, *128*, 672-673; Hippius, C.; Schlosser, F.; Vysotsky, M. O.; Bohmer, V.; Wurthner, F. *J. Am. Chem. Soc.* **2006**, *128*, 3870-3871; Neuteboom, E. E.; Janssen, R. A. J.; Meijer, E. W. *Synthetic. Met.* **2001**, *121*, 1283-1284; Wang, W.; Wan, W.; Zhou, H. H.; Niu, S. Q.; Li, A. D. Q. *J. Am. Chem. Soc.* **2003**, *125*, 5248-5249.

(9) Li, A. D. Q.; Wang, W.; Wang, L. Q. *Chem. Eur. J.* **2003**, *9*, 4594-4601; Neuteboom, E. E.; Meskers, S. C. J.; Meijer, E. W.; Janssen, R. A. J. *Macromol. Chem. Physic.* **2004**, *205*, 217-222; Wang, W.; Li, L. S.; Helms, G.; Zhou, H. H.; Li, A. D. Q. *J. Am. Chem. Soc.* **2003**, *125*, 1120-1121.

(10) Cornelissen, J. J. L. M.; Rowan, A. E.; Nolte, R. J. M.; Sommerdijk, N. A. J. M. *Chem. Rev.* **2001**, *101*, 4039-4070.

(11) Nolte, R. J. M. *Chem. Soc. Rev.* **1994**, *23*, 11-19; Okamoto, Y.; Nakano, T. *Chem. Rev.* **1994**, *94*, 349-372; Suginome, M.; Ito, Y. *Adv. Polym. Sci.* **2004**, *171*, 77-136.

(12) Vriezema, D. M.; Hoogboom, J.; Velonia, K.; Takazawa, K.; Christianen, P. C. M.; Maan, J. C.; Rowan, A. E.; Nolte, R. J. M. *Angew. Chem., Int. Ed.* **2003**, *42*, 772-776.

(13) de Witte, P. A. J.; Castriciano, M.; Cornelissen, J. J. L. M.; Scolaro, L. M.; Nolte, R. J. M.; Rowan, A. E. *Chem. Eur. J.* **2003**, *9*, 1775-1781.

(14) de Witte, P. A. J.; Hernando, J.; Neuteboom, E. E.; van Dijk, E. M. H. P.; Meskers, S. C. J.; Janssen, R. A. J.; van Hulst, N. F.; Nolte, R. J. M.; Garcia-Parajo, M. F.; Rowan, A. E. *J. Phys. Chem. B* **2006**, *110*, 7803-7812; Hernando, J.; de Witte, P. A. J.; van Dijk, E. M. H. P.; Korterik, J.; Nolte, R. J. M.; Rowan, A. E.; Garcia-Parajo, M. F.; van Hulst, N. F. *Angew. Chem., Int. Ed.* **2004**, *43*, 4045-4049.

(15) Otten, M. B. J. PhD thesis: Functionalized Polyisocyanides, Radboud University, **2010**.

(16) Cornelissen, J. J. L. M.; Graswinckel, W. S.; Adams, P. J. H. M.; Nachtegaal, G. H.; Kentgens, A. P. M.; Sommerdijk, N. A. J. M.; Nolte, R. J. M. *J. Polym. Sci., Part A: Polym. Chem.* **2001**, *39*, 4255-4264.

(17) Demmig, S.; Langhals, H. *Chem. Ber.* **1988**, *121*, 225-230.

(18) Kaiser, H.; Lindner, J.; Langhals, H. *Chem. Ber.* **1991**, *124*, 529-535.

(19) Bellamy, L. *The Infra Red Spectra of Complex Molecules*; 3 ed., 1975.

(20) Kamer, P. C. J.; Nolte, R. J. M.; Drenth, W. *J. Am. Chem. Soc.* **1988**, *110*, 6818-6825.

(21) Prokhorova, S. A.; Sheiko, S. S.; Moller, M.; Ahn, C. H.; Percec, V. *Macromol. Rapid. Comm.* **1998**, *19*, 359-366.

(22) Cornelissen, J. J. L. M.; Donners, J. J. J. M.; de Gelder, R.; Graswinckel, W. S.; Metselaar, G. A.; Rowan, A. E.; Sommerdijk, N. A.; Nolte, R. J. M. *Science* **2001**, *293*, 676-80.

(23) Cornelissen, J.; Graswinckel, W. S.; Rowan, A. E.; Sommerdijk, N.; Nolte, R. J. M. *J. Polym. Sci., Part A: Polym. Chem.* **2003**, *41*, 1725-1736.

(24) Spano, F. C. *J. Chem. Phys.* **2005**, *122*, 234701; Spano, F. C. *J. Chem. Phys.* **2007**, *126*, 159901.

(25) van der Boom, T.; Hayes, R. T.; Zhao, Y. Y.; Bushard, P. J.; Weiss, E. A.; Wasielewski, M. R. *J. Am. Chem. Soc.* **2002**, *124*, 9582-9590.

(26) Cornelissen, J. J. L. M.; Sommerdijk, N. A. J. M.; Nolte, R. J. M. *Macromol. Chem. Physic.* **2002**, *203*, 1625-1630.

(27) Wurthner, F.; Chen, Z. J.; Hoeben, F. J. M.; Osswald, P.; You, C. C.; Jonkheijm, P.; von Herrikhuyzen, J.; Schenning, A. P. H. J.; van der Schoot, P. P. A. M.; Meijer, E. W.; Beckers, E. H. A.; Meskers, S. C. J.; Janssen, R. A. J. *J. Am. Chem. Soc.* **2004**, *126*, 10611-10618.

(28) Kasha, M.; Rawls, H.; El-Bayoumi, M. *Pure Appl. Chem* **1965**, *11*, 371.

(29) Harada, N.; Nakanishi.K *Circular Dichroism Spectroscopy. Exciton Coupling in Organic Stereochemistry*; Univ Sci. Books: California, 1983; Harada, N.; Nakanish.K *Acc. Chem. Res.* **1972**, *5*, 257-263.

(30) Metselaar, G. A.; Cornelissen, J. J. L. M.; Rowan, A. E.; Nolte, R. J. M. *Angew. Chem., Int. Ed.* **2005**, *44*, 1990-1993.

(31) A Guide to Recording Fluorescence Quantum Yields: http://www.jobinyvon.com/usadivisions/fluorescence/applications/quantumyieldstrad.pdf.

(32) Bisht, P. B.; Fukuda, K.; Hirayama, S. *Chem. Phys. Lett.* **1996**, *258*, 71-79; Ford, W. E.; Kamat, P. V. *J. Phys. Chem.* **1987**, *91*, 6373-6380.

(33) Katoh, R.; Sinha, S.; Murata, S.; Tachiya, M. *J. Photoch. Photobio. A* **2001**, *145*, 23-34; Masuko, M.; Ohtani, H.; Ebata, K.; Shimadzu, A. *Nucleic Acids. Res.* **1998**, *26*, 5409-5416.

(34) Palermo, V.; Otten, M. B. J.; Liscio, A.; Schwartz, E.; de Witte, P. A. J.; Castriciano, M. A.; Wienk, M. M.; Nolde, F.; De Luca, G.; Cornelissen, J. J. L. M.; Janssen, R. A. J.; Mullen, K.; Rowan, A. E.; Nolte, R. J. M.; Samori, P. *J. Am. Chem. Soc.* **2008**, *130*, 14605-14614.

(35) Foster, S.; Finlayson, C. E.; Keivanidis, P. E.; Huang, Y.-S.; Hwang, I.; Friend, R. H.; Otten, M. B. J.; Lu, L.-P.; Schwartz, E.; Nolte, R. J. M.; Rowan, A. E. *Macromolecules* **2009**, *42*, 2023-2030.

(36) P3HT: Poly-3-hexylthiophene; PFB: Poly(9,9′-dioctylfluorene-co-bis-N,N′-(4-butylphenyl)-bis-N,N′-phenyl-1,4-phenyl-diamine) and F8BT: Poly(9,9-dioctylfluorene-co-benzothidiazole)

(37) Campbell, I. H.; Rubin, S.; Zawodzinski, T. A.; Kress, J. D.; Martin, R. L.; Smith, D. L.; Barashkov, N. N.; Ferraris, J. P. *Phys. Rev B.* **1996**, *54*, 14321-14324.

(38) The carrier mobility as a function of temperature were also studied; a measured mobility of order 10^{-3} $cm^2 V^{-1} s^{-1}$ is reached at 360 K.

(39) de Boer, R. W. I.; Gershenson, M. E.; Morpurgo, A. F.; Podzorov, V. *Physica Status Solidi A -Applied Research* **2004**, *201*, 1302-1331.

(40) Adler, A. D.; Shergali.W; Longo, F. R. *J. Am. Chem. Soc.* **1964**, *86*, 3145-3149; Adler, A. D.; Longo, F. R.; Finarell.Jd; Goldmach.J; Assour, J.; Korsakof.L *J. Org. Chem.* **1967**, *32*, 476.

(41) The rodlike nature of the purified polymers prevented us from obtaining information about its molecular weight and polydispersity by means of the usual techniques, such as MALDITOF,MS, or GPC. For an estimation of the Mws see reference 42.

(42) Schwartz, E.; Palermo, V.; Finlayson, C. E.; Huang, Y.-S.; Otten, M. B. J.; Liscio, A.; Trapani, S.; González-Valls, I.; Brocorens, P.; Cornelissen, J. J. L. M.; Peneva, K.; Müllen, K.; Spano, F.; Yartsev, A.; Westenhoff, S.; Friend, R. H.; Beljonne, D.; Nolte, R. J. M.; Samori, P.; Rowan, A. E. *Chem. Eur. J.* **2009**, *15*, 2536-2547.

(43) Huang, Y.-S. PhD thesis: Chapter 6: Sequential energy and electron transfer in polyisocyanopeptides based multichromophoric arrays, Cambridge University, **2008**.

(44) The insertion of platinum in into the porphyrin, gives rise to a strong spin-orbit coupling. If there is a strong spin-orbit coupling available, then intersystem crossing (ISC) can occur, which might induce a singlet-triplet transition. Subsequent emission form the triplet excited state to the ground stead leads to phosphorescence

(45) Mezyk, J.; Kalinowski, J.; Meinardi, F.; Tubino, R. *Appl. Phys. Lett.* **2005**, *86*, 111916; Kalinowski, J.; Stampor, W.; Szmytkowski, J.; Cocchi, M.; Virgili, D.; Fattori, V.; Di Marco, P. *J. Chem. Phys.* **2005**, *122*, 154710.

(46) Bansal, A. K.; Holzer, W.; Penzkofer, A.; Tsuboi, T. *Chemical Physics* **2006**, *330*, 118-129.

(47) Osuka, A.; Shimidzu, H. *Angew. Chem., Int. Ed.* **1997**, *36*, 135-137; Nagata, T.; Osuka, A.; Maruyama, K. *J. Am. Chem. Soc.* **1990**, *112*, 3054-3059.

(48) Kasha, M.; Rawls, H. R.; El-Bayoumi, M. A. *Pure. Appl. Chem.* **1965**, *11*, 371-92.

(49) Kaletas, B. K.; Dobrawa, R.; Sautter, A.; Wurthner, F.; Zimine, M.; De Cola, L.; Williams, R. M. *J. Phys. Chem. A* **2004**, *108*, 1900-1909.

(50) Shibano, Y.; Umeyama, T.; Matano, Y.; Tkachenko, N. V.; Lemmetyinen, H.; Araki, Y.; Ito, O.; Imahori, H. *J. Phys. Chem. C* **2007**, *111*, 6133-6142.

(51) Loewe, R. S.; Tomizaki, K.-y.; Youngblood, W. J.; Bo, Z.; Lindsey, J. S. *J. Mater. Chem.* **2002**, *12*, 3438-3451.

(52) Okamoto, K.; Mori, Y.; Yamada, H.; Imahori, H.; Fukuzumi, S. *Chem. Eur. J.* **2004**, *10*, 474-483.

(53) Oneil, M. P.; Niemczyk, M. P.; Svec, W. A.; Gosztola, D.; Gaines, G. L.; Wasielewski, M. R. *Science* **1992**, *257*, 63-65.

(54) Ambroise, A.; Kirmaier, C.; Wagner, R. W.; Loewe, R. S.; Bocian, D. F.; Holten, D.; Lindsey, J. S. *J. Org. Chem.* **2002**, *67*, 3811-3826; Miller, M. A.; Lammi, R. K.; Prathapan, S.; Holten, D.; Lindsey, J. S. *J. Org. Chem.* **2000**, *65*, 6634-6649.

(55) Prathapan, S.; Yang, S. I.; Seth, J.; Miller, M. A.; Bocian, D. F.; Holten, D.; Lindsey, J. S. *J. Phys. Chem. B* **2001**, *105*, 8237-8248; Yang, S. I.; Lammi, R. K.; Prathapan, S.; Miller, M. A.; Seth, J.; Diers, J. R.; Bocian, D. F.; Lindsey, J. S.; Holten, D. *J. Mater. Chem.* **2001**, *11*, 2420-2430; Yang, S. I.; Prathapan, S.; Miller, M. A.; Seth, J.; Bocian, D. F.; Lindsey, J. S.; Holten, D. *J. Phys. Chem. B* **2001**, *105*, 8249-8258.

(56) Ghirotti, M.; Chiorboli, C.; You, C.-C.; Wurthner, F.; Scandola, F. *J. Phys. Chem. A* **2008**, *112*, 3376-3385; You, C.-C.; Wurthner, F. *Organic Letters* **2004**, *6*, 2401-2404.

(57) Kelley, R. F.; Tauber, M. J.; Wasielewski, M. R. *J. Am. Chem. Soc.* **2006**, *128*, 4779-4791; Kelley, R. F.; Shin, W. S.; Rybtchinski, B.; Sinks, L. E.; Wasielewski, M. R. *J. Am. Chem. Soc.* **2007**, *129*, 3173-3181.

(58) Mathew, S.; Johnston, M. R. *Chem. Eur. J.* **2009**, *15*, 248-253.

(59) Goutermann, M. In *The Porphyrins: Physical Chemistry, Part A*; Dolphin, D., Ed.; Academic Press Inc: London, 1978; Vol. 3.

(60) Fisher, A. W. In *Pigment Handbook: Properties and Economics* Patton, T. C., Ed.; Whiley & Sons: New York, 1973; Vol. 1.

(61) Goutermann, M. *J. Chem. Phys.* **1959**, *30*, 1139.

(62) Kircher, T.; Lohmannsroben, H. G. *Phys. Chem. Chem. Phys.* **1999**, *1*, 3987-3992.

(63) Skorna, G.; Ugi, I. *Angew. Chem., Int. Ed.* **1977**, *16*, 259-260.

(64) Creedon, S. M.; Crowley, H. K.; McCarthy, D. G. *Journal of the Chemical Society, Perkin Transactions 1: Organic and Bio-Organic Chemistry* **1998**, 1015-1018; Khapli, S.; Dey, S.; Mal, D. *Journal of the Indian Institute of Science* **2001**, *81*, 461-476.

(65) Ugi, I.; Meyr, R. *Angew. Chem., Int. Ed.* **1958**, *70*, 702-703.

(66) Böhme, H.; Fuchs, G. *Chem. Ber.* **1970**, *103*, 2775-2779.

(67) Walborsky, H. M.; Niznik, G. E. *J. Org. Chem.* **1972**, *37*, 187.

(68) Van der Eijk, J. M.; Nolte, R. J. M.; Drenth, W. *Recueil des Travaux Chimiques des Pays-Bas* **1978**, *97*, 46-9.

(69) Wittmann, R. *Angew. Chem., Int. Ed.* **1961**, *73*, 219.

(70) Porcheddu, A.; Giacomelli, G.; Salaris, M. *J. Org. Chem.* **2005**, *70*, 2361-2363.

(71) Nielsen, C. B.; Krebs, F. C. *Tetrahedron Letters* **2005**, *46*, 5935-5939.

(72) Krapcho, A. P.; Kuell, C. S. *Synthetic. Commun.* **1990**, *20*, 2559-2564.

4

Synthesis, characterisation and chiroptical properties of ‘click’able polyisocyanopeptides[§]

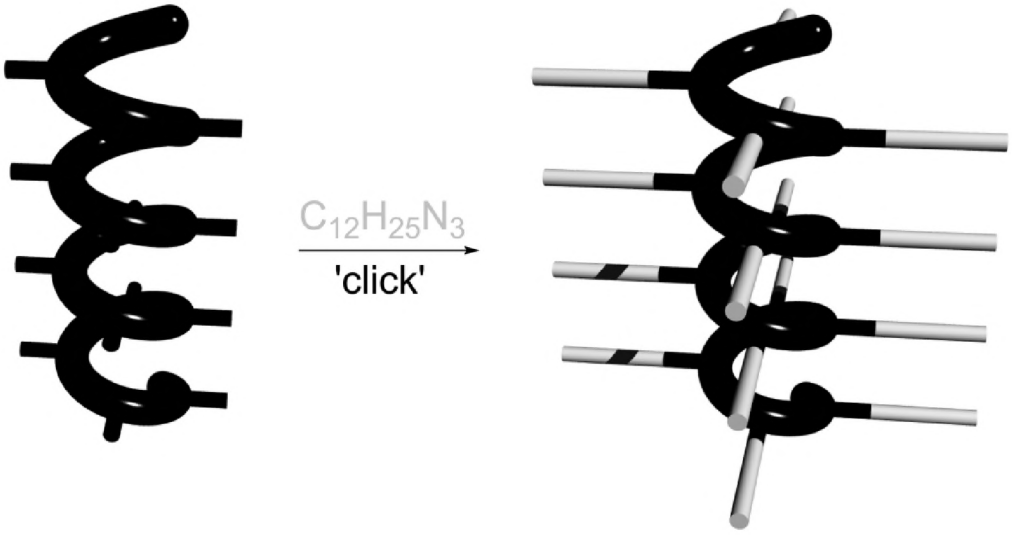

[§]Parts of this work have been published: Schwartz, E.; Kitto, H. J.; de Gelder, R.; Nolte, R. J. M.; Rowan, A. E.; Cornelissen, J. J. L. M. *Journal of Materials Chemistry* **2007**, *17*, 1876–1884.

4.1 Introduction

The utility of click chemistry to prepare novel materials has received wide attention in different fields in recent years. The use of this elegant class of reactions is mainly based on its near quantitative yield, selectivity, regiospecific conversion and its high compatibility with a broad range of functional groups and reaction conditions. Originally developed by Sharpless, Fokin and co-workers[1] and widely utilised in the synthesis of small organic molecules, the copper catalysed click reaction (Scheme 1) between acetylenes and azides is now also used in the synthesis of dendrimers,[2] biologically derived architectures,[3] DNA metallisation[4] and (bio)polymers.[5] In this last area, click chemistry has led to the construction of well-defined functional polymer materials. Emrick and co-workers applied the copper-catalysed click reaction to graft oligopeptides to acetylene-functionalised aliphatic polyesters, which are considered to be of interest as polymer-based biomaterials due to their biocompatibility and biodegradability.[6] Recently, the copper-catalysed coupling of an alkyne with an azide to link two polymers together, has been demonstrated by van Hest et al. [7] The post-functionalisation of polymers by the click reaction has also been shown,[8,9] but to date, these investigations have mainly been focussed on random coil polymers.

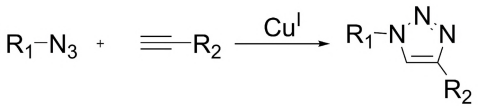

Scheme 1. Cu(I) catalyzed cyclo addition of an azide and an acetylene to form the triazole (1,4-regioisomer).

Polyisocyanides,[10] also known as polyisonitriles or polyiminomethylenes, are most commonly prepared by nickel(II) induced polymerisation of isocyanide monomer units. A special characteristic of polyisocyanides is the fact that every carbon atom in the polymer backbone bears a substituent, leading to considerable steric hindrance. The C–C bonds of the backbone twist and adopt a helical structure in order to minimise the steric hindrance. Polyisocyanides have a well-defined 4_1 helical conformation (i.e., 4 repeat units per helical turn), which is only stable when sterically demanding side-chains are present.[11] Cornelissen et al. introduced chiral peptide substituents onto the side chain in order to stabilise the helical arrangement of the polyisocyanides, leading to a preference for a left (*M*) or a right (*P*) handed helical arrangement of the polymer.[12] The peptide containing polymers have been studied in detail with ^{1}H NMR spectroscopy, Infrared spectroscopy (IR), Circular Dichroism (CD) and by Atomic Force Microscopy (AFM) techniques and it was found that the well-defined hydrogen bonding network between the peptide side chains at position n and (n+4), with a stacking distance of 4.6 Å, led to extremely stiff polymers with a persistence length of 76 nm.[13]

Previous work from our group has demonstrated that, using the concept of polyisocyanides as a scaffold, porphyrins,[14] thiophenes[15] and perylenes[16] could be organised over a large distance resulting in highly ordered functional polymers. The synthesis of these functionalised polyisocyanides is, however, laborious and not always straightforward. Therefore, we synthesised acetylene containing isocyanopeptides to use as (modular) building blocks for the construction of functionalised polyisocyanides, making use of the copper-catalysed cycloaddition with derivatised azides. In this chapter the synthesis and the characterisation of the acetylene functionalised polyisocyanides is discussed. The potential for derivatisation of these materials using click chemistry was successfully demonstrated by the reaction of these polymers with aliphatic tails functionalised with azide moieties.

4.2 Results and Discussion

The stepwise synthesis of the isocyanide monomers allowed for the building of different stereoisomers (e.g., DL, LD or LL) and on treatment with Ni(II) resulted in formation of either *M* or *P* polymers, allowing CD spectroscopic investigations to be carried out. A Cotton effect in the CD spectrum in the range λ = 250 nm to 350 nm is characteristic for helical polyisocyanides and originates from the n-π* transition of the helically arranged imine groups in the polymer backbone.[17] Two types of CD spectra can be observed for polyisocyanopeptides: (i) A Cotton effect around λ = 310 nm, or (ii) around λ = 280 nm of a significantly lower intensity.[17-19] The first type of spectra is observed for polymers that have a well-defined hydrogen bonding array, e.g. DL-PIAA (poly(D-isocyanoalanyl-L-alanine methyl ester)) or LD-PIAA. The latter spectra are obtained when no well-defined hydrogen bonding arrays are present, as in the case of for example L-PIAG (poly(L-isocyanoalanyl-glycine methyl ester)).[18]

The synthetic route to the DL-acetylene functionalised polymer is outlined in Scheme 2. The coupling of 2-propynol to Boc-L-Ala-OH using 1-(3-dimethylaminopropyl)-3-ethylcarbodiimide hydrochloride (EDC) generated **1**. The Boc-protecting group of **1** was removed with an HCl-saturated solution of ethyl acetate and the resulting amine salt was subsequently coupled to Boc-D-Ala-OH under EDC conditions. The N-formylated dipeptide was prepared by cleavage of the Boc-protecting group of **2** using acid, followed by refluxing of the resulting amine HCl salt in ethyl formate in the presence of sodium formate. The isocyanide **4** was obtained by dehydration of the formamide **3** with diphosgene and N-methylmorpholine at –30 °C in THF.[20]

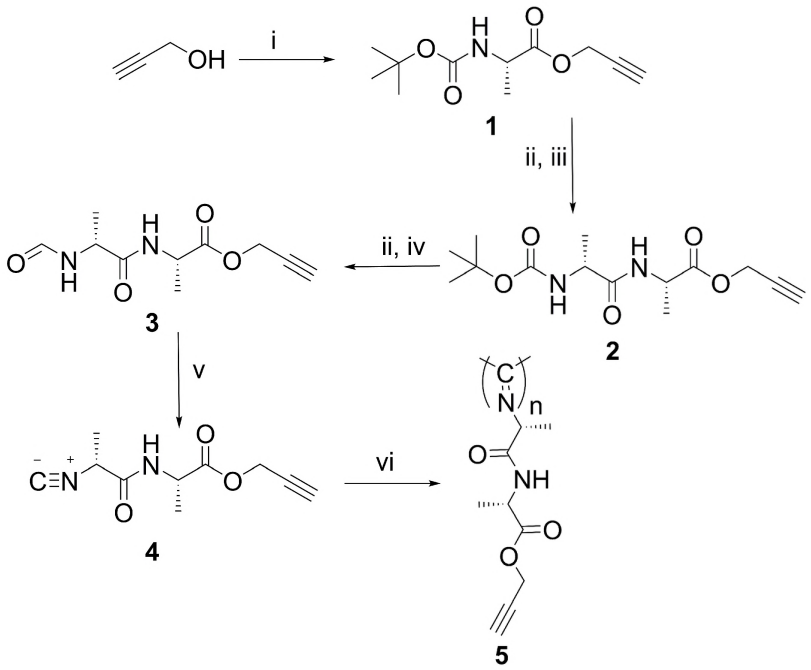

Scheme 2. Synthesis of polyisocyanide **5**; reagents and conditions. (i) EDC, HOBt, DIPEA, Boc-L-Ala-OH, CH_2Cl_2; (ii) EtOAc·HCl; (iii) EDC, HOBt, DIPEA, Boc-D-Ala-OH, CH_2Cl_2; (iv) Ethyl formate, $NaHCO_2$, reflux; (v) *N*-Methylmorpholine, diphosgene, THF, –30 °C; (vi) $Ni(ClO_4)_2·6H_2O$, CH_2Cl_2.

The isocyanide monomer **4** could be recrystallised from ethanol/hexane, offering crystals suitable for X-ray analysis. Compound **4** crystallises in the triclinic system, space group P1, with one molecule in the unit cell. The X-ray analysis has established the conformation and relative stereochemistry and shows (Figure 1) that the molecules are linked by N–H···O hydrogen bonds in the *a*-direction, with N···O 2.843 (7) Angstroms and N–H···O 167 degrees. These H-bonded chains are linked to adjacent chains by well-defined C–H···O hydrogen bonds involving the acetylenic C–H of one chain and a carboxyl oxygen of an adjacent chain, with C···O 3.256 (9) Angstrom and C–H···O 178 degrees, to generate sheets of molecules in the *ab* plane.

The polymerisation of monomer **4** with 3 mol% $Ni(ClO_4)_2·6H_2O$ in CH_2Cl_2/EtOH (98:2 v/v) was monitored using CD spectroscopy. A negative Cotton effect around 310 nm was clearly observed (Figure 2, left), indicating formation of the expected left-handed helix with a well-defined hydrogen bonding network.[19]

Recently, it was found that polyisocyanide **2** could be prepared by acid initiation resulting in polymers with the same chiroptical properties as those prepared using a nickel(II) catalyst, however, with a much higher molecular weight as observed by AFM.[21] In agreement with these studies **9** could be polymerised with acid, leading to polymers with a similar CD spectrum as observed during the nickel catalysed polymerisation of **9** (Figure 2, right).

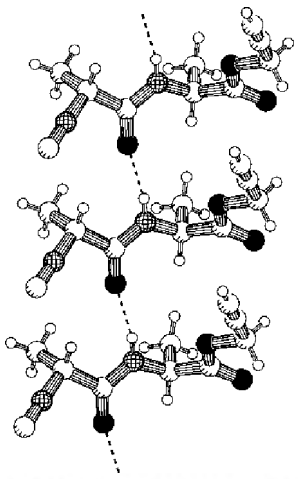

Figure 1. X-ray structure of monomer **4** showing the presence of hydrogen bonding between three stacked isocyanide molecules. The structure confirmed the presence of the acetylene with a bond C≡C bond distance of 1.151Å and a C-C≡C angle of 178.95°.

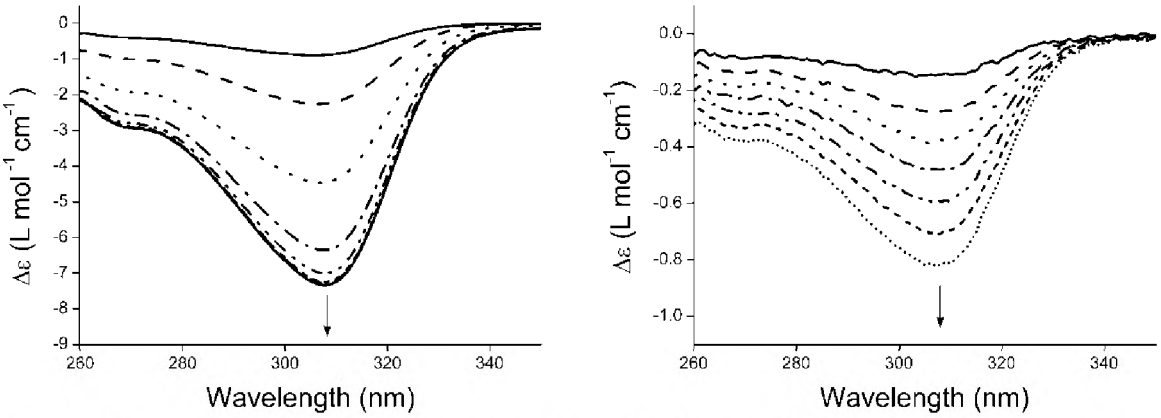

Figure 2. CD monitored polymerisation of **4** with 1/30 equiv. of Ni(II) (left) or 1/16 equiv. of TFA (right).

The polymerisation of isocyanopeptides can also be confirmed using infrared spectroscopy. Upon polymerisation of the isocyanopeptides the N-H stretching vibration and the amide I vibration shift to lower wavenumbers, as is expected when hydrogen bonds are formed between the amide groups in the side chains. Using IR spectroscopy the polymerisation reaction in dichloromethane was followed over time (Figure 3) by the disappearance of the CN stretching vibration at ν = 2136 cm^{-1}, the shift of the N-H stretching vibration from ν = 3430 cm^{-1} to 3261 cm^{-1} and the shift of the amide I vibrations from ν = 1710 cm^{-1} and ν = 1692 cm^{-1} to ν = 1657 cm^{-1}; the last two shifts point to the formation of a hydrogen bonding network. The unaltered signals at ν = 3303 cm^{-1} and ν = 1754 cm^{-1} are assigned to the C-H alkyne stretch and the C=O stretch vibration of the ester, respectively.

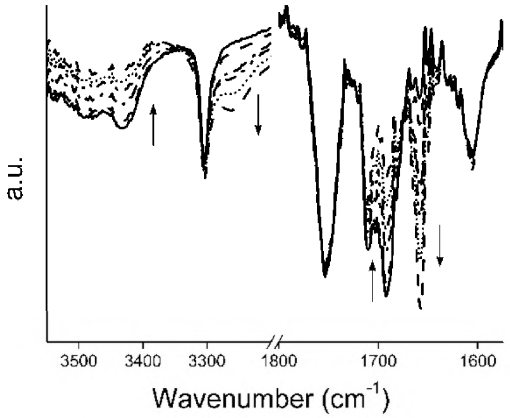

Figure 3. Polymerisation of **4** with 1/30 equiv. of Ni(II) monitored with Infrared spectroscopy. Arrows indicate the increasing or decreasing signals.

The polymerisation of compound **4** to give **5** could be monitored by spectroscopic techniques at relatively low dilution. However, at higher concentrations **5** was insoluble in organic solvents, e.g., $CHCl_3$ or CH_2Cl_2. The insolubility can be explained in three ways: (*i*) the polymer material is insoluble because of its molecular structure, (*ii*) during the polymerisation the acetylene function is also polymerised or (*iii*) occasionally an acetylene is built into the growing polymer chain instead of an isocyanide. Options *ii* and *iii* will result in cross-linked polymers and consequently lead to an insoluble material. Although CD and IR spectroscopic results indicated that the acetylene moiety was not involved in the polymerisation, an isocyanide monomer in which the acetylene function is protected by a trimethyl silyl group (**6)** was synthesised to exclude this possibility (Scheme 3). The monomer **6** was prepared following the same procedure as that used for **4**, but instead of 2-propynol, its derivative, trimethyl silyl 2-propynol, was used. During the work-up a tendency of the monomer **6** to gelate forming micrometer long bundles was observed, as is illustrated in the TEM micrograph (Figure 4, left).

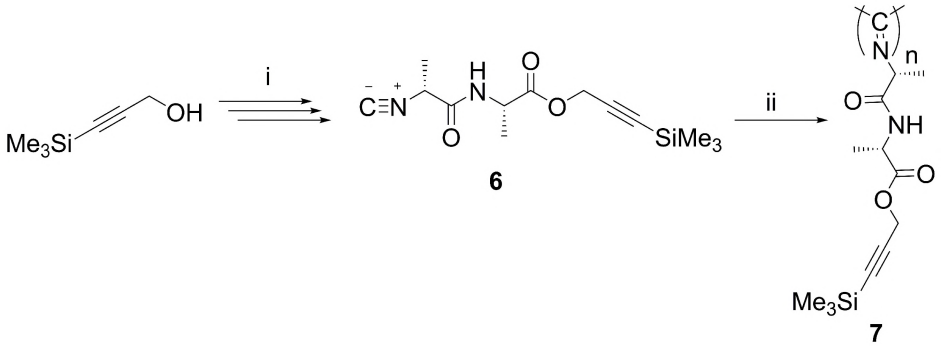

Scheme 3. Synthesis of polyisocyanide **7**; reagents and conditions. (i) see scheme 2; (ii) $Ni(ClO_4)_2 \cdot 6H_2O$, CH_2Cl_2.

Polymerisation of **6** to give **7** was very slow compared to the polymerisation of **6** and did not proceed to completion even after 5 days of stirring. The CD spectrum of **7**, in contrast to the CD spectrum of **5**, shows a positive Cotton effect at λ = 290 nm with a smaller intensity (Figure 4, right). This is indicative of a polymer product having a less defined architecture as is also reflected in the less pronounced downfield chemical shift of the amide NH resonance in the ^{1}H NMR spectrum.[22]

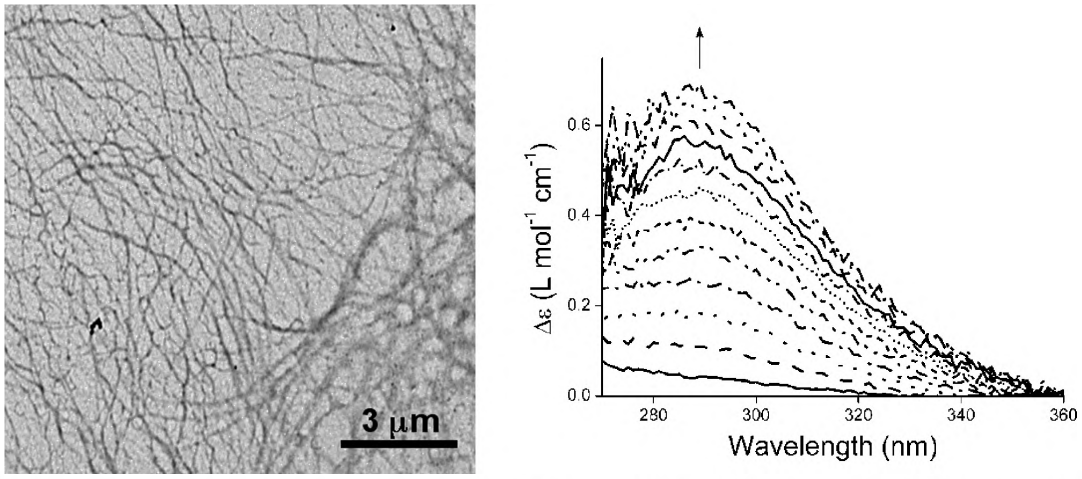

Figure 4. Transmission Electron Microscopy (TEM) image of the gel-like structure of **6** in hexane (left). CD spectrum following the polymerisation of **6** with 1/30 equiv. of Ni(II) (right).

The IR spectrum of **7** shows a shift from ν = 3427 cm^{-1} compared to **11** ν = 3268 cm^{-1} (broad) and a peak at 3320 (shoulder) for the N-H stretching vibration, demonstrating that not all amide groups participate in the hydrogen bonding. These results can be explained by the presence of the bulky trimethylsilyl groups, which hamper the polymerisation and consequently lead to a polymer with a less well-defined character.[18] In contrast to **5**, however, **7** is completely soluble in $CHCl_3$ allowing AFM measurements to be conducted (Figure 5). The AFM images obtained show the presence of fibre-like structures having lengths up to 300 nm.

The trimethyl silyl groups of polymer **7** were cleaved off using tetrabutylammonium fluoride (TBAF) and resulted in the precipitation of polymer **5**. The formation of the precipitate strengthens the assumption, based on CD and IR spectroscopy, that the acetylene functionality is not involved in the polymerisation reaction and that polymer **5** is insoluble due to its molecular structure.

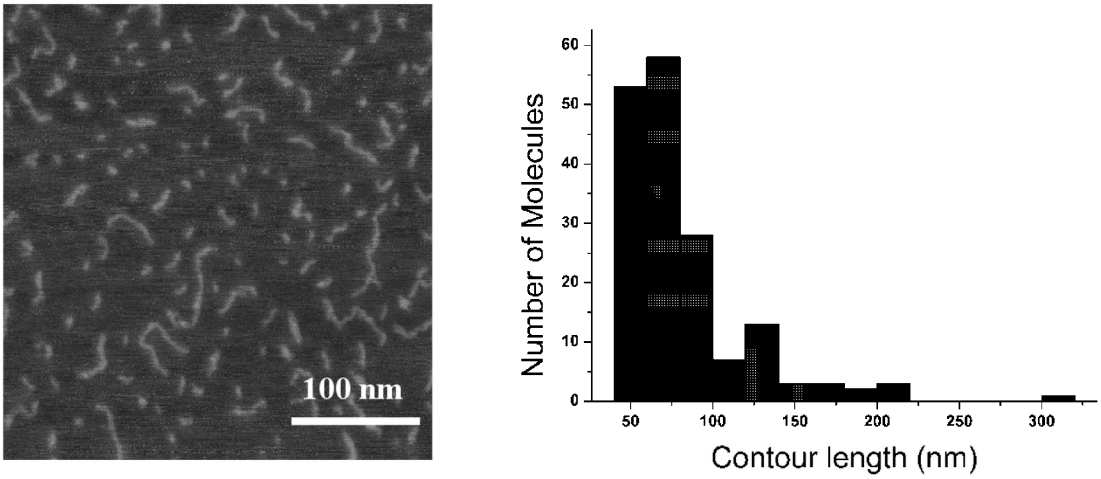

Figure 5. Atomic Force Micrograph of polymer **7** and the histogram of the contour length obtained for **7** from the AFM images. From these contour lengths, DP = 710 and $M_n = 2 \cdot 10^5$ g mol^{-1} were calculated.[13]

In order to overcome the insolubility problems encountered thus far, polyisocyanides **8** (the diastereoisomer of **5**), **9** and **10** (containing longer alkyl groups in the side chains) were prepared (Chart 1) and investigated by CD and IR spectroscopy. To obtain the monomers used for **9** and **10** commercially available 2-heptyn-1-ol was converted into 6-heptyn-1-ol via the acetylene zipper reaction, which allows isomerisation of an internal alkynyl into a terminal alkyne with sodium 2-aminoethylamide generated in situ from sodium hydride and ethylenediamine.[23]

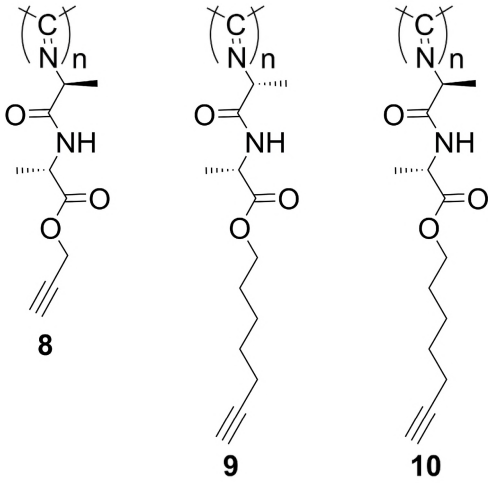

Chart 1. Acetylene functionalised polyisocyanopeptides **8** (LL), **9** (DL) and **10** (LL).

As expected, the CD spectrum of **8** shows a strong positive Cotton effect around λ = 310 nm, pointing to a right-handed (*P*) helix (Figure 6). During the polymerisation to obtain **9**, an intense negative Cotton effect at λ = 310 nm disappears within several minutes; simultaneously the appearance of a positive effect at λ = 290 nm and a negative effect at λ = 360 nm are observed (Figure 7, left). The λ = 290 / 360 nm couplet is usually observed

in polyisocyanopeptides when no-well defined hydrogen bonding arrays are present in the side-arm of the polymer.[18] The IR spectrum of **10** shows the amide I vibration shifted to a lower wave number compared to the monomer (Table 1) consistent with a change in the arrangement of the side arms from the well-organised kinetic product of the polymerisation reaction, to a stable situation in which the hydrogen bonds are no longer mainly between side chain *n* and (*n* + 4).[24] In the case of the formation of polymer **10**, a CD spectrum displaying a couplet was immediately observed (Figure 7, right); the presence of the heptyne fragment in the monomer prevents the formation of the well-defined hydrogen bonding array along the polymeric back bone. The ^{1}H NMR data of both **9** and **10** also confirm this situation, as a less pronounced shift of the NH proton towards low field is observed (Table 1).

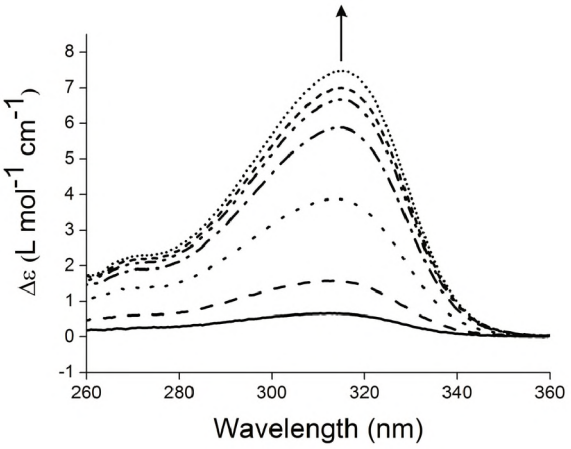

Figure 6. CD spectrum following the polymerisation of L-isocyanoalanyl-L-alanine prop-2-ynol ester with 1/30 equiv. of Ni(II) to give **8**.

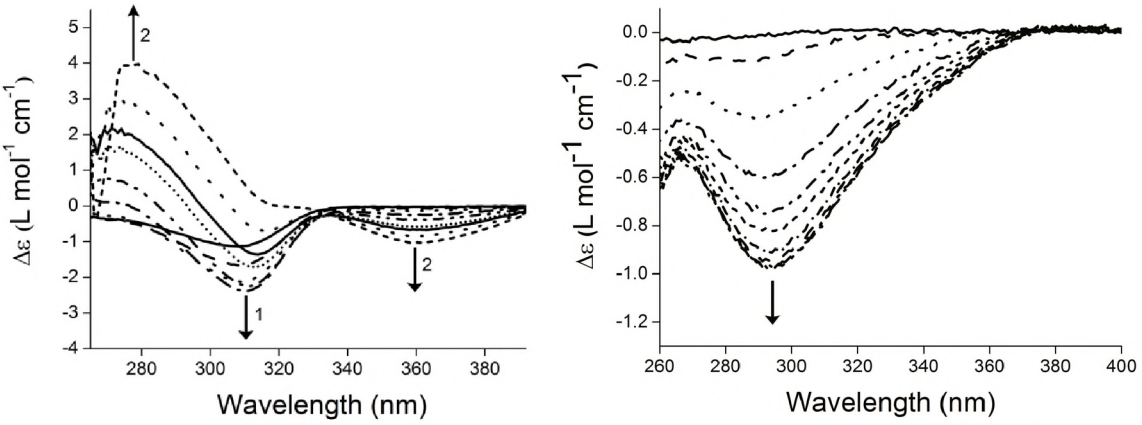

Figure 7. CD spectrum monitored in time during the formation of polymer **9** (left). Black arrow (1) indicates initial changes; black arrows (2) point to the second series of changes. On the right the CD monitored polymerisation of L-isocyanoalanyl-L-alanine hept-6-ynol ester with 1/30 equiv. of Ni (II) to give **10** is depicted.

Table 1 Selected IR[a] and ^{1}H NMR chemical shift[b] displacements indicative of hydrogen bonding

	Monomer				Polymer				
	ν_{NH} (CH_2Cl_2)	$\nu_{amide\ I}$ (CH_2Cl_2)	ν_{NH} (KBr)	$\nu_{amide\ I}$ (KBr)	ν_{NH} (CH_2Cl_2)	$\nu_{amide\ I}$ (CH_2Cl_2)	ν_{NH} (KBr)	$\nu_{amide\ I}$ (KBr)	$\Delta\delta_{NH}$ ($CDCl_3$)
D-Isocyanoalanyl-L-alanine prop-2-ynol ester	3434	1692[c]	3277	1665	3264	1657	3271	1653	–[f]
L-Isocyanoalanyl-L-alanine prop-2-ynol ester	3430	1694[c]	3281	1665	3261	1656	3271[d]	1655	2.4
D-Isocyanoalanyl-L-alanine-(3-trimethylsilyl) prop-2-ynol ester	3427	1692[c]	3318	1668	3294[d]	1657	3284	1655	1.5
D-isocyanoalanyl-L-alanine hept-6-ynol ester	3431	1689	3299	1673	3266	1656	3264	1655	2
L-isocyanoalanyl-L-alanine hept-6-ynol ester	3429	1689	3291	1672	3288	–[g]	3284[e]	1664[d]	1.8
L-isocyanoalanyl-L-alanine methyl ester[h]	3430[d]	1688	3279	1669	3265	1657	3276	1657	2.4

[a]In cm^{-1}. [b]Chemical shift displacement upon polymerisation (in ppm). [c] Major amide I absorbance band, weaker band observed at 1710 cm^{-1}. [d]Split signal, average values are given. [e] Major NH absorbance band, weaker band observed at 3356 cm^{-1}. [f]Could not be obtained due to insolubility of the polymer. [g] No shift observed for the amide I vibration. [h]See ref. 12.

The ability to functionalise, by click chemistry, these rigid polyisocyanides was demonstrated using polymer **8**; the only polymer synthesised that is sufficiently soluble and still displays the characteristics of the well-defined hydrogen bonding array along the polymer back bone. A suspension of polymer **8** was treated with dodecylazide in the presence of copper bromide and pentamethyl diethylene triamine (PMDETA) in dichloromethane. The introduction of long aliphatic chains in the polymer is expected to lead to an increased solubility and the potential of these macromolecules to form thermotropic liquid crystals.[25,26] After stirring at ambient temperature for 4 days, the copper catalyst was removed by extraction of the reaction mixture with an EDTA solution. The polymer was separated from excess dodecylazide using a Bio-Beads size-exclusion column.

As expected the solubility of the product **11** was greater than that of the starting polymer as a result of the dodecyl chains; evident by the appearance of a transparent solution after removal of the copper catalyst. The presence of the dodecyl tails on the side arms was confirmed by the appearance of a peak at δ = 7.8 in the ^{1}H NMR spectrum corresponding to the proton of the generated triazole ring and also by the increased concentration of aliphatic signals between δ = 1.0 and δ = 2.1 ppm. In addition, stretching frequencies due to the triazole ring can be seen in the IR spectrum at ν = 1692 cm^{-1} and ν = 1487 cm^{-1}. The absence of any residual acetylene CC stretching vibrations point to complete grafting of the polyisocyanopeptides. The CD spectrum of **11**, surprisingly no longer showed a positive Cotton effect at λ = 310 nm, but instead a broad negative signal around λ = 290 nm with a decreased intensity. (Figure 8). The change in the CD spectrum could be the result of the prolonged time in solution leading to (partial) unfolding of the helical organisation, the presence of the more bulky dodecyl chains or a slight change in helical pitch. Although helix

inversion can not be excluded this is highly unlikely as this process has a high energy of activation.[24]

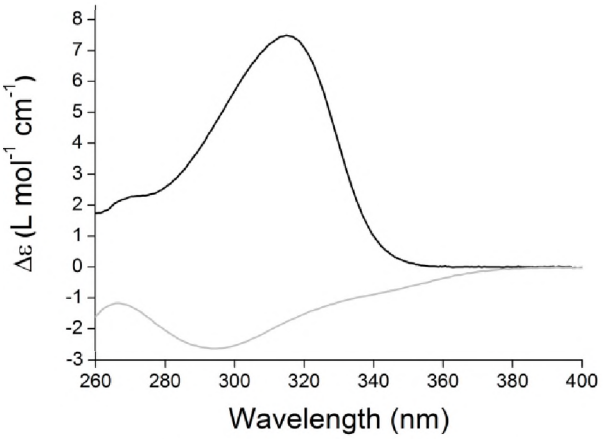

Figure 8. CD spectra of polymer **8** (black line) and **11** (light grey line) in $CHCl_3$.

AFM studies were carried out to determine the molecular properties of the dodecyl functionalised polymer compared with the starting polymer (Figure 9). From the AFM images and the corresponding contour length histograms, it is clearly visible that **8** and **11** have different topological properties. In the case of polymer **11**, the contour length is no longer a good representation of the molecular weight properties, likely caused by the strong interaction of the long alkyl tails with the mica substrate.[27] In brush-like macromolecules such processes have led to chain scission,[27] however, for helical polyisocyanides conformational changes will also result in a different topology. Another explanation for the observed contour lengths of polymer **11** might be due to the work-up procedure. In case of **11** a Bio-Beads size-exclusion column was used to remove excess diodecylazide; this might, however, also have led to a 'separation in size', in which larger polymer stick on the column, while the shorter polymers elute from the column.

Initial studies towards the liquid crystalline properties of polymer **11** showed no ordered mesophases in the range between room temperature and 230 °C. Above this temperature the material melted to form a viscous liquid that only slowly solidified upon cooling with no clear transition temperature. The high temperature melting of the functionalised polyisocyanopeptide is likely accompanied by the loss of the ester groups, as was observed previously for polyisocyanides based on dialanine.[28]

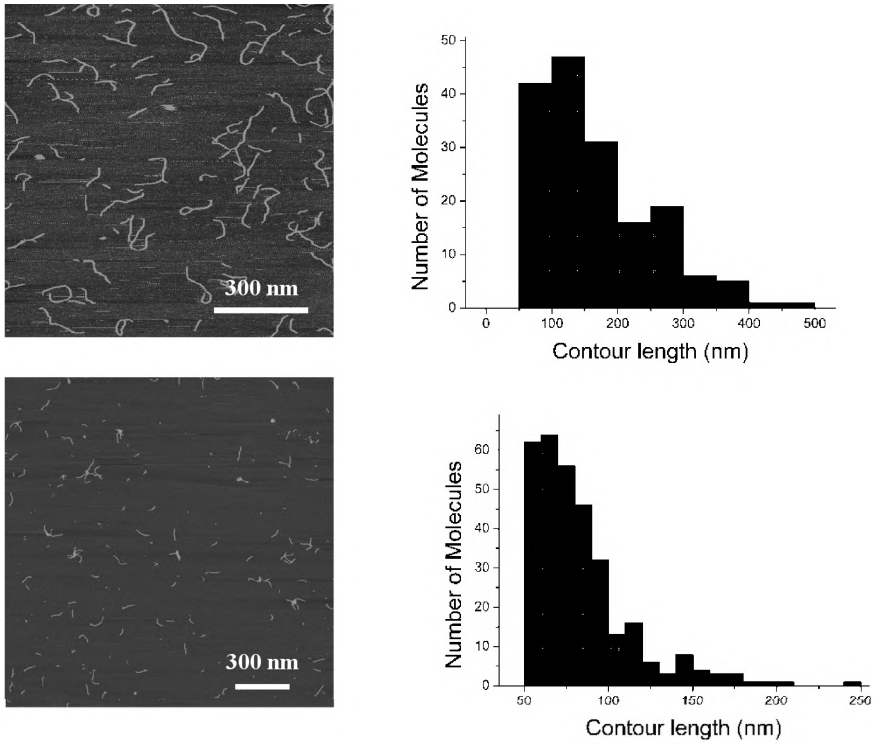

Figure 9. Atomic Force Microscopy images of polymers **8** and the corresponding histograms of the contour lengths obtained from the AFM images (top) and **11** (bottom), respectively; for **8**, DP = 1465 and $M_n = 3 \cdot 10^5$ $g\ mol^{-1}$. In the case of **11**, the relation between the molecular weight parameters and the contour length is unclear.

4.3 Conclusion

Isocyanopeptides containing acetylene functionalities could be prepared by peptide coupling procedures. The resulting polymers showed distinctly different solubility properties, which could be altered by changing the stereochemistry of the constituent (alanine) amino acids, by the introduction of bulky trimethyl silyl groups or by increasing the spacer length between the dipeptide and the acetylene moiety. Using a combination of CD, IR and NMR spectroscopic studies we found that only in the case of polymer **8** the rigidity imposed by the well-defined hydrogen bonding array along the helical back bone was combined with satisfactory solubility. All other synthesised polymers were either insoluble or the spectroscopic data obtained pointed to a decreased degree of hydrogen bonding organisation and consequently a reduced rigidity. Initial copper catalysed 'clicking' experiments with **11** and dodecyl azide showed this procedure can be efficiently employed to graft functional groups to these rigid macromolecules. This opens the way to use these polyisocyanide building blocks to graft various azides in order to obtain a wide range of materials.

4.4 Experimental

General

All solvents were distilled prior to use, all other chemicals were commercials products. Column chromatography was performed using silica gel (40–60 µm) purchased from Merck. TLC-analyses were carried out on silica 60 F_{254} coated glass from Merck and the compounds were visualised using Ninhydrine or $Ni(ClO_4)_2 \cdot 6H_2O$ in EtOH. The click reactions were performed under Schlenk conditions. ^1H NMR and ^{13}C NMR spectra were recorded on a Bruker AC-300 MHz instrument operating at 300 MHz and 75 MHz respectively, unless otherwise stated. FT-infrared spectra were recorded on a ThermoMattson IR300 spectrometer equipped with a Harrick ATR unit; compounds were measured as an oil or solid. Melting points were measured on a Buchi B-545 and are reported uncorrected. Mass spectrometry measurements were performed on a VG 7070E instrument (EI/CI) or on a JEOL Accutof instrument (ESI). Elemental analyses were carried out on a Carlo Erba 1180 instrument and optical rotations were measured on a Perkin Elmer 241 Polarimeter at room temperature and are reported in 10^{-1} deg cm^2 g^{-1}. CD spectra were recorded on a Jasco 810 instrument equipped with a Peltier temperature control unit. AFM experiments were performed using a Nanoscope III instrument from Digital Instruments. Solutions of 7, 8 and 11 (~10^{-6} M in $CHCl_3$) were spin-coated (1600 RPM) onto freshly cleaved Muscovite Mica. All images were recorded with the AFM operating in tapping mode in air at room temperature with a resolution of 512 × 512 pixels using moderate scan rates (1–2 lines/sec.). Commercial tapping-mode tips (NT-MDT) were used with a typical resonance frequency around 300 kHz. Length and heights were evaluated using image recognition software "Scanning Adventure" developed by Jaques Barbet. The isocyanide monomer 4 could be recrystallised from ethanol/hexane, offering crystals suitable for X-ray analysis. A single crystal was mounted in air on a glass fibre. Intensity data were collected at -65 degrees C. A Nonius KappaCCD single-crystal diffractometer was used (ϕ and ω scan mode) using graphite monochromated Mo-Kalpha radiation. Unit cell dimensions were determined from the angular setting of 23 reflections. Intensity data were corrected for Lorentz and polarisation effects. SADABS multiscan correction was applied.[29] The structure was solved by the program CRUNCH[30] and was refined with standard methods using SHELXL97[31] with anisotropic parameters for the nonhydrogen atoms. TEM micrographs were recorded on a JEOL JEM-1010 instrument.

Crystal data for **4**: translucent colourless, $C_{10}H_{12}N_2O_3$, M = 208.22, triclinic, space group P1, a = 4.7566(12), b = 6.225(2), c = 10.116(17) Å, α = 72.97(6), β = 85.49(8), γ = 80.83(3)°, U = 282.6(5) $Å^3$, T = 298(2) K, Z = 1, µ(Mo-Kα) = 0.092 mm^{-1}, 4505 reflections measured, 1167 unique (R_{int} = 0.0695), final R1 0.0698, wR2 0.1399 (I › 2σ(I)). CCDC reference number 637825.

Synthesis

6-Heptyn-1-ol[23] and dodecylazide[32] were synthesised according to literature procedures.

Boc-L-alanine prop-2-ynol ester 1

Boc-L-alanine-OH (4.40 g, 23.3 mmol) and 2-propynol (1.54 g, 27.5 mmol, 1.2 equiv.) were dissolved in CH_2Cl_2 (300 mL). To this solution diisopropylethylamine (DIPEA; 4.3 mL, 26 mmol, 1.1 equiv.), 1-hydroxybenzatriazole (HOBt; 3.97 g, 25.9 mmol, 1.1 equiv.) and finally 1-(3-dimethylaminopropyl)-3-ethylcarbodiimide hydrochloride (EDC; 4.9 g, 25.6 mmol, 1.1 equiv.) were added. After stirring for 10 hours the solvent was evaporated *in vacuo* and the product was redissolved in $CHCl_3$ (200 mL). This solution was subsequently washed with an aqueous

10% (w/w) citric acid solution (2 × 200 mL), H_2O (200 mL), an aqueous 10 % (w/w) sodium carbonate solution (2 × 200 mL) and H_2O (200 mL). The organic layer was dried (Na_2SO_4), concentrated and subjected to column chromatography (2% MeOH in $CHCl_3$), yielding 92% of 6 as a colorless oil. $[\alpha]_D$ –17 (*c* 0.8 in $CHCl_3$). ^{1}H NMR (δ ppm, $CDCl_3$): 5.03 (s, 1H, NH), 4.71 (m, 2H, C≡CC*H*$_2$), 4.32 (m, 1H, CH Ala), 2.47 (t, 1H, HC≡C, *J* 2.4), 1.41 (s, 9H, C(C*H*$_3$)$_3$), 1.38 (d, 3H, C*H*$_3$ Ala, *J* 7.2). ^{13}C NMR (δ ppm, $CDCl_3$): 172.3, 154.8 (C=O), 80.0 (*C*(CH$_3$)$_3$, 77.2 (HC≡*C*CH$_2$), 75.4 (H*C*≡CCH$_2$), 52.8 (CH Ala), 49.3 (HC≡*C*CH$_2$), 28.6 (C(*C*H$_3$)$_3$), 18.6 (CH$_3$ Ala). FT-IR (cm^{-1}, ATR): 3299 (NH), 2128 (C≡C), 1748 (C=O ester), 1701 (Amide I), 1506 (amide II). MS-CI: m/z = 228 $[M+H]^+$. HRMS for $C_{11}H_{18}NO_4$: Calcd 228.1236. Found: 228.1230.

Boc-L-alanyl-L-alanine prop-2-ynol ester 2

Compound **1** (2.03 g, 8.9 mmol) was dissolved in HCl-saturated ethyl acetate (100 mL). The mixture was stirred for 5 hours after which the reaction mixture was concentrated to a small volume, *t*-BuOH/CH_2Cl_2 was added and evaporated under reduced pressure twice, to remove the excess of HCl. The resulting L-alanine prop-2-ynol ester HCl salt was dissolved in CH_2Cl_2 (200 mL). To this solution Boc-L-alanine-OH (1.88 g, 9.9 mmol, 1.1 equiv.), DIPEA (3.3 mL, 20 mmol, 2.2 equiv.), HOBt (1.52 g, 9.9 mmol, 1.1 equiv.) and finally EDC (1.92 g, 10.0 mmol, 1.1 equiv.) were added. After stirring for 36h the solvent was evaporated *in vacuo* and the product was redissolved in $CHCl_3$ (150 mL). This solution was washed with an aqueous 10% (w/w) citric acid solution (2 × 150 mL), H_2O (150 mL), an aqueous 10 % (w/w) sodium carbonate solution (2 × 150 mL) and H_2O (150 mL). The organic layer was dried (Na_2SO_4), concentrated and subjected to column chromatography (2% MeOH in $CHCl_3$), yielding 1.9 g of the title compound in 72% yield as a white powder. Mp: 84 °C. $[\alpha]_D$ –41 (*c* 0.9 in $CHCl_3$). ^{1}H NMR (δ ppm, $CDCl_3$): 7.07 (s, 1H, NH), 5.38 (d, 1H, NH, *J* 7.5), 4.67 (m, 2H, HC≡CC*H*$_2$), 4.52 (quintet, 1H, CH Ala *J* 7.2), 2.45 (t, 1H, HC≡C, *J* 6.0), 1.36 (s, 9H, C(CH$_3$)$_3$), 1.29 (m, 6H, CH$_3$ Ala). ^{13}C NMR (δ ppm, $CDCl_3$): 172.7, 171.9, 155.5 (C=O), 79.9 (*C*(CH$_3$)$_3$, 77.2 (HC≡*C*CH$_2$), 75.5 (H*C*≡CCH$_2$), 52.8 (CH Ala), 49.8 (HC≡*C*CH$_2$), 47.9 (CH Ala), 28.3 (C(*C*H$_3$)$_3$), 18.5, 17.7 (CH$_3$ Ala). FT-IR (cm^{-1}, ATR): 3270 (NH), 2135 (C≡C), 1738 (C=O ester), 1679, 1653 (Amide I), 1555, 1518 (amide II). MS-CI: m/z = 299 $[M+H]^+$. HRMS for $C_{14}H_{23}N_2O_5$: Calcd 299.1607. Found: 299.1595.

Boc-D-alanyl-L-alanine prop-2-ynol ester 2

Starting from **1** and Boc-D-alanine-OH, following the same procedure as for Boc-L-alanyl-L-alanine prop-2-ynol ester, the title compound was obtained as a viscous colorless oil (yield 46%).$[\alpha]_D$ +24 (*c* 1.3 in $CHCl_3$). ^{1}H NMR (δ ppm, $CDCl_3$): 6.76 (s, 1H, NH), 4.98 (s, 1H, NH), 4.72 (m, 2H, HC≡CC*H*$_2$), 4.59 (quintet, 1H, CH Ala *J* 7.2), 2.48 (t, 1H, HC≡C, *J* 2.4), 1.44 (s, 9H, C(CH$_3$)$_3$), 1.42 (d, 4H, CH$_3$ Ala, *J* 7.2), 1.35 (d, 4H, CH$_3$ Ala, *J* 6.9). ^{13}C NMR (δ ppm, $CDCl_3$): 172.4, 172.2, 155.7 (C=O), 80.5 (*C*(CH$_3$)$_3$), 77.2 (HC≡*C*CH$_2$), 75.5 (H*C*≡CCH$_2$), 52.9 (CH Ala), 50.1 (HC≡*C*CH$_2$), 48.0 (CH Ala), 28.4 (C(*C*H$_3$)$_3$), 18.2, 17.3 (CH$_3$ Ala). FT-IR (cm^{-1}, ATR): 3297 (NH), 2128 (C≡C), 1747 (C=O ester), 1700, 1660 (Amide I), 1512 (br, amide II). MS-CI: m/z = 299 $[M+H]^+$. HRMS for $C_{14}H_{23}N_2O_5$: Calcd 299.1607. Found: 299.1600.

***N*-Formyl-L-alanyl-L-alanine prop-2-ynol ester**

The Boc-protecting group of Boc-L-alanyl-L-alanine prop-2-ynol ester (1.59 g, 5.3 mmol) was removed by dissolving the dipeptide in HCl-saturated ethyl acetate (150 mL). The mixture was stirred for 5 hours after which time the solvent was evaporated *in vacuo* and the excess of HCl was removed by addition of *t*-BuOH/CH_2Cl_2 and subsequent evaporation. The resulting L-alanyl-L-alanine prop-2-ynol ester HCl salt was taken up in ethyl formate (200 mL) and sodium formate (1.6 g, 24.3 mmol, 4.6 equiv.) was added. The

mixture was stirred under reflux for 72 hours, before the solid was filtered off and washed thoroughly with $CHCl_3$. The solvent was removed from the filtrate and the crude product was recrystallised from ethanol/diisopropyl ether to give 1.0 g (83%) of white crystals. Mp: 112 °C. $[\alpha]_D$ –71 (*c* 1.6 in THF). ^{1}H NMR (δ ppm, DMSO-d_6): 8.24 (s, 1H, NH), 8.07 (s, 1H, NH), 7.96 (s, 1H, HCO), 4.70 (m, 2H, HC≡CCH_2), 4.34 (m, 2H, CH Ala), 3.54 (t, 1H, HC≡C, *J* 2.7), 1.29 (d, 3H, CH_3 Ala, *J* 7.5), 1.24 (d, 3H, CH_3 Ala, *J* 6.9)). ^{13}C NMR (δ ppm, DMSO-d_6): 171.9, 169.1 (C=O), 160.6 (HCO), 78.1 (HC≡*C*CH_2), 77.9 (H*C*≡CCH_2), 52.3 (CH Ala), 47.5 (HC≡*C*CH_2), 46.3 (CH Ala), 18.5, 16.6 (CH_3 Ala). FT-IR (cm^{-1}, ATR): 3283, 3237 (NH), 2127 (C≡C), 1748 (C=O ester), 1640 (Amide I), 1550 (amide II). MS-CI: m/z = 227 $[M+H]^+$. HRMS for $C_{10}H_{15}N_2O_4$: Calcd 227.1039. Found: 227.1032. El. Anal. Calcd. for $C_{10}H_{14}N_2O_4$: C, 53.09; H, 6.24; N, 12.38. Found: C, 53.12; H, 6.26; N, 12.59.

_N_-Formyl-D-alanyl-L-alanine prop-2-ynol ester 3

Starting from **2** following the same procedure as for *N*-Formyl-L-alanyl-L-alanine prop-2-ynol ester, **3** was obtained as a white crystalline product (yield 62%). Mp: 123 °C. $[\alpha]_D$ +25 (*c* 1.0 in THF). ^{1}H NMR (δ ppm, DMSO-d_6): 8.44 (d, 1H, NH, *J* 6.9), 8.23 (s, 1H, NH, *J* 7.8), 7.96 (s, 1H, HCO), 4.71 (d, 2H, HC≡CCH_2, *J* 2.7), 4.41 (quintet, 1H, CH Ala, *J* 7.2), 4.27 (quintet, 1H, CH Ala, *J* 7.2), 3.53 (t, 1H, HC≡C, *J* 2.4), 1.28 (d, 3H, CH_3 Ala, *J* 7.2), 1.20 (d, 3H, CH_3 Ala, *J* 7.2)). ^{13}C NMR (δ ppm, DMSO-d_6): 171.8, 171.7 (C=O), 160.6 (HCO), 78.2 (HC≡*C*CH_2), 77.9 (H*C*≡CCH_2), 52.3 (CH Ala), 47.5 (HC≡*C*CH_2), 46.3 (CH Ala), 18.9, 16.8 (CH_3 Ala). FT-IR (cm^{-1}, ATR): 3345, 3319 (NH), 2119 (C≡C), 1747 (C=O ester), 1660, 1640 (Amide I), 1544, 1508 (amide II). MS-ESI m/z = 249 $[M+Na]^+$. HRMS for $C_{10}H_{14}N_2O_4Na$: Calcd 249.0841. Found: 249.0851. El. Anal. Calcd. for $C_{10}H_{14}N_2O_4$: C, 53.09; H, 6.24; N, 12.38. Found: C, 52.79; H, 6.34; N, 12.30.

L-Isocyanoalanyl-L-alanine prop-2-ynol ester

N-Formyl-L-alanyl-L-alanine prop-2-ynol ester (1.0 g, 4.4 mmol) was dissolved in THF (80 mL) under an N_2 atmosphere and N-methyl morpholine (1.75 mL, 16.4 mmol, 3.7 equiv.) was added. The resulting solution was cooled to –30 °C (acetone/CO_2) and diphosgene (0.3 mL, 2.4 mmol, 0.6 equiv.) in THF (8 mL) was added dropwise to over a period of 15 minutes, while the temperature was maintained at –30 °C. After complete addition of diphosgene, the orange solution was allowed to warm to 0 °C and an ice-cold saturated aqueous sodium bicarbonate solution (10 mL) was added and stirred vigorously for 10 minutes. The product was extracted with $CHCl_3$ (25 mL) and subsequently washed with an aqueous 10% (w/w) sodium bicarbonate solution. The organic layer was dried (Na_2SO_4) and evaporated *in vacuo* resulting in a yellow/orange oil. The product was purified using column chromatography (2% MeOH, 0.5% Et_3N in $CHCl_3$) and subsequently recrystallised two times from ethanol/hexane to yield 458 mg (50%) of white needles. Mp: 89 °C. $[\alpha]_D$ +11 (*c* 0.6 in CH_2Cl_2). ^{1}H NMR (δ ppm, $CDCl_3$): 6.86 (s, 1H, NH), 4.76 (m, 2H, HC≡CCH_2), 4.60 (quintet, 1H, CH Ala, *J* 7.2), 4.27 (q, 1H, CH Ala, *J* 7.2), 2.51 (t, 1H, HC≡C, *J* 5.8), 1.66 (d, 3H, CH_3 Ala, *J* 6.9), 1.24 (d, 3H, CH_3 Ala, *J* 7.2)). ^{13}C NMR (δ ppm, $CDCl_3$): 171.5, 165.9 (C=O), 161.8 (CN), 76.9 (HC≡*C*CH_2), 75.8 (H*C*≡CCH_2), 54.0 (HC≡*C*CH_2), 53.3, 48.6 (CH Ala), 19.7, 18.0 (CH_3 Ala). FT-IR (cm^{-1}, ATR): 3280 (NH), 2154, 2132 (CN, C≡C), 1742 (C=O ester), 1665 (Amide I), 1552 (amide II). MS-CI: m/z = 209 $[M+H]^+$. HRMS for $C_{12}H_{13}N_2O_3$: Calcd 209.0926. Found: 209.0921. El. Anal. Calcd. for $C_{10}H_{12}N_2O_3$: C, 57.68; H, 5.81; N, 13.45. Found: C, 57.32; H, 5.74; N, 13.31.

D-Isocyanoalanyl-L-alanine prop-2-ynol ester 4

Starting from **3** following the same procedure as for L-Isocyanoalanyl-L-alanine prop-2-ynol ester, **4** was obtained as a white crystalline product (yield 48%). Mp: 98 °C. $[\alpha]_D$ –17 (*c* 0.6 in CH_2Cl_2). ^{1}H NMR (δ ppm,

$CDCl_3$): 6.88 (s, 1H, NH), 4.79 (m, 2H, HC≡CCH_2), 4.61 (quintet, 1H, CH Ala, *J* 7.3), 4.27 (q, 1H, CH Ala, *J* 7.3), 2.51 (t, 1H, HC≡C, *J* 2.6), 1.66 (d, 3H, CH_3 Ala, *J* 7.1), 1.50 (d, 3H, CH_3 Ala, *J* 7.3)). ^{13}C NMR (δ ppm, $CDCl_3$): 171.4, 166.0 (C=O), 161.0 (CN), 76.8 (HC≡*C*CH_2), 75.8 (H*C*≡CCH_2), 53,5 (t, HC≡*C*CH_2), 53.3, 48.6 (CH Ala), 19.9, 18.0 (CH_3 Ala). FT-IR (cm^{-1}, ATR): 3277 (NH), 2152, 2141 (CN, C≡C), 1737 (C=O ester), 1665 (Amide I), 1564 (amide II). MS-CI: m/z = 209 $[M+H]^+$. HRMS for $C_{12}H_{13}N_2O_3$: Calcd 209.0926. Found: 209.0924. El. Anal. Calcd. for $C_{10}H_{12}N_2O_3$: C, 57.68; H, 5.81; N, 13.45. Found: C, 57.50; H, 5.74; N, 13.48.

Poly(L-Isocyanoalanyl-L-alanine prop-2-ynol ester) 8

To a stirred solution of L-Isocyanoalanyl-L-alanine prop-2-ynol ester (178 mg, 0.85 mmol) in $CHCl_3$ (2 mL) was added $Ni(ClO_4)_2{\cdot}6H_2O$ (0.03 equiv.; 24 mL of a 0.0012 mM $CHCl_3$/EtOH (98/2 v/v) solution). The solution turned red/brown immediately and after 12 hours the solvent was evaporated off. The glassy solid was taken up in a minimal amount of $CHCl_3$ and the polymer precipitated out by dropping this solution into MeOH/H_2O (100 mL (2:1 v/v)) with vigorous stirring. The product was filtered off and washed with MeOH. Drying *in vacuo* gave the polymer as a brown solid in 57% yield (102 mg). $[\alpha]_D$ +154 (*c* 0.03 in CH_2Cl_2). ^{1}H NMR (δ ppm, $CDCl_3$): 9.3 (br, 1H, NH), 5.5–3.5 (br, 4H,HC≡CCH_2, CH Ala), 2.6–2.2 (br, 1H, HC≡C), 2–0.5 (br, 6H, CH_3 Ala). FT-IR (cm^{-1}, ATR): 3263 (NH), 2129 (C≡C), 1746 (C=O ester), 1656 (Amide I), 1525 (amide II).

Poly(D-Isocyanoalanyl-L-alanine prop-2-ynol ester) 5

This polymer was prepared as described for polymer **8**, resulting in the immediate precipitation of insoluble **5.** FT-IR (cm^{-1}, ATR): 3270 (NH), 2128 (C≡C), 1746 (C=O ester), 1651 (Amide I), 1529 (amide II). Because the polymer was insoluble, no further characterisation could be obtained.

Boc-L-alanine-(3-trimethylsilyl) prop-2-ynol ester

Following a similar procedure as for **1**, the title compound was obtained in 77% yield as a colorless oil. $[\alpha]_D$ –16 (*c* 0.8 in $CHCl_3$). ^{1}H NMR (δ ppm, $CDCl_3$): 5.03 (s, 1H, NH), 4.71 (d, 2H, HC≡CCH_2, *J* 1.8), 4.31 (m, 1H, CH Ala), 1.42 (s, 9H, $C(CH_3)_3$), 1.38 (d, 3H, CH_3 Ala J =7.2), 0.15 (s, 9H, Si-CH_3). ^{13}C NMR (δ ppm, $CDCl_3$): 172.7, 155.2 (C=O), 98.6 (C≡*C*CH_2), 92.7 (*C*≡CCH_2), 80.0 (*C*$(CH_3)_3$), 53.6 (C≡C*C*H_2), 49.3 (CH Ala), 28.4 (C(*C*$H_3)_3$), 18.6 (CH_3 Ala), 0.1 (Si-CH_3). FT-IR (cm^{-1}, ATR): 3277 (NH), 2187 (C≡C), 1747 (C=O ester), 1714 (Amide I), 1505 (amide II), 1250 (Si-CH_3). MS-ESI m/z = 322 $[M+Na]^+$. HRMS for $C_{14}H_{25}NO_4SiNa$: Calcd 322.1434. Found: 322.1450.

Boc-D-alanyl-L-alanine-(3-trimethylsilyl) prop-2-ynol ester

Following a similar procedure as for **2**, the title compound was obtained as a colorless oil in 75% yield. $[\alpha]_D$ +28 (*c* 1.2 in $CHCl_3$).^{1}H NMR (δ ppm, $CDCl_3$): 7.05 (s, 1H, NH), 5.40 (s, 1H, NH), 4.63 (d, 2H, HC≡CCH_2, CH Ala, *J* 2.0), 4.52 (quintet, 1H, CH Ala, *J* 7.3), 1.35 (m, 12H, $C(CH_3)_3$), CH_3 Ala), 1.26 (d, 3H, CH_3 Ala, *J* 7.1), 0.07 (s, 9H, Si-CH_3). ^{13}C NMR (δ ppm, $CDCl_3$): 172.6, 172.1, 155.5 (C=O), 98.4 (C≡*C*CH_2), 92.5 (*C*≡CCH_2), 79.9 (*C*$(CH_3)_3$), 53.5 (C≡C*C*H_2), 49.9, 47.9 (CH Ala), 28.3 (C(*C*$H_3)_3$), 18.3, 17.9 (CH_3 Ala), –0.4 (Si-CH_3). MS-ESI m/z = 393 $[M+Na]^+$. HRMS for $C_{17}H_{30}N_2O_5SiNa$: Calcd 393.1826. Found: 393.1822. FT-IR (cm^{-1}, ATR): 3313 (br,NH), 2186 (C≡C), 1747 (C=O ester), 1661 (Amide I), 1514 (amide II), 1250 (Si-CH_3).

N-Formyl-D-alanyl-L-alanine-(3-trimethylsilyl) prop-2-ynol ester

Following a similar procedure as for **3**, the title compound was obtained as a colorless oil in 45% yield. $[\alpha]_D$ +45 (*c* 0.9 in $CHCl_3$). ^{1}H NMR (δ ppm, $CDCl_3$, 200 MHz): 8.02 (s, 1H, HCO), 7.69 (d, 1H, NH. *J* 7.3), 7.50

(d, 1H, NH, *J* 7.9), 4.58 (m, 3H, HC≡CC*H*$_2$, CH Ala), 4.39 (q, 1H, CH Ala, *J* 7.3), 1.29 (m, 6H, CH_3 Ala), 0.05 (s, 9H, Si-CH_3). ^{13}C NMR (*δ* ppm, $CDCl_3$, 25 MHz): 172.3, 171.9 (C=O), 161.5 (HCO), 98.3 (C≡*C*CH$_2$), 92.5 (*C*≡CCH$_2$), 53.5 (CH Ala), 48.0 (C≡C*C*H$_2$), 47.2 (CH Ala), 18.4, 17.3 (CH_3 Ala), –0.5 (Si-CH_3). FT-IR (cm^{-1}, ATR): 3282 (NH), 2186 (C≡C), 1747 (C=O ester), 1650 (Amide I), 1540 (amide II), 1250 (Si-CH_3). MS-ESI m/z = 321 [M+Na]$^+$. HRMS for $C_{13}H_{22}N_2O_4SiNa$: Calcd 321.1243. Found: 321.1246.

D-Isocyanoalanyl-L-alanine-(3-trimethylsilyl) prop-2-ynol ester 6

Following a similar procedure as for **4**, with the exception that the reaction was carried out in CH_2Cl_2, the title compound was obtained after precipitation in hexane as a slightly yellow solid in 59% yield.

Mp: 75 °C. [α]$_D$ –12 (*c* 0.9 in $CHCl_3$). ^{1}H NMR (*δ* ppm, $CDCl_3$, 200 MHz): 6.99 (d, 1H, NH, *J* 7.1), 4.69 (d, 2H, HC≡CC*H*$_2$, *J* 1), 4.54 (quintet, 1H, CH Ala, *J* 6.8), 4.25 (q, 1H, CH Ala, *J* 7.1), 1.59 (d, 3H, CH_3 Ala *J* 7.0), 1.43 (d, 3H, CH_3 Ala, *J* 7.2), 0.12 (s, 9H, Si-CH_3). ^{13}C NMR (*δ* ppm, $CDCl_3$, 25 MHz): 171.2, 165.7 (C=O), 160.9 (CN), 97.8 (C≡*C*CH$_2$), 92.7 (*C*≡CCH$_2$), 53.7 (CH Ala), 53.0 (C≡C*C*H$_2$), 48.2 (CH Ala), 19.4, 17.5 (CH_3 Ala), –0.6 (Si-CH_3). FT-IR (cm^{-1}, ATR): 3318 (NH), 2188 (C≡C), 2144 (CN), 1748 (C=O ester), 1668 (Amide I), 1543 (amide II), 1250 (Si-CH_3). MS-ESI m/z = 303 [M+Na]$^+$. HRMS for $C_{13}H_{20}N_2O_3SiNa$: Calcd 303.1141. Found: 303.1144. El. Anal. Calcd. for $C_{13}H_{20}N_2O_3Si$: C, 55.69; H, 7.19; N, 9.99. Found: C, 55.70; H, 7.28; N, 9.71.

Poly(D-Isocyanoalanyl-L-alanine-(3-trimethylsilyl) prop-2-ynol ester 7

Following a similar procedure as for **8**, **7** was obtained as a brown solid in 6% yield.

[α]$_D$ +67 (*c* 0.02 in $CHCl_3$). ^{1}H NMR (*δ* ppm, $CDCl_3$): 8.5 (br, 1H, NH), 5.2–3.8 (br, 4H, C≡CC*H*$_2$, CH Ala), 2–0.8 (br, 6H, CH_3 Ala), 0.3–0.1 (br, 9H, Si-CH_3). FT-IR (cm^{-1}, ATR): 3284 (NH), 2186 (C≡C), 1748 (C=O ester), 1655 (Amide I), 1531 (amide II), 1250 (Si-CH_3).

Boc-L-alanine hept-6-ynol ester

Starting from Boc-L-alanine-OH and hept-6-ynol, the title compound was prepared following a similar procedure as for **1**, with the exception that the product was purified by column chromatography (Heptane-EtOAc 7:3 v/v, followed by 2% MeOH in $CHCl_3$). The title compound was obtained as a colorless oil (yield 78%). [α]$_D$ –4 (*c* 2.1 in $CHCl_3$). ^{1}H NMR (*δ* ppm, $CDCl_3$): 5.03 (d, 1H, NH, *J* 7.8), 4.28 (m, 1H, CH Ala), 4.13 (m, 3H, OCH_2, CH Ala), 2.19 (m, 2H, HC≡CC*H*$_2$), 1.93 (t, 1H, *H*C≡CCH$_2$, *J* 2.7), 1.65 (quintet, 2H, CH_2, *J* 7.2), 1.52 (m, 4H, CH_2), 1.42 (s, 9H, C(CH_3)$_3$), 1.36 (d, 3H, CH_3 Ala, *J* 7.2). ^{13}C NMR (*δ* ppm, $CDCl_3$): 173.5, 155.2 (C=O), 84.2 (C≡*C*CH$_2$), 80.0 (*C*(CH_3)$_3$), 68.6 (*C*≡CCH$_2$), 65.2 (OCH_2), 49.4 (CH Ala), 28.4 (C(*C*H$_3$)$_3$), 28.2, 28.1, 25.0, 18.9 (CH_2), 18.4 (CH_3 Ala). FT-IR (cm^{-1}, ATR): 3377, 3303 (NH), 2111 (C≡C), 1710 (br, C=O ester, amide I), 1510 (amide II). MS-ESI m/z = 306 [M+Na]$^+$. HRMS for $C_{15}H_{25}N_1O_4Na$: Calcd 306.1681. Found: 301.1701.

Boc-D-alanyl-L-alanine hept-6-ynol ester

Following a similar procedure as for **2**, the title compound was obtained in 75 % yield as a colorless oil. [α]D +28 (c 0.8 in CHCl3). 1H NMR (δ ppm, CDCl3): 6.82 (s, 1H, NH), 5.14 (d, 1H, NH, J 7.5), 4.51 (quintet, 2H, CH Ala, J 7.2), 4.12 (m, 3H, OCH2, CH Ala), 2.16 (m, 2H, HC≡CCH2), 1.91 (t, 1H, HC≡CCH2, J 2.7), 1.63 (quintet, 2H, CH2, J 6.9), 1.48 (m, 4H, CH2), 1.41 (s, 9H, C(CH3)3), 1.36 (d, 3H, CH3 Ala, J 7.2), 1.32 (d, 3H, CH3 Ala, J 7.2). 13C NMR (δ ppm, CDCl3): 172.9, 172.3, 155.5 (C=O), 84.2 (C≡CCH2), 80.1 (C(CH3)3), 68.6 (C≡CCH2), 65.3 (OCH2), 50.3, 48.1 (CH Ala), 28.4 (C(CH3)3), 28.1, 28.0, 24.9 (CH2), 18.4 (CH3 Ala), 18.3

(CH2, CH3 Ala). FT-IR (cm–1, ATR): 3299 (NH), 2116 (C≡C), 1711 (C=O ester), 1663 (Amide I), 1513 (amide II). MS-ESI m/z = 377 [M+Na]+. HRMS for $C_{18}H_{30}N_2O_5Na$: Calcd 377.2052 Found: 377.2050.

Boc-L-alanyl-L-alanine hept-6-ynol ester

Following a similar procedure as for **2**, the title compound was obtained in 60% yield as a colorless oil. $[\alpha]_D$ –18 (*c* 0.9 in $CHCl_3$). ^{1}H NMR (δ ppm, $CDCl_3$): 6.79 (s, 1H, NH), 5.18 (d, 1H, NH, *J* 7.8), 4.51 (quintet, 1H, CH Ala, *J* 7.2), 4.10 (m, 3H, OCH_2, CH Ala), 2.16 (m, 2H, HC≡CCH_2), 1.92 (t, 1H, *H*C≡CCH_2, *J* 2.7), 1.63 (quintet, 2H, CH_2, *J* 7.0), 1.49 (m, 4H, CH_2), 1.40 (s, 9H, $C(CH_3)_3$), 1.36 (d, 3H, CH_3 Ala, *J* 7.2), 1.32 (d, 3H, CH_3 Ala, *J* 7.0). ^{13}C NMR (δ ppm, $CDCl_3$, 50 M): 172.8, 172.4, 155.5 (C=O), 84.1 (C≡*C*CH_2), 80.0 (*C*$(CH_3)_3$), 68.6 (*C*≡CCH_2), 65.3 (OCH_2), 50.0, 48.1 (CH Ala), 28.4 ($C(CH_3)_3$), 28.1, 28.0, 24.9 (CH_2), 18.5 (CH_3 Ala), 18.4 (CH_2), 18.3 (CH_3 Ala). FT-IR (cm^{-1}, ATR): 3299 (NH), 2116 (C≡C), 1736 (C=O ester), 1661 (Amide I), 1519 (amide II). MS-ESI m/z = 377 $[M+Na]^+$. HRMS for $C_{18}H_{30}N_2O_5Na$: Calcd 377.2052 Found: 377.2040.

N-Formyl-L-alanyl-L-alanine hept-6-ynol ester

Starting from Boc-L-alanyl-L-alanine hept-6-ynol ester following the same procedure as for **3**, the title compound was obtained as a white crystalline product (yield 44%). Mp: 73 °C. $[\alpha]_D$ –39 (*c* 1.4 in CH_2Cl_2). ^{1}H NMR (δ ppm, $CDCl_3$): 8.11 (s, 1H, HCO), 7.14 (d, 1H, NH, *J* 7.2), 6.97 (d, 1H, NH, *J* 7.5), 4.66 (quintet, 2H, CH Ala, *J* 7.2), 4.48 (quintet, 1H, CH Ala, *J* 7.2), 4.11 (m, 2H, OCH_2), 2.16 (m, 2H, HC≡CCH_2), 1.93 (t, 1H, *H*C≡CCH_2, *J* 2.4), 1.50 (m, 12H, CH_3 Ala, CH_2). ^{13}C NMR (δ ppm, $CDCl_3$): 172.7, 171.8 (C=O), 161.0 (HCO), 84.2 (C≡*C*CH_2), 68.7 (*C*≡CCH_2), 65.5 (OCH_2), 48.3, 47.4 (CH Ala), 28.1, 28.0, 24.9 (CH_2), 18.9 (CH_3 Ala), 18.0 (CH_2, CH_3 Ala). FT-IR (cm^{-1}, ATR): 3284 (NH), 2113 (C≡C), 1737 (C=O ester), 1641 (Amide I), 1554, 1510 (amide II). MS-CI: m/z = 283 $[M+H]^+$. HRMS for $C_{14}H_{23}N_2O_4$: Calcd 283.1658. Found: 283.1664. El. Anal. Calcd. for $C_{14}H_{22}N_2O_4$: C, 59.56; H, 7.85; N, 9.92. Found: C, 59.33; H, 7.79; N, 9.86.

N-Formyl-D-alanyl-L-alanine hept-6-ynol ester

Starting from Boc-D-alanyl-L-alanine hept-6-ynol ester following the same procedure as for **3**, the title compound was obtained as a white crystalline product (yield 32%).

Mp: 96 °C. $[\alpha]_D$ +25 (*c* 0.7 in CH_2Cl_2). ^{1}H NMR (δ ppm, DMSO-d_6): 8.37 (d, 1H, NH, *J* 7.2), 8.22 (d, 1H, NH, *J* 7.5), 7.96 (s, 1H, HCO), 4.42 (quintet, 2H, CH Ala, *J* 7.2), 4.42 (quintet, 1H, CH Ala, *J* 7.2), 4.02 (m, 2H, OCH_2), 2.72 (t, 1H, *H*C≡CCH_2, *J* 2.7), 2.15 (m, 2H, HC≡CCH_2), 1.45 (m, 6H, CH_2), 1.27 (d, 3H, CH_3 Ala, *J* 7.5), 1.19 (d, 3H, CH_3 Ala, *J* 7.2). ^{13}C NMR (δ ppm, DMSO-d_6): 172.4, 171.7 (C=O), 160.5 (HCO), 84.4 (C≡*C*CH_2), 71.2 (*C*≡CCH_2), 64.3 (OCH_2), 47.7, 46.3 (CH Ala), 27.5, 24.5, 19.1 (CH_2), 18.9 (CH_3 Ala), 17.0 (CH_2, CH_3 Ala). FT-IR (cm^{-1}, ATR): 3285 (NH), 2113 (C≡C), 1734 (C=O ester), 1650 (Amide I), 1530 (amide II). MS-CI: m/z = 283 $[M+H]^+$. HRMS for $C_{14}H_{23}N_2O_4$: Calcd 283.1658. Found: 283.1656. El. Anal. Calcd. for $C_{14}H_{22}N_2O_4$: C, 59.56; H, 7.85; N, 9.92. Found: C, 59.42; H, 8.00; N, 10.08

L-isocyanoalanyl-L-alanine hept-6-ynol ester

Following a similar procedure as for L-Isocyanoalanyl-L-alanine prop-2-ynol ester, but using CH_2Cl_2 as the solvent, the title compound was obtained afterrecrystallisation from ethanol/diisopropylether as a white crystalline solid in 40% yield. Mp: 58 °C. $[\alpha]_D$ +19 (*c* 0.8 in CH_2Cl_2). ^{1}H NMR (δ ppm, $CDCl_3$): 6.92 (d, 1H, NH, *J* 5.7), 4.54 (quintet, 1H, CH Ala, *J* 7.2), 4.22 (m, 3H, OCH_2, CH Ala), 2.21 (m, 2H, HC≡CCH_2), 1.94 (t, 1H, *H*C≡CCH_2, *J* 2.7), 1.56 (m, 9H, CH_2, CH_3 Ala), 1.47 (d, 3H, CH_3 Ala, *J* 7.2) ^{13}C NMR (δ ppm, $CDCl_3$): 172.0, 165.7 (C=O), 161.7 (CN), 84.2 (C≡*C*CH_2), 68.7 (*C*≡CCH_2), 65.8 (OCH_2), 53.4 (t, HC≡CCH_2), 48.8 (CH Ala), 28.1, 28.0, 25.0, 19.8 (CH_2), 18.4, 18.3 (CH_3 Ala). FT-IR (cm^{-1}, ATR): 3291 (NH), 2139 (CN, C≡C (shoulder)), 1738

(C=O ester), 1672 (Amide I), 1539 (amide II). MS-CI: m/z = 265 $[M+H]^+$. HRMS for $C_{14}H_{21}N_2O_3$: Calcd 265.1552. Found: 265.1543. Anal. Calcd. for $C_{14}H_{20}N_2O_3$: C, 63.62; H, 7.63; N, 10.60. Found: C, 63.55; H, 7.70; N, 10.63.

D-isocyanoalanyl-L-alanine hept-6-ynol ester

Following a similar procedure as for L-Isocyanoalanyl-L-alanine prop-2-ynol ester, the title compound was obtained after recrystallisation from ethanol/diisopropylether as a white crystalline solid in 40% yield. Mp: 44 °C. $[\alpha]_D$ +3 (*c* 0.6 in CH_2Cl_2). ^{1}H NMR (δ ppm, $CDCl_3$): 6.92 (d, 1H, NH, *J* 6.9), 4.55 (quintet, 1H, CH Ala, *J* 7.2), 4.21 (m, 3H, OCH_2, CH Ala), 2.21 (m, 2H, HC≡CCH_2), 1.95 (t, 1H, *H*C≡CCH_2, *J* 2.7), 1.56 (m, 6H, CH_2), 1.47 (d, 3H, CH_3 Ala, *J* 6.9), 1.12 (d, 3H, CH_3 Ala, *J* 6.3). ^{13}C NMR (δ ppm, $CDCl_3$): 172.2, 165.8 (C=O), 161.7 (CN), 84.2 (C≡*C*CH_2), 68.7 (*C*≡CCH_2), 65.8 (OCH_2), 53.5 (t, HC≡*C*CH_2), 48.8 (CH Ala), 28.1, 28.0, 25.0, 19.8 (CH_2), 18.4, 18.3 (CH_3 Ala). FT-IR (cm^{-1}, ATR): 3299 (NH), 2139 (CN, C≡C (shoulder)), 1738 (C=O ester), 1673 (Amide I), 1539 (amide II). MS-CI: m/z = 265 $[M+H]^+$. HRMS for $C_{14}H_{21}N_2O_3$: Calcd 265.1552. Found: 265.1545. EI. Anal. Calcd. for $C_{14}H_{20}N_2O_3$: C, 63.62; H, 7.63; N, 10.60. Found: C, 63.94; H, 7.70; N, 10.63.

Poly(D-isocyanoalanyl-L-alanine hept-6-ynol ester) 9

Following a similar procedure as for **8**, **9** was obtained as a brown solid in 58% yield. $[\alpha]_D$ +116 (*c* 0.04 in $CHCl_3$). ^{1}H NMR (δ ppm, $CDCl_3$): 8.9 (br, 1H, NH), 8.52 (br, 1H, NH), 5.5–5.1 (br, 1H, CH Ala), 5.0–3.5 (br, 4H, OCH_2, CH Ala), 2.3–2.1 (br, 2H, HC≡CCH_2), 2.1–1.9 (br, 1H, *H*C≡CCH_2), 1.9–0.6 (br, 12H, CH_2, CH_3 Ala). FT-IR (cm^{-1}, ATR): 3264 (NH), 2984, 2936, 2863 (CH_2), 2116 (C≡C), 1736 (C=O ester), 1656 (Amide I), 1531 (amide II).

Poly(L-isocyanoalanyl-L-alanine hept-6-ynol ester) 10

Following a similar procedure as for **8**, **10** was obtained as a brown solid in 56% yield. $[\alpha]_D$ –204 (*c* 0.02 in $CHCl_3$). ^{1}H NMR (δ ppm, $CDCl_3$): 8.7 (br, 1H, NH), 7.62 (br, 1H, NH), 4.7–3.5 (br, 4H, CH Ala, OCH_2), 2.3–2.1 (br, 2H, HC≡CCH_2), 2.1–1.8 (br, 1H, *H*C≡CCH_2), 1.8–0.8 (br, 12H, CH_2, CH_3 Ala). FT-IR (cm^{-1}, ATR): 3356, 3284 (NH), 2989, 2938, 2864 (CH_2), 2115 (C≡C), 1737 (C=O ester), 1685, 1644 (Amide I), 1531 (amide II).

Polyisocyanide 11

To a suspension of polymer **8** (18mg, 0.09mmol) in freshly distilled CH_2Cl_2 (16 mL) was subsequently added dodecylazide (0.9 mL, 3.8 mmol, 42 equiv.), PMDETA (0.6 mL, 2.5 mmol, 28 equiv.) and CuBr (40 mg, 0.28 mmol, 3 equiv.) The pale green solution was stirred for 96 hours, after which time the precipitated copper salts were removed by filtration. The resulting green solution was washed with an aqueous 10% (w/w) EDTA solution, dried (Na_2SO_4), concentrated and subjected to size exclusion chromatography (Bio Bead S-X1, $CHCl_3$) resulting in a yellow solid (17 mg). $[\alpha]_D$ –82 (*c* 0.03 in $CHCl_3$). ^{1}H NMR (δ ppm, $CDCl_3$, 400 MHz): 7.77 (br, 1H, triazole H), 7.1, 6.6 (br, 2H, NH), 5.5–4.9 (br, 2H, OCH_2), 4.5–3.8 (br, 4H, CH Ala, NCH_2), 2.1–1.0 (br, 26H, CH_2 dodecyl, CH_3 Ala), 0.9–0.6 (br, 3H, CH_3). FT-IR (cm^{-1}, ATR): 3289 (NH), 2955, 2923, 2853 (CH_2), 1737 (C=O ester), 1692 (C=C), 1646 (Amide I), 1548 (amide II), 1487 (N=N).

4.5 References & Notes

(1) Rostovtsev, V. V.; Green, L. G.; Fokin, V. V.; Sharpless, K. B. *Angew. Chem. Int. Ed.* **2002**, *41*, 2596-2599.

(2) Joralemon, M. J.; O'Reilly, R. K.; Matson, J. B.; Nugent, A. K.; Hawker, C. J.; Wooley, K. L. *Macromolecules* **2005**, *38*, 5436-5443; Malkoch, M.; Schleicher, K.; Drockenmuller, E.; Hawker, C. J.; Russell, T. P.; Wu, P.; Fokin, V. V. *Macromolecules* **2005**, *38*, 3663-3678; Wu, P.; Feldman, A. K.; Nugent, A. K.; Hawker, C. J.; Scheel, A.; Voit, B.; Pyun, J.; Frechet, J. M. J.; Sharpless, K. B.; Fokin, V. V. *Angew. Chem. Int. Ed.* **2004**, *43*, 3928-3932; Wu, P.; Malkoch, M.; Hunt, J. N.; Vestberg, R.; Kaltgrad, E.; Finn, M. G.; Fokin, V. V.; Sharpless, K. B.; Hawker, C. J. *Chem. Commun.* **2005**, 5775-5777.

(3) Beatty, K. E.; Liu, J. C.; Xie, F.; Dieterich, D. C.; Schuman, E. M.; Wang, Q.; Tirrell, D. A. *Angew. Chem. Int. Ed.* **2006**, *45*, 7364-7367; Link, A. J.; Vink, M. K. S.; Tirrell, D. A. *J. Am. Chem. Soc.* **2004**, *126*, 10598-10602.

(4) Burley, G. A.; Gierlich, J.; Mofid, M. R.; Nir, H.; Tal, S.; Eichen, Y.; Carell, T. *J. Am. Chem. Soc.* **2006**, *128*, 1398-1399.

(5) Diaz, D. D.; Punna, S.; Holzer, P.; Mcpherson, A. K.; Sharpless, K. B.; Fokin, V. V.; Finn, M. G. *J. Polym. Sci. Pol. Chem.* **2004**, *42*, 4392-4403; Hawker, C. J.; Wooley, K. L. *Science* **2005**, *309*, 1200-1205; O'Reilly, R. K.; Hawker, C. J.; Wooley, K. L. *Chem. Soc. Rev.* **2006**, *35*, 1068-1083.

(6) Parrish, B.; Breitenkamp, R. B.; Emrick, T. *J. Am. Chem. Soc.* **2005**, *127*, 7404-7410.

(7) Opsteen, J. A.; van Hest, J. C. M. *Chem. Commun.* **2005**, 57-59.

(8) Mantovani, G.; Ladmiral, V.; Tao, L.; Haddleton, D. M. *Chem. Commun.* **2005**, 2089-2091; Wang, X. Y.; Kimyonok, A.; Weck, M. *Chem. Commun.* **2006**, 3933-3935.

(9) Helms, B.; Mynar, J. L.; Hawker, C. J.; Frechet, J. M. J. *J. Am. Chem. Soc.* **2004**, *126*, 15020-15021; Malkoch, M.; Vestberg, R.; Gupta, N.; Mespouille, L.; Dubois, P.; Mason, A. F.; Hedrick, J. L.; Liao, Q.; Frank, C. W.; Kingsbury, K.; Hawker, C. J. *Chem. Commun.* **2006**, 2774-2776.

(10) Cornelissen, J. J. L. M.; Rowan, A. E.; Nolte, R. J. M.; Sommerdijk, N. A. J. M. *Chem. Rev.* **2001**, *101*, 4039-4070; Nolte, R. J. M. *Chem. Soc. Rev.* **1994**, *23*, 11-19.

(11) Clericuzio, M.; Alagona, G.; Ghio, C.; Salvadori, P. *J. Am. Chem. Soc.* **1997**, *119*, 1059-1071; Ishikawa, M.; Maeda, K.; Mitsutsuji, Y.; Yashima, E. *J. Am. Chem. Soc.* **2004**, *126*, 732-733; Kollmar, C.; Hoffmann, R. *J. Am. Chem. Soc.* **1990**, *112*, 8230-8238; Millich, F.; Baker, G. K. *Macromolecules* **1969**, *2*, 122-128; Nolte, R. J. M.; Van Beijnen, A. J. M.; Drenth, W. *J. Am. Chem. Soc.* **1974**, *96*, 5932-3.

(12) Cornelissen, J. J. L. M.; Donners, J. J. J. M.; de Gelder, R.; Graswinckel, W. S.; Metselaar, G. A.; Rowan, A. E.; Sommerdijk, N. A. J. M.; Nolte, R. J. M. *Science* **2001**, *293*, 676-680.

(13) Samori, P.; Ecker, C.; Goessl, I.; de Witte, P. A. J.; Cornelissen, J. J. L. M.; Metselaar, G. A.; Otten, M. B. J.; Rowan, A. E.; Nolte, R. J. M.; Rabe, J. P. *Macromolecules* **2002**, *35*, 5290-5294.

(14) de Witte, P. A. J.; Castriciano, M.; Cornelissen, J. J. L. M.; Scolaro, L. M.; Nolte, R. J. M.; Rowan, A. E. *Chem. Eur. J.* **2003**, *9*, 1775-1781.

(15) Vriezema, D. M.; Hoogboom, J.; Velonia, K.; Takazawa, K.; Christianen, P. C. M.; Maan, J. C.; Rowan, A. E.; Nolte, R. J. M. *Angew. Chem. Int. Ed.* **2003**, *42*, 772-776.

(16) de Witte, P. A. J.; Hernando, J.; Neuteboom, E. E.; van Dijk, E. M. H. P.; Meskers, S. C. J.; Janssen, R. A. J.; van Hulst, N. F.; Nolte, R. J. M.; Garcia-Parajo, M. F.; Rowan, A. E. *J. Phys. Chem. B* **2006**, *110*, 7803-7812; Hernando, J.; de Witte, P. A. J.; van Dijk, E. M. H. P.; Nolte, R. J. M.; Rowan, A. E.; Garcia-Parajo, M. F.; van Hulst, N. F. *Abstr. Pap. Am. Chem. S.* **2004**, *227*, U302-U302; Schwartz, E.; Palermo, V.; Finlayson, C. E.; Huang, Y.-S.; Otten, M. B. J.; Liscio, A.; Trapani, S.; González-Valls, I.; Brocorens, P.; Cornelissen, J. J. L. M.; Peneva, K.; Müllen, K.; Spano, F.; Yartsev, A.; Westenhoff, S.; Friend, R. H.; Beljonne, D.; Nolte, R. J. M.; Samori, P.; Rowan, A. E. *Chem. Eur. J.* **2009**, *15*, 2536-2547.

(17) Vanbeijnen, A. J. M.; Nolte, R. J. M.; Naaktgeboren, A. J.; Zwikker, J. W.; Drenth, W.; Hezemans, A. M. F. *Macromolecules* **1983**, *16*, 1679-1689.

(18) Cornelissen, J. J. L. M. *Pure. Appl Chem.* **2002**, *74*, 2021-2030.

(19) Cornelissen, J. J. L. M.; Sommerdijk, N. A. J. M.; Nolte, R. J. M. *Macromol. Chem. Physic.* **2002**, *203*, 1625-1630.

(20) Skorna, G.; Ugi, I. *Angew Chem Int Edit* **1977**, *16*, 259-260.

(21) Metselaar, G. A.; Cornelissen, J. J. L. M.; Rowan, A. E.; Nolte, R. J. M. *Angew. Chem. Int. Ed.* **2005**, *44*, 1990-1993.

(22) The $\Delta\delta_{NH}$ upon polymerisation of **6** to give **7** amounts to 1.5 ppm, whereas for LD-PIAA the $\Delta\delta_{NH}$ is 2.4 ppm.

(23) Denmark, S. E.; Yang, S. M. *Tetrahedron* **2004**, *60*, 9695-9708; Macaulay, S. R. *J. Org. Chem.* **1980**, *45*, 734-735; Brown, C. A.; Yamashita, A. *J. Am. Chem. Soc.* **2002**, *97*, 891-892.

(24) Wezenberg, S. J.; Metselaar, G. A.; Rowan, A. E.; Cornelissen, J. J. L. M.; Seebach, D.; Nolte, R. J. M. *Chemistry--A European Journal* **2006**, *12*, 2778-2786.

(25) Kajitani, T.; Okoshi, K.; Sakurai, S. I.; Kumaki, J.; Yashima, E. *J. Am. Chem. Soc.* **2006**, *128*, 708-709; Metselaar, G. A.; Wezenberg, S. J.; Cornelissen, J. J. L. M.; Nolte, R. M.; Rowan, A. E. *J. Polym. Sci. Pol. Chem.* **2007**, *45*, 981-988.

(26) Okoshi, K.; Saxena, A.; Naito, M.; Suzaki, G.; Tokita, M.; Watanabe, J.; Fujiki, M. *Liquid Crystals* **2004**, *31*, 279-283.

(27) Sheiko, S. S.; Sun, F. C.; Randall, A.; Shirvanyants, D.; Rubinstein, M.; Lee, H.; Matyjaszewski, K. *Nature* **2006**, *440*, 191-194.

(28) Cornelissen, J. J. L. M.; Graswinckel, W. S.; Adams, P. J. H. M.; Nachtegaal, G. H.; Kentgens, A. P. M.; Sommerdijk, N. A. J. M.; Nolte, R. J. M. *J. Polym. Sci. Pol. Chem.* **2001**, *39*, 4255-4264.

(29) Sheldrick, G. M. (1996) *SADABS. Program for Emperical Absorption Correction*.

(30) de Gelder, R.; de Graaff, R. A. G.; Schenk, H. *Acta. Crystallogr. A* **1993**, *49*, 287-293.

(31) Sheldrick, G.M. *SHELXL-97. Program for the refinement of crystal structures*, University of Gottingen: Germany, 1997.

(32) Henkel, K.; Weygand, F. *Chem. Ber.* **1943**, *76*, 812-818.

5

Post-modification of helical dipeptido polyisocyanides using the ‘click' reaction[§]

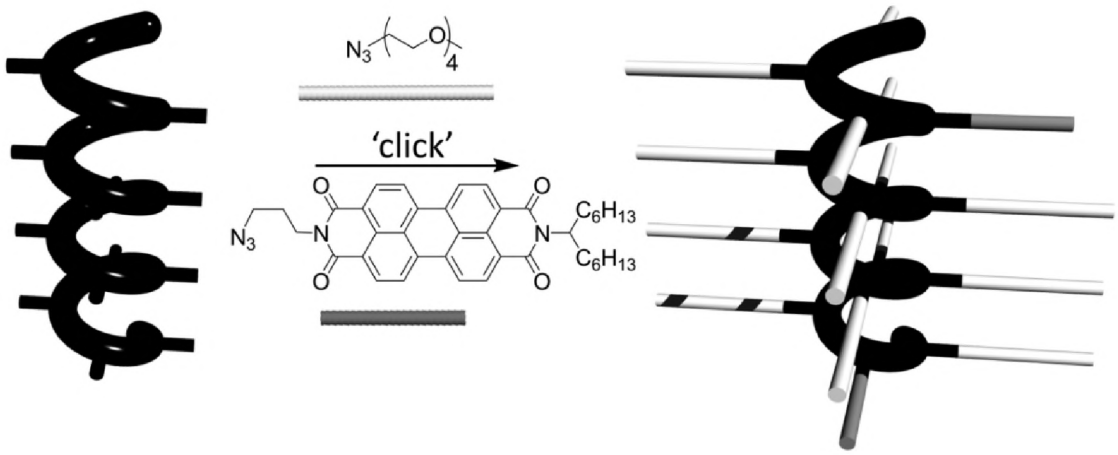

[§]Parts of this work have been published: Kitto, H. J.; Schwartz, E.; Nijemeisland, M.; Koepf, M.; Cornelissen, J. J. L. M.; Rowan, A. E.; Nolte, R. J. M. *Journal of Materials Chemistry* **2008**, *18*, 5615–5624.

5.1 Introduction

The assembling of functional dyes into ordered arrays is an area of great current interest in the materials sciences, with a number of potential applications, particularly in the fields of molecular photonics and electronics.[1] New materials, which possess the architecture and mimic the function natural systems, e.g. in the sense that they display unique photophysical and electronic properties as a result of excitonic interactions between neighbouring dye units, are highly sought after. The light-harvesting antenna and photosynthetic centres used by green plants and purple bacteria employ organised assemblies of bacteriochlorophyll molecules that are held together with the help of protein scaffolds.[2] The precise arrangement of the chromophoric pigments results in the efficient absorption and transportation of light energy and its subsequent conversion into chemical energy.[3]

In order to mimic these highly efficient natural systems one can utilise molecular-recognition and self-assembly as tools to construct synthetic structures that display similar properties. In this respect supramolecular interactions such as π–π stacking, hydrogen bonding, metal–ligand interactions, or electrostatic forces are important parameters. These interactions can be used to organise molecular building blocks into well-defined arrays, but eventually only limited control over the final structure can be obtained. An alternative approach is the use of covalent synthesis to link the building blocks together.[4] The step-wise construction of such assemblies is a frequently used approach, but is cumbersome because it involves multi-step syntheses and the desired products are often obtained in low yields. We and others have used polymers as scaffolds to covalently organise chromophoric molecules in well-defined arrays.[5,6,7]

Of particular interest in this connection are helical polyisocyanides, which have been developed by our group and are discussed in Chapter 1.[8] Polyisocyanides, such as poly(L-isocyanoalanyl-L-alanine methyl ester), form very stable β-helical architectures due to the presence of four hydrogen-bonding arrays parallel to the polymer backbone; the hydrogen bonding network rigidifies the chains, resulting in extremely stiff polymers (persistence length 76 nm) and prevents the unwinding of the helix.[9] Polyisocyanides possess a 4_1 helical conformation (i.e., four repeat units per helical turn) with an average spacing between the side chains *n* and (*n* + 4) of 4.7 Å. In addition, the chiral centres of the peptide units control the handedness (left- or right-handed) of the helix, allowing the tuning of the architectures; a right-handed (*P*) helix is generated on formation of poly(L-isocyanoalanyl-L-alanine methyl ester).

The introduction of chromophoric units, such as porphyrins and perylenes (see Chapter 1) into these polymers can be achieved by the synthesis of a chromophore-appended monomer and subsequent polymerisation with nickel ions. Previous studies on these

chromophoric macromolecules showed that defined polyisocyanides with chromophoric units have promising photophysical properties when arranged in a helical environment. One disadvantage, however, is that the synthesis of the materials and in particular of the chromophore-containing isocyanide monomers is tedious and considerable problems are often encountered in the final dehydration step of the formamide to form the isocyanide. The work in this chapter presents an alternative way to prepare the costly chromophoric polyisocyanides, namely by post-modification of a well-defined polyisocyanide scaffold, which is synthesised from readily available starting materials. The polymer scaffold has side arms containing two alanine groups and an acetylene functionality and was described in Chapter 4[10]; post-modification can be achieved by applying click chemistry to generate a product that contains a dye linked to the scaffold through a triazole ring. The scaffold itself is only mildly soluble in organic solvents, but it was found that reaction of this polymer with dodecyl azide under click chemistry conditions led to a polymer with greatly increased solubility in organic solvents and modified properties as concluded from AFM and CD spectroscopic studies. In this chapter we extend the above mentioned clicking approach, i.e. by post-modification of acetylene containing polyisocyanides with both chromophoric and water-soluble azides to yield water-soluble systems.

5.2 Results & Discussion

Two azides, one containing a perylene moiety and the other one possessing ethylene glycol units, were prepared in order to study the scope of the click reaction involving the polyisocyanide scaffold. The perylene azide **4** was synthesised in three steps from the commercially available 3,4:9,10-perylenetetracarboxydianhydride using a method reported by Langhals[11] and Nagao[12] (Scheme 1). The first step involved the reaction of the perylene dianhydride **1** with potassium hydroxide in water, followed by addition of acetic acid to generate the potassium salt **2**. The salt was treated with 1-azido-3-amino propane and after stirring overnight, the addition of potassium carbonate yielded the asymmetric perylene monoimide monoanhydride **3**. The reaction of this imide with 1-hexylheptyl amine in the presence of imidazole lead to the isolation of the desired diimide **4**, which was purified by column chromatography.

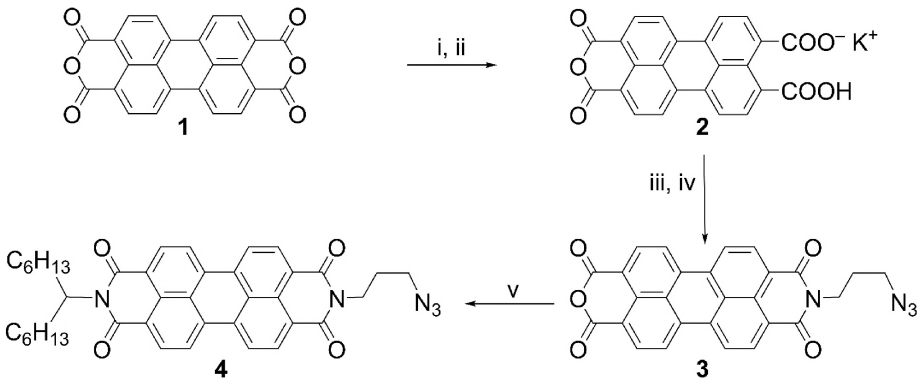

Scheme 1. Synthesis of PDI **4**; reagents and conditions. (i) KOH, H_2O, 90 °C, 2h; (ii) acetic acid, 90 °C, 40 min; (iii) 1-azido-3aminopropane, H_2O, K_2CO_3, 90 °C, 48h; (iv) 2M HCl; (v) 1-hexylheptylamine, imidazole, DMF, 120 °C.

The second azide contains a tetraethylene glycol unit and was synthesised by converting tetraethylene glycol monomethyl ether **5** into the corresponding tosylate **6** under standard tosylation conditions (Scheme 2). The tosylate was then treated with sodium azide in ethanol at elevated temperatures to generate the desired azide **7**, which was obtained, after purification by chromatography, as a colourless oil.

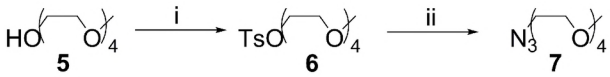

Scheme 2. Synthesis of azide **7**; reagents and conditions. (i) TsCl, Triethyl amine, CH_2Cl_2, 0 °C ; (ii) NaN_3, ethanol, reflux.

The click reaction of the polymeric scaffold poly(L-isocyanoalanyl-L-alanine prop-2-ynol ester) with the azides was performed under an inert argon atmosphere. The polymer was suspended in dichloromethane and the azide added. The resulting mixture was subsequently treated with PMDETA and copper bromide and stirred overnight. The copper salts were removed from solution by complexation with EDTA and the clicked polymers were subjected to size-exclusion chromatography to remove any unreacted azides. All polymers generated this way were analysed by different physical techniques including circular dichroism (CD), ultraviolet–visible absorption (UV–Vis), infrared (IR), NMR and fluorescence spectroscopy, by gel permeation chromatography (GPC) and in some cases atomic force microscopy (AFM).

In order to determine whether the polymers obtained from the click reaction approach have the same properties as those obtained from the polymerisation of isocyanide monomers several comparison experiments were performed. In the first instance two perylene-containing polymers were prepared and their properties compared. The first polymer (**9**) was obtained from the nickel-induced polymerisation of the perylene isocyanide monomer **8** in dichloromethane. The second, “clicked”, polymer was generated by reaction of poly(L-

isocyanoalanyl-L-alanine prop-2-ynol ester) (**10**) with an excess of the perylene azide **4** to give the triazole ring containing polymer **11**. In order to compare these two polymers, solutions were prepared in which the concentration was calculated on the effective monomer unit (in the case of the clicked polymer this involves the monomer–triazole–perylene unit and it was assumed that the click reaction was 100% efficient).[13]

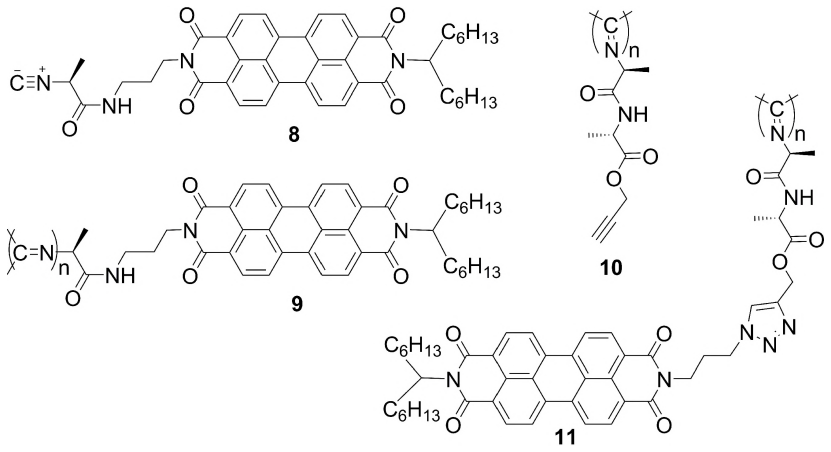

Chart 1. Molecular structure of the molecules **8**–**11**.

The absorption spectra (Figure 1, top left) of these compounds were recorded at three different concentrations. At each concentration, for both polymers, several well-defined aborption bands were observed in the region of 400–550 nm, with λ_{max} = 469, 492 and 533 nm; the perylene isocyanide monomer **8** had peaks in the same region with λ_{max} = 432, 459, 490 and 527 nm (Figure 1, top left), however, these peaks differ in intensity and width to those of the polymer **9**. The red-shifted broadening of the absorption peaks in the region 550–600 nm is evident in the polymer spectra and is indicative of strong Coulombic (exciton) interactions between the transition dipole moments of nearby perylene moieties, indicating short inter-chromophoric distances. At each concentration both polymers exhibited the same features indicating that exciton migration is present in both cases and that the presence of the triazole moiety does not significantly disorder the chromophoric array. The fluorescence emissions of the two polymers and that of the monomer are compared in Figure 1 (top right). The fluorescence spectrum of the perylene monomer **8** is represented by a strong vibronic band at λ = 535 nm and a second weaker band at λ = 578 nm; the polymer of **8** has a broad peak centred around λ = 620 nm. The red-shifted emission observed for the polymer compared to that of the monomer is consistent with the formation of excimer-like perylenediimide species, favoured by exciton interactions and charge transfer, often seen in perylene arrays. The polymer obtained by clicking also had a broad peak centred at λ = 620

nm, however, of lower intensity than that of the homopolymer (Figure 1, top right). In this case fluorescence due to monomer emission was also observed.

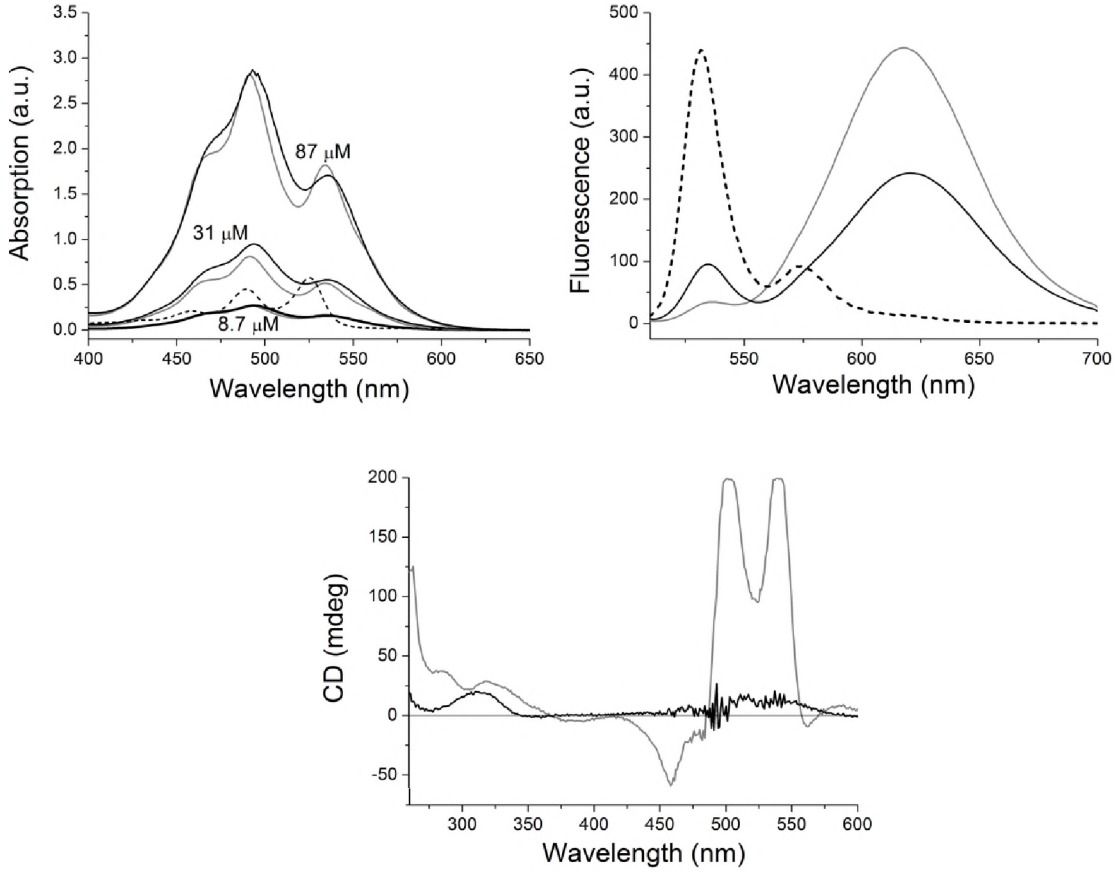

Figure 1. Spectroscopic properties of **9** (grey line) and **11** (black line) in dichloromethane. UV–Vis spectra at various concentrations: 8.7 μM, 31 μM and 87 μM (top left); Fluorescence spectra at 0.87 μM (top right) and CD spectra at 87 μM (bottom). Data of the monomer **8** (dotted line) are shown as comparison.

The monomer emission could result from the presence of some residual perylene azide, but since extensive washing and purification by size exclusion chromatography was applied, it is more likely causes by irregularities in the grafting process of the azide onto the polymers. The perylenes situated at the defects can be expected to exhibit more monomer-like emission. The difference in the intensity of the monomer emission compared to that of the polymer indicates that ca. 9% of the perylenes on the polymer backbone were in a non-excimer environment. This is in contrast to **9**, in which all the perylenes are in an excimer-like environment (see Chapter 3).

In contrast to the fluorescence spectra, which were similar, the CD spectra of the two polymers showed very different signatures (Figure 1, bottom). Polymer **9** had strong positive Cotton signals in the region of λ = 450–550 nm where the absorption bands due to interacting perylenediimides are located. In this polymer, signals having much lower intensity could also be seen at ca. λ = 290 and 330 nm. The CD spectrum of the clicked

polymer did not exhibit any effect reminiscent of that observed for the former polymer in the region of λ = 450–550 nm. In this region a slight increase of the signal from the baseline could be seen, however, no well-defined peaks were observed; increasing or decreasing the concentration did not result in peaks giving any information. A positive peak was present at λ = 320 nm , arising from the polyimine groups present in the backbone of the polymer; this spectrum is similar to the polymer scaffold **10** and shows that the inner core of the helix is not influenced by the clicking. The difference in the position of the peaks of the two polymers in the λ = 280–350 nm region could result from the fact that the homopolymer has only one alanine unit in the side-chain, whereas the clicked polymer has two alanine units making the hydrogen bonding network stronger, therefore having an effect on the helical pitch of the polymer. The absence of any signal due to the perylene units in the clicked polymer suggests that due to the presence of the two alanine units and the triazole moiety, the perylenes are too far away from the helical backbone to be influenced by it. This lack of ordering of the perylenes may also in part account for the slight differences in the fluorescence spectra.

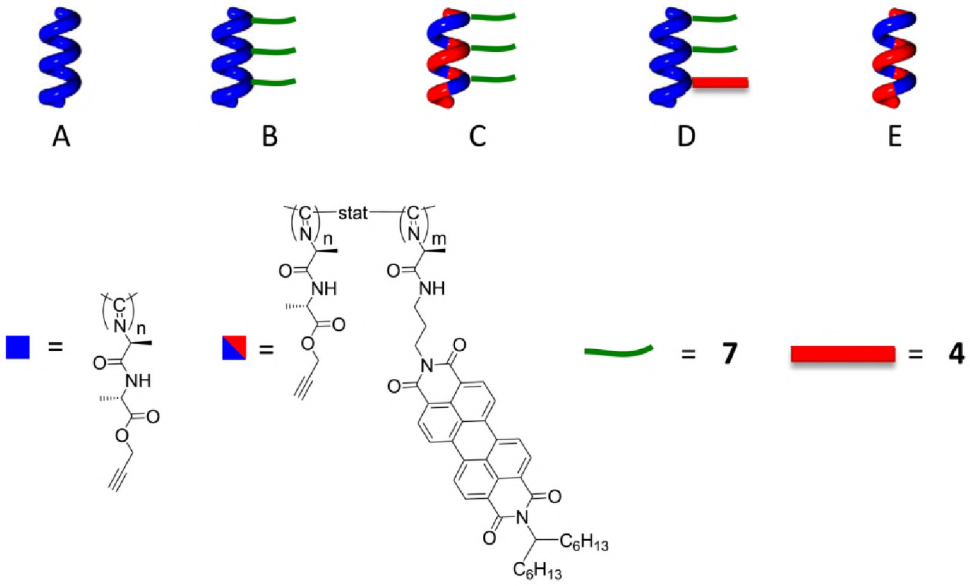

Figure 2. Schematic representation of the five compounds (**A**–**E**) that were used to study the formation of statistical copolymers by click chemistry.

A second set of experiments was carried out to determine whether the formation of statistical copolymers could also be efficiently achieved using the click chemistry approach. Five compounds were prepared and analysed by spectroscopic techniques. The five samples, represented in schematic diagrams in Figure 2, were as follows: **A**) the polymer scaffold poly(L-isocyanoalanyl-L-alanine prop-2-ynol ester) **10**; **B**) the polymeric scaffold with clicked ethylene glycol units; **C**) a statistical copolymer formed from L-isocyanoalanyl-L-alanine prop-

2-ynol ester (99%) and perylene isocyanide **8** (1%) followed by a click reaction with an excess of **7**; **D**) polymer **10** statistically clicked to perylene azide **4** (1%) and ethylene glycol azide **7** (99%); **E**) a statistical copolymer formed from **10** (99%) and perylene isocyanide **8** (1%). Solutions of these polymers (ca. 0.75 mM) were prepared taking into account the molecular weight of the effective monomer unit and neglecting, if necessary, any incorporated perylene. In the cases where the click reaction had been used, it was assumed, for calculating concentrations, that the click reaction had an efficiency of 100%.

The absorption spectra of the samples containing the perylene chromophore (**C**–**E**) are shown in Figure 3 (top left). The intensities of the bands varied, but in each case an absorption band similar to that seen for the perylene monomer absorption was observed. In the case of **D**, however, there was a noticeable broadening and a red shift in the λ = 520–570 nm region in the UV–Vis spectrum. This shift occurred after polymerisation of the perylene isocyanide and is a result of the stacking of perylene molecules within the polymer. This stacking was further confirmed by the presence of an absorption in the excimer region of the fluorescence spectrum (Figure 3, top right). Although the three samples **A**–**C** showed fluorescence reminiscent to that of monomer emission, as would be expected for the presence of such a small quantity of perylene, polymer **D** displayed, in the range of λ = 600–650 nm, a slight broadening, which was not present in the case of **C**, indicating that interactions exist between neighbouring chromophores (Figure 3, top right, inset). It is of interest to note that the fluorescence emission of the two polymers containing ethylene glycol units had a lower intensity than that of the statistically clicked polymer, indicating that the presence of the ethylene glycol units leads to a slight quenching of the perylene fluorescence.

The CD spectra of the five samples (Figure 3, bottom left) showed interesting trends. In the case of the polymers with no ethylene glycol incorporated (**A** and **E**), a positive CD effect was observed at λ = 320 nm arising from the polyimine backbone. The polymers containing the clicked ethylene glycol units exhibited a negative CD effect of a much lower intensity at λ = 290 nm. The click reaction of the polymer scaffold with dodecyl azide[10] also generated a sample for which a similar change in CD signal was observed (see Chapter 4). One of the reasons for the observed difference can be attributed to an induced small change in the helical pitch of the polymer backbone due to the presence of the triazole ring resulting in changes in the hydrogen bonding array. Since no change in the CD signal was observed when perylene azide is clicked to the polymeric scaffold, the present change in signal seen here might be attributed to properties of the azido derivatized compounds being clicked. It is of interest to note that the three samples displaying negative CD effects (**B**–**D**) all exhibited the same spectra when measured in water (Figure 3, bottom right).

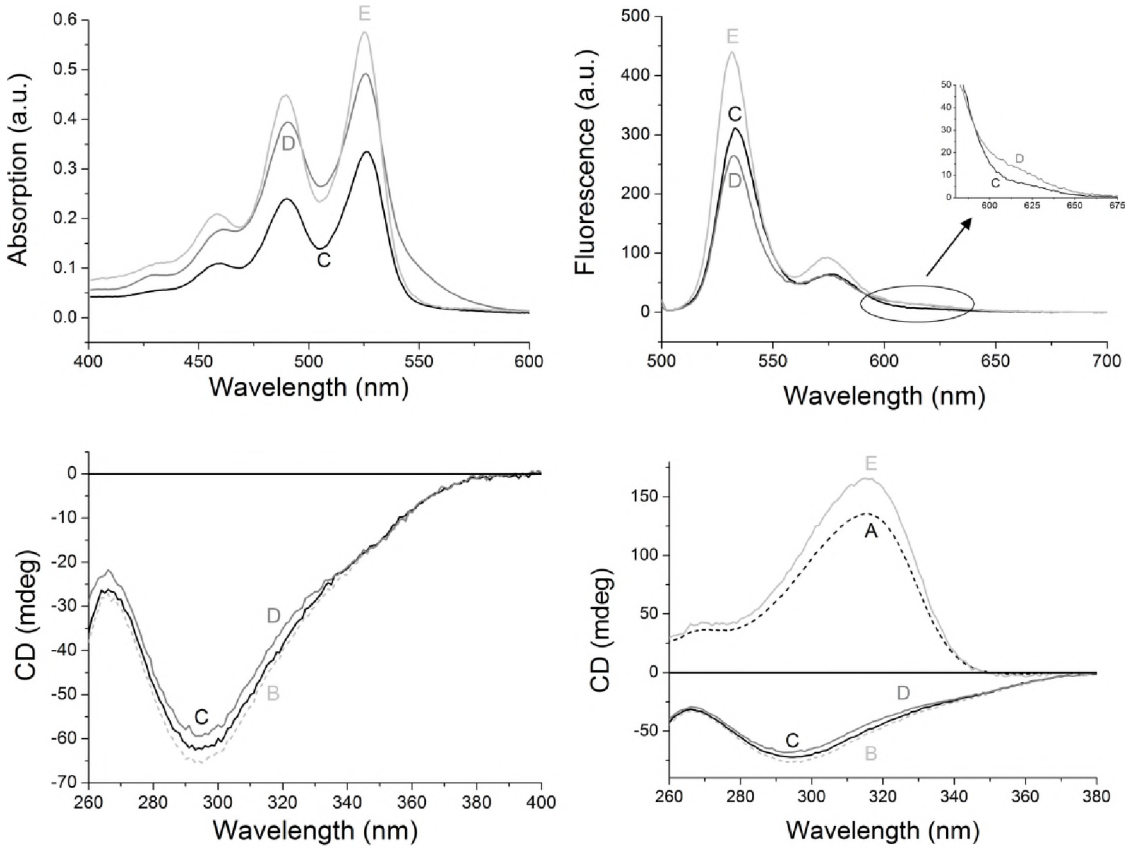

Figure 3. Spectroscopic data for the statistical copolymers and reference polymers in dichloromethane: **A** (dotted line); **B** (grey dashed); **C** (black line); **D** (grey line); **E** (light grey line). UV–Vis spectra (0.75 mM) (top left); Fluorescence spectra (5.90 μM), λ_{exc} = 492 nm (the inset shows the red-shifted broad absorption band of the polymer **D**) (top right). CD spectra (0.75 mM) in CH_2Cl_2 (bottom left) and CD spectra (0.75 mM) of **B** (grey dashed); **C** (black line); **D** (grey line) in H_2O (bottom right).

In order to study the cooperative effect seen in the UV–Vis and fluorescence spectra of sample **D** in more detail, a family of polymers were synthesised consisting of different percentages of perylene and ethylene glycol moieties statistically clicked to the polymer scaffold. The prepared samples are given in Table 1.

Table 1 Polymers synthesised with varying degrees of perylene azide **4** incorporated

Polymer	**P0**	**P1**	**P2**	**P3**	**P4**	**P5**	**P6**	**P7**	**P8**	**P9**	**P10**
% **4**	0	0.5	1	2	5	7	10	15	20	50	100

The UV–Vis spectra of samples **P0–P8** are shown in Figure 4 (left). On increasing the percentage of perylene a change in the absorption spectrum is observed similar to that when the perylene monomer is converted into the polymer. It involves a broadening and red-shift as well as changes in intensity and position of the absorption maxima. It is of

interest to note that a close to linear relationship is observed when the absorption at λ = 498 nm is plotted against the percentage of perylene in the sample (Figure 4, right).

The fluorescence spectra of samples **P0–P8** are shown in Figure 5a. Sample **P1**, containing 0.5% perylene, was seen to have only monomer-like emission. On increasing the percentage of perylene to 1%, the intensity of the monomer emission also increased, however, in the region of the spectrum between λ = 600–650 nm a slight broadening was observed. With greater percentages of perylene the monomer emission was found to decrease, whilst that of the excimer emission increased. Separate fluorescence spectroscopic measurements were conducted on **P9** and **P10** at much lower concentrations as the intensity of the measurements when the samples were prepared analogous to the other samples were out of the range of the machines used. The absorption spectra of these two polymers were reminiscent of the spectra observed for interacting chromophores and the fluorescence spectra showed excimer-like emission, however, in both cases monomer-like emission could also be seen.

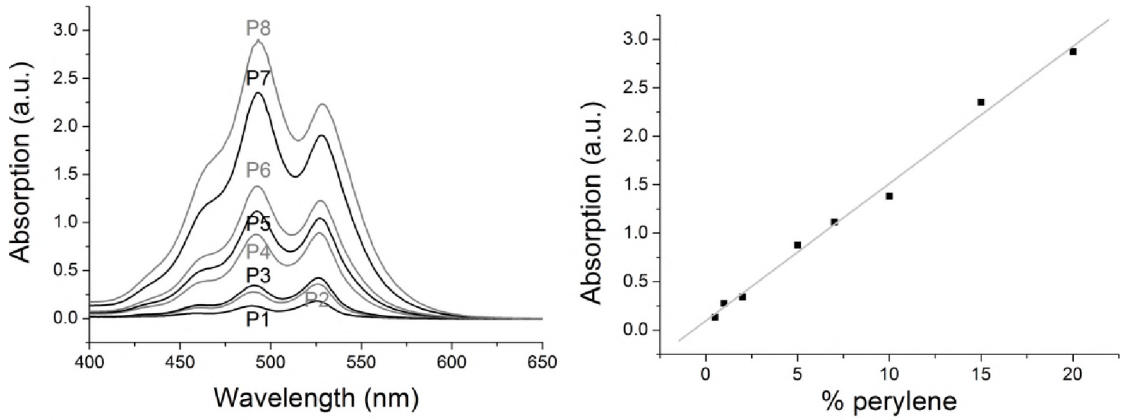

Figure 4. UV-Vis data for the statistically clicked polymers **P0–P8** in dichloromethane. UV-Vis spectra (1 mg in 5 mL) (left) and plot of the absorption at λ = 492 nm against percentage of perylene (right).

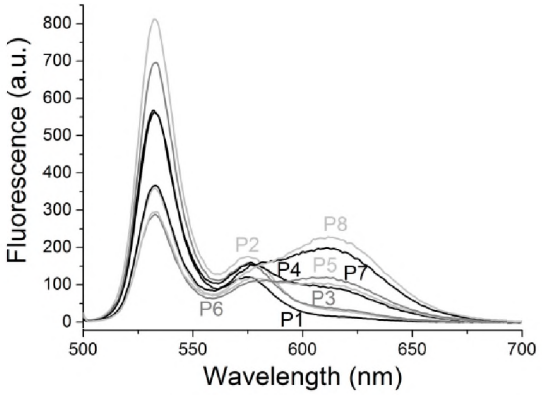

Figure 5. a) Fluorescence spectra (25 μg in 5 mL; λ_{exc} = 492 nm) of the statistically clicked polymers **P0–P8** in dichloromethane.

The CD spectra of **P0**–**P10** measured in dichloromethane are shown in Figure 6. The polymer samples containing only ethylene glycol units and sample having low percentages of perylene displayed negative Cotton effects at λ = 290 nm. As the percentage of perylene in the samples increased the intensity of the peak at λ = 290 nm decreased and a positive peak at λ = 320 nm appeared. Samples **9** and **10**, containing 50 and 100% perylene, have only positive peaks at λ = 320 nm. This leads one to conclude that the ethylene glycol units affect the arrangement of the inner core of the helix while the perylene units do not. To determine whether the trend observed was dependent on the concentration of the solution, the CD spectra were measured on solutions that had an absorption of ca. 0.8 a.u. at λ = 492 nm in the UV–Vis spectrum. The spectra obtained under these conditions had the same shape as those seen in Figure 6, albeit with different intensities. Further dilution or concentration of the samples did not yield CD spectra with different shapes.

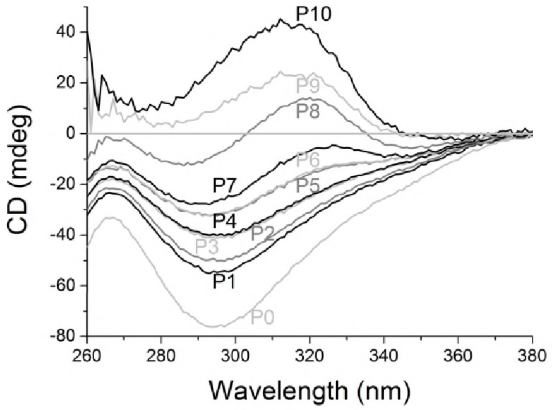

Figure 6. CD spectra (1 mg in 5 mL) of the statistically clicked polymers **P0**–**P8** in dichloromethane.

Temperature dependent CD spectra were recorded for polymers **P0** and **P10** in chloroform (1 mg in 5 mL) at 10, 20, 30, 40 and 50 °C. For both polymers no change was observed in the temperature range studied. In order to go to higher temperatures an attempt was made to dissolve the polymers in toluene, however, neither of the polymers had any solubility in this solvent, which is in strong contrast to the perylene homopolymer obtained from **8**, which was readily soluble in toluene.[7] The ethylene glycol polymer **P0** was dissolved in water (1 mg in 5 mL) and CD spectra were measured at 10, 20 and 50 °C. No changes were apparent at these temperatures, but on heating the sample to 80 °C the solution became turbid, due to the decreased solubility of ethylene glycol at high temperatures,[14] and a slight decrease of the CD signal was observed. The original spectrum was, however, restored on cooling of the solution back to 50 °C. The fact that no change in the CD spectra of the polymers was observed on changing the concentration, solvent or temperature confirms that the various side-chains have no effect on the helical backbone, although in the case of the ethylene glycol side-chains a slight unwinding of the helix might have occurred.

Polymers **P1–P8** were studied to see if the ethylene glycol units would provide solubility in water. Disappointingly, it was found that only the polymers with up to 2% of perylene (**P0–P3**) were soluble in water.

In a final series of experiments statistical copolymers were synthesised by clicking two dyes (i.e. perylene and coumarin) to the polyisocyanide scaffold. Reaction of poly(L-isocyanoalanyl-L-alanine prop-2-ynol ester) **10** with equimolar equivalents of perylene azide **4** and 3-Azido-7-hydroxycoumarin[15] was performed to generate **P11**. The coumarin azide has very little fluorescence, but on formation of the triazole moiety, its fluorescence intensity is greatly increased. For comparison also polymer **P12**, in which the scaffold was reacted with 100% coumarin, was prepared. The absorption spectrum of a dichloromethane solution of **P12** (0.26 mM based on effective monomer unit) revealed a maximum at λ = 340 nm as shown in Figure 7 (top left). The absorption spectrum of **P11** (53 μM, based on half the sum of the two effective monomer units, assuming that clicking of the azide units is equally efficient) showed, in the region of the absorption of the perylene, bands reminiscent of those of the homopolymer. In addition, two broad and overlapping bands centred at λ = 322 and 370 nm corresponding to the coumarin dye were also seen. The extinction coefficient of 7-hydroxycoumarin is known to be 40 000 L mol^{-1} cm^{-1} at λ = 409 nm,[16] while that of perylene is 385 000 L mol^{-1} cm^{-1} at λ = 435.75 nm.[17] The differences in these extinctions coefficients were reflected in the concentrations of the solutions used to record the fluorescence spectra (Figure 7, top right). The fluorescence spectrum of a solution of **P11** (53 μM), when excited at 340 nm, exhibited broad overlapping bands in the coumarin region of λ = 375–500 nm. Polymer **P12** containing only coumarin (0.64 μM) had a fluorescence emission at λ = 462 nm. When a solution of **P11** (2 μM) was excited at λ = 492 nm the fluorescence corresponding to the perylene was observed. In this case, as expected, there were bands corresponding to both monomer and excimer emission. The existence of multiple peaks for **P11** in both the UV–Vis and fluorescence spectra indicates that there is communication between the coumarin and the perylene dyes; the coumarin molecules in close proximity of a perylene molecule display a largely quenched and blue-shifted emission. The CD spectrum (Figure 7, bottom) obtained of copolymer **P11** showed a positive Cotton effect at λ = 320 nm. The spectrum of **P12**, however, was very different. In this case there was a small negative band at λ = 340 nm and a positive band of twice the intensity at 290 nm. It is clear from the CD spectra obtained in these and earlier experiments that the perylene molecules dominate the arrangement of the helical backbone in the cases where clicking involves more than one azide.

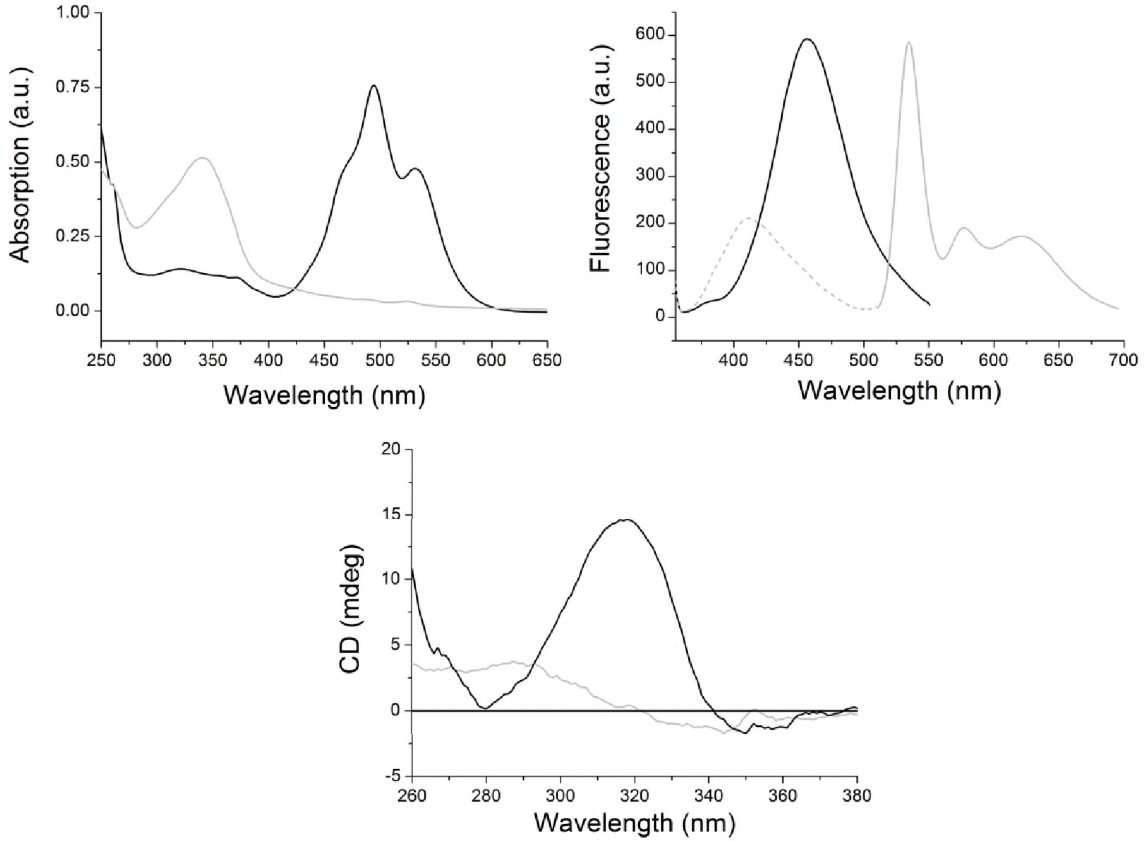

Figure 7. Spectroscopic data for polymers obtained from the statistical clicking of perylene and coumarin dyes. UV–Vis spectra of **P11** (53 μM, black line) and **P12** (0.26 mM, grey line) (top left). Fluorescence spectra of **P11** (54 μM, λ_{exc} = 340 nm, dotted grey line; 2 μM, λ_{exc} = 492 nm, grey line) and **P12** (0.64 μM, λ_{exc} = 340 nm, black line) (top right) and CD spectra of **P11** (0.32 mM, grey line) and **P12** (0.51 mM, black line) (bottom).

AFM micrographs of polymers **P11** and **P12** were recorded (Figure 8). A sample of **P12** before size exclusion chromatography (Figure 8, left) was found to contain polymers of much greater lengths than a sample after the chromatography (Figure 8, right). In fact, the latter micrographs did not show polymer strands clearly, instead aggregates of very short polymers were observed. This leads to the conclusion that the click reaction conditions do not destroy the polymer molecules, but that merely the long polymers are sticking to the biobeads and are being removed from the samples.

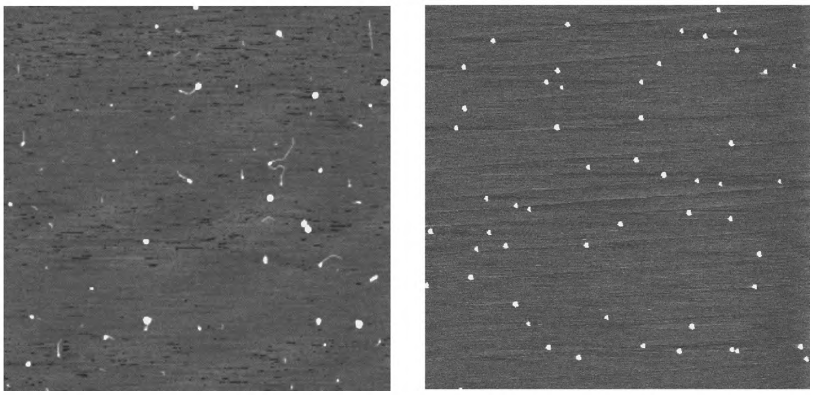

Figure 8. AFM micrographs of **P12** spin-coated on mica from chloroform. Before size exclusion chromatography (left, 3 μm × 3 μm) and after size exclusion chromatography (right, 5 μm × 5 μm).

5.3 Conclusion

The post-modification of the polymer scaffold poly(L-isocyanoalanyl-L-alanine prop-2-ynol ester) **10** can be effectively achieved by click chemistry using a variety of compounds that contain azide moieties. Although the fluorescence intensity of the polymer obtained from clicking a perylene azide onto the scaffold is not as large as that of the homopolymer prepared from an perylene functionalised isocyanide monomer, the clicking method is versatile and very useful for making statistical copolymers and there are indications that in the click reactions cooperative interactions lead to blocks of perylene units interacting along the polymer backbone. The use of an ethylene glycol azide leads to the formation of water-soluble polymers, and further incorporation of the perylene azide gave chromophoric water-soluble polymers with CD spectra that are the same in water and in dichloromethane. The click reaction also allowed the incorporation of a second chromophore (i.e. a coumarin dye) yielding statistical copolymers, in which the characteristic absorption and emission features from both polymers could be observed. It was found that in these compounds, interaction between the chromophores took place, evidenced by a quenched and blue-shifted emission of the coumarin dyes that are in close proximity to a perylene molecule. It can be concluded that the clicking method is an effective method for preparing polymers from compounds that are costly and for which the synthesis of the isocyanide monomer may not be straightforward. In particular the ability to form water soluble dye containing polymers, which can be modified by the addition of biomolecules, such as antibodies, proteins and peptides, offers perspectives for the preparations of materials that can function as biomarkers.

5.4 Experimental

General

All click reactions were performed under Schlenk conditions using distilled solvents. Tetraethylene glycol monomethyl ether, sodium azide and PMDETA were purchased from ACROS chemicals. Copper bromide, 3,4:9,10-perylenetetracarboxydianhydride and sodium azide were purchased from Sigma Aldrich. All purchased chemicals were used as received. Column chromatography was performed using silica gel (40–60 μm) purchased from Merck. TLC analyses were carried out using silica 60 F_{254} coated glass obtained from Merck and the compounds were visualised with ninhydrine, iodine or $Ni(ClO_4)\cdot 6H_2O$ in ethanol. Size exclusion chromatography was performed using Bio Bead S-X1 using $CHCl_3$ as eluant. ^{1}H NMR spectra were recorded, at 20 °C, on a Varian Inova400 or Bruker AC-300 machines operating at 400 and 300 MHz, respectively. ^{13}C NMR spectra were recorded on a Bruker AC-300 machines operating at 75 MHz. FT-IR spectra were recorded on a ThermoMattson IR300 spectrometer equipped with a Harrick ATR unit; compounds were measured as an oil or as an solid. Melting points were measured on a Buchi B-545 apparatus and are reported uncorrected. Mass spectrometry measurements were performed on a VG 7070E instrument (EI/CI) or on a JEOL Accutof instrument (ESI). CD spectra were recorded on a Jasco 810 instrument equipped with a Peltier temperature control unit and were measured at 20 ºC unless otherwise stated. AFM experiments were performed using a Nanoscope IV instrument from Digital Instruments. Solutions of the samples were spin-coated onto freshly cleaved Muscovite mica. All images were recorded with the AFM operating in tapping mode in air at room temperature with a resolution of 512 × 512 pixels using moderate scan rates (1–2 lines s^{-1}). Commercial tapping-mode tips (NT-MDT) were used with a typical resonance frequency around 300 kHz.

Compounds

1-Azido-3-amino propane,[18] 1-hexylheptyl amine,[19] 3-azido-7-hydroxycoumarin[15] and poly(L-isocyano-L-alanine prop-2-ynol ester **10**)[10] were prepared according to literature procedures.

3,4,9,10-Perylenetetracarboxy-3,4-anhydride potassium salt 2.

3,4:9,10-Perylenetetracarboxydianhydride (10.0 g, 25.5 mmol) was placed in a 3-necked round bottom flask and water (800 mL) was added. Potassium hydroxide (40.0 g, 0.71 mol) was added and the resulting mixture was stirred at 90 °C for 2 h, over which time the reaction mixture changed from red to green. Addition of acetic acid (50 mL) resulted in a colour change to brown and after stirring at 90 °C for 40 min the purple solid (11.0 g, 96%) was removed by filtration and washed thoroughly with methanol before being dried at 120 °C. Due to the insolubility of this compound in all solvents, characterisation could not be performed.

***N*^{1}-(3-Azidopropyl)-3,4,9,10-Perylenetetracarboxy-3,4-anhydride-9,10-imide 3**

3,4,9,10-Perylenetetracarboxy-3,4-anhydride potassium salt (1.92 g, 4.30 mmol) and 1-azido-3-amino propane (2.15 g, 21.50 mmol) were placed in a round bottom flask and water (60 mL) was added. The solution was stirred at 90 ºC for 48 h after which aqueous potassium carbonate (25%, 200 mL) was added. The solution was heated at 90 ºC for 3 h, over which time the colour changed from purple to green. The solid was filtered off and washed from the filter with a mixture of water (300 mL) and triethylamine (10 mL). The filtrate was diluted with aqueous HCl (2 M, 500 mL) and after standing for one day the precipitated solid was filtered off and washed with methanol. The product was obtained as a purple solid (2.0 g, 98%). Due to the insolubility of this compound in all solvents, characterisation could not be performed.

N^1-(3-Azidopropyl)-N^2-(1-hexylheptyl)-3,4:9,10-perylenetetracarboxydiimide 4

N^1-(3-Azidopropyl)-3,4,9,10-perylenetetracarboxy-3,4-anhydride-9,10-imide (1.10 g, 2.31 mmol) and 1-hexylheptyl amine (0.92 g, 4.63 mmol) were suspended in a solution of imidazole (49 g) and DMF (60 mL). The mixture was heated overnight at 120 °C after which it was cooled to room temperature. The addition of ethanol (200 mL) followed by the addition of aqueous citric acid (10%, 200 mL) generated a solid, which was removed by filtration. The crude solid was subjected to column chromatography ($CHCl_3$) to give the product as a dark red solid (0.82 g, 54%) having mp > 218 °C (dec.). ^{1}H NMR (300 MHz, $CDCl_3$): δ = 0.83 (t, 6 H, $^3J_{HH}$ = 6.90 Hz, CH_3), 1.20–1.41 (overlapping multiplets, 16 H, (CH_2)$_4$CH$_3$), 1.92 (m, 2 H, NCHCH_2), 2.06 (p, 2 H, $^3J_{HH}$ = 6.90 Hz, CH_2CH$_2$N$_3$), 2.26 (m, 2 H, NCHCH_2), 3.46 (t, 2 H, $^3J_{HH}$ = 6.90 Hz, CH_2N$_3$), 4.24 (t, 2 H, $^3J_{HH}$ = 6.90 Hz, CH_2CH$_2$CH$_2$N$_3$), 5.16 (m, 1 H, NC*H*), 8.21 (d, 2 H, $^3J_{HH}$ = 8.43 Hz, perylene), 8.28 (d, 2 H, $^3J_{HH}$ = 8.10 Hz, perylene), 8.36 (d, 2 H, $^3J_{HH}$ = 7.80 Hz, perylene), 8.49 (d, 2 H, $^3J_{HH}$ = 6.60 Hz, perylene). ^{13}C-NMR (75 MHz, $CDCl_3$): δ = 14.0 (*C*H$_3$), 22.5 (*C*H$_2$CH$_3$), 27.0, 27.6 (*C*H$_2$), 29.2 (CH$_2$*C*H$_2$N$_3$), 31.8 (*C*H$_2$), 32.3 (NCH*C*H$_2$), 38.0 (N*C*H$_2$), 49.4 (*C*H$_2$N$_3$), 54.9 (N*C*H), 122.6, 122.8, 125.8, 125.8, 128.9, 129.2, 130.9, 133.6, 134.2 (perylene C), 162.9 (*C*=O). FT-IR (cm^{-1}, ATR) 2954, 2919, 2850 (C-H stretch), 2094 (N$_3$), 1692, 1640 (amide) 1588, 1573 (C=C aromatic), 1333 (C-N stretch), 806, 741 (CH aromatic). MS-ESI *m/z* = 1333 [2M + Na]$^+$. Anal. Calcd for $C_{40}H_{41}N_5O_4$: C, 73.26; H, 6.30; N, 10.68. Found: C, 73.51; H, 6.30; N, 10.48.

11-Methoxy-3,6,9-trioxaundecyl *p*-toluenesulphonate 6

Tetraethylene glycol monomethyl ether (2.20 g, 10.57 mmol) and triethyl amine (1.62 mL, 11.62 mmol) were placed in a Schlenk flask under nitrogen and dissolved in dichloromethane (50 mL). The solution was cooled to 0 °C and tosyl chloride (2.22 g, 11.62 mmol) in dichloromethane (60 mL) was added dropwise over 1 h. The solution was left stirring overnight at room temperature after which time a TLC showed residual tosyl chloride and the desired product. The crude mixture was subject to column chromatography; dichloromethane was used to elute the excess tosyl chloride and 2% MeOH in CH_2Cl_2 to elute the desired compound. The product was obtained as a colourless oil (2.55 g, 67%). ^{1}H NMR (400 MHz, $CDCl_3$, 20 °C): δ = 2.44 (s, 3 H, CH_3), 3.37 (s, 3 H, OCH_3), 3.53–3.70 (overlapping multiplets, 14 H, CH_2CH_2OMe), 4.16 (t, 2 H, $^3J_{HH}$ = 4.84 Hz, CH_2OTS), 7.34 (d, 2 H, $^3J_{HH}$ = 8.08 Hz, ArH ortho to OMe), 7.79 (d, 2 H, $^3J_{HH}$ = 8.32 Hz, ArH ortho to OTs). ^{13}C NMR (300 MHz, $CDCl_3$, 20 ºC): δ = 21.6 (CH_3), 59.0 (OCH3), 68.7, 69.2, 70.5, 70.5, 70.6, 70.6, 71.9 (*C*H$_2$CH$_2$), 128.0, 129.0 (ArC), 133.0 (CSO_2), 144.8 (*C*CH$_3$). FT-IR (cm^{-1}, ATR): 2870 (br, CH_2/CH_3), 1175 (S=O). Anal. Calcd for $C_{16}H_{26}O_7S$: C, 53.02; H, 7.23. Found: C, 53.01; H, 7.42.

1-Azido-11-methoxy-3,6,9-trioxaundecane 7

Tosylate **6** (0.68 g, 1.88 mmol) was dissolved in ethanol (50 mL) and sodium azide (0.25 g, 3.77 mmol) was added. The solution was heated under reflux for 2.5 h, after which time TLC (10% MeOH in $CHCl_3$) showed that no starting material was left. The solvent was removed under vacuum and CH_2Cl_2 was added to the residue. The organic layer was extracted with water (3 ×) and dried ($MgSO_4$). The solvent was removed and the crude product was purified on silica (2% MeOH in CH_2Cl_2) to give the product as a colourless oil (0.43 g, 99%). ^{1}H NMR (400 MHz, $CDCl_3$, 20 °C): δ = 3.38 (s, 3 H, OCH_3), 3.40 (br s, 2 H, CH_2N$_3$) 3.53–3.56 (m, 2 H, CH_2CH$_2$N$_3$), 3.64–3.69 (overlapping multiplets, 12 H, –CH_2CH_2OMe). ^{13}C NMR (300 MHz, $CDCl_3$, 20 °C): δ = 50.7 (*C*N$_3$), 59.0 (O*C*H$_3$), 70.0, 70.5, 70.6, 70.6, 70.7, 70.7 72.9 (–*C*H$_2$CH$_2$O). FT-IR (cm^{-1}, ATR): 2872 (br, CH_2/CH_3), 2101 (N$_3$), 1105 (C–O–C). Mass or elemental analyses could not be obtained.

Typical procedure for the statistical click reactions

The polymer scaffold was suspended in a solution of CH_2Cl_2 (10 mL) (under an inert atmosphere) and the azides were added (in the case of coumarin THF was added to avoid precipitation). The addition of PMDETA and CuBr was carried out and the solutions were stirred overnight. The precipitated copper salts were removed from the solution by the repeated addition of a saturated aqueous EDTA solution and removal of the water layer from the top. The organic layer was dried over $MgSO_4$ and the solvent evaporated to give the polymer produtc as a solid. The polymers were subjected to size exclusion chromatography to remove any unreacted azides.

^{1}H NMR Spectroscopy. The spectra were broadened as expected for a polymer. The acetylene peak seen at 2.51 ppm in the polymeric scaffold **10** was no longer present and there was an additional peak at 7.60 ppm corresponding to the proton of the triazole ring. This peak is very evident in the samples in which the percentage of perylene is low, however, in samples with a high perylene content, the aromatic region of the spectrum becomes broad and the triazole peak disappeared in the broad resonances of the perylene protons.

IR spectroscopy. After each click reaction the IR spectrum of the product was recorded. The peak corresponding to the acetylene stretching frequency at 2129 cm^{-1} was no longer visible and in addition no azide peaks, which would indicate unreacted azide in the sample, were seen.

5.4 References & Notes

(1) Whitesides, G. M.; Mathias, J. P.; Seto, C. T. *Science* **1991**, *254*, 1312-1319; Philp, D.; Stoddart, J. F. *Angew. Chem., Int. Ed.* **1996**, *35*, 1155-1196; Lehn, J. M. *Science* **2002**, *295*, 2400-2403.

(2) Mcdermott, G.; Prince, S. M.; Freer, A. A.; Hawthornthwaitelawless, A. M.; Papiz, M. Z.; Cogdell, R. J.; Isaacs, N. W. *Nature* **1995**, *374*, 517-521.

(3) Pullerits, T.; Sundstrom, V. *Acc. Chem. Res.* **1996**, *29*, 381-389.

(4) Burrell, A. K.; Officer, D. L.; Plieger, P. G.; Reid, D. C. W. *Chem. Rev.* **2001**, *101*, 2751-2796; Kim, D.; Osuka, A. *Acc. Chem. Res.* **2004**, *37*, 735-745.

(5) de Witte, P. A. J.; Castriciano, M.; Cornelissen, J. J. L. M.; Scolaro, L. M.; Nolte, R. J. M.; Rowan, A. E. *Chem. Eur. J.* **2003**, *9*, 1775-1781.

(6) de Witte, P. A. J.; Hernando, J.; Neuteboom, E. E.; van Dijk, E. M. H. P.; Meskers, S. C. J.; Janssen, R. A. J.; van Hulst, N. F.; Nolte, R. J. M.; Garcia-Parajo, M. F.; Rowan, A. E. *J. Phys. Chem. B* **2006**, *110*, 7803-7812; Hernando, J.; de Witte, P. A. J.; van Dijk, E. M. H. P.; Korterik, J.; Nolte, R. J. M.; Rowan, A. E.; Garcia-Parajo, M. F.; van Hulst, N. F. *Angew. Chem., Int. Ed.* **2004**, *43*, 4045-4049.

(7) Schwartz, E.; Palermo, V.; Finlayson, C. E.; Huang, Y.-S.; Otten, M. B. J.; Liscio, A.; Trapani, S.; González-Valls, I.; Brocorens, P.; Cornelissen, J. J. L. M.; Peneva, K.; Müllen, K.; Spano, F.; Yartsev, A.; Westenhoff, S.; Friend, R. H.; Beljonne, D.; Nolte, R. J. M.; Samori, P.; Rowan, A. E. *Chem. Eur. J.* **2009**, *15*, 2536-2547.

(8) Millich, F. *Chem. Rev.* **1972**, *72*, 101-113; Millich, F. *Advances in Polymer Science* **1975**, *19*, 117-41; Drenth, W.; Nolte, R. J. M. *Acc. Chem. Res.* **1979**, *12*, 30-35; Nolte, R. J. M. *Chem. Soc. Rev.* **1994**, *23*, 11-19; Takei, F.; Yanai, K.; Onitsuka, K.; Takahashi, S. *Angewandte Chemie, International Edition in English* **1996**, *35*, 1554-1556; Takahashi, S.; Onitsuka, K.; Takei, F. *P Jpn Acad B-Phys* **1998**, *74*, 25-30; Amabilino, D. B.; Ramos, E.; Serrano, J.-L.; Sierra, T.; Veciana, J. *J. Am. Chem. Soc.* **1998**, *120*, 9126-9134; Hasegawa, T.; Kondoh, S.; Matsuura, K.; Kobayashi, K. *Macromolecules* **1999**, *32*, 6595-6603; Cornelissen, J.; Rowan, A. E.; Nolte, R. J. M.; Sommerdijk, N. *Chem. Rev.* **2001**, *101*, 4039-4070; Yamada, Y.; Kawai, T.; Abe, J.; Iyoda, T. *J. Polym. Sci., Part A: Polym. Chem.* **2002**, *40*, 399-408; Suginome, M.; Ito, Y. *Adv. Polym. Sci.* **2004**, *171*, 77-136; Kajitani, T.; Okoshi, K.; Sakurai, S. I.; Kumaki, J.; Yashima, E. *J. Am. Chem. Soc.* **2006**, *128*, 708-709; Amabilino, D. B.; Serrano, J. L.; Sierra, T.; Veciana,

J. *J. Polym. Sci., Part A: Polym. Chem.* **2006**, *44*, 3161-3174; Kajitani, T.; Okoshi, K.; Yashima, E. *Macromolecules* **2008**, *41*, 1601-1611.

(9) Cornelissen, J. J. L. M.; Donners, J. J. J. M.; de Gelder, R.; Graswinckel, W. S.; Metselaar, G. A.; Rowan, A. E.; Sommerdijk, N. A.; Nolte, R. J. M. *Science* **2001**, *293*, 676-80; Samori, P.; Ecker, C.; Goessl, I.; de Witte, P. A. J.; Cornelissen, J. J. L. M.; Metselaar, G. A.; Otten, M. B. J.; Rowan, A. E.; Nolte, R. J. M.; Rabe, J. P. *Macromolecules* **2002**, *35*, 5290-5294.

(10) Schwartz, E.; Kitto, H. J.; de Gelder, R.; Nolte, R. J. M.; Rowan, A. E.; Cornelissen, J. J. L. M. *J. Mater. Chem.* **2007**, *17*, 1876-1884.

(11) Kaiser, H.; Lindner, J.; Langhals, H. *Chem. Ber.* **1991**, *124*, 529-535.

(12) Nagao, Y.; Naito, T.; Abe, Y.; Misono, T. *Dyes and Pigments* **1996**, *32*, 71-83.

(13) Assumption based on the absence of acetylene stretching frequency in the IR spectrum and acetylene proton in the ^{1}H NMR spectrum.

(14) Bekiranov, S.; Bruinsma, R.; Pincus, P. *Phys Rev E* **1997**, *55*, 577-585.

(15) Sivakumar, K.; Xie, F.; Cash, B. M.; Long, S.; Barnhill, H. N.; Wang, Q. *Organic Letters* **2004**, *6*, 4603-4606.

(16) Zlokarnik, G.; Negulescu, P. A.; Knapp, T. E.; Mere, L.; Burres, N.; Feng, L. X.; Whitney, M.; Roemer, K.; Tsien, R. Y. *Science* **1998**, *279*, 84-88.

(17) Berlman, I. *Handbook of Fluorescence Spectra of Aromatic Molecules*; 2nd ed.; Academic Press: New York, 1971.

(18) Hatzakis, N. S.; Engelkamp, H.; Velonia, K.; Hofkens, J.; Christianen, P. C. M.; Svendsen, A.; Patkar, S. A.; Vind, J.; Maan, J. C.; Rowan, A. E.; Nolte, R. J. M. *Chem. Commun.* **2006**, 2012-2014.

(19) Che, Y. K.; Datar, A.; Balakrishnan, K.; Zang, L. *J. Am. Chem. Soc.* **2007**, *129*, 7234-7235.

6

Water soluble azido polyisocyanopeptides as functional β-sheet mimics[§]

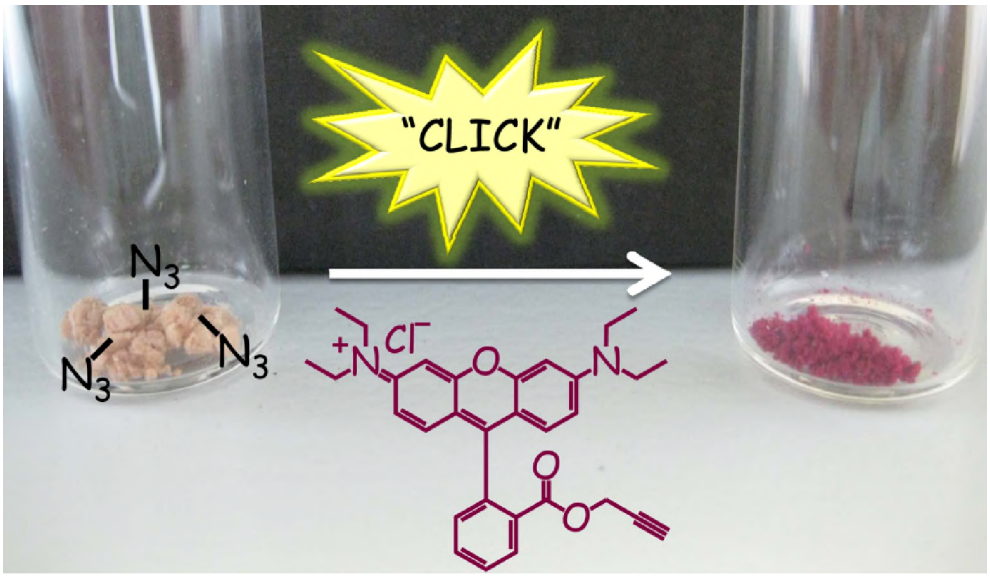

[§]Parts of this work have been published: Schwartz, E.; Koepf, M.; Kitto, H. J.; Espelt-Ripoll, M.; Nebot-Carda, V.J.; de Gelder, R.; Nolte, R. J. M.; Cornelissen, J. J. L. M.; Rowan, A. E. *Journal of Polymer Chemistry: Part A: Polymer Science* **2009**, *16*, 4150-4163.

6.1 Introduction

To synthesise water soluble polymers which retain a stable hydrogen bonding secondary structure in water, and can still be readily functionalized remains a major challenge in polymer chemistry. As a biomimetic scaffold we use polyisocyanides[1] which possess a unique polymer backbone that adopts a rigid helical conformation, which is stabilised by steric interaction induced by bulky side chains or π-π stacking and/or hydrogen bonding between the side groups. The use of specific noncovalent interactions to stabilize the conformation of polyisocyanides was initially reported by Cornelissen et al.[2] When introducing peptide substituents into the side chains, it was found that a strong intramolecular hydrogen bonding network could be formed, which stabilised the native helical structure of the backbone. The side groups of the growing chain are involved in a 4_1 helix, in which the stacked peptide chains at positions n and (n+4) have a distance of ~4.6 Å. This results in a β-sheet arrangement of the hydrogen bonds between the side groups, and consequently in a strong stabilisation of the helical structure of these polymers.[2] Polyisocyanides that possess these hydrogen bonding arrays are, therefore, a very attractive scaffold to which functional groups can be attached to give well-defined arrays, thus giving the opportunity to develop new materials with unique properties.[3] Recently we demonstrated that by polymerisation of an acetylenic dipeptido-isocyanide,[4,5] a well-defined rigid polymer can be obtained onto which a wide variety of azide-functionalised groups can be quantitatively grafted using the Cu(I)-catalysed Huisgen 1,3-dipolar coupling.[6] This very robust, efficient, versatile and highly selective chemical reaction, typically known as 'click chemistry', has been applied in both synthetic (in)organic chemistry as well as in polymer chemistry and offers an easy route towards elaborate materials.[7] To date, the post-modification of polymers using the Cu(I) catalysed click reaction has been carried out mainly with nonchiral materials, with only a few examples of click chemistry on optically active polymers having been described.[8] Recently, Yashima and co-workers used the click reaction to modify azido functionalised helical poly(phenylacetylenes) with acetylenes.[9] In this way optically diverse active poly(phenylacetylene)s can be obtained. Our approach to the post-modification of polymers makes use of helical polyisocyanides bearing acetylene moieties (Chapter 3 & 4), is less suitable for water soluble clicking due to the hydrophobic nature of the acetylenic homopolymer and the lower solubility of the acetylene compounds.

As consequence we choose to invert the approach and introduce azide groups onto the polymer backbone for post modification with acetylene-containing compounds. In order to enhance the water solubility of these polymers a second monomer was incorporated containing a terminal ester bond, resulting in a statistical copolymer consisting of both azide and ester functionalised isocyanopeptides. It was shown previously that polymers containing this latter function can be saponified to give water soluble helical polymers.[2] The synthesis

and properties of these aforementioned azide containing homo- and the water soluble helical β-sheet co-polymers, and their post-modification with acetylenic chromophores is presented in this chapter.

6.2 Results & Discussion

The synthesis of the azide functionalised polyisocyanopeptide **P1** is outlined in Scheme 1. Starting from 3-azidopropanol, obtained upon the reaction of sodium azide with 3-bromopropanol, and Boc-L-alanine-OH, the azido derived alanine **1** was obtained in 60% yield. Removal of the Boc protecting group of **1**, followed by EDC coupling with Boc-L-alanine-OH gave the dipeptide **2**. The treatment of **2** with acid to remove the protecting group and the subsequent heating at reflux of the amine salt in ethyl formate and sodium formate gave in 65% yield the formylated dialanine **3**. Using the procedure developed by Skorna and Ugi[10] dehydration of **3** resulted in isocyanide **4**. Purification of the isocyanide by column chromatography and subsequent recrystallisation gave monomer **4**. The single X-ray structure of compound **4** was obtained, confirming the expected structure, stereochemistry and revealing a hydrogen bonding network between the stacked isocyanide molecules in the solid state (Figure 1).

The polymerisation of **4** with 1/30 equivalents of $Ni(ClO_4)_2 \cdot 6H_20$ in CH_2Cl_2 was monitored with Infrared spectroscopy (IR) and Circular Dichroism (CD). After the addition of the nickel catalyst to the monomer solution the isocyanide stretch at ν = 2135 cm^{-1}, which appeared as a shoulder on the azide stretch at ν = 2105 cm^{-1}, disappears. Concurrently, the NH stretching vibration shifts from ν = 3430 to ν = 3281 cm^{-1} and the amide I vibration from ν = 1689 to ν = 1660 cm^{-1}. These shifts are indicative of the formation of a hydrogen bonding network between the side arms of the polymer; albeit that the latter shift is less pronounced.

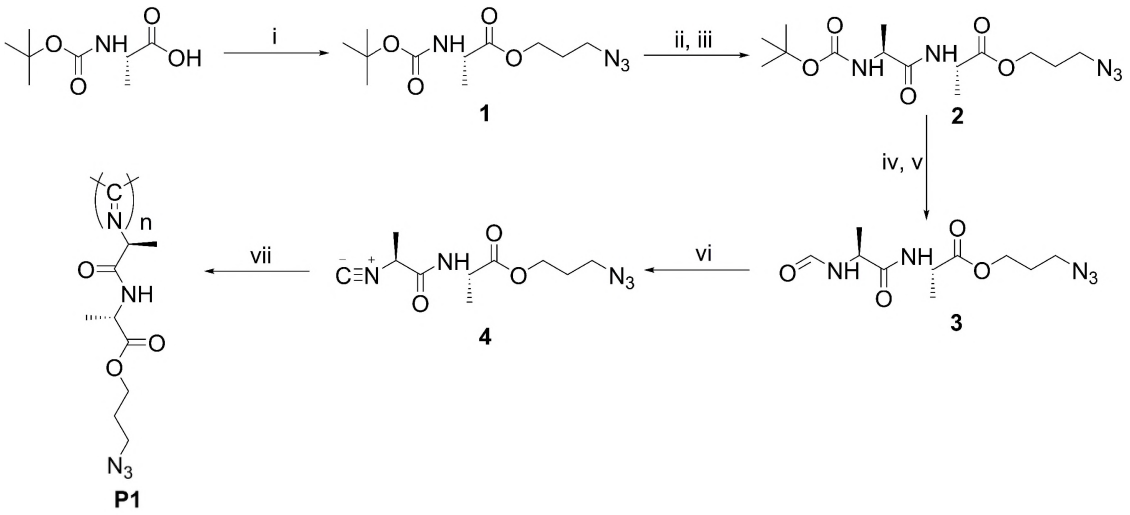

Scheme 1. Synthesis of polyisocyanide **P1**. (i) EDC, HOBt, 3-azidopropanol, CH_2Cl_2 (59%); (ii) EtOAc·HCl; (iii) EDC, HOBt, Boc-L-alanine-OH, DIPEA, CH_2Cl_2 (76%); (iv) EtOAc·HCl; (v) $NaHCO_2$, HCO_2Et, reflux (65%); (vi) N-methylmorpholine, diphosgene, CH_2Cl_2, –30°C (49%); (vii) $Ni(ClO_4)_2{\cdot}6H_2O$, CH_2Cl_2 (42%).

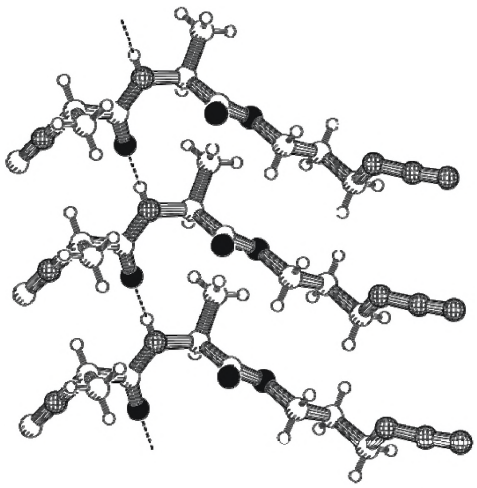

Figure 1. X-ray structure of three stacked hydrogen bonding molecules of monomer **4** showing the stereochemistry of the monomer and the azide end group.

The vibrational shifts observed in the infrared spectrum upon formation of polymer **P1** are somewhat smaller, than those of poly(L-isocyanoalanyl-L-alanine methyl ester)[2] and those of the acetylene functionalised polymer (poly(L-isocyanoalanyl-L-alanine propynol ester).[4] This observation implies that interactions between the azide side groups may partially disrupt the hydrogen bonding of **P1** and results in a polymer with a slightly less defined architecture.[11] This decreased helical definition is also reflected in the nature of the CD signal observed during the polymerisation reaction of **4**. A negative Cotton effect was seen around λ = 290 nm, whereas the simple poly(L-isocyanoalanyl-L-alanine methyl ester showed a positive signal at λ = 310 nm of much greater intensity upon polymerisation.[2] For

polyisocyanopeptides, this (strong) Cotton effect is assumed to originate from the ordering of amides, thereby creating a large permanent dipole that influences the n-π* transition of the imine chromophore.[12] It would seem that although incorporation of dipeptidoazides into the polyisocyanopeptides was successful, the azido group appears to have a significant electronic/steric effect on the architecture of the polymer in solution leading to a different hydrogen bonding arrangement of the amide groups as evidenced by the spectroscopic studies of **P1**.

Since a prerequisite of the material design was that a well-defined scaffold was required our attention was directed towards polymers **P2** and **P3** (Scheme 2). These polymers have a similar molecular structure to **P1**, except 3-azidopropyl amine was used instead of 3-azidopropanol. Starting from 3-azidopropane amine results in monomers containing two amide linkages which can both be involved in intramolecular hydrogen bonding after polymerisation. The presence of two hydrogen bonding networks within the polymers chains leads to an enhanced rigidity of these polymers[13] and hopefully to a well-defined architecture of the polymer. The polymer was built up stepwise, by the Boc-protection chemistry strategy, allowing the construction of the LL (**P2**) and DL (**P3**) polymers.

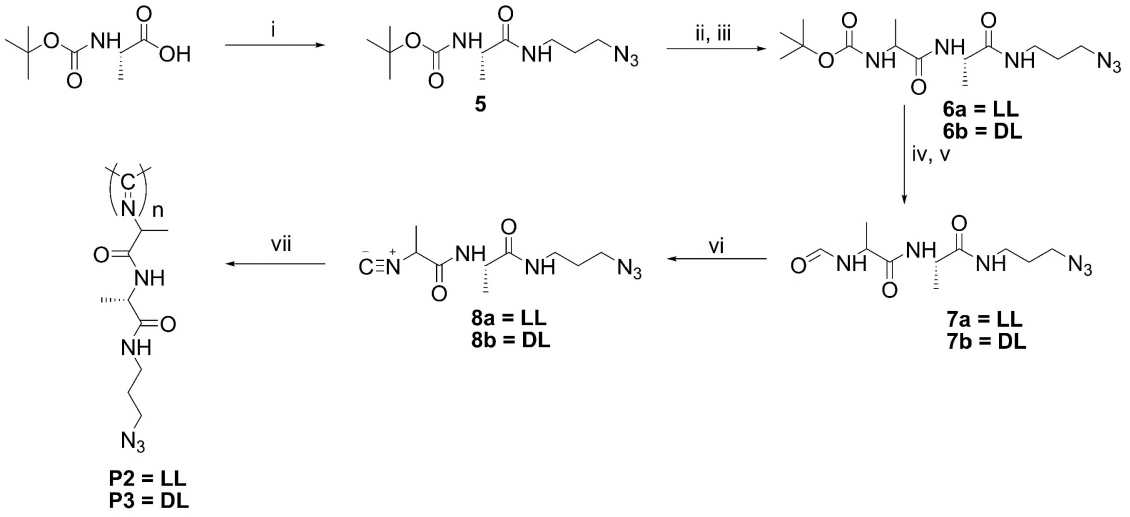

Scheme 2. Synthesis of polyisocyanides **P2** and **P3**. (i) EDC, HOBt, 3-azidopropane amine, CH_2Cl_2 (66%); (ii) EtOAc·HCl; (iii) EDC, HOBt, Boc- L(or D)-Ala-OH, DIPEA, CH_2Cl_2 (**6a**: 51%; **6b**: 76%); (iv) EtOAc·HCl; (v) $NaHCO_2$, HCO_2Et, reflux (**7a**: 64%; **7b**: 64%); (vi) N-methylmorpholine, diphosgene, CH_2Cl_2, –30ºC (**8a**: 20%; **8b**: 48%); (vii) $Ni(ClO_4)_2·6H_2O$, CH_2Cl_2 (**P2**: 70%).

The polymerisation of monomers **8a** and **8b** was again followed by IR and CD spectroscopies. Upon polymerisation of monomer **8a**, a single NH-stretching vibration at ν = 3300 cm^{-1} was visible for the polymer (Figure 2, top left) and the Amide I vibration shifted from ν = 1677 cm^{-1} to ν = 1640 cm^{-1}, which is similar to that seen for parallel-chain β-sheet (1637 cm^{-1}).[14]

These observed frequency shifts indicate a hydrogen bonding network in which the two amide bonds in **P2** are equivalent in strength. During the polymerisation of monomer **8a** to obtain **P2**, a positive cotton effect around λ = 310 nm arises in the CD spectrum after several minutes, indicated by the black arrow in Figure 2. After the initial 10 minutes of the polymerisation reaction, a second change in the CD signal was observed (grey arrows in Figure 2, top right).

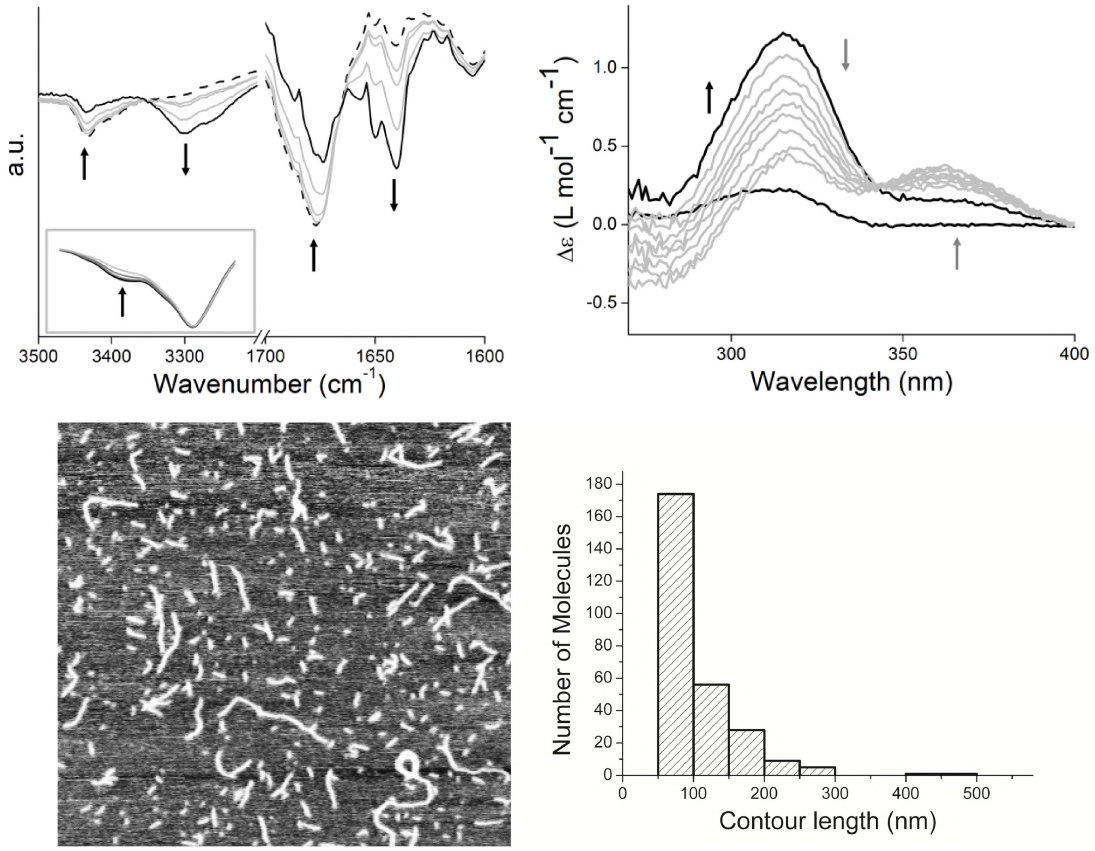

Figure 2. Polymerisation of **8a** monitored by infrared spectroscopy (inset shows the disappearance of the isocyanide stretch at ν = 2133 cm^{-1} , which appears as a shoulder on the large azide stretch vibration; arrows indicate the decreasing or increasing signals (top left) and Circular Dichroism (black arrow indicates initial changes; grey arrows point to the second series of changes (top right). Atomic Force Micrograph of polymer **P2** and (bottom left) the histogram of the contour lengths (bottom right). From these plots the degree of polymerisation (DP) = 870 and a weight-average apparent length (L_w) of 134 nm and a number average apparent length (L_n) of 103 nm were calculated.[16] Assuming a 4_1 type helix with a helical pitch of 0.46 nm (as measured by Powder X-ray diffraction of poly(L-isocyanoalanyl-L-alanine methyl ester)[2] these values[17] amount to a M_w of 293 kg/mol and a M_n of 226 kg/mol. This gives a polydispersity (PD) of 1.3 which is comparable with the PD measured for poly(L-isocyanoalanyl-L-alanine methyl ester) (1.4), indicating comparable initiation and propagation rates and thus similar control over the degree of polymerisation.

The signal at λ = 310 nm was found to decrease and simultaneously a positive effect around λ = 360 nm became visible. This behaviour has been previously observed and is thought to

originate from a change in the arrangement of the side arms from the well-organised kinetic product to a more stable arrangement in which an alternative hydrogen bond network is formed, involving the second amide, which is no longer predominantly between side chain *n* and (n+4).[4,11,15]

Since it is not possible to determine the molecular weights of the polyisocyanides by Gel Permeation Chromatography (GPC) or Maldi-TOF (ms) due to the rod like nature of the polyisocyanides, AFM was used to determine the molecular weight (Figure 2). Analysis of several AFM images resulted in a M_w 293 kg/mol for **P2**. We also investigated the diastereoisomer of **P2**, since the incorporation of D-alanine into the monomer is known to lead to a more stable molecular arrangement of the polymer.

The CD and IR spectroscopic data during the polymerisation of **8b** are depicted in Figure 3. From the IR plots of the polymerisation it is clearly visible that for **P3** the NH-stretch vibration is split, indicating that in this polymer there are two unique amide groups which are non-equivalent in hydrogen bonding strength. The extent to which the NH-stretching frequency shifts towards lower wavenumbers correlates with the hydrogen bonding strengths. The amide I and amide II vibrations shift to lower and higher wavenumbers, respectively. The NH stretch at ν = 3430 cm^{-1} in the monomer shifts to lower wavenumbers in the polymer (ν = 3295 cm^{-1} and ν = 3255 cm^{-1}). The observed NH stretch shift is comparable with polyisocyanoalanyl-alanine methyl esters.[2] It was proposed that in poly(L-isocyanoalanyl-D-alanine methyl ester) the hydrogen bonding is stronger than for poly(L-isocyanoalanyl-L-alanine methyl ester) as a result of negative steric interactions between the first alanine methyl group in the side chain *n* with the second alanine methyl group in side chain *n+1* (Figure 3, top). The differences between the observed spectra of **P2** and **P3** could also be explained based upon these postulated interactions. When the hydrogen bonding between the amide closest to the polymer backbone (A in Figure 3, top) increases, the angle between the *n* and the *n +4* side chain increases and makes the distance between the amide at the periphery (B in Figure 3, top) too large to form strong and stable hydrogen bonds.[22] In Figure 3 (bottom) the changes in the secondary structure, as monitored by CD spectroscopy are shown. At first a strong negative cotton effect is observed, as expected for the polymerisation of a DL-isocyanodialanine (black arrow in Figure 3, bottom). This effect disappears and concomitantly a broad positive effect around λ = 290 nm and a negative effect around λ = 360 nm appears (grey arrow). Similar changes are also seen for **P2**, however for **P3** the process is considerably faster (several minutes for **P3** compared to hours for **P2**). The dotted arrow indicates the final change observed in the CD spectrum and most likely arises from the slow precipitation of the polymer from solution.

The insolubility of **P3**, which is a result of its increased stiffness, also hampered further investigations of the polymer by additional characterisation techniques.[18] Overall, the azide functionalised polyisocyanopeptides described above have a surprisingly different architecture when compared to their methyl and acetylene analogues. Apparently, a homopolymer of azido functionalised isocyanopeptides leads to a less-defined overall polymer architecture. This is tentatively ascribed to the charge repulsion effects between the azide groups in the beta-sheets and needs further investigations.

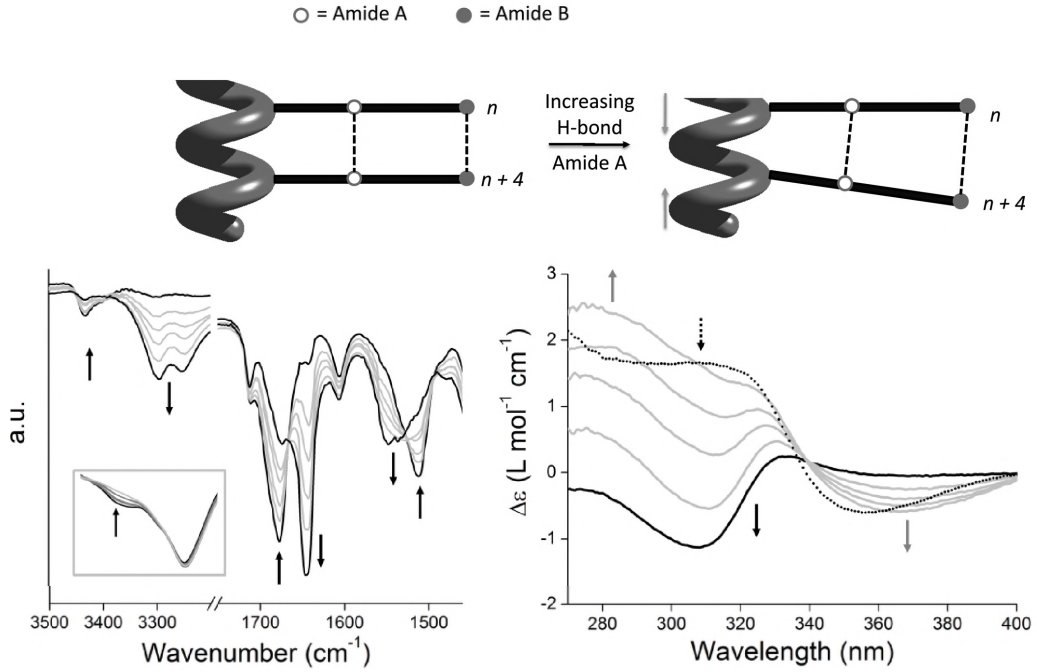

Figure 3. Schematic representation of hydrogen bond strength. Polymerisation of **8b** monitored by infrared spectroscopy (top left) (inset shows the disappearance of the isocyanide stretch, which is a shoulder on the large azide stretch vibration; arrows indicate the decreasing or increasing signals. CD spectra monitored in time during the formation of polymer **P3** with 1/30 equiv of Ni(II) and (black arrow indicates initial changes (kinetic structure); grey arrows point to the second series of changes (thermodynamic structure) and dotted arrow to the final change) (bottom right)

All three polymers described above, disappointingly, do not display the characteristics of a really well-defined hydrogen bonding network. The goal was to obtain a polymer with a precise architecture containing an array of azide groups which could be post-modified by click chemistry. The proposed repulsion of the azide group could be overcome by diluting the polymer with another isocyanide, whilst retaining the helical structure. Therefore we copolymerised monomer **8b** and D-isocyanoalanyl-L-alanine methyl ester (Scheme 3) to give polymer **P4**.[5,19] This creates a polymer with a well-defined architecture containing two amide hydrogen bonding networks, in which the methyl ester can be further saponified to give a water soluble polymer possessing azido groups, which can then be post-functionalised.

Using a monomer ratio of 30:1 D-isocyanoalanyl-L-alanine methyl ester: **8b**, respectively) and a $Ni(ClO_4)_2 \cdot 6H_2O$ catalyst ratio of 0.02% the statistical copolymer **P4** was obtained in reasonable yield (80%). As expected, the CD spectrum of **P4** shows a strong negative Cotton effect around λ = 310 nm pointing to a well-defined hydrogen bonding network similar to the methyl and acetylene analogues (Figure 4, left).[20] In the Infrared spectrum of the polymer, the presence of the azide absorption at ν = 2105 cm^{-1} confirmed the successful incorporation of monomer **8b** into the polymer. The shifts of the NH (ν = 3295 cm^{-1}) and amide I (1656 cm^{-1}) stretching vibrations, as compared to those of the monomer indicate the existence of a hydrogen bonding network comparable to poly(D-isocyanoalanyl-L-alanine methyl ester).

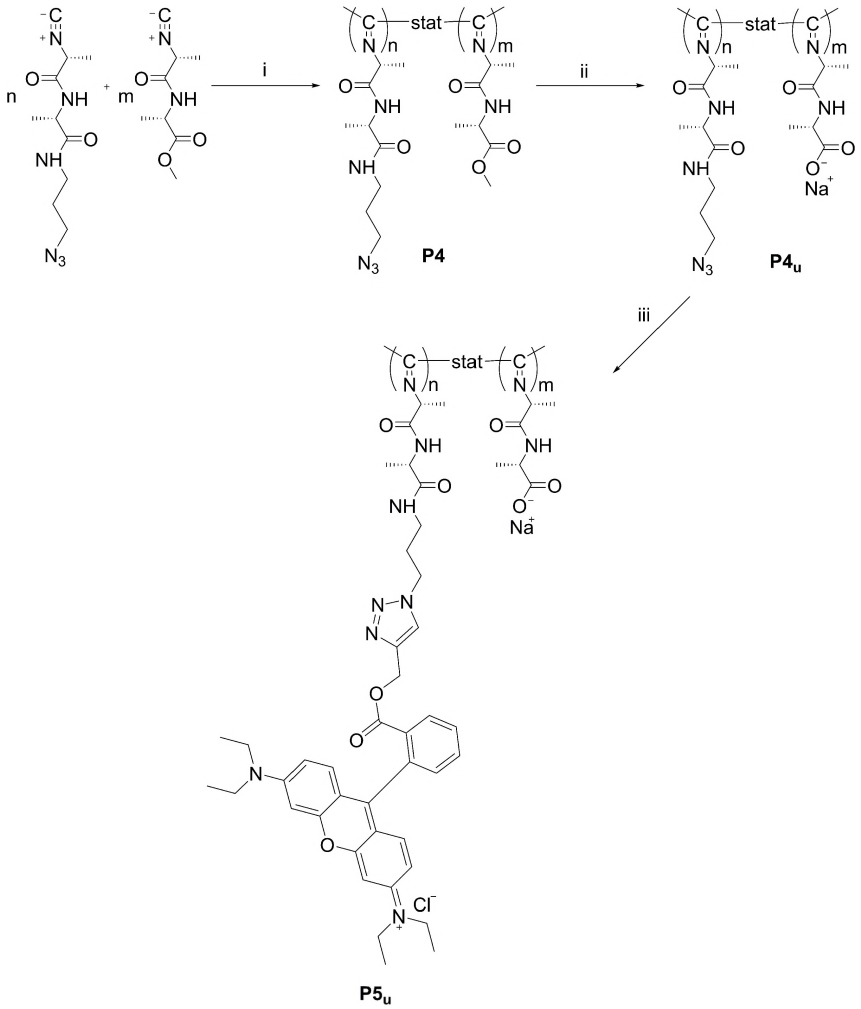

Scheme 3. Synthesis of polyisocyanide **P5u**. (i) $Ni(ClO_4)_2 \cdot 6H_2O$, CH_2Cl_2 (70%); (ii) NaOH, H_2O (80%); (iii) $CuSO_4$, ascorbic acid sodium salt, rhodamine dye **10**, (Tris((1-((O-ethyl)carboxymethyl)-(1,2,3-triazole-4-yl))methyl)amine **11** (68%).

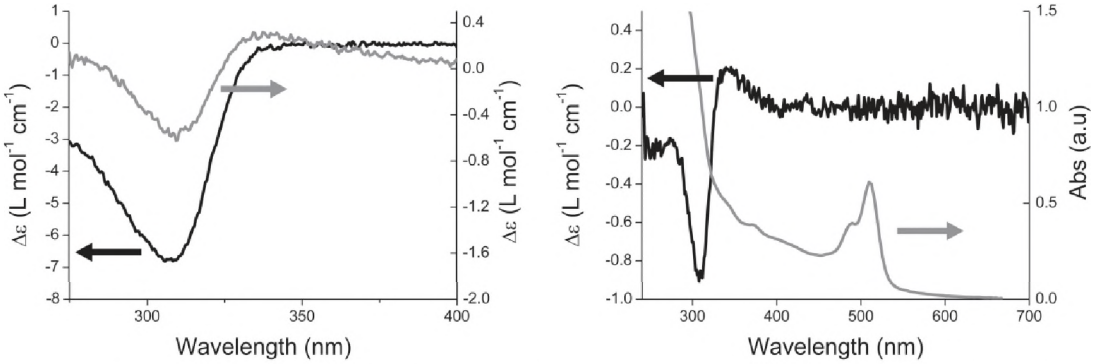

Figure 4. (a) CD spectra of **P4** in $CHCl_3$ (~10^{-3} M, black line) and **P4**$_u$ in H_2O (~10^{-3} M, grey line). (b) CD (~10^{-3} M, black line) and UV (~10^{-4} M, grey line) spectra of **P5**$_u$, respectively.[21]

Since the β-helical polymer poly(D-isocyanoalanyl-L-alanine methyl ester) is known to retain its secondary structure in an aqueous solution after removal of the ester functions in the side chain,[2] we used a similar approach to hydrolyse polymer **P4**. Following the procedure developed by Cornelissen and co-workers, **P4** was hydrolysed by stirring the polymer in aqueous 0.5 M NaOH (9 mL) at 37 °C until a clear solution was obtained (3 days). After dialysis and subsequent freeze-drying, the water soluble polymer **P4**$_u$ was obtained as a fluffy powder. Infrared spectroscopy confirmed the presence of the carboxylate group and the azide moiety, which is not affected by the hydrolysis (Figure 5). The CD spectrum of **P4**$_u$ showed a negative cotton effect around λ = 310 nm, similar to **P4**, albeit with a smaller intensity, which was also observed for the hydrolysed polymer of poly(D-isocyanoalanyl-L-alanine methyl ester and might indicate some partial unfolding of the helix during the hydrolysis for an extensive time or may also be a change in CD due the polarity of the solvent (Figure 4,left, grey line). The resulting water-soluble polyisocyanopeptide possesses a well-defined architecture characteristic of poly(D-isocyanoalanyl-L-alanine methyl ester) as concluded by IR and CD. Polymer **P4**$_u$ was functionalised by click chemistry with an acetylene functionalised rhodamine **10** (Scheme 3). The excess of compound **10** was removed by dialysis against an aqueous 5% NaCl solution, until the dialysis solution was colourless and then further dialysed against mQ water to remove the excess of NaCl. Analysis by IR, UV-Visible, Fluorescence, and CD spectroscopies revealed that the click reaction was successful. The IR spectrum of the polymer showed the disappearance of the azide vibration and the absence of the acetylene vibration of the rhodamine dye.

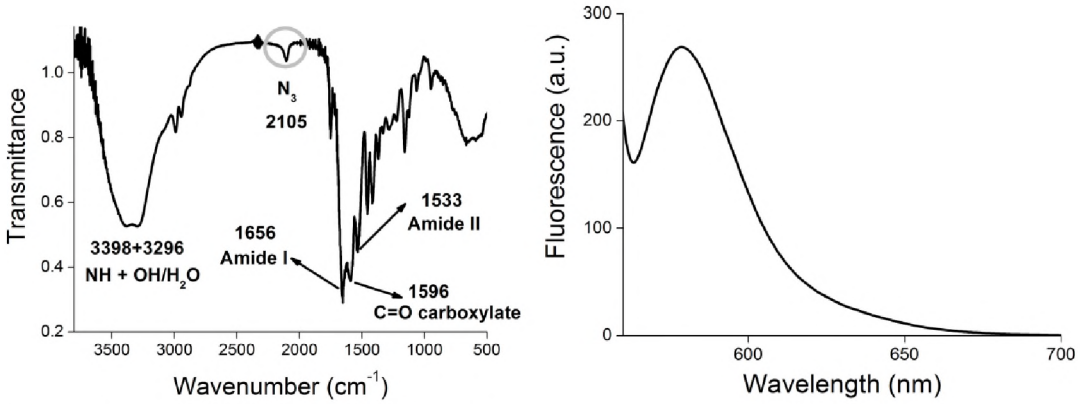

Figure 5. IR spectrum of polymer **P4$_u$** showing the N_3 absorbance at 2105 cm^{-1}(left) and Fluorescence spectrum of polymer **P5$_u$** (λ_{exc} = 539 nm; λ_{em} = 579 nm; ~10^{-6} M in H_2O) (right).

The UV-Visible spectrum of polymer **P5$_u$** showed the characteristic profile of a rhodamine dye, that is vibronic bands of the S_0-S_1 optical transition at λ = 539 and 559 nm (Figure 4, right). The fluorescence spectrum of **P5$_u$** showed a broad emission with a maximum at λ = 579 nm as expected (Figure 5). The CD spectrum showed that **P5$_u$** has the same characteristic Cotton effect as **P4** and **P4$_u$** at λ = 310 nm indicating a well-defined polymer (Figure 4, right). Due, however, to the relatively strong dilution of the chromophores on the polyisocyanopeptide scaffold, no chiral interactions between the rhodamine side groups were observed, and hence no cotton effect was observed around 540–560 nm.

6.3 Conclusion

Polyisocyanopeptides bearing azide functionalities have been successfully synthesised. These homopolymers showed a hydrogen bonding network in the side chain, although the hydrogen bonding strength was somewhat diminished as compared to related polyisocyanopeptides. Only in the case of statistical copolymers was a well-defined polymer obtained, as revealed by IR and CD spectroscopies. Hydrolysis of the statistical copolymer offered a functional water soluble polyisocyanide, in which the polymer has retained its hydrogen bonding network even in water forming functional β-sheet macromolecules. The post-modification of the water soluble polymer scaffold was achieved using an acetylene functionalised rhodamine dye. The CD spectrum of the resulting water soluble polymer dye displays a similar Cotton effect at λ = 310 nm as obtained for related polyisocyanopeptides. This route opens the way to use the polyisocyanide as effective water soluble scaffolds to which a variety of acetylene functionalised biomolecules can be added.[22]

6.4 Experimental

General

All solvents were distilled on $CaCl_2$ or sodium prior to use. All other chemicals were commercials products and used as received. Column chromatography was performed using silica gel (40–60 µm) purchased from Merck. TLC-analyses were carried out on silica 60 F_{254} coated glass from Merck and the compounds were visualised using Ninhydrine, $KMnO_4$ or $Ni(ClO_4)_2 \cdot 6H_2O$ in EtOH. ^1H NMR and ^{13}C NMR spectra were recorded on a Bruker AC-300 MHz instrument operating at 300 MHz and 75 MHz respectively, unless otherwise stated. FT-infrared spectra were recorded on a ThermoMattson IR300 spectrometer equipped with a Harrick ATR unit and the compounds were measured as a solid or an oil. KBr and liquid IR spectra were recorded on a Bruker Tensor 27. Mass spectrometry measurements were performed on a JEOL Accutof instrument (ESI) or Thermo LCQ. Optical rotations were measured on a Perkin Elmer 241 Polarimeter at room temperature and are reported in 10^{-1} deg cm^2 g^{-1}. UV-Visible spectra were recorded on a Varian Cary 50 spectrometer and fluorescence spectra on a Perkin Elmer Luminescence spectrometer LS50B. AFM measurements of the polymer **P2** for analysis of the length were prepared using 10^{-6} M solutions of **P2** in $CHCl_3$ spin-coated (1600 RPM) onto freshly cleaved Muscovite Mica. All AFM images were recorded on Multimode IV microscope controlled with a NanoscopeIII controller (Digital Instruments, Santa Barbara CA) operating in tapping mode in air at room temperature with a resolution of 512 × 512 pixels using moderate scan rates (1–2 lines/sec.). Commercial tapping-mode tips (NSG10, NT-MDT) were used with a typical resonance frequency around 300 kHz. Length and heights were evaluated using image recognition software "Scanning Adventure" developed by Jaques Barbet. All values derived from AFM data presented in this paper carry an error notated as the standard deviation of the values from different measurements sessions. CD spectra were recorded on a Jasco 810 instrument equipped with a Peltier temperature control unit. Elemental analyses were carried out on a Carlo Erba 1180 instrument. The isocyanide monomer **4** could be recrystallised from diethyl ether, offering crystals suitable for X-ray analysis. A single crystal was mounted in air on a glass fibre. Intensity data were collected at -65 degrees C. A Nonius KappaCCD single-crystal diffractometer was used (ϕ and ω scan mode) using graphite monochromated Mo-Kalpha radiation. Unit cell dimensions were determined from the angular setting of 50 reflections. Intensity data were corrected for Lorentz and polarisation effects. SADABS multiscan correction was applied[23]. The structure was solved by the program CRUNCH[24] and was refined with standard methods using SHELXL97[25] with anisotropic parameters for the nonhydrogen atoms. All hydrogens were placed at calculated positions and were refined riding on the parent atoms. A PLUTON[26] drawing is shown in Figure 1. Dialysis tubing (regenerated cellulose membrane) with a molecular cut-off (MWCO) of 3.5 (used for $\mathbf{P4_u}$) and 1 kDa (used for $\mathbf{P5_u}$) was obtained from Spectra/Por.

Crystal data for **4**: translucent colourless, $C_{10}H_{15}N_5O_3$, M = 253.27, monoclinic, space group P21, a = 4.8734(3), b = 10.3977(10), c = 12.8583(5) Å, α = 90, β = 90.233(4), γ = 90°, U = 651.55(7) $Å^3$, T = 208(2) K, Z = 2, µ(Mo-Kα) = 0.092 mm^{-1}, 9832 reflections measured, 2279 unique (R_{int} = 0.0546), final R1 0.0535, wR2 0.0728 (I › 2σ(I)).

Synthesis

The synthesis of the tris coordinating ligand (Tris((1-((O-ethyl)carboxymethyl)-(1,2,3-triazole-4-yl))methyl)amine (tris-triazole ligand **11**) was synthesised according to literature procedures.[27]

Boc-L-alanine azidopropyl ester 1

Sodium azide (23.5 g, 361.2 mmol, 5 equiv) and 3-bromopropanol (10.1 g, 72.8 mmol) were dissolved in DMF (100 ml). The reaction mixture was heated to 100 °C and stirred for 72 hours, after which time the white

precipitate was filtered off. To the filtrate DMF (100 mL), Boc-L-Alanine (15.3 g, 80.6 mmol, 1.1 equiv), HOBt (10.7 g, 79.4 mmol, 1.1 equiv), DIPEA (14 ml, 78.8 mmol, 1.1 equiv) and EDC (15.3 g, 79.8 mmol 1.1 equiv) were added. After stirring for 10 hours, the solvent was evaporated *in vacuo* and the product was dissolved in $CHCl_3$ (200 mL). This solution was subsequently washed with an aqueous 10% (w/w) citric acid solution (2 × 200 mL), H_2O (200 mL), an aqueous 10 % (w/w) sodium carbonate solution (2 × 200 mL) and H_2O (200 mL). The organic layer was dried (Na_2SO_4), concentrated and subjected to column chromatography (1% MeOH in $CHCl_3$), yielding 59% of **1** as a slightly yellow oil. $[\alpha]_D$ ($CHCl_3$, *c* 1.6) = –5. ^{1}H NMR (δ ppm, $CDCl_3$, 300 MHz): 5.03 (br, 1H, NH), 4.25 (m 1H, CH Ala), 4.19 (t, 2H, OCH_2, *J* = 3.2 Hz), 3.38 (t, 2H, CH_2, *J* = 6.6 Hz), 1.90 (qn, 2H, CH_2, *J* = 12 Hz), 1.42 (s, 9H, $C(CH_3)_3$), 1.36 (d, 3H, CH_3, *J* = 7.2 Hz). ^{13}C NMR (δ ppm, $CDCl_3$, 75 MHz): 172.8, 154.6 (C=O), 84.6 ($C(CH_3)_3$), 61.6 (CH_2O), 48.7 (CH Ala), 47.5 (N_3CH_2), 27.6 ($C(CH_3)_3$), 27.6 ($CH_2CH_2CH_2$), 18.0 (CH_3 Ala). IR (cm^{-1}, ATR): 3374 (NH), 2097 (N_3), 1740 (C=O, ester), 1709 (C=O, amide I), 1511 (amide II). MS-ESI: *m/z* = 295 $[M+Na]^+$. HRMS for $C_{11}H_{20}N_4O_4Na$: Calcd, 295.1369. Found, 295.1382.

Boc-L-alanyl-L-alanine azidopropyl ester 2

Boc-L-alanine-azidopropyl ester (11.6 g, 42.7 mmol) was dissolved in ethyl acetate (50 mL) and a solution of HCl-saturated ethyl acetate (50 mL) was added. The reaction mixture was stirred for 12 hours, when according to TLC (10% MeOH in $CHCl_3$), the starting material had been consumed. The solvent was partially evaporated and the excess HCl was removed by the addition of tert-butanol and subsequent evaporation. The resulting L-alanine azidopropyl ester HCl salt was dissolved in CH_2Cl_2 (200 mL). To this solution Boc-L-alanine (9.2 g, 44.6 mmol, 1.05 equiv), HOBt (6.7 g, 49.4 mmol, 1.1 equiv), DIPEA (17 ml, 95.6 mmol, 2.2 equiv) and EDC (9.5 g, 49.7 mmol, 1.1 equiv) were added. After stirring for 12 hours, the solvent was evaporated *in vacuo* and the product was dissolved in $CHCl_3$ (150 mL). This solution was washed with an aqueous 10% (w/w) citric acid solution (2 × 150 mL), H_2O (150 mL), an aqueous 10 % (w/w) sodium carbonate solution (2 × 150 mL) and H_2O (150 mL). The organic layer was separated, dried (Na_2SO_4), concentrated, and subjected to column chromatography (0.5 % MeOH in $CHCl_3$), yielding **2** in 76% yield as a colourless oil. $[\alpha]_D$ ($CHCl_3$, *c* 0.88) = –22. ^{1}H NMR (δ ppm, $CDCl_3$, 300 MHz): 6.79 (br, 1H, NH), 5.13 (d, 1H, NH, *J* = 7.5 Hz), 4.51 (m, 1H, CH Ala), 4.20 (m, 3H, CH Ala + OCH_2), 3.37 (t, 2H, NCH_2, *J* = 6.6 Hz), 1.89 (m, 2H, CH_2), 1.41 (s, 9H, $C(CH_3)$), 1.35 (q, 6H, CH_3 Ala, *J* = 6.9Hz). ^{13}C NMR (δ ppm, $CDCl_3$, 75 MHz): 172.1, 171.9, 155.0 (C=O), 79.5 ($C(CH_3)_3$), 61.8 (OCH_2), 49.5 (2CH Ala), 47.6 (NCH_2), 27.8 ($C(CH_3)_3$), 27.6 ($CH_2CH_2CH_2$), 17.8, 17.6 (CH_3 Ala). IR (cm^{-1}, ATR): 3313 (NH), 2097 (N_3), 1740 (C=O, ester), 1660 (C=O, amide I), 1520 (amide II). MS-ESI: *m/z* = 366 $[M+Na]^+$. HRMS for $C_{14}H_{25}N_5O_5Na$: Calcd, 366.1746. Found, 366.1753.

N-Formyl- L-alanyl-L-alanine azidopropyl ester 3

The Boc-protecting group of **2** (8.5 g, 24.9 mmol) was removed by dissolving the dipeptide in HCl-saturated ethyl acetate (150 mL). The mixture was stirred for 5 hours after which time the solvent was evaporated *in vacuo* and the excess HCl was removed by addition of *t*-BuOH/CH_2Cl_2 and subsequent evaporation. The resulting L-alanyl-L-alanine azidopropyl ester HCl salt was taken up in ethyl formate (200 mL) and sodium formate (7.0 g, 103.8 mmol, 4.2 equiv) was added. The mixture was stirred under reflux for 72 hours before the solid was filtered off and washed thoroughly with $CHCl_3$. The solvent was removed from the filtrate and the crude product was recrystallised from ethanol/diisopropyl ether to give 4.4 g (65%) of **3** as white crystals. Mp: 77 °C. $[\alpha]_D$ ($CHCl_3$, *c* 1.0) = –41. ^{1}H NMR (δ ppm, DMSO, 300 MHz): 8.41 (d, 1H, NH, *J* = 6.9 Hz), 8.26 (d, 1H, NH, *J* = 7.5 Hz), 7.97 (s, 1H, HCO), 4.40 (m, 1H, CH Ala), 4.26 (m, 1H, CH Ala), 4.11 (t, 2H, N_3CH_2, *J* = 6 Hz), 3.42 (t, 2H, CH_2O), 1.83 (m, 2H, $CH_2CH_2CH_2$), 1.30 (d, 3H, CH_3 Ala, *J* = 7.2 Hz), 1.22 (d, 3H, CH_3 Ala, *J* = 7.2 Hz). ^{13}C NMR (δ ppm, DMSO, 75 MHz): 172.9, 172.4 (C=O), 161.2 (C=O ester), 62.2 (CH_2), 48.3, 48.0, 46.9 (CH Ala/CH/N_3CH_2),

28.2 (CH_2), 19.0 (CH_3 Ala), 17.3 (CH_3 Ala). IR (cm^{-1}, ATR): 3292 (NH), 2099 (N_3), 1739 (C=O, ester), 1650 (C=O, amide I), 1536 (amide II). MS-ESI: *m/z* = 294 $[M+Na]^+$. HRMS for $C_{10}H_{17}N_5O_4Na$: Calcd, 294.1169. Found, 294.1178.

L-isocyanoalanyl-L-alanine azidopropyl ester 4

Compound **3** (1.0 g, 3.7 mmol) was dissolved in CH_2Cl_2 (400 mL) under an N_2 atmosphere and N-methyl morpholine (1.0 mL, 9.2 mmol, 2.5 equiv) was added. The resulting solution was cooled to –30 °C (acetone/dry ice) and diphosgene (0.37 mL, 1.85 mmol, 0.5 equiv) in CH_2Cl_2 (30 mL) was added drop wise over a period of 60 minutes, while the temperature was maintained at –30 °C. After complete addition of the diphosgene, the orange solution was warmed to 0 °C and an ice-cold saturated aqueous sodium bicarbonate solution (2 mL) was added and stirred vigorously for 10 minutes. The product was extracted with $CHCl_3$ (25 mL) and subsequently washed with an aqueous 10% (w/w) sodium bicarbonate solution. The organic layer was dried (Na_2SO_4) and evaporated *in vacuo* resulting in a yellow/orange oil. The product was purified using column chromatography (1% MeOH in $CHCl_3$) and recrystallised from diethyl ether to yield 458 mg (49 %) of white needles. Mp: 57 °C. $[\alpha]_D$ ($CHCl_3$, *c* 0.68) = 22. ^{1}H NMR (δ ppm, $CDCl_3$, 300 MHz): 6.88 (br, 1H, NH), 4.55 (m, 1H, CH Ala), 4.27 (s, 1H, CH Ala), 4.25 (s, 2H, OCH_2), 3.41 (t, 2H, NCH_2, *J* = 6.3Hz), 1.94 (t, 2H, CH_2 CH_2CH_2, *J* = 6Hz), 1.65 (d, 3H, CH_3 Ala, *J* = 6.9), 1.47 (m, 3H, CH_3 Ala). ^{13}C NMR (δ ppm, $CDCl_3$, 75 MHz): 172.5, 166.3 (C=O), 162.0 (CN), 63.3 (CH_2O), 53.9 (CH Ala), 49.2, 48.6 (CH/ N_3CH_2), 28.6 ($CH_2CH_2CH_2$), 20.17 (CH_3 Ala), 18.6 (CH_3 Ala). IR (cm^{-1}, ATR): 3332 (NH), 2137 (CN), 2099 (N_3), 1742 (C=O, ester), 1677 (C=O, amide I), 1535 (amide II). MS-ESI: *m/z* = 276 $[M+Na]^+$. HRMS for $C_{10}H_{15}N_5O_3Na$: Calcd, 276.1061. Found, 276.1073. El. Anal. Calcd. for $C_{10}H_{15}N_5O_3$: C, 47.43; H, 5.97; N, 27.65. Found, C, 47.77; H, 6.06; N, 27.11.

Poly(L-isocyanoalanyl-L-alanine azidopropyl ester) P1

To a stirred solution of **4** (0.12 g, 0.40 mmol) in CH_2Cl_2 (1 mL) was added $Ni(ClO_4)_2{\cdot}6H_2O$ (0.03 equiv; 12.8 mL of a 1.15 mM CH_2Cl_2/EtOH (98/2 v/v) solution). The solution turned brown immediately and after 5 hours the solvent was evaporated off. The glassy solid was taken up in a minimal amount of $CHCl_3$ and the polymer precipitated out by dropping this solution into a MeOH/H_2O (50 mL (3:1 v/v)) solution with vigorous stirring. The product was filtered off and washed with MeOH/H_2O (3:1 v/v) and MeOH. Drying *in vacuo* gave the polymer as a brown solid in 42% yield (50 mg). $[\alpha]_D$ ($CHCl_3$, *c* 0.015) = –248°, ^{1}H NMR (δ ppm, $CDCl_3$, 300 MHz): 8.60 (br, NH), 4.15 (br, 2CH Ala), 3.63 (br, OCH_2), 3.40 (br, NCH_2), 1.90 (br, CH_2 CH_2CH_2), 1.38 (br, $2CH_3$). IR (cm^{-1}, ATR): 3292 (NH), 2109 (N_3), 1752 (C=O, ester), 1656 (C=O, amide I), 1538 (amide II).

Boc- L-alanine azidopropyl amide 5

Starting from 3-azido propyl amine and Boc-L-alanine-OH, following the same procedure as for **1**, compound **5** was obtained as a viscous colourless oil (overall yield 66%). $[\alpha]_D$ (CH_2Cl_2, *c* 2.0) = –28°. ^{1}H NMR (δ ppm, $CDCl_3$, 300 MHz): 6.99 (s, 1H, NH), 5.48 (d, 1H, NH, *J* = 7.2 Hz), 4.12 (m, 1H, CH Ala), 3.28 (m, 4H, CH_2), 1.72 (qn, 2H, $CH_2CH_2CH_2$, *J* = 6.6 Hz), 1.37 (s, 9H, $C(CH_3)_3$), 1.28 (d, 3H, CH_3 Ala, *J* =7.0 Hz). ^{13}C NMR (δ ppm, $CDCl_3$, 75 MHz): 173.2, 155.6 (C=O), 79.9 ($C(CH_3)_3$), 50.1 (CH Ala), 49.0 (N_3CH_2), 36.8 (CH_2NH), 28.7 ($CH_2CH_2CH_2$), 28.3 ($C(CH_3)_3$), 18.6 (CH_3 Ala). FT-IR (cm^{-1}, ATR): 3320 (NH), 2097 (N_3), 1691 (Amide I), 1540 (amide II). MS-ESI: *m/z* = 294 $[M+Na]^+$. HRMS for $C_{11}H_{21}N_5O_3Na$: Calcd, 294.1542. Found, 294.1560.

Boc-L-alanyl-L-alanine azidopropyl amide 6a

Starting from **5**, following the same procedure as for **2**, compound **6a** was obtained as a white solid in 51%. Mp: 158 °C. $[\alpha]_D$ (CH_2Cl_2, *c* 1.3) = –46°. ^{1}H NMR (δ ppm, $CDCl_3$, 300 MHz): 7.19 (m, 2H, NH), 5.49 (d, 1H, NH, *J* = 6 Hz),

4.46 (qn, 1H, CH Ala, *J* = 7.2 Hz), 4.15 (m, 1H, CH Ala), 3.27 (m, 4H, CH_2), 1.74 (qn, 2H, $CH_2CH_2CH_2$, *J* = 6.9 Hz), 1.39 (s, 9H, $C(CH_3)_3$), 1.31 (m, 6H, CH_3 Ala). ^{13}C NMR (δ ppm, $CDCl_3$, 50 MHz): 173.0, 172.5, 155.6 (C=O), 80.3 ($C(CH_3)_3$), 50.7 (CH Ala), 49.1 (N_3CH_2), 48.9 (CH Ala), 36.8 (CH_2NH), 28.6 ($CH_2CH_2CH_2$), 28.3 ($C(CH_3)_3$), 18.4, 18.3 (CH_3 Ala). FT-IR (cm^{-1}, ATR): 3276 (NH), 2095 (N_3), 1673, 1635 (Amide I), 1524 (amide II).MS-ESI: *m/z* = 365 $[M+Na]^+$. HRMS for $C_{14}H_{26}N_6O_4Na$: Calcd, 365.1913. Found, 365.1925.

Boc-D-alanyl-L-alanine azidopropyl amide 6b

Starting from **5**, following the same procedure as for **2**, compound **6b** was obtained as a white solid in 76 % yield. Mp: 98 °C. $[\alpha]_D$ (CH_2Cl_2, *c* 1.1) = –21 °. ^{1}H NMR (δ ppm, $CDCl_3$, 200 MHz): 7.24 (m, 2H, NH), 5.54 (d, 1H, NH, *J* = 6.2 Hz), 4.47 (qn, 1H, CH Ala, *J* = 7.2 Hz), 4.15 (qn, 1H, CH Ala, *J* = 6.8 Hz), 3.27 (m, 4H, CH_2), 1.74 (qn, 2H, $CH_2CH_2CH_2$, *J* = 6.7 Hz), 1.39 (s, 9H, $C(CH_3)_3$), 1.32 (m, 6H, CH_3 Ala). ^{13}C NMR (δ ppm, $CDCl_3$, 50 MHz): 173.2, 172.5, 155.7 (C=O), 80.2 ($C(CH_3)_3$), 50.6 (CH Ala), 49.1 (N_3CH_2, CH Ala), 36.9 (CH_2NH), 28.7 ($CH_2CH_2CH_2$), 28.3 ($C(CH_3)_3$), 18.3, 18.2 (CH_3 Ala). FT-IR (cm^{-1}, ATR): 3284 (NH), 2095 (N_3), 1647 (Amide I), 1524 (amide II). MS-ESI: *m/z* = 365 $[M+Na]^+$. HRMS for $C_{14}H_{26}N_6O_4Na$: Calcd, 365.1913. Found, 365.1929.

N-Formyl-L-alanyl-L-alanine azidopropyl amide 7a

Following a similar procedure as for **3**, compound **7a** was obtained in 64% yield as a white solid.

Mp: 174 °C. $[\alpha]_D$ (DMSO, *c* 0.90) = -31°. ^{1}H NMR (δ ppm, DMSO-D_6, 300 MHz):8.27 (d, 2H, NH, *J* = 7.2 Hz), 8.06 (d, 2H, NH, *J* = 7.5 Hz), 7.97 (s, 1H, HCO), 7.84 (t, 1H, NH, *J* = 5.7 Hz), 4.34 (qn, 1H, CH Ala, *J* = 7.2 Hz), 4.18 (qn, 1H, CH Ala, *J* = 7.2 Hz), 3.33 (m, 2H, CH_2), 3.11 (m, 2H, CH_2), 1.64 (qn, 2H, $CH_2CH_2CH_2$, *J* = 6.9 Hz), 1.19 (d, 6H, CH_3 Ala, *J* = 7.2Hz). ^{13}C NMR (δ ppm, $CDCl_3$, 75 MHz): 172.1, 171.5 (C=O), 160.9 (HCO), 48.4 (CH Ala), 48.3 (N_3CH_2), 46.9 (CH Ala), 35.8 (CH_2NH), 28.3 ($CH_2CH_2CH_2$), 18.3, 18.1 (CH_3 Ala). FT-IR (cm^{-1}, ATR): 3285 (NH), 2101 (N_3), 1662, 1628 (Amide I), 1550, 1527 (amide II). MS-ESI: *m/z* = 293 $[M+Na]^+$. HRMS for $C_{10}H_{18}N_6O_3Na$: Calcd, 293.1338. Found, 293.1335. El. Anal. Calcd. for $C_{10}H_{18}N_6O_3$: C, 44.44; H, 6.71; N, 31.09. Found, C, 44.27; H, 6.94; N, 30.84.

N-Formyl- D-alanyl-L-alanine azidopropyl amide 7b

Following a similar procedure as for **3**, compound **7b** was obtained in 54% yield as a white solid.

Mp: 165 °C. $[\alpha]_D$ (DMSO, *c* 0.77) = 1°. ^{1}H NMR (δ ppm, DMSO-D_6, 300 MHz): 8.34 (d, 2H, NH, *J* = 6.3 Hz), 8.25 (d, 2H, NH, *J* = 7.5 Hz), 7.97 (s, 1H, HCO), 7.83 (t, 1H, NH, *J* = 5.4 Hz), 4.30 (qn, 1H, CH Ala, *J* = 6.9 Hz), 4.17 (qn, 1H, CH Ala, *J* = 7.2 Hz), 3.32 (t, 2H, CH_2, *J* = 6.9 Hz), 3.11 (m, 2H, CH_2), 1.65 (qn, 2H, $CH_2CH_2CH_2$, *J* = 6.6 Hz), 1.20 (d, 3H, CH_3 Ala, *J* = 7.2Hz), 1.19 (d, 3H, CH_3 Ala, *J* = 6.9 Hz). ^{13}C NMR (δ ppm, $CDCl_3$, 75 MHz): 172.0, 171.7 (C=O), 161.1 (HCO), 48.4 (CH Ala), 48.3 (N_3CH_2), 47.3 (CH Ala), 35.9 (CH_2NH), 28.4 ($CH_2CH_2CH_2$), 18.4, 18.0 (CH_3 Ala). FT-IR (cm^{-1}, ATR): 3277 (NH), 2096 (N_3), 1666, 1633 (Amide I), 1555, 1526 (amide II). MS-ESI: *m/z* = 293 $[M+Na]^+$. HRMS for $C_{10}H_{18}N_6O_3Na$: Calcd, 293.1338. Found, 293.1339. El. Anal. Calcd. for $C_{10}H_{18}N_6O_3.0.5H_2O$: C, 43.00; H, 6.86; N, 30.09. Found, C, 42.89; H, 6.68; N, 29.85.

L-isocyanoalanyl-L-alanine azidopropyl amide 8a

Following a similar procedure as for **4**, compound **8a** was obtained in 20% yield as a white solid.

Mp: 125 °C. $[\alpha]_D$ ($CHCl_3$, *c* 0.55) = –10°. ^{1}H NMR (δ ppm, $CDCl_3$, 300 MHz): 6.96 (s, 1H, NH), 6.03 (s, 1H, NH), 4.37 (qn, 1H, CH Ala, *J* = 6.9 Hz), 4.25 (q, 1H, CH Ala, *J* = 7.2 Hz), 3.38 (m, 4H, CH_2), 1.81 (qn, 2H, $CH_2CH_2CH_2$, *J* = 6.6 Hz), 1.66 (d, 3H, CH_3 Ala, *J* = 7.2 Hz), 1.44 (d, 3H, CH_3 Ala, *J* = 7.2 Hz). ^{13}C NMR (δ ppm, $CDCl_3$, 75 MHz): 171.5, 166.3 (C=O), 161.6 (CN), 53.3 (CH Ala), 49.5 (N_3CH_2), 49.4 (CH Ala), 37.5 (CH_2NH), 28.7 ($CH_2CH_2CH_2$), 19.8, 18.5 (CH_3 Ala). FT-IR (cm^{-1}, ATR): 3300, 3265 (NH), 2155, 2133 (CN), 2103 (N_3), 1690, 1636 (Amide I), 1545 (amide II).

MS-ESI: *m/z* = 275 $[M+Na]^+$. HRMS for $C_{10}H_{16}N_6O_2Na$: Calcd, 275.1232. Found, 275.1247. El. Anal. Calcd. for $C_{10}H_{16}N_6O_2$: C, 47.61; H, 6.39; N, 33.31. Found, C, 47.37; H, 6.39; N, 33.26.

D-isocyanoalanyl-L-alanine azidopropyl amide 8b

Following a similar procedure as for **4**, compound **8a** was obtained in 48% yield as a white solid.
Mp: 136 °C. $[\alpha]_D$ ($CHCl_3$, *c* 0.53) = –29°. ^{1}H NMR (δ ppm, $CDCl_3$, 300 MHz): 6.98 (d, 1H, NH, *J* = 5.7 Hz), 6.09 (s, 1H, NH), 4.39 (qn, 1H, CH Ala, *J* = 7.2 Hz), 4.17 (q, 1H, CH Ala, *J* = 7.2 Hz), 3.39 (m, 4H, CH_2), 1.81 (qn, 2H, $CH_2CH_2CH_2$, *J* = 6.3 Hz), 1.77 (d, 3H, CH_3 Ala, *J* = 6.9 Hz), 1.44 (d, 3H, CH_3 Ala, *J* = 7.2 Hz). ^{13}C NMR (δ ppm, $CDCl_3$, 75 MHz): 171.6, 166.4 (C=O), 161.4 (CN), 53.4 (CH Ala), 49.5 (N_3CH_2), 49.4 (CH Ala), 37.4 (CH_2NH), 28.7 ($CH_2CH_2CH_2$), 19.9, 18.6 (CH_3 Ala). FT-IR (cm^{-1}, ATR): 3280 (NH), 2142 (CN), 2099 (N_3), 1648 (Amide I), 1554 (amide II). MS-ESI: *m/z* = 275 $[M+Na]^+$. HRMS for $C_{10}H_{16}N_6O_2Na$: Calcd, 275.1232. Found, 275.1254. El. Anal. Calcd. for $C_{10}H_{16}N_6O_2.0.5H_2O$: C, 45.97; H, 6.56; N, 32.16. Found, C, 46.08; H, 6.37; N, 32.11.

Poly(L-isocyanoalanyl-L-alanine azidopropyl amide) P2

Following a similar procedure as for **P1**, polymer **P2** was obtained from the polymerisation of **8a** in 70% yield as a brown powder.
$[\alpha]_D$ ($CHCl_3$, *c* 0.02) = –117°. ^{1}H NMR (δ ppm, $CDCl_3$, 300 MHz): 9.25 (br, 1H, NH), 5.4–4.3 (br, 2H, CH Ala), 3.6–3.0 (br, 4H, CH_2), 2–0.9 (br, 8H, CH_3 Ala, CH_2). FT-IR (cm^{-1}, ATR): 3296, 3258 (NH), 2093 (N_3), 1649 (Amide I), 1534 (amide II).

Poly(D-isocyanoalanyl-L-alanine azidopropyl amide) P3

This polymer was prepared as described for polymer **P2** (starting from monomer **8b**), resulting in the precipitation of insoluble **P2.** FT-IR (cm^{-1}, ATR): 3281 (NH), 2095 (N_3), 1645 (Amide I), 1532 (amide II). Since the polymer was highly insoluble, no further characterisation data could be obtained.

Poly(D-isocyanoalanyl-L-alanine azidopropyl amide)-*statistical*-Poly(D-isocyanoalanyl-L-alanine methyl ester) P4

To a stirred solution of D-isocyanoalanyl-L-alanine methyl ester (110 mg, 0.60 mmol) and **8b** (5 mg, 0.020 mmol, 0.03 equiv) in CH_2Cl_2 (2 ml) was added $Ni(ClO_4)_2{\cdot}6H_2O$ (0.02 equiv; 10.9 mL of a 1.14 mM CH_2Cl_2 /EtOH (98/2 v/v) solution). The solution turned red/brown immediately and after 12 hours the solvent was evaporated off. The glassy solid was taken up in a minimal amount of $CHCl_3$ and the polymer precipitated out by dropping this solution into MeOH/H_2O (100 mL (3:1 v/v)) with vigorous stirring. The product was filtered off and washed extensively with MeOH. Drying *in vacuo* gave the polymer as an off-white solid in 70% yield.
[?]$_D$ ($CHCl_3$, *c* 0.03) = –384°. ^{1}H NMR (δ ppm, $CDCl_3$, 300 MHz): 9.4 (br, 3H, NH), 5.4–4.3 (br, 4H, CH Ala), 3.6–3.0 (br, 6H, CH_2, OCH_3), 2–0.6 (br, 14H, CH_3 Ala, CH_2). FT-IR (cm^{-1}, ATR): 3256 (NH), 2098 (N_3), 1743 (C=O ester), 1654 (Amide I), 1614 (C=N), 1527 (amide II).

N-(6-(diethylamino)-9-(2-((prop-2-ynyloxy)carbonyl)phenyl)-3H-xanthen-3-ylidene)-N-ethylethanaminium chloride (rhodamine 10)

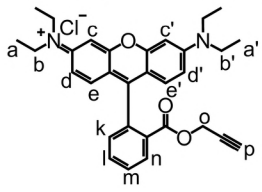

To a solution of rhodamine B (1.0 gr, 2.1 mmol) in acetonitrile (100 ml) was added EDC (420 mg, 2.2 mmol) and the reaction mixture was stirred for 5 min at room temperature. Propargyl alcohol (350 ul, 6.1 mmol, 3 equiv.) and DMAP (24 mg, 0.2 mmol, 0.1 equiv.) were subsequently added to the reaction mixture which was then stirred for 4 hours. The solvent was evaporated and the crude product was purified

by column chromatography (Acetone / CH_2Cl_2 1: 4 v/v to 4:1). The product was eluted with 10% MeOH in CH_2Cl_2 to give 387 mg of **10** as a red / purple powder (38%). ^{1}H NMR (δ ppm, $CDCl_3$, 300 MHz): 8.30 (dd, 1H, n, J_1 = 7.8 Hz, J_2 = 1.2 Hz), 7.83 (dt, 1H, l, J_1 = 7.5 Hz, J_2 = 1.2 Hz), 7.73 (dt, 1H, m, J_1 = 7.8 Hz, J_2 = 1.5 Hz), 7.32 (dd, 1H, k, J_1 = 7.5 Hz, J_2 = 0.9 Hz), 7.04 (d, 2H, c,c', J = 9.3 Hz), 6.89 (dd, 2H, d,d', J_1 = 9.6 Hz, J_2 = 2.4 Hz), 6.81 (d, 2H, e,e', J = 2.7 Hz), 4.60 (d, 2H, o, J = 2.7 Hz), 3.63 (q, 8H, b,b', J = 7.2 Hz), 2.40 (tr, 1H, p, J = 2.7 Hz), 1.29 (tr, 12H, a,a', J = 7.2 Hz). ^{13}C NMR (δ ppm, $CDCl_3$, 75 MHz):163.8 (C=O), 157.6, 157.3, 155.1, 133.3, 133.0, 131.0, 130.7, 130.0, 129.9, 128.7, 113.9, 113.1, 95.9 (CH aromatic), 76.8 ($CH_2C{\equiv}C$), 75.1 ($CH_2C{\equiv}C$), 52.4 ($CH_2C{\equiv}C$), 45.7 (CH_2CH_3), 12.2 (CH_2CH_3). FT-IR (cm^{-1}, ATR): 2171 (C=N$^+$), 2118 (C≡C), 1722 (C=O), 1586 (C=C). MS-ESI: *m/z* = 481.4 $[M\text{-}Cl]^+$ Calcd. $C_{31}H_{33}N_2O_3$: 481.3.

Poly (D-isocyanoalanyl-L-alanine azidopropyl amide)-*statistical*-Poly (D-isocyanoalanyl-L-alanine sodium carboxylate) P4$_u$

The water soluble polyisocyanide **P4$_u$** was obtained by stirring **P4** (45 mg) in aqueous NaOH (9mL, 0.5 M) at a temperature of 37 °C until a clear solution was obtained (3 days). The brown solution was dialysed against three changes of Milli-Q (24 hours per change) and subsequently freeze-dried to yield 36 mg (80%) of a brown fluffy powder. ^{1}H NMR (δ ppm, D_2O, 300 MHz): 8.5 (br, 3H, NH), 4.8–3.9 (br, 4H, CH Ala), 3.4–3.2 (br, 2H, CH_2), 2.1–0.5 (br, 16H, CH_3 Ala, CH_2). IR (cm^{-1}, KBr): 3500–3200 (OH, H_2O), 3296 (NH), 2105 (N_3), 1656 (Amide I), 1601 (C=O carboxylate), 1533 (amide II).

Polymer P5$_u$

To a solution of **P4$_u$** (10.9 mg, 56 mmol) and rhodamine **10** (1.33 mg, 2.37 mmol, 0.04 equiv; i.e. 1.27 equiv compared to available amount of azides in polymer **P4$_u$**) in H_2O/CH_3CN (6 mL (3/1 v/v)) was added a $CuSO_4$/ ligand **11**/ascorbic acid solution (444 µL (this solution was prepared from a 1 mL H_2O solution of $CuSO_4$ (2.09 mg, 8.3 µmmol) and ascorbic acid (11.53 mg, 58 mmol; 7 equiv compared to $CuSO_4$) by taking 222 µL (in total 1.84 µmmol $CuSO_4$) and adding it to 222 µL of ligand **11** in CH_3CN (3.6 µmmol) and the mixture was stirred for 12 hours. The red solution was dialysed against three changes of an aqueous 5% EDTA solution (3 hours per change) followed by dialysis against three changes of an aqueous 10% NaCl solution (24 hours per change) and finally dialysed against Milli-Q (8 hours) until the dialysis solution was colourless. The polymer solution was freeze-dried to yield 8 mg (68%) of a red fluffy powder.

^{1}H NMR (δ ppm, D_2O, 300 MHz): Broad signals at 8.4, 7.6, 7.0, 6.9 (NH, triazole, aromatic rhodamine), 4.5–3.9 (br, 4H, CH Ala), 3.6–3.4 (br, 2H, CH_2), 1.9–1 (br, 16H, CH_3 Ala, CH_2). IR (cm^{-1}, KBr): 3500-3200 (OH, H_2O), 3257 (NH), 1657 (Amide I), 1596 (C=O carboxylate), 1530 (amide II). UV-Visible (H_2O): λ_{max} (ε) = 530 (651), 560 (1002, mol^{-1} L cm^{-1}). Fluorescence (H_2O, λ_{exc} = 559 nm): λ_{max} = 579.[21]

6.5 References & Notes

(1) Nolte, R. J. M. *Chem. Soc. Rev.* **1994**, *23*, 11-19; Suginome, M.; Ito, Y. *Adv. Polym. Sci.* **2004**, *171*, 77-136; Otten, M. B. J.; Metselaar, G. A.; Cornelissen, J. J. L. M.; Rowan, A. E.; Nolte Roeland, J. M. In *Foldamers: Structure, Properties, and Applications*; Hecht, S., Huc, I., Eds.; Weinheim: Wiley-VCH: 2007.

(2) Cornelissen, J. J. L. M.; Donners, J. J. J. M.; de Gelder, R.; Graswinckel, W. S.; Metselaar, G. A.; Rowan, A. E.; Sommerdijk, N. A.; Nolte, R. J. M. *Science* **2001**, *293*, 676-80.

(3) Palermo, V.; Otten, M. B. J.; Liscio, A.; Schwartz, E.; de Witte, P. A. J.; Castriciano, M. A.; Wienk, M. M.; Nolde, F.; De Luca, G.; Cornelissen, J. J. L. M.; Janssen, R. A. J.; Mullen, K.; Rowan, A. E.; Nolte, R. J. M.; Samori, P. *J. Am. Chem. Soc.* **2008**, *130*, 14605-14614; Finlayson, C. E.; Friend Richard, H.; Otten, M. B. J.; Schwartz, E.; Cornelissen, J. J. L. M.; Rowan, A. E.; Samori, P.; Palermo, V.; Liscio, A.; Peneva, K.;

Mullen, K.; Trapani, S.; Beljonne, D. *Adv. Funct. Mater.* **2008**, *18*, 3947-3955; Schwartz, E.; Palermo, V.; Finlayson, C. E.; Huang, Y.-S.; Otten, M. B. J.; Liscio, A.; Trapani, S.; González-Valls, I.; Brocorens, P.; Cornelissen, J. J. L. M.; Peneva, K.; Müllen, K.; Spano, F.; Yartsev, A.; Westenhoff, S.; Friend, R. H.; Beljonne, D.; Nolte, R. J. M.; Samori, P.; Rowan, A. E. *Chem. Eur. J.* **2009**, *15*, 2536-2547.

(4) Schwartz, E.; Kitto, H. J.; de Gelder, R.; Nolte, R. J. M.; Rowan, A. E.; Cornelissen, J. J. L. M. *J. Mater. Chem.* **2007**, *17*, 1876-1884.

(5) Kitto, H. J.; Schwartz, E.; Nijemeisland, M.; Koepf, M.; Cornelissen, J. J. L. M.; Rowan, A. E.; Nolte, R. J. M. *J. Mater. Chem.* **2008**, *18*, 5615-5624.

(6) Tornoe, C. W.; Christensen, C.; Meldal, M. *J. Org. Chem.* **2002**, *67*, 3057-3064; Rostovtsev, V. V.; Green, L. G.; Fokin, V. V.; Sharpless, K. B. *Angew. Chem., Int. Ed.* **2002**, *41*, 2596-2599.

(7) Hawker, C. J.; Wooley, K. L. *Science* **2005**, *309*, 1200-1205; Binder, W. H.; Sachsenhofer, R. *Macromol. Rapid. Comm.* **2007**, *28*, 15-54; Lutz, J. F. *Angew. Chem., Int. Ed.* **2007**, *46*, 1018-1025; Dirks, A. J.; Cornelissen, J. J. L. M.; van Delft, F. L.; van Hest, J. C. M.; Nolte, R. J. M.; Rowan, A. E.; Rutjes, F. P. J. T. *Qsar Comb. Sci.* **2007**, *26*, 1200-1210; Nandivada, H.; Jiang, X. W.; Lahann, J. *Adv. Mater.* **2007**, *19*, 2197-2208; Fournier, D.; Hoogenboom, R.; Schubert, U. S. *Chem. Soc. Rev.* **2007**, *36*, 1369-1380; Meldal, M. *Macromol. Rapid. Comm.* **2008**, *29*, 1016-1051; Binder, W. H.; Sachsenhofer, R. *Macromol. Rapid. Comm.* **2008**, *29*, 952-981; Le Drournaguet, B.; Velonia, K. *Macromol. Rapid. Comm.* **2008**, *29*, 1073-1089; Johnson, J. A.; Finn, M. G.; Koberstein, J. T.; Turro, N. J. *Macromol. Rapid. Comm.* **2008**, *29*, 1052-1072; Lundberg, P.; Hawker, C. J.; Hult, A.; Malkoch, M. *Macromol. Rapid. Comm.* **2008**, *29*, 998-1015.

(8) Kumin, M.; Sonntag, L. S.; Wennemers, H. *J. Am. Chem. Soc.* **2007**, *129*, 466-467; Ikeda, M.; Hasegawa, T.; Numata, M.; Sugikawa, K.; Sakurai, K.; Fujiki, M.; Shinkai, S. *J. Am. Chem. Soc.* **2007**, *129*, 3979-3988.

(9) Kobayashi, S.; Itomi, K.; Morino, K.; Iida, H.; Yashima, E. *Chem. Commun.* **2008**, 3019-3021.

(10) Skorna, G.; Ugi, I. *Angew. Chem., Int. Ed.* **1977**, *16*, 259-260.

(11) Cornelissen, J. J. L. M. *Pure. Appl. Chem.* **2002**, *74*, 2021-2030.

(12) Cornelissen, J. J. L. M.; Graswinckel, W. S.; Adams, P. J. H. M.; Nachtegaal, G. H.; Kentgens, A. P. M.; Sommerdijk, N. A. J. M.; Nolte, R. J. M. *J. Polym. Sci., Part A: Polym. Chem.* **2001**, *39*, 4255-4264.

(13) Metselaar, G. A.; Adams, P. J. H. M.; Nolte, R. J. M.; Cornelissen, J. L. L. M.; Rowan, A. E. *Chem. Eur. J.* **2007**, *13*, 950-960.

(14) Bandekar, J.; Krimm, S. *Biopolymers* **1988**, *27*, 909-921; Bandekar, J.; Krimm, S. *Biophysical Journal* **1986**, *49*, A295-A295.

(15) In the case of **P2**, however, no λ = 290/360 couplet is observed, even after several hours. This couplet is usually observed for polyisocyanides that exhibit a less defined hydrogen bonding network. In the case of **P2** this couplet was only observed after work-up.

(16) Prokhorova, S. A.; Sheiko, S. S.; Moller, M.; Ahn, C. H.; Percec, V. *Macromol. Rapid. Comm.* **1998**, *19*, 359-366; Samori, P.; Ecker, C.; Goessl, I.; de Witte, P. A. J.; Cornelissen, J. J. L. M.; Metselaar, G. A.; Otten, M. B. J.; Rowan, A. E.; Nolte, R. J. M.; Rabe, J. P. *Macromolecules* **2002**, *35*, 5290-5294; Sheiko, S. S.; da Silva, M.; Shirvaniants, D.; LaRue, I.; Prokhorova, S.; Moeller, M.; Beers, K.; Matyjaszewski, K. *J. Am. Chem. Soc.* **2003**, *125*, 6725-6728.

(17) The molecular weight of the monomer unit is 252 g mol^{-1}. To estimate the molecular weight of the polymer 274 polymer fibers were selected and statistically analysed.

(18) Analogous to related D,L-isocyanopeptides, **8b** could also be polymerised by initiation of acid leading to polymers having the same chiroptical properties as those obtained with nickel catalysis. Since the polymerisation of **P3** with acid is slower as compared to the nickel catalysed polymerisation, the λ = 290/360 nm couplet is immediately observed and slowly diminish over time.

(19) Kamer, P. C. J.; Cleij, M. C.; Nolte, R. J. M.; Harada, T.; Hezemans, A. M. F.; Drenth, W. *J. Am. Chem. Soc.* **1988**, *110*, 1581-7; Hong, B.; Fox, M. A. *Macromolecules* **1994**, *27*, 5311-5317; King, R. B.; Borodinsky, L.; Greene, M. J. *J. Polym. Sci., Part A: Polym. Chem.* **1987**, *25*, 2165-2173; Deming, T. J.; Novak, B. M. *Macromolecules* **1991**, *24*, 326-328.

(20) Cornelissen, J. J. L. M.; Sommerdijk, N. A. J. M.; Nolte, R. J. M. *Macromol. Chem. Physic.* **2002**, *203*, 1625-1630.

(21) To calculate the Δε, the molecular weight of the monomer units used was based on the assumption that both monomers were 100% incorporated into the polymer. This would give a monomer molecular weight of 186 g mol^{-1} for **P4,** a monomer molecular weight of 195 g mol^{-1} for $\mathbf{P4_u}$ and a monomer molecular weight of 212 g mol^{-1} for $\mathbf{P5_u}$.

(22) Lutz, J. F.; Zarafshani, Z. *Adv. Drug Deliver Rev.* **2008**, *60*, 958-970.

(23) Sheldrick, G. M. (1996) *SADABS. Program for Emperical Absorption Correction*.

(24) de Gelder, R.; de Graaff, R. A. G.; Schenk, H. *Acta Crystallogr., Sect. A* **1993**, *49*, 287-293.

(25) Sheldrick, G.M. *SHELXL-97. Program for the refinement of crystal structures*, University of Gottingen: Germany, 1997.

(26) Spek, A.L. *PLATON, A Multipurpose Crystallographic Tool*, Utrecht University, Utrecht, The Netherlands, 2004.

(27) Chan, T. R.; Hilgraf, R.; Sharpless, K. B.; Fokin, V. V. *Organic Letters* **2004**, *6*, 2853-2855.

7

Self-trapped vibrational states in synthetic β-sheet helices observed by nonlinear infrared spectroscopy[§]

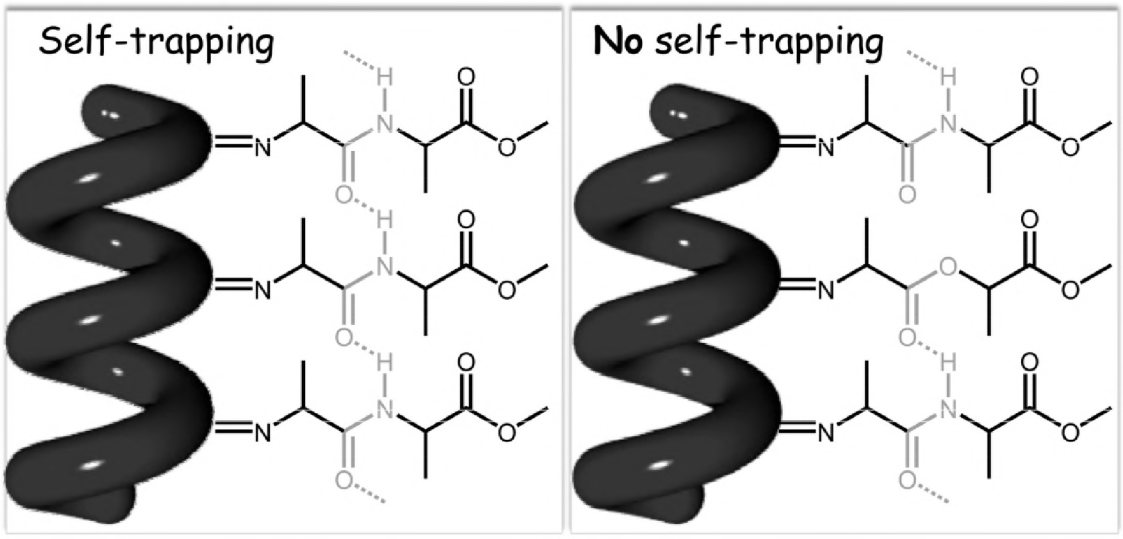

[§]Parts of this work have been published: Schwartz, E.; Bodis, P.; Koepf, M.; Cornelissen, J. J. L. M.; Rowan, A. E.; Woutersen, S.; Nolte, R. J. M. *Chem. Commun.* **2009**, 4675-4677; Bodis, P.; Schwartz, E.; Koepf, M.; Cornelissen, J. J. L. M.; Rowan, A. E.; Nolte, R.J. M.; Woutersen, S. *J. Chem. Phys.* **2009**, *131*, 124503.

7.1 Introduction

In 1973 Davydov hypothesised that the energy-transport mechanism in proteins and enzymes, which remains to this date largely unknown, may actually occur by a vibrational soliton mechanism.[1-3] It was suggested that in an α-helix, coupling between the amide I (CO-stretching) mode of the amide units and the NH···OC hydrogen bonds can lead to localisation (self-trapping) of vibrational energy. The vibrational excitation would then be accompanied by a local contraction of the hydrogen-bonded chain. This self-trapping makes it possible to transport the vibrational energy along the hydrogen-bonded chain in the form of a dispersionless wave packet, which would be spread out over only a few consecutive amide units in the hydrogen-bonded chain. As a consequence, the energy generated at one site of the protein could thus be transported to another site without any dispersion of the energy packet. [1-5]

In order to verify the soliton concept the amide I vibrational self-trapping has been extensively studied over the last decades in particular in crystalline acetanilide, a solid compound with a well-defined array of hydrogen bonds, often used as a model for α-helices.[4] Despite this considerable interest, to date only Hamm and co-workers have reported a direct observation of self-trapped vibrational states in an α-helix.[3] They observed self-trapping of the NH-stretch (rather than the amide I) mode in poly-γ-benzyl-L-glutamate. Using femtosecond infrared pump–probe spectroscopy Edler and Hamm could directly monitor the self-trapped vibrational states through their anharmonicity.[3] Upon excitation of the NH-stretching mode, two positive excited-state bands in the pump–probe response were observed, which were attributed to self-trapped NH-stretch excitations. Interestingly, the NH-stretch mode has an energy approximately equal to that of ATP→ADP conversion, relating it to the transport of energy in biological systems.

Here, we investigate whether NH-stretch self-trapping can also occur in ß-sheet structures.[6] To this purpose, we study the self-trapped vibrational states in synthetic β-sheet helices, i.e. polyisocyanopeptides. These helical polymers possess peptide side chains that form well-defined NH···OC hydrogen-bonded networks, which are arranged in the form of four ß-sheet type arrays along the polymer back bone. By engineering the structure of this polymer, i.e. by the inclusion of side arms without amide functions, the hydrogen-bonded NH···OC chain in which the self-trapping occurs can be readily modified without significantly changing the secondary structure allowing the self-trapping process to be more easily quantified. Polyisocyanides can be readily prepared by nickel(II) induced polymerisation of isocyanide monomers to give helical macromolecules.[7] The introduction of a chiral peptide substituent (e.g. L or D-alanine) as side chain both stabilizes the helix and induces a preferred helix handedness (Figure 1).[8]

Dipeptide derived polyisocyanides possess a highly defined rigid (persistent length of 76 nm)[9] secondary structure in which the side arms form the above mentioned β-sheet-like arrays of hydrogen bonds.

The resulting polymers are extremely stable and remain ordered even in competitive hydrogen bonding solvents such as methanol and DMSO. Disruption of the β-sheet network of the polymer is only possible by addition of strong acids, such as trifluoroacetic acid. This well-defined hydrogen bonding network and stiffness makes the helical polyisocyanopeptide ideal for the study of the NH-stretched self-trapped states using femtosecond vibrational pump-probe spectroscopy.[10] In order to further quantify the self-trapping states a statistical copolymer[11] has also been synthesised in which the hydrogen-bonding chain is interrupted. The copolymer allows one to manipulate the degree of connectivity of the hydrogen-bonded chain of NH moieties without changing the secondary structure.

In this chapter the synthesis of the (statistical) (co)polyisocyanides and their NH-stretch self-trapping are discussed. The complicated theoretical framework,[2] carried out using full quantum models and advanced mathematical methods[12] or semi-classical descriptions,[13] of the Davydov model will not be discussed in this chapter.[14]

7.2 Results & Discussion

To investigate vibrational self-trapping in β-sheet polymers, we measure the change in the NH-stretch absorption spectrum upon excitation of the NH-stretch mode. Upon excitation of the NH-stretch mode with a short (100 fs) infrared pulse (centre frequency 3260 cm^{-1}), the optical response can be observed using a time-delayed probing pulse which is detected in a frequency dispersed manner.[15] At first the pump-probe response (see experimental section) of the isocyanide LD-IAA, in which no self-trapping can occur, was measured (Figure 1). The grey curve shows the typical absorption spectrum of LD-IAA. At 3425 cm^{-1} the NH-stretch absorption band is shown, with a small splitting due to the presence of a conformer with a weak intramolecular hydrogen bond.[16] Upon resonantly exciting, under magic angle-polarisation conditions to eliminate the effects of orientational diffusion of the molecule,[17] the NH-stretch mode at 3425 cm^{-1} a clear absorption shift is visible (points in Figure 1). The transient absorption spectrum (Δα) is the regular response of an anharmonic oscillator.[18] The spectrum exhibits a negative Δα upon $\nu = 0 \rightarrow 1$ excitation of the NH-stretch mode, at the fundamental frequency due to ground state bleaching and stimulated emission ($\nu = 1 \rightarrow 0$) and a positive Δα peak at 3276 cm^{-1} due to $\nu = 1 \rightarrow 2$ excited state absorption. The –150 cm^{-1} anharmonic shift of the $\nu = 1 \rightarrow 2$ frequency with respect to the $\nu = 0 \rightarrow 1$ frequency is due to the

anharmonicity of the NH-stretch potential. The response is typical for normal vibrational excitations in which only a single-excited-state absorption peak is observed.[18]

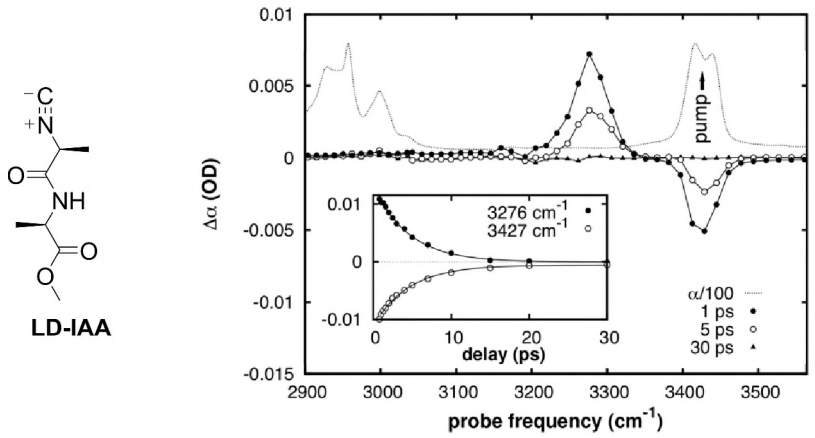

Figure 1. Molecular structure of LD-IAA and the transient absorption change in LD-IAA at different pump-probe delays (connected points). The thin grey line represents the conventional absorption spectrum. Inset: Delay dependence at two probing frequencies, showing the decay due to $\nu = 1 \rightarrow 0$ excited state population relaxation of the NH-stretch mode. The curves are least-squares of single-exponential decays with time constants of 4.5 ± 0.5 ps (3276 cm^{-1}) and 4.2 ± 0.4 ps (3427 cm^{-1}).

As evidenced from IR spectroscopy the amide I vibrations are shifted to lower wavenumbers upon polymerisation due to the hydrogen bonding network formed between amide groups in the side chains *n* and (*n* +4). The red shift of the NH-stretch frequency, as compared to the LD-IAA monomer, at 3260 cm^{-1} is close to the 3280 cm^{-1} observed in poly(L-alanine) β-sheets.[19] The response to the short (100 fs) infra red pulse (centre frequency 3260 cm^{-1}) is very different from that of the monomer, as can be seen in Figure 2. As for the monomer, a negative Δα at the fundamental frequency is observed in the transient absorption spectrum. There are, however, two positive Δα bands, where as in the monomer only one Δα band is observed. The identical delay (see inset) and polarisation[10] dependence implies that the two excited-state absorption peaks are both due to the NH-stretching mode (Figure 3). This anomalous response, is very similar to the one observed by Hamm and co-workers for self-trapped states in α-helices.[3] The two peaks represent absorptions of two-vibron bound states (TVBS) in which the vibrational energy is localised on a single NH-group, i.e. trapping of the vibrons at the same site, (TVBS-I) and on nearest-neighbouring NH-groups (TVBS-II), respectively.[3]

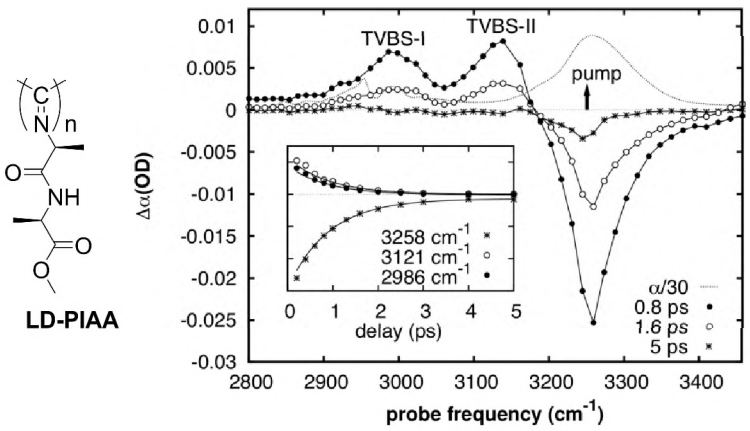

Figure 2. Transient absorption change of LD-PIAA upon NH-stretch excitation, at three delay times (see below). The thin curve represents the steady-state absorption spectrum. The inset shows the time dependence of the absorption change for three probing frequencies, together with least-squares-fitted exponential decays with time constants of 0.80±0.04 ps (3258 cm^{-1}), 0.78±0.11 ps (3121 cm^{-1}), and 0.73±0.05 ps (2986 cm^{-1}).

Using a displaced-oscillator model[2,20] the vibrational self-trapping can be described as follows. The NH-stretch mode of each amide unit is coupled to both of the hydrogen bonds connected to it and the couplings to these two hydrogen bonds are of comparable strength. Excitation of an amide group results in a contraction of both hydrogen bonds, because of the NH-stretch/hydrogen bond couplings (Figure 3). The hydrogen bond decreases in length and hence causes a lowering of the NH-stretch frequencies of the excited and of the two neighbouring NH groups. This effect can be seen as the vibrational analogue of a Stokes shift.[21] Because the NH-stretch frequency of the excited amide group is coupled to two contracting hydrogen bonds it lowers more than that of the two neighbouring amide groups, which are only coupled to one contracting hydrogen bond. This leads, upon excitation of the NH-stretch mode, to a red-shifted positive Δα band due to the amide unit with $\nu_{NH} = 1$ and a positive Δα band due to the two neighbouring NH groups.[13]

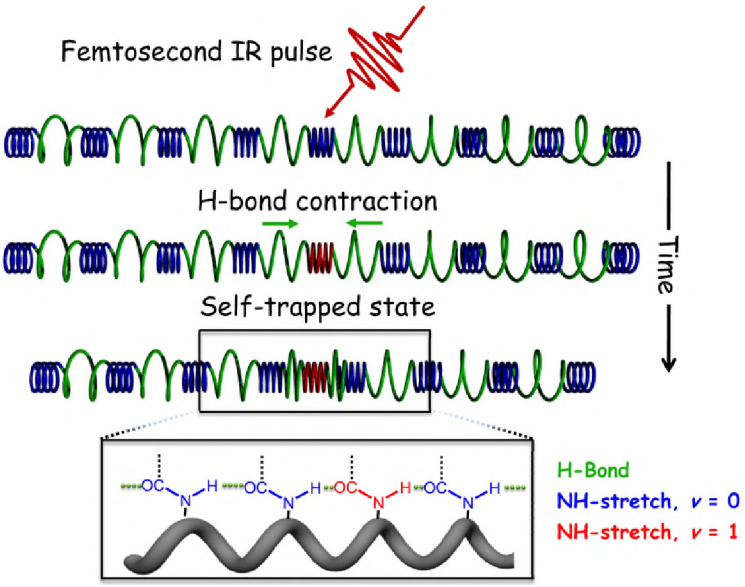

Figure 3. Schematic drawing of the vibrational self-trapping process. An ultrashort (100 fs) infrared pulse is used to resonantly excite an NH bond in the hydrogen-bonded chain to the v = 1 state. This causes contraction of the hydrogen bonds attached to the amide group, which in turn causes a lowering of the stretching frequency of the excited NH bond. The excited NH group is thus no longer in resonance with its neighbouring NH groups. This prevents delocalisation (hence 'traps') of the vibrational excitation.

To investigate if we could modify or change the self-trapping behaviour without influencing the secondary structure, the transient absorption change of a statistical copolymer, in which the hydrogen-bonding chain is interrupted, was also measured. It was presumed that this should lead to isolated NH moieties and consequently a low chance of two neighbouring NH groups interacting with each other. We chose to incorporate a non-hydrogen bonding isocyanide (with similarities to the bis-alanine derived isocyanide) instead of denaturing the secondary structure (by acid or high temperature)[3], as the latter method would change the overall conformation of the polymer and lead to a complex, inhomogeneously broadened infrared spectrum.

To disrupt the one-dimensional hydrogen bonding network in the side chain we initially focused on the incorporation of an N-methylated alanine unit in the isocyanopeptide. The synthesis of this non-hydrogen-bonding isocyanide was carried out by the conversion of Boc-L-*N*-methyl-Ala-OH into the corresponding L-*N*-methylalanine methyl ester HCl salt and subsequent coupling to Boc-D-ala-OH using 1-(3-dimethylaminopropyl)-3-ethyl carbodiimide hydrochloride (EDC) and 1-hydroxybenzatriazole (HOBt) to give **1** (Scheme 1). Removal of the Boc-protecting group of **1** with HCl gave the HCl salt **2** of the N-methylated dipeptide. Conversion into the formamide using similar conditions to previous work,[22] i.e., refluxing in ethyl formate in the presence of sodium formate, was, however, unsuccessful, as illustrated by the absence of the formyl proton and the complete disappearance of the methoxy protons in the ^{1}H NMR spectrum. Apparently, the *N*-methylated dipeptide had cyclised by

attack of the amine on the ester moiety via the Z-amide. Reaction of **2** using various conditions (0-4 equivalents of sodium formate, different temperatures, reaction with 2,4,5 trichloro phenyl formate, acetic anhydride / formic acid) give either the cyclised product or no product. The cyclisation was further confirmed by X-ray diffraction of crystals that were obtained by slow diffusion of diisopropylether into an ethanol solution of the obtained product, revealing the structure of the *cyclo*-alanyl-N-alanyl (**3**) (Figure 4). The formation of diketopiperazines is a known problem with N-methylated amino acids.[23] It can be prevented by switching to the tert-butyl ester derivative as illustrated by Wenger [24] (for MeLeu-MeVal-O^{t}Bu) and McDermott[25] (Ala-MeLeu-O^{t}Bu). The deprotection of *Cbz*-L-Ala-D-MeAla-O^{t}Bu **(4)** with Pd/H_2 followed by reaction of the liberated amine in ethyl formate, however, also resulted in the formation of a cyclised compound.[26] To avoid the diketopiperazine formation, N-formyl-Ala-OH can be coupled to an N-methylated alanine, although in this case there is the disadvantage of epimerisation due to an enhanced reactivity of the acid group. A successful coupling product could, however, not be obtained.

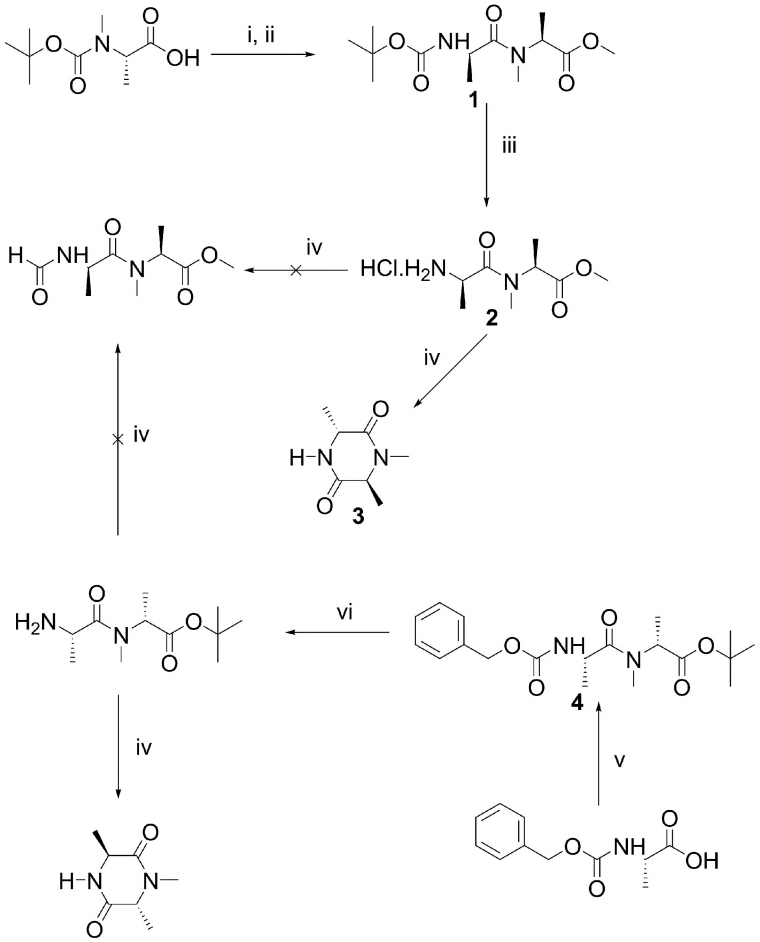

Scheme 1. Reagents and reaction conditions: (i) $SOCl_2$, MeOH; (ii) Boc-D-alanine, EDC, HOBt, DIPEA, CH_2Cl_2; (iii) EtOAc·HCl; (iv) $EtHCO_2$, $NaHCO_2$, various conditions / 2,4,5-trichlorophenyl formate, DIPEA, CH_2Cl_2; (v) Boc-D-N-methyl-alanine-O^{t}Bu, EDC, HOBt, CH_2Cl_2; (vi) Pd/H_2, MeOH.

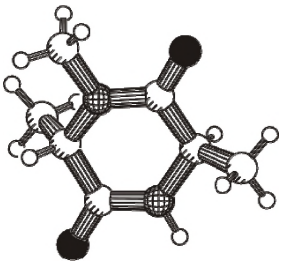

Figure 4. X-ray structure of **3** showing the piperazine (cyclo-alanyl-N-alanyl) structure.

Since formation of the formylated N-methylated dipeptide was unsuccessful, we shifted our focus on displacing the amide moiety with an ester functionality. Therefore, Boc-L-Ala-OH (**5a**) was coupled, using carbodiimide chemistry, to methyl (*R*)-(+)-lactate methyl ester to give **6a** (Scheme 2). Liberation of the free amine of **6a** with acid followed by refluxing in ethyl formate in the presence of sodium formate offered, after column chromatography, the formamide **7a** as a colourless oil in 75% yield. Dehydration of the *N*-formyl moiety with diphosgene and *N*-methylmorpholine resulted in the isocyanide derivative **8**. ^{1}H NMR spectroscopy of this compound (Figure 5 and 6), however, revealed complete epimerisation of the first 'amino acid' residue, as also indicated by the doubling of the signals in the ^{13}C NMR spectrum. The formamide was optically pure as evidenced by the comparison of the optical rotation of the formamide precursor **7a** (LD) ($[\alpha]_D$ = + 17° (*c* 1.2, $CHCl_3$)) with the enantiomer of the formamide (**7b**) (DL) ($[\alpha]_D$ = –17° (*c* 1.2, $CHCl_3$). Epimerisation was further confirmed by chiral HPLC, which showed two retention times for the isocyanide (7.32 min. and 8.29 min.) (Figure 7).

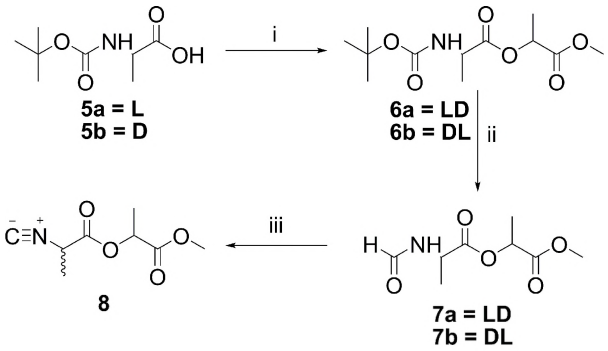

Scheme 2. Reagents and reaction conditions: (i) (*R*)-(+)-lacatate methyl ester, EDC, CH_2Cl_2; (ii) EtOAc·HCl / $EtHCO_2$, $NaHCO_2$, reflux (iii) diphosgene, N-Methylmorpholine, CH_2Cl_2, –30°C.

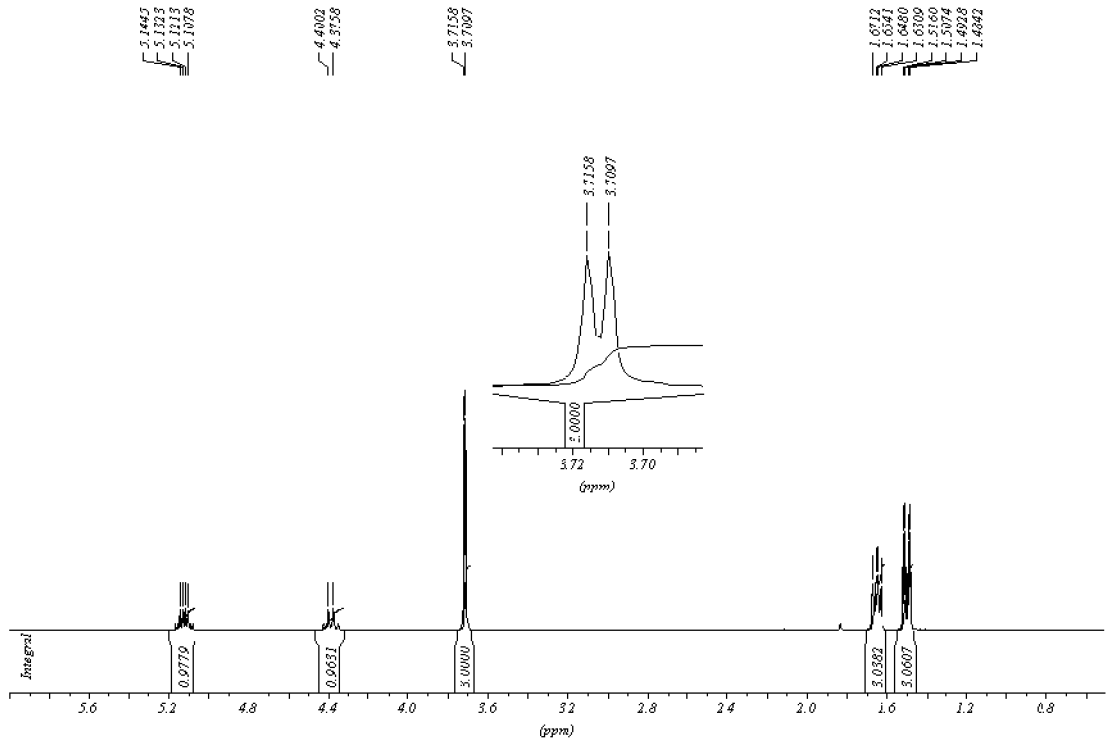

Figure 5: ^{1}H NMR (300 MHz) spectrum of isocyanide **8** in $CDCl_3$. Inset shows the two signals attributed to the methoxy protons.

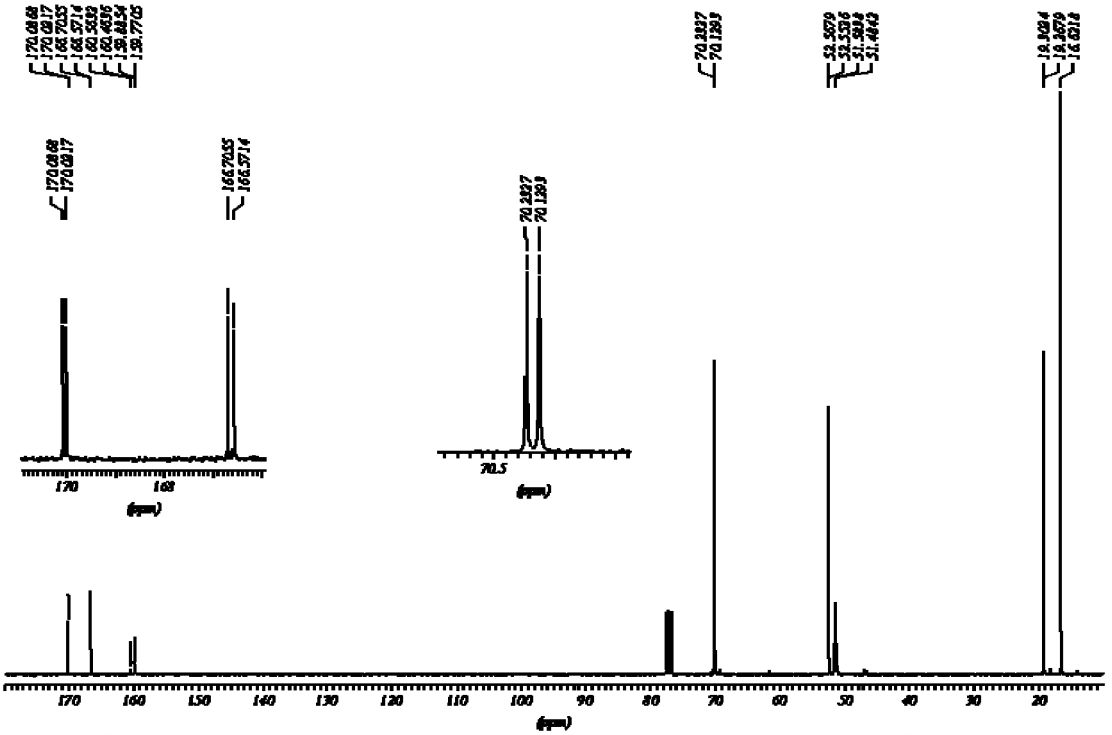

Figure 6: ^{13}C NMR (75 MHz) spectrum of isocyanide **8** in $CDCl_3$. Inset shows the doubling of the signals for the C=O and O-CH_3 carbons.

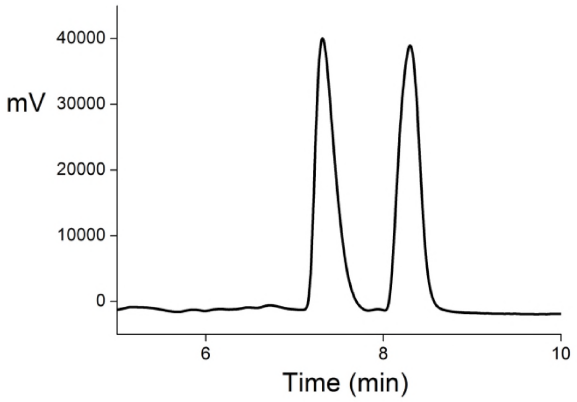

Figure 7: HPLC chromatogram of isocyanide **8** showing two retention times with similar intensities. (10µL of a 1mg / 1mL solution in isopropanol / heptane (80:20 v/v). Column: ODH2. Detector: 213 nm.

To further confirm that it is indeed the C_1 that is prone to epimerisation an isocyanide (**9**), derived from ß-homoalanine instead of alanine was synthesised allowing us to establish where the eprimerisation occured (Scheme 3). This compound was obtained enantiomerically pure, as concluded from the absence of double signals in both the ^{1}H NMR and ^{13}C NMR spectrum.

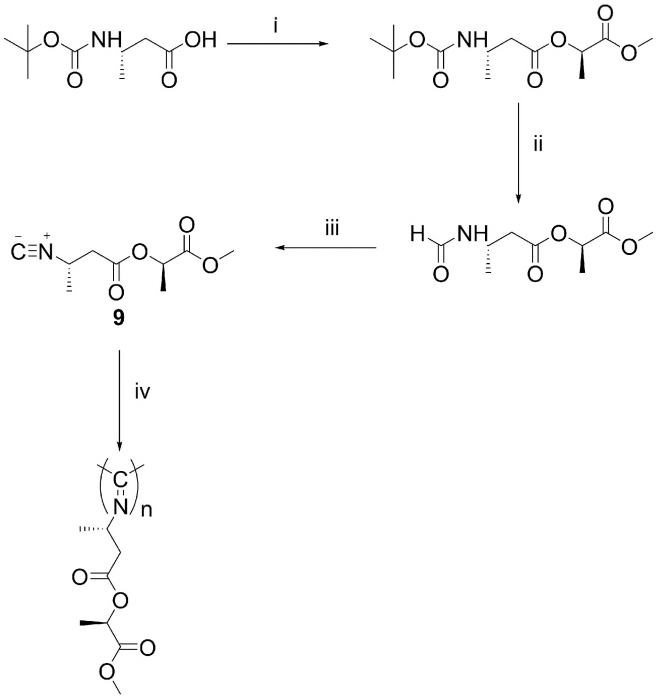

Scheme 3: Reagents and reaction conditions: (i) Boc-D-Ala-OH, EDC, CH_2Cl_2; (ii) EtOAc.·HCl/ $EtHCO_2$, $NaHCO_2$, reflux (iii) diphosgene, N-Methylmorpholine, CH_2Cl_2, –30 °C. (iv) 0.03 equivalents $Ni(ClO_4)_2 \cdot 6H_2O$, MeOH, CH_2Cl_2.

The polymerisation behaviour of this polymer, however, deviated from most other isocyanodipeptides (it was inert to polymerisation) preluding the use of this monomer as a good non-H-bonding model. We tentatively assigned the low yield of the polymerisation of

ß-homoalanine derived isocyanide to chelating of the monomer to the nickel centre hampering the polymerisation process. In contrast to the ß-homoalanine derived isocyanide, polymerisation of **8** proceeded much faster and therefore in further experiments monomer **8** was chosen for the statistical copolymerisation with DL-IAA.

Despite the fact that monomer **8** occurs as a mixture of diastereoisomers, which would result in two helices of opposite handedness, the self-trapping could still be studied since the hydrogen-bonding network in the two opposite helices would be identical. Therefore, a statistical copolymerisation based on isocyanides **8** and DL-IAA (with a 15:1 ratio of **8**:DL-IAA),[8,11] was carried out at room temperature with $Ni(ClO_4)_2 \cdot 6H_2O$ as a catalyst. In the to be formed polymer, the remaining NH groups are still hydrogen bonded to carbonyl groups in the same way as in the β-sheet helix, but no longer form a hydrogen bonding chain. The resulting polymer **10** was precipitated from diethyl ether, obtained as a powder, characterised by ^{1}H and ^{13}C NMR and IR spectroscopy and investigated by vibrational spectroscopy. Incorporation of both monomers into the polymer was demonstrated by varying the ratio between the monomers **8** and DL-IAA (15:1, 1:2, 1:0 and 0:1, respectively). Infrared spectroscopy showed different intensities of the NH, Amide I and Amide II vibrations and in the NMR spectra differences in the integration of the OCH (^{1}H NMR and ^{13}C NMR) and NH (^{1}H NMR) resonances were observed.

The pump-probe experiments performed on the NH:O statistical copolymer **10** (Figure 8), when compared to those performed on the regular β-sheet helix revealed that disruption of the hydrogen-bonded NH···OC chains in the β-sheet structure leads to a dramatic change in the vibrational response. Upon disturbance of the hydrogen-bond structure the NH-stretch vibrational response becomes completely regular (exhibiting a single excited state absorption peak) and shows no evidence of self-trapping

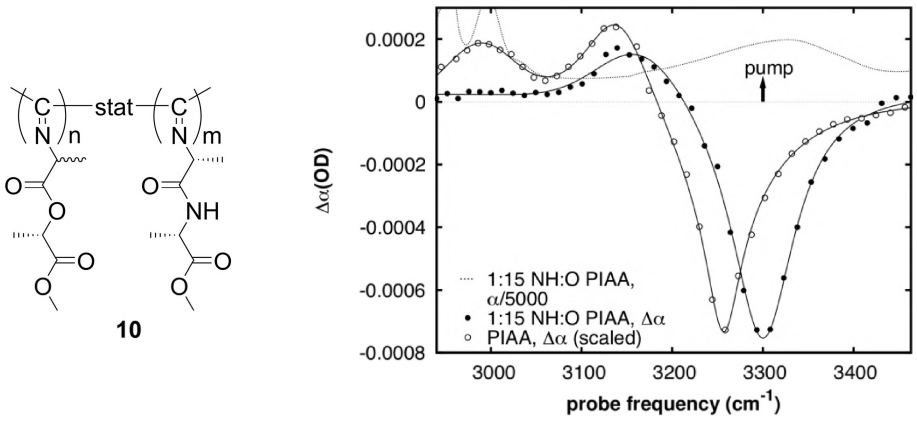

Figure 8. Molecular structure of the statistical copolymer **10** and the absorption change upon NH-stretch excitation of LD-PIAA and of statistical copolymer **10** (red line 1: 15 NH:O). Disruption of the hydrogen-bond network completely eliminates vibrational self-trapping.

We also performed self-trapping studies on a polyisocyanide with tripeptide side chains, i.e. LDL-PIAA (Figure 9). From previous studies we know that this polymer had two sets of hydrogen bonding arrays in its side chains, one close to the helical backbone with a hydrogen bonding strength similar to that in polyisocyano*di*peptides (inner chain) and another one, more remote from the helical backbone (outer chain) with a lower hydrogen bonding strength comparable to the one formed in a stretched out β-sheet. The inner chain has an NH-stretch frequency of 3260 cm^{-1} and the outer chain of 3400 cm^{-1}.[27] We investigated if the two hydrogen bonding chains in LDL-PIAA (Figure 9) also displayed different self-trapping behaviour. The response upon excitation of either one of the two NH-stretch modes is shown in Figure 9. The inner chain (centre frequency 3280 cm^{-1}) exhibits NH-stretch self-trapping (two positive Δα bands) similar as observed for LD-PIAA. The outer chain, with the weaker hydrogen bonding array, shows a regular pump-probe response, i.e. only one positive Δα band is visible. Apparently, the stretching of the β-sheet structure sufficiently decreases the NH-stretch/hydrogen bond coupling making the self-trapping effect so weak as to be unobservable.

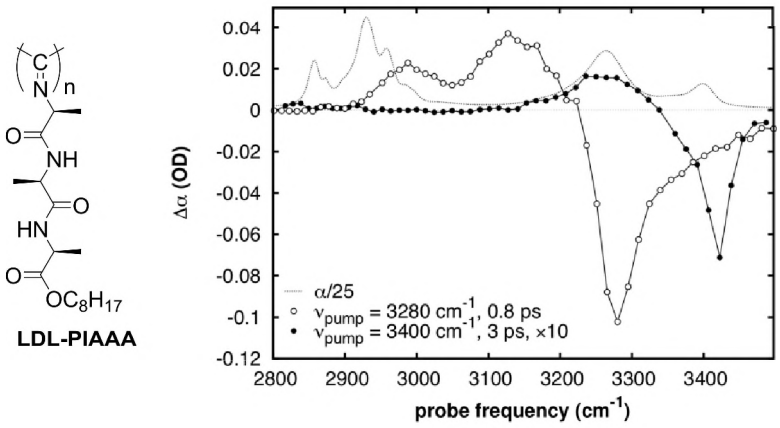

Figure 9. Molecular structure of the polyisocyanotripeptide used in this study and the transient absorption changes observed in this polymer. No self-trapping is observed for the chain with stretched hydrogen bonds.

7.3 Conclusion

We have observed self-trapping of NH-stretch vibrational excitations in β-sheet-like polyisocyanides by measuring the response of the NH-stretch mode upon $\nu_{NH} = 0 \rightarrow 1$ excitation in a time- and frequency resolved manner. Our studies show that NH-stretch vibrational self-trapping not only can occur in α-helices but also in synthetic β-sheet helical polymers. This implies that delocalisation (spreading out) of the vibrational excitation can be eliminated, which is one of the requirements for vibrational energy transport by means of Davydov solitons.[1-3] At present, the role of Davydov solitons in

energy transport in proteins is still under debate, and needs further investigations. The high persistence length of peptide-based polyisocyanides, combined with their structural integrity allows one to further tailor their hydrogen-bonding structure, making these synthetically well-accessible polymers excellent model systems for the study of vibrational self-trapping and energy transport in biosystems.

7.4 Experimental

General

All solvents were distilled prior to use. All other chemicals were commercials products and used as received. Column chromatography was performed using silica gel (40–60 μm) purchased from Merck. TLC-analyses were carried out on silica 60 F_{254} coated glass from Merck and the compounds were visualised using Ninhydrine, $KMnO_4$ or $Ni(ClO_4)_2 \cdot 6H_2O$ in EtOH. ^1H NMR and ^{13}C NMR spectra were recorded on a Bruker AC-300 MHz instrument operating at 300 MHz and 75 MHz, respectively, unless otherwise stated. FT-infrared spectra were recorded on a ThermoMattson IR300 spectrometer equipped with a Harrick ATR unit; compounds were measured as solid or oil. Mass spectrometry measurements were performed on a JEOL Accutof instrument (ESI). Optical rotations were measured on a Perkin Elmer 241 Polarimeter at room temperature and are reported in 10^{-1} deg cm^2 g^{-1}. High Performance Liquid Chromatography (HPLC) analysis was performed on a Shimadzu VP LC10 instrument equipped with a 250 mm ´ 4 ´ 4.6 mm^2 Daicel Chiralpak OD-H column, using isocratic flow rates of 1 mL min^{-1} of hexane and 2-propanol as eluent in various ratios. Detection took place at λ = 215 and 254 nm. The piperazine **3** was recrystallised from ethanol / diisopropyl ether, offering crystals suitable for X-ray analysis. A single crystal was mounted in air on a glass fibre. Intensity data were collected at -65 degrees C. A Nonius KappaCCD single-crystal diffractometer was used (ϕ and ω scan mode) using graphite monochromated Mo-Kα radiation. Unit cell dimensions were determined from the angular setting of 86 reflections. Intensity data were corrected for Lorentz and polarisation effects. SADABS multiscan correction was applied.[28] The structure was solved by the program CRUNCH[29] and was refined with standard methods using SHELXL97[30] with anisotropic parameters for the non-hydrogen atoms. All hydrogen atoms were placed at calculated positions and were refined riding on the parent atoms. A PLUTON[31] drawing is shown in Figure 5. Femto-second pump-probe experiments were carried out using a setup described previously.[15,32] Mid-infrared pump and probe pulses with energies of 10 μJ and ~100 nJ respectively, which are independently tunable from 2800 to 4000 cm^{-1}, were generated. The pulses have a duration and bandwidth of 150 fs and ~80 cm^{-1}, respectively. The cross correlation function was measured using two-photon absorption in InAs placed in a sample cell identical to the one used in the experiments on the solution samples. Transient absorption changes were measured as a function of frequency and pump-probe delay time using frequency-dispersed detection of the probe and reference pulses using a 2 × 32 MCT array, and a continuously variable path-length differences between the pump and probe pulses. To cover the entire frequency region of interest, the centre frequency of the probe pulse was subsequently tuned to three of four values, chosen such that the observed transient-absorption spectra had sufficient overlap, and the spectra were merged afterwards. The probe polarisation was at 45° with respect to that of the pump, and using a polarizer after the sample, either the parallel or the perpendicular polarisation component of the probe pulse was measured. All experiments were carried out at room temperature on ~10mM solutions (concentration of repeating units; To ensure that the results are not dependent on inter-molecular aggregation IR experiments were performed at various concentrations (including

more diluted solutions, in $CDCl_3$ kept between two CaF_2 windows separated by a 1 mm Teflon spacer). These experiments did not reveal any changes in the shift of the NH and amide I vibrational stretch vibrations.

Crystal data for **3**: translucent colourless, $C_7H_{12}N_2O_2$, M = 156.19, monoclinic, space group P21, a = 10.2526(5), b = 10.5948(5), c = 12.3707(7) Å, α = 90, β = 113.367(5), γ = 90°, U = 1233.55(11) $Å^3$, T = 208(2) K, Z = 6, μ(Mo-Kα) = 0.093 mm^{-1}, 25039 reflections measured, 4345 unique (R_{int} = 0.0322), final R1 0.0381, wR2 0.0722 (I › 2σ(I)).

Synthesis

LD-PIAA,[33] DL-PIAA,[34] and LDL-PIAAA,[27] were synthesised according to literature procedures.

(*S*)-Methyl 2-methyl–((*R*)-2-(tertbutoxycarbonylamino)-*N*-methylpropanamido)propanoate 1

$SOCl_2$ (6 mL) was slowly added to MeOH (50 mL) at –78 °C. After addition of Boc-L-N-methyl-Ala-OH (2.05 g, 10.1 mmol) the mixture was warmed up to room temperature and stirred for 24 hrs. After this time the reaction mixture was concentrated and *t*-BuOH was added and the solvent was evaporated under reduced pressure twice, to remove excess of HCl. The resulting L-*N*-methylalanine methyl ester HCl salt was dissolved in CH_2Cl_2 (200 mL). To this solution Boc-D-alanine-OH (2.19 g, 11.6 mmol, 1.15 equiv), DIPEA (4.0 mL, 23.4 mmol, 2.3 equiv), HOBt (1.74 g, 11.4 mmol, 1.13 equiv) and EDC (2.12 g, 11.0 mmol, 1.09 equiv) were added. After stirring for 18 hrs the reaction mixture was washed with an aqueous 10% (w/w) citric acid solution (2 × 150 mL), H_2O (150 mL), aqueous 10 % (w/w) sodium carbonate solution (2 × 150 mL) and H_2O (150 mL). The organic layer was dried (Na_2SO_4), concentrated and subjected to column chromatography (3% MeOH in $CHCl_3$), yielding **1** in 82% yield as a colourless oil. $[\alpha]_D$ – 44° (*c* 1.1, $CHCl_3$). ^{1}H NMR (δ ppm, $CDCl_3$, 300 MHz, rotamers): 5.51 and 5.39 (br d, *J* = 7.3 Hz, 1H, NH), 5.03 (q, *J* = 7.0 Hz, 1H, NHC*H*), 4.24 (rotameric m, 1H, CH_3NCH), 3.75 and 3.70 (rotameric s, 3H, OCH_3), 3.00 and 2.82 (rotameric s, 3H, NCH_3), 1.47 and 1.40 (rotameric d, *J* = 7.0 Hz, 3H, CH_3NCHCH_3), 1.43 (s, 9H, $C(CH_3)_3$), 1.30 (d, *J* = 7.0 Hz, 3H, $NHCHCH_3$). ^{13}C NMR (δ ppm, $CDCl_3$, 75 MHz, rotamers): 173.2, 172.8, 171.8, 171.3 (rotameric C=O), 155.0 (C=O Boc), 79.4 ($C(CH_3)_3$), 54.9 and 53.1 (CH_3NCH), 52.6 and 52.3 (rotameric OCH_3), 46.6 and 46.1 (rotameric NHCH), 31.8 and 29.3 (rotameric CH_3NCH), 28.4 ($C(CH_3)_3$), 19.2 and 19.0 (rotameric $NHCHCH_3$), 15.4 and 14.8 (rotameric CH_3NCHCH_3). FT-IR (cm^{-1}, ATR): 3417, 3314 (NH), 1742 (ester), 1705, 1690 (Amide I), 1645 (N-CH_3) 1558 (amide II). MS-ESI: m/z = 311 $[M+Na]^+$. HRMS for $C_{13}H_{24}N_2O_5Na$: Calcd 311.1583. Found: 311.1572.

(3*R*, 6*S*)-1,3,6-Trimethylpiperazine-2,5-dione (*cyclo*-alanyl-*N*-alanyl) 3

The cyclic title title compound was obtained after treatment of **1** or **3** using various formylation conditions (i.e. $EtHCO_2$, $NaHCO_2$ or various amounts of 2,4,5-trichlorophenyl formate, DIPEA, CH_2Cl_2) as described in the text; yield 60 %.

Mp: 111 °C. ^{1}H NMR (δ ppm, $CDCl_3$, 300 MHz): 7.7 (br, 1H, NH), 4.03 (q, *J* = 6.9 Hz, 1H, CH), 3.85 (q, *J* = 7.2 Hz, 1H, CH), 2.93 (s, NCH_3,3H,), 1.46 (d, *J* = 6.9 Hz, 3H, CH_3), 1.45 (d, *J* = 7.2 Hz, 3H, CH_3). ^{13}C NMR (δ ppm, $CDCl_3$, 75 MHz): 172.0, 167.1 (C=O), 58.8, 49.7 (CH), 32.4 (NCH_3), 18.3, 17.1 (CH_3). FT-IR (cm^{-1}, ATR): 3235 (NH), 1648 (br, Amide I).

(*R*)-*tert*-Butyl 2-((*S*)-2-(benzyloxycarbonylamino)-N-methylpropanamido)propanoate 4

Starting from Cbz-L-alanine-OH and D-*N*-methylalanine *tert*-butyl ester and following the same procedure as for **1**, **4** was obtained in 69 % yield as a colourless oil.

$[\alpha]_D$ + 41° (*c* 1.1, $CHCl_3$). ^{1}H NMR (δ ppm, $CDCl_3$, 300 MHz, rotamers): 7.32–7.28 (m, ArH, 5H), 5.85(d, *J* = 7.5 Hz, 1H, NH), 5.06 (s, 2H, CH_2), 4.84 and 4.52 (rotameric q, *J* = 7.2 Hz, 1H, CH_3NCH), 4.65 (rotameric m, 1H, NHC*H*), 2.97 and 2.80 (rotameric s, 3H, NCH_3), 1.43–1.30 (rotameric m, 6H, CH_3NCHCH_3 and $NHCHCH_3$), 1.40 (s, 9H, $C(CH_3)_3$). ^{13}C NMR (δ ppm, $CDCl_3$, 75 MHz, rotamers): 172.5, 172.4, 170.3, 169.7 (rotameric C=O), 155.6, 155.5 (rotameric C=O *tert*-butyl ester), 136.5, 136.4 (rotameric ArC *ipso* to OCH_2), 128.5–127.9 (rotameric m, ArC), 82.4, 81.6 (rotameric $C(CH_3)_3$), 66.7, 66.6 (rotameric CH_2) 55.7, 54.0 (CH_3NCH), 47.1 and 46.8 (rotameric NHCH), 31.9 and 29.1 (rotameric CH_3NCH), 27.9, 27.94 (rotameric $C(CH_3)_3$), 19.2 and 18.9 (rotameric $NHCHCH_3$), 15.5 and 14.3 (rotameric CH_3NCHCH_3). FT-IR (cm^{-1}, ATR): 3291 (NH), 1735 (ester), 1716, 1696 (Amide I), 1645 (N-CH_3), 1558 (amide II). MS-ESI: m/z = 387 $[M+Na]^+$. HRMS for $C_{19}H_{28}N_2O_5Na$: Calcd 387.1896. Found: 387.1889.

(*S*)-((*R*)-1-Methoxy-1-oxopropan-2-yl)2-(*tert*-butoxycarbonylamino)propanoate 6a

Methyl (*R*)-(+)-lacatate methyl ester (3.1 mL, 32.4 mmol) and Boc- L-alanine-OH (6.86 g, 36.3, 1.1 equiv mmol) were dissolved in CH_2Cl_2 (200 mL). To this solution diisopropylethylamine (DIPEA; 6.1 mL, 35.7 mmol, 1.1 equiv), 1-hydroxybenzatriazole (HOBt; 5.55 g, 36.2 mmol, 1.1 equiv), a catalytic amount of dimethylaminopyridine (DMAP) and 1-(3-dimethylaminopropyl)-3-ethylcarbodiimide hydrochloride (EDC; 6.83 mmol, 1.1 equiv) were added. After stirring for 10 hrs the solvent was evaporated *in vacuo* and the product was redissolved in $CHCl_3$ (200 mL). This solution was subsequently washed with an aqueous 10% (w/w) citric acid solution (2 × 200 mL), H_2O (200 mL), an aqueous 10 % (w/w) sodium carbonate solution (2 × 200 mL) and H_2O (200 mL). The organic layer was dried (Na_2SO_4), concentrated and subjected to column chromatography (2% MeOH in $CHCl_3$), yielding 73% of **6a** as a colourless oil.

$[\alpha]_D$ + 16° (*c* 2.1, $CHCl_3$). ^{1}H NMR (δ ppm, $CDCl_3$, 300 MHz): 5.13 (q, *J* = 6.9 Hz, 1H, OC*H*), 5.06 (br, 1H, NH), 4.34 (m, 1H, NHC*H*), 3.70 (s, 3H, OCH_3), 1.46 (d, *J* = 6.9 Hz, 3H, $OCHCH_3$), 1.40 (s, 9H, $C(CH_3)_3$), 1.38 (d, *J* = 7.2 Hz, 3H, $NHCHCH_3$). ^{13}C NMR (δ ppm, $CDCl_3$, 75 MHz): 172.6, 170.8, 155.0 (C=O), 79.8 ($C(CH_3)_3$), 69.2 (OCH), 52.4 (OCH_3), 49.4 (NHCH), 28.4 ($C(CH_3)_3$), 18.5 ($NHCHCH_3$), 16.9 ($OCHCH_3$). FT-IR (cm^{-1}, ATR): 3378 (NH), 1745 (ester), 1699 (Amide I), 1510 (amide II). MS-ESI: m/z = 294 $[M+Na]^+$. HRMS for $C_{12}H_{21}NO_6Na$: Calcd 294.1267. Found: 294.1258.

(*R*)-((*S*)-1-methoxy-1-oxopropan-2-yl)2-(*tert*-butoxycarbonylamino)propanoate 6b

Following the same procedure as for **6a**, **6b** was obtained in 68% yield as a colourless oil. $[\alpha]_D$ –15° (*c* 0.9, $CHCl_3$). ^{1}H NMR (δ ppm, $CDCl_3$, 300 MHz): 5.13 (q, *J* = 7.0 Hz , 1H, OCH), 5.04 (br, 1H, NH), 4.36 (m, 1H, NHC*H*), 3.73 (s, 3H, OCH_3), 1.49 (d, *J* = 7.0 Hz, 3H, $OCHCH_3$), 1.43 (s, 9H, $C(CH_3)_3$), 1.40 (d, *J* =7.7 Hz, 3H, $NHCHCH_3$,). ^{13}C NMR (δ ppm, $CDCl_3$, 75 MHz): 172.6, 170.8, 155.1 (C=O), 79.9 ($C(CH_3)_3$), 69.3 (OCH), 52.5 (OCH_3), 49.4 (NHCH), 28.4 ($C(CH_3)_3$), 18.6 ($NHCHCH_3$), 16.9 ($OCHCH_3$). FT-IR (cm^{-1}, ATR): 3382 (NH), 1744 (ester), 1711 (Amide I), 1512 (amide II). MS-ESI: m/z = 294 $[M+Na]^+$. HRMS for $C_{12}H_{21}NO_6Na$: Calcd 294.1267. Found: 294.1256.

(*S*)-((*R*)-1-Methoxy-1-oxopropan-2-yl)2-formamidopropanoate) 7a

The Boc-protecting group of the **6a** (2.12 g, 7.7 mmol) was removed by dissolving the **6a** in HCl-saturated ethyl acetate (150 mL). The mixture was stirred for 5 hrs after which time the solvent was evaporated *in vacuo* and the excess of HCl was removed by addition of *t*-BuOH/CH_2Cl_2 and subsequent evaporation. The resulting HCl salt was taken up in ethyl formate (150 mL) and sodium formate (2.15 g, 31.6 mmol, 4.1 equiv) was added. The mixture was stirred under reflux for 72 hrs, after which the solid was filtered off and washed thoroughly with

$CHCl_3$. The filtrate was evaporated and the crude product was purified by column chromatography (2% MeOH in $CHCl_3$) to yield 75% of a colourless oil. $[\alpha]_D$ + 17° (*c* 1.2, $CHCl_3$). ^{1}H NMR (δ ppm, $CDCl_3$, 300 MHz): 8.18 (s, 1H, HCO), 6.28 (br, 1H, NH), 5.14 (q, *J* = 7.0 Hz, 1H, OCH), 4.77 (qn, *J* = 7.0 Hz, 1H, NHC*H*), 3.74 (s, 3H, OCH_3), 1.51 (d, *J* = 7.0 Hz, 3H, NHCHCH_3), 1.47 (d, *J* = 7.0 Hz, 3H, OCHCH_3). ^{13}C NMR (δ ppm, $CDCl_3$, 75 MHz): 171.9, 170.6 (C=O), 160.5 (HCO), 69.7 (OCH), 52.6 (OCH_3), 47.0 (NHCH), 18.5 (NHCHCH_3), 17.0 (OCHCH_3). FT-IR (cm^{-1}, ATR): 3313 (NH), 1748 (ester), 1683 (Amide I), 1558 (amide II). MS-ESI: m/z = 226 $[M+Na]^+$. HRMS for $C_8H_{13}NO_5Na$: Calcd 226.0691. Found: 226.0692.

(*R*)-((*S*)-1-Methoxy-1-oxopropan-2-yl)2-formamidopropanoate) 7b

Following the same procedure as for the (*S,R*) diastereoisomer, the title compound was obtained in 81% yield as a colourless oil. $[\alpha]_D$ –17° (*c* 1.2, $CHCl_3$). ^{1}H NMR (δ ppm, $CDCl_3$, 300 MHz): 8.17 (s, 1H, HCO), 5.13 (d, *J* = 6.9 Hz, 1H, NH), 5.12 (q, *J* = 7.2 Hz, 1H, OCH), 4.70 (qn, *J* = 7.2 Hz, 1H, NHCH), 3.75 (s, 3H, OCH_3), 1.51 (d, *J* = 6.9 Hz, 3H, NHCHCH_3), 1.46 (d, *J* =7.2 Hz, 3H, OCHCH_3). ^{13}C NMR (δ ppm, $CDCl_3$, 75 MHz): 171.3, 170.2 (C=O), 160.9 (HCO), 68.9 (OCH), 51.9 (OCH_3), 46.2 (NHCH), 17.2 (NHCHCH_3), 16.2 (OCHCH_3). FT-IR (cm^{-1}, ATR): 3313 (NH), 1746 (ester), 1683 (Amide I), 1558 (amide II). MS-ESI: m/z = 226 $[M+Na]^+$. HRMS for $C_8H_{13}NO_5Na$: Calcd 226.0691. Found: 226.0694.

(*R*)-1-Methoxy-1-oxopropan-2-yl)2-isocyanopropanoate) 8

The formamide **7a** (305 mg, 1.5 mmol) was dissolved in dry CH_2Cl_2 (60 mL) under an N_2 atmosphere and N-methyl morpholine (0.33 mL, 3.0 mmol, 2.0 equiv) was added. The resulting solution was cooled to –50 °C (acetone/CO_2) and diphosgene (90 µL, 0.75 mmol, 0.5 equiv) in CH_2Cl_2 (10 mL) was added dropwise to the reaction mixture over a period of 30 min, while the temperature was maintained at –50 °C. After complete addition of diphosgene, the pale yellow solution was allowed to warm to 0 °C and an ice-cold saturated aqueous sodium bicarbonate solution (3 mL) was added while stirring for 10 min. The product was extracted with $CHCl_3$ (10 mL) and subsequently washed with an aqueous 10% (w/w) sodium bicarbonate solution and water (10 mL). The organic layer was dried (Na_2SO_4) and evaporated *in vacuo* resulting in a pale yellow oil. The product was purified using column chromatography (2% MeOH in $CHCl_3$). Analysis by NMR spectroscopy and HPLC revealed epimerisation of the isocyanide. Bulb–to–bulb distillation of the pale yellow isocyanide with a Kugelrohr apparatus offered the epimerised isocyanide **8** as a colourless oil in 60% yield. ^{1}H NMR (δ ppm, $CDCl_3$, 300 MHz): 5.12 (m, 2H, OCH), 4.38 (q, *J* = 7.0 Hz, 2H, NCH), 3.72 (s, 3H, OCH_3), 3.71 (s, 3H, OCH_3), 1.66 (d, *J* = 7.0 Hz, 3H, NCHCH_3), 1.64 (d, *J* = 7.0 Hz, 3H, NCHCH_3), 1.50 (d, *J* = 7.0 Hz, 3H, OCHCH_3), 1.49 (d, *J* = 7.0 Hz, 3H, OCHCH_3). ^{13}C NMR (δ ppm, $CDCl_3$, 75 MHz): 170.1, 170.0 (C=O), 166.7, 166.6 (C=O), 159.9, 159.8 (CN), 70.2, 70.1 (OCH), 52.6, 52.5 (OCH_3), 51.6, 51.5 (NCH), 19.3, 19.3 (NCHCH_3), 16.6, 16.5 (OCHCH_3). FT-IR (cm^{-1}, ATR): 2145 (CN), 1746 (ester). MS-ESI: m/z = 208 $[M+Na]^+$. HRMS for $C_8H_{11}NO_4Na$: Calcd 208.0586. Found: 208.0587. HPLC (Column ODH2, 1 mg/mL, 2-propanol / heptane 4:1 v/v): 7.32 min., 8.29 min.

Statistical copolymer 10

To **8** (396 mg, 2.14 mmol) and DL-IAA (26.4 mg, 0.14 mmol, 0.065 equiv) in CH_2Cl_2 (5mL) was added 0.03 equiv of $Ni(ClO_4)_2{\cdot}6H_2O$ (90 µL of a 0.85 mM MeOH solution). The solution turned reddish brown immediately and after 12 h the solvent was evaporated. The glassy solid was taken up in a minimal amount of THF and the polymer was precipitated out by dropping this solution into diethyl ether (200 mL) with vigorous stirring. The product was filtered off and washed extensively with ether. Drying *in vacuo* gave the polymer as a brown solid in 40% yield. ^{1}H NMR (*δ* ppm, $CDCl_3$, 300 MHz): 5.3–4.8 (br, 1H, OCH), 4.4–3.9 (br, 2H, NCH, CH ala), 3.9–3.4

(br, 6H, OCH_3), 1.9–0.9 (br, 12H, CH_3). ^{13}C NMR (δ ppm, $CDCl_3$, 75 MHz). 171 (br, C=O), 70 (br, OCH), 53–53 (br, OCH_3, CH), 17.5–16 (br, CH_3. FT-IR (cm^{-1}, ATR): 1739 (C=O ester), 1629 (C=N), 1092 (C-O-C).

(*S*)-((*R*)-1-Methoxy-1-oxopropan-2-yl)3-(*tert*-butoxycarbonylamino)butanoate

Starting from Boc-L-ß-homoalanine-OH and methyl (*R*)-(+)-lactate methyl ester and following the same procedure as for **10a**, the title compound was obtained in 76 % yield as a colourless oil. $[\alpha]_D$ –14° (*c* 0.8, $CHCl_3$). ^1H NMR (δ ppm, $CDCl_3$, 300 MHz): 5.05 (m, 2H, NH, OCH), 3.97 (m, 1H, CH ß-homo-Ala), 3.69 (s, 3H, OCH_3), 2.52 (d, *J* = 5.4 Hz, 2H, CH_2), 1.42 (d, *J* = 7.2 Hz, 3H, OCH*C*H_3), 1.37 (s, 9H, $C(CH_3)_3$), 1.16 (d, *J* = 6.6 Hz, 3H, CH_3 ß-homo-Ala). ^{13}C NMR (δ ppm, $CDCl_3$, 75 MHz): 171.2, 170.8, 155.1 (C=O), 79.1 (*C*$(CH_3)_3$), 69.3 (OCH), 52.4 (OCH_3), 49.4 (CH ß-homo-Ala), 40.3 (CH_2), 28.4 (C(*C*$H_3)_3$), 20.1 (CH_3 ß-homo-Ala), 16.9 (OCH*C*H_3). FT-IR (cm^{-1}, ATR): 3382 (NH), 1740 (ester), 1711, 1688 (Amide I), 1513 (amide II). MS-ESI: m/z = 312 $[M+Na]^+$. HRMS for $C_{13}H_{23}NO_6Na$: Calcd 312.1423. Found: 312.1425.

(*S*)-((*R*)-1-Methoxy-1-oxopropan-2-yl)3-formamidobutanoate)

Following the same procedure as for the formamide precursor of **3**, the title compound was obtained in 84% yield as a colourless oil. $[\alpha]_D$ – 44° (*c* 1.0, $CHCl_3$). ^1H NMR (δ ppm, $CDCl_3$, 200 MHz, rotamers): 7.93 and 7.88 (rotameric s, 1H, HCO), 6.95 and 6.80 (rotameric d, *J* = 7.3 Hz, 1H, NH,), 4.90 (q, *J* = 7.1 Hz, 1H, OCH), 4.24 (sextet, 1H, *J* = 6.5 Hz, CH ß-homo-Ala), 3.55 (s, 3H, OCH_3), 2.42 (d, *J* = 5.6 Hz, 2H, CH_2,), 1.29 (d, *J* = 7.1 Hz, 3H, OCH*C*H_3,), 1.11 and 1.06 (rotameric d, *J* = 6.8 Hz, 3H, CH_3 ß-homo-Ala). ^{13}C NMR (δ ppm, $CDCl_3$, 50 MHz, rotamers): 171.0, 170.9, 170.2, 169.8 (rotameric C=O), 164.1, 160.7 (rotameric HCO), 68.5, 68.3 (rotameric OCH), 52.1 (OCH_3), 45.1, 41.4 (rotameric CH ß-homo-Ala), 40.6, 39.6 (rotameric CH_2), 21.4, 20.6 (rotameric CH_3 Ala ß-homo-Ala), 19.5, 16.5 (rotameric OCH*C*H_3). FT-IR (cm^{-1}, ATR): 3378 (NH), 1736 (ester), 1661 (Amide I), 1528 (amide II). MS-ESI: m/z = 240 $[M+Na]^+$. HRMS for $C_9H_{15}NO_6Na$: Calcd 240.0848. Found: 240.0858.

(*S*)-((*R*)-1-Methoxy-1-oxopropan-2-yl)3-isocyanobutanoate) (β-alanine derived isocyanide) 9

Following a similar procedure as for **3**, compound **5** was obtained in 68% yield as a colourless oil. $[\alpha]_D$ + 68° (*c* 1.2, $CHCl_3$). ^1H NMR (δ ppm, $CDCl_3$, 300 MHz): 5.13 (q, *J* = 6.9 Hz, 1H, OCH), 4.10 (sextet, *J* = 6.9 Hz, 1H, CH ß-homo-Ala), 3.73 (s, 3H, OCH_3), 2.80 (m, 1H, CH_2), 2.64 (m, 1H, CH_2), 1.49 (d, *J* = 7.2 Hz, 3H, OCH*C*H_3), 1.45 (m, 3H, CH_3 ß-homo-Ala). ^{13}C NMR (δ ppm, $CDCl_3$, 75 MHz): 170.8, 168.8 (C=O), 156.3 (tr, *J* = 4.6 Hz), 69.2 (OCH), 52.5 (OCH_3), 46.4 (tr, *J* = 6.3 Hz, CH ß-homo-Ala), 41.3 (CH_2), 21.4, (CH_3 ß-homo-Ala), 16.9 (OCH*C*H_3). FT-IR (cm^{-1}, ATR): 2148 (CN), 1745 (ester). MS-ESI: m/z = 222 $[M+Na]^+$. HRMS for $C_9H_{13}NO_4Na$: Calcd 220.0742. Found: 220.0750.

7.5 References & Notes

(1) Davydov, A. S. *Journal of Theoretical Biology* **1973**, *38*, 559-569; Davydov, A. S. *Journal of Theoretical Biology* **1977**, *66*, 377-387.

(2) Scott, A. *Phys Rep* **1992**, *217*, 1-67.

(3) Edler, J.; Pfister, R.; Pouthier, V.; Falvo, C.; Hamm, P. *Physical Review Letters* **2004**, *93*, 106405.

(4) Careri, G.; Buontempo, U.; Carta, F.; Gratton, E.; Scott, A. C. *Physical Review Letters* **1983**, *51*, 304-307; Careri, G.; Buontempo, U.; Galluzzi, F.; Scott, A. C.; Gratton, E.; Shyamsunder, E. *Phys. Rev B.* **1984**, *30*, 4689-4702; Blanchet, G. B.; Fincher, C. R. *Physical Review Letters* **1985**, *54*, 1310-1312; Alexander, D. M. *Physical Review Letters* **1985**, *54*, 138-141; Alexander, D. M.; Krumhansl, J. A. *Phys. Rev B.* **1986**, *33*, 7172-7185; Fann, W.; Rothberg, L.; Roberson, M.; Benson, S.; Madey, J.; Etemad, S.; Austin, R. *Physical Review Letters* **1990**, *64*, 607-610; Johnson, S. W.; Barthes, M.; Eckert, J.; McMullan, R. K.; Muller, M. *Physical Review Letters* **1995**, *74*, 2844-2844; Edler, J.; Hamm, P.; Scott, A. C. *Physical Review Letters*

2002, *88*; Edler, J.; Hamm, P. *J. Chem. Phys.* **2002**, *117*, 2415-2424; Edler, J.; Hamm, P. *J. Chem. Phys.* **2003**, *119*, 2709-2715; Edler, J.; Hamm, P. *Phys. Rev B.* **2004**, *69*, 214301; Hamm, P.; Edler, J. *Phys. Rev B.* **2006**, *73*.

(5) Long, Y. T.; Abu-Rhayem, E.; Kraatz, H. B. *Chem. Eur. J.* **2005**, *11*, 5186-5194.

(6) Yoder, M. D.; Keen, N. T.; Jurnak, F. *Science* **1993**, *260*, 1503-1507.

(7) Nolte, R. J. M. *Chem. Soc. Rev.* **1994**, *23*, 11-19; Suginome, M.; Ito, Y. *Adv. Polym. Sci.* **2004**, *171*, 77-136.

(8) Cornelissen, J. J. L. M.; Donners, J. J. J. M.; de Gelder, R.; Graswinckel, W. S.; Metselaar, G. A.; Rowan, A. E.; Sommerdijk, N. A.; Nolte, R. J. M. *Science* **2001**, *293*, 676-80.

(9) Samori, P.; Ecker, C.; Goessl, I.; de Witte, P. A. J.; Cornelissen, J. J. L. M.; Metselaar, G. A.; Otten, M. B. J.; Rowan, A. E.; Nolte, R. J. M.; Rabe, J. P. *Macromolecules* **2002**, *35*, 5290-5294.

(10) Bodis, P.; Schwartz, E.; Koepf, M.; Cornelissen, J. J. L. M.; Rowan, A. E.; Nolte, R. J. M.; Woutersen, S. *The Journal of chemical physics* **2009**, *131*, 124503.

(11) Kamer, P. C. J.; Cleij, M. C.; Nolte, R. J. M.; Harada, T.; Hezemans, A. M. F.; Drenth, W. *J. Am. Chem. Soc.* **1988**, *110*, 1581-1587; Hong, B.; Fox, M. A. *Macromolecules* **1994**, *27*, 5311-5317; King, R. B.; Borodinsky, L.; Greene, M. J. *J. Polym. Sci., Part A: Polym. Chem.* **1987**, *25*, 2165-2173; Deming, T. J.; Novak, B. M. *Macromolecules* **1991**, *24*, 326-328; Kitto, H. J.; Schwartz, E.; Nijemeisland, M.; Koepf, M.; Cornelissen, J. J. L. M.; Rowan, A. E.; Nolte, R. J. M. *J. Mater. Chem.* **2008**, *18*, 5615-5624.

(12) Falvo, C.; Pouthier, V. *J. Chem. Phys.* **2005**, *123*, 184709; Falvo, C.; Pouthier, V. *J. Chem. Phys.* **2005**, *123*, 184710; Pouthier, V. *Phys Rev E* **2003**, *68*, 021909.

(13) Woutersen, S. *J. Chem. Phys.* **2007**, *126*, 226101.

(14) Davydov's original motivation and papers are based on solitons. It is nowadays however, established that what is observed in crystalline acetanilide, as well as in the poly-γ-benzyl-L-glutamate system studied by Edler and co-workers[4] is rather a polaron. Polarons, as discussed by Pouthier[4] have a large effective mass, i.e. they are essentially dispersion less, which allows spatial localization. With a large effective mass, however, one would not expect polarons to be very mobile, in contrast to Davydov's original idea.

(15) Bodis, P.; Timmer, R.; Yeremenko, S.; Buma, W. J.; Hannam, J. S.; Leigh, D. A.; Woutersen, S. *Journal of Physical Chemistry C* **2007**, *111*, 6798-6804.

(16) Ditter, W.; Luck, W. A. P. *Berichte Der Bunsen-Gesellschaft Fur Physikalische Chemie* **1969**, *73*, 526.

(17) Graener, H.; Seifert, G.; Laubereau, A. *Chem. Phys. Lett.* **1990**, *172*, 435-439.

(18) Mukamel, S. *Principles of Nonlinear Optical Spectroscopy*; Oxford University Press: New York, 1995.

(19) Elliott, A. *Proceedings of the Royal Society of London Series a-Mathematical and Physical Sciences* **1954**, *226*, 408-421.

(20) Hamm, P.; Edler, J. *Phys. Rev B.* **2006**, *73*, 094302.

(21) Woutersen, S.; Bakker, H. J. *Physical Review Letters* **1999**, *83*, 2077-2080.

(22) Schwartz, E.; Kitto, H. J.; de Gelder, R.; Nolte, R. J. M.; Rowan, A. E.; Cornelissen, J. J. L. M. *J. Mater. Chem.* **2007**, *17*, 1876-1884.

(23) Humphrey, J. M.; Chamberlin, A. R. *Chem. Rev.* **1997**, *97*, 2243-2266.

(24) Wenger, R. M. *Helvetica Chimica Acta* **1983**, *66*, 2672-2702.

(25) McDermot.Jr; Benoiton, N. L. *Can. J. Chem.* **1973**, *51*, 2562-2570.

(26) Because we used a L,D dialanine in this case the enantiomer of **3** is obtained.

(27) Metselaar, G. A.; Adams, P. J. H. M.; Nolte, R. J. M.; Cornelissen, J. L. L. M.; Rowan, A. E. *Chem. Eur. J.* **2007**, *13*, 950-960.

(28) Sheldrick, G. M. (1996) *SADABS. Program for Emperical Absorption Correction.*

(29) de Gelder, R.; de Graaff, R. A. G.; Schenk, H. *Acta Crystallogr., Sect. A* **1993**, *49*, 287-293.

(30) Sheldrick, G.M. *SHELXL-97. Program for the refinement of crystal structures*, University of Gottingen: Germany, 1997.

(31) Spek, A.L. *PLATON, A Multipurpose Crystallographic Tool*, Utrecht University, Utrecht, The Netherlands, 2004.

(32) Dokter, A. M.; Woutersen, S.; Bakker, H. J. *J. Chem. Phys.* **2007**, *126*, 124507.

(33) Cornelissen, J. J. L. M.; Donners, J. J. J. M.; de Gelder, R.; Graswinckel, W. S.; Metselaar, G. A.; Rowan, A. E.; Sommerdijk, N. A. J. M.; Nolte, R. J. M. *Science* **2001**, *293*, 676-680; Cornelissen, J. J. L. M.; Graswinckel, W. S.; Adams, P. J. H. M.; Nachtegaal, G. H.; Kentgens, A. P. M.; Sommerdijk, N. A. J. M.; Nolte, R. J. M. *J. Polym. Sci., Part A: Polym. Chem.* **2001**, *39*, 4255-4264.

(34) Metselaar, G. A.; Cornelissen, J. J. L. M.; Rowan, A. E.; Nolte, R. J. M. *Angew. Chem., Int. Ed.* **2005**, *44*, 1990-1993.

8

Synthesis and characterisation of surface-initiated helical polyisocyanopeptide brushes[§]

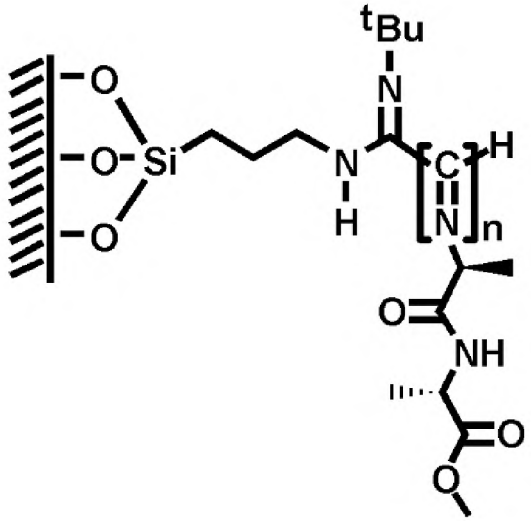

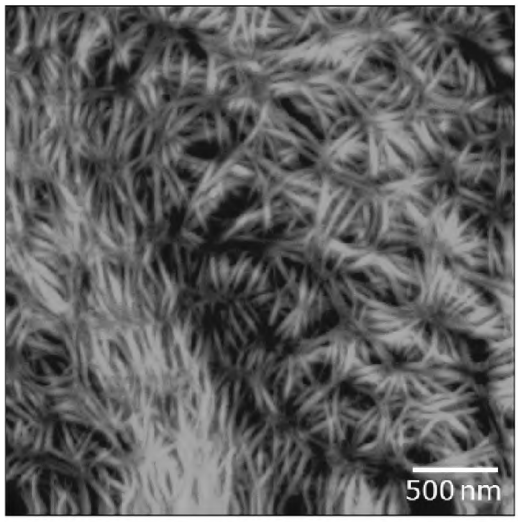

[§]Parts of this work have been published: Lim, E.; Tu, G.; Schwartz, E.; Cornelissen, J. J. L. M.; Rowan, A. E.; Nolte, R. J. M.; Huck, W. T. S. *Macromolecules* **2008**, *41*, 1945–1951.

8.1 Introduction

Polymer brushes have emerged as a powerful tool to control the morphology and properties of polymer thin films. By surface-tethering polymers in sufficiently high grafting densities, the polymer chains are forced to stretch away from the surface, leading to more or less aligned thin polymer films.[1] Such so-called polymer brushes can be used to improve the charge transport properties of films[2] or to generate surface coatings that can respond to changes in temperature, pH, salt concentration and solvent conditions.[3] Furthermore, the alignment of the polymer chains allows a rapid and unidirectional response, which is a prerequisite for the development of nanoscale actuators.[4] A further level of control can be achieved when the polymers adopt well-defined conformations. Schouten and co-workers have reported the synthesis of surface grafted poly(L-glutamates) through the ring-opening polymerisation of *N*-carboxyanhydride (NCA) monomers.[5] These polypeptides form helical structures that can be aligned perpendicular to the surface and have very interesting optical and piezoelectrical properties.[6] In practice, robust alignment is difficult and the NCA polymerisation seems to yield rather thin (<25 nm) films. We were therefore interested in exploring routes to grow helical polymer brushes using another major class of helix-forming polymers, namely the polyisocyanides.

Polyisocyanides have been most commonly prepared by a Ni(II)-catalyzed polymerisation in which the monomers first coordinate to the nickel centre and, upon initiation by a nucleophile, then link through a series of consecutive insertion reactions.[7] Due to steric crowding, the polymers adopt helical structures and the use of optically active Ni(II) catalysts or enantiopure monomers gives rise to an excess of either left- or right-handed helices.[8] Chiral peptide substituents have been introduced into the polyisocyanide backbone,[9,10] which force the helical backbone to be stabilised by hydrogen bonds between adjacent amide groups and result in β-sheet-like arrangements. Moreover, the incorporation of electroactive side groups such as porphyrin, perylene, ferrocene, triphenylamine and tetrathiafulvalene (TTF), offers routes to polymers suitable for optical and electronic applications.[11] The helical, chiral polyisocyanides bearing ferrocenyl groups exhibited reversible conformational changes on electrical stimuli, which would be a promising feature when using these materials in actuators.[12] In this chapter, the first synthesis of polyisocyanide brushes from amine-terminated self-assembled monolayers on various surfaces using a Ni-catalyst is presented.[13] By controlling the reaction time, monomer concentration and growth conditions, brushes up to 250 nm could be prepared. The morphology of the brush films and the helical structure were characterised using AFM, CD spectroscopy and Fourier transform IR. In addition, we expanded the approach and were able to grow carbazole functionalised polyisocyanide brushes, which were used to get a more detailed characterisation of the polymer.

8.2 Results and Discussion

The synthetic routes developed for surface-initiated polymerisation are shown in Scheme 1. We followed two strategies for the immobilisation of the Ni(II)-catalysts onto the surface: either (tBuNC)$_4$Ni(ClO$_4$)$_2$ from solution was allowed to coordinate to amino-terminated self-assembled monolayers (SAMs) or a triethoxysilane Ni(II) derivative (**1**) was initially synthesised and then used to form activated, Ni-functionalised SAMs directly. The poly(L-isocyanoalanyl-L-alanine methyl ester) (LL-PIAA) brushes prepared from the two-step immobilisation route (Scheme 1a) resulted in rather thin brushes of up to 19 nm. The formation of high quality APTS (aminopropyl triethoxysilane) SAMs is difficult and it is possible that the surface density of the Ni(II) catalyst is too low to provide efficient brush growth. Nevertheless, the morphology of these thin polymer films is very interesting as can be seen in Figure 1. Very thin (5 nm) brushes (Figure 1a), show a moss-like appearance (root-mean-square (rms) of 1.2 nm) whereas the 19 nm thick brushes show feather-like bundles (rms of 4.4 nm). This is a most unusual morphology for polymer brush films, which are always featureless except for block copolymer brushes, from which rounded features develop upon exposure to different solvents.[14] The very high stiffness (persistence length 76 nm) of the polyisocyanides must be a contributing factor in the development of these structures.[15] The thickness of the brush layer is less than the persistence length of polymer chains, which indicates that the feather-like morphologies observed most likely consist of stiff bundles of polyisocyanide chains that are more or less aligned in the *x,y*-plane. A careful analysis of the AFM images revealed that the length and width of the feathery patterns are in the order of 220 $\pm$ 20 and 30 $\pm$ 7 nm (average of over 50 features), respectively. In addition, exposure of the brushes to toluene resulted in an increase in film thickness from 19 to 34 nm, with a concomitant decrease in refractive index (from 1.52 to 1.30) indicating a much rougher surface. AFM analysis indeed showed an increase in surface roughness and an increase in rms value of 4.4 to over 9. This change in surface morphology is likely related to a different molecular organisation before and after solvent treatment.[16]

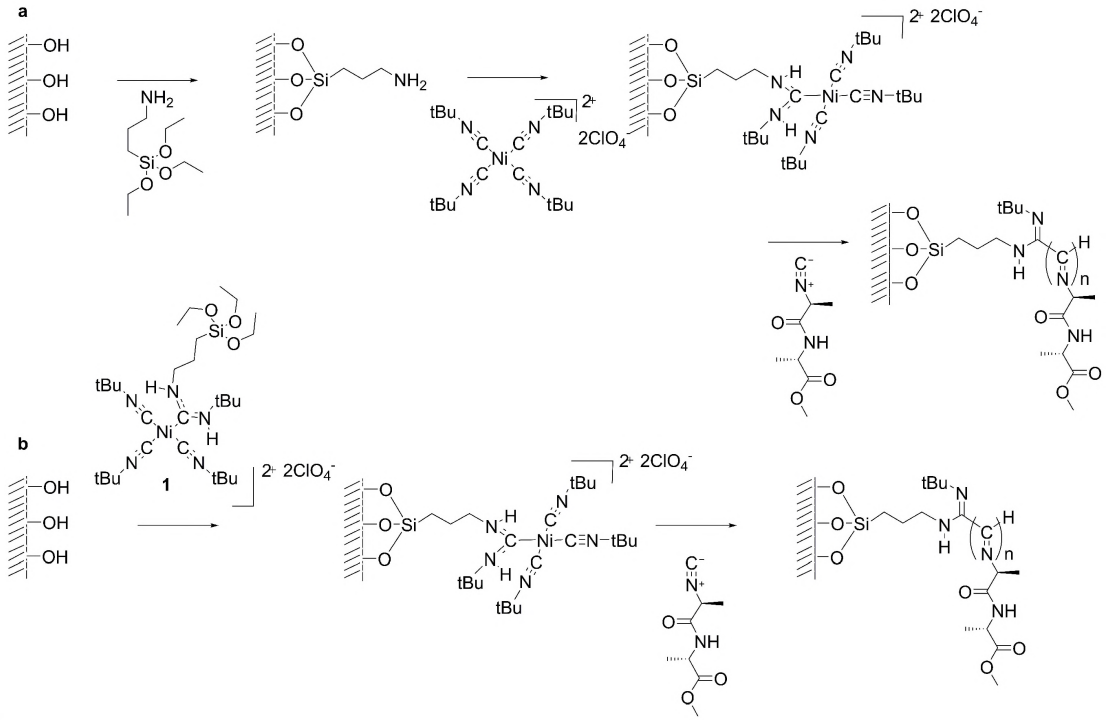

Scheme 1. Synthetic procedure for surface-initiated polymerisation of polyisocyanopeptide brushes.

To increase the thickness of the brush layer, the carbene-like Ni(II) complex (**1**, Scheme 1b) was synthesised and immobilised on Si/SiO_2 surfaces. The Ni-functionalised SAMs gave an ellipsometric thickness of about 1.4 nm, which indicates a good monolayer formation. These surfaces provided an activated Ni complex and efficient initiation and growth of LL-PIAA brushes of up to 200 nm could be achieved in three hours. In addition, the refractive index of all brushes, as measured by spectroscopic ellipsometry at λ = 632.8 or 532 nm, was found to be 1.52 $\pm$ 0.015. Water contact angles for all the brushes were found to be around 72°. The polyisocyanide brushes showed no changes in morphologies for samples stored under a N_2-atmosphere for six months.

The polymerisation reaction could be controlled by variations in the reaction time and monomer concentration, as shown in Table 1. No extra precautions regarding the purification of solvents or the exclusion of oxygen or water were required. By using a monomer concentration of 16 mM, an almost linear dependence of polymer growth versus time was observed (Figure 2) during the first three hours of the polymerisation; this led to brushes of approximately 60 nm thick. After this time, the growth became non-linear, as is often observed for brush growth using controlled radical polymerisations,[17] which indicated competition from termination as well as chain transfer processes. The latter also accounted for the formation of non-grafted polymeric material, which leads to a slight thickening of the polymerisation solution. Thicker brushes could be obtained by using higher monomer concentration (48 mM) while maintaining the same reaction time (Table 1 and Figure 2).

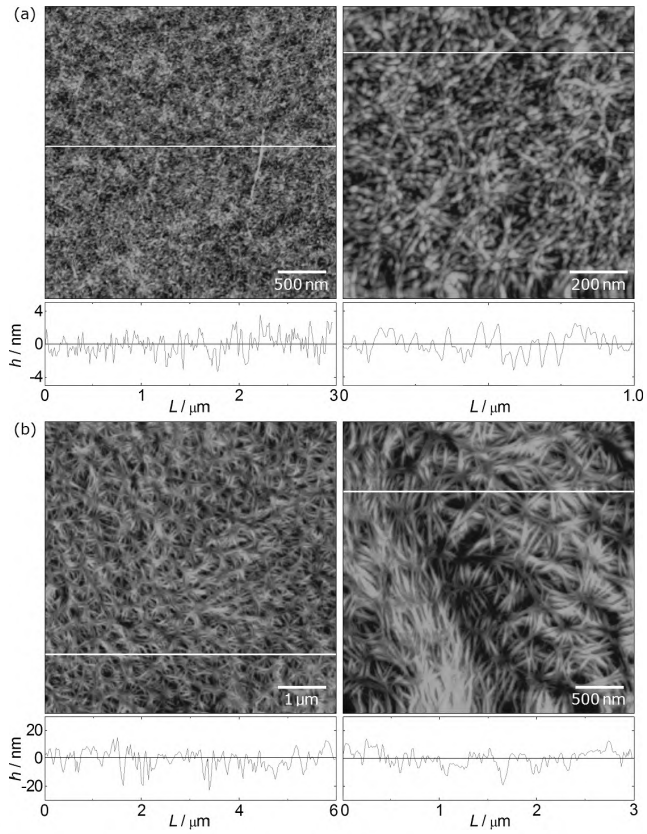

Figure 1. AFM images showing morphology of LL-PIAA brushes grown on APTS-modified silicon wafers (a) 5 nm thick and (b) 19 nm thick brushes.

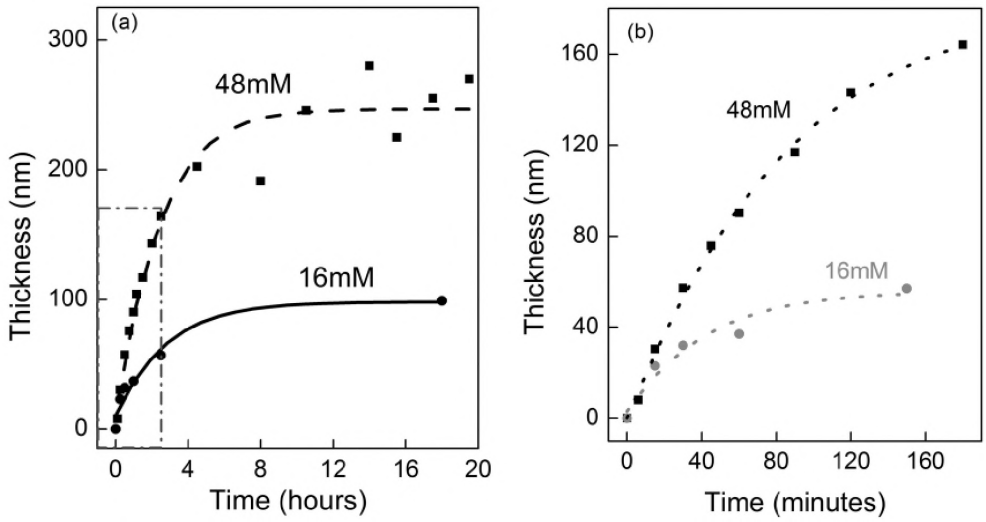

Figure 2. Film thickness as function of polymerisation time and monomer concentration using the procedure of Scheme 1b (left) and zoom-in of the boxed area in the left Figure (right).

AFM studies on a 56 nm thick brush (Figure 3a, rms of 1.3 nm) again showed the interesting morphologies already observed on the very thin brushes (Figure 1), whereas the 387 nm thick brush (Figure 3b, rms of 2.0 nm) exhibited a film morphology with less well-defined

features. We believe that as these films are much thicker than the persistence length of the chains, there is no reason for the chains to align in the plane and the order is lost. Due to the relatively small overall surface areas (1 x 1 cm^2) and the inherent difficulties with the determination of the molecular weights of stiff polyisocyanides,[18] we did not attempt to elucidate the molecular weights of these polymer brushes, although this would give us valuable information on the grafting density of the films and clues about the orientation of the chains.

Table 1 Film thickness of PIAA brushes from various reaction time and monomer concentrations[a]

	Thickness (nm)[c]		
Polymerisation time (hours)[b]	16 mM[d]	48 mM[d]	80 mM[d]
0.1	2	8	–
0.25	23	30	–
0.5	32	47	–
1	37	82	147
1.2	45	105	178
2	46	143	–
2.5	57	168	–
17	162	317	462

[a]Polymerised according the procedure b shown in Scheme 1. [b]Polymerisation time for LL-IAA after the immobilisation of the catalyst complex **1**. [c]Average values for separate brush samples prepared using the same conditions and from at least three spots on each sample. [d]Monomer concentration.

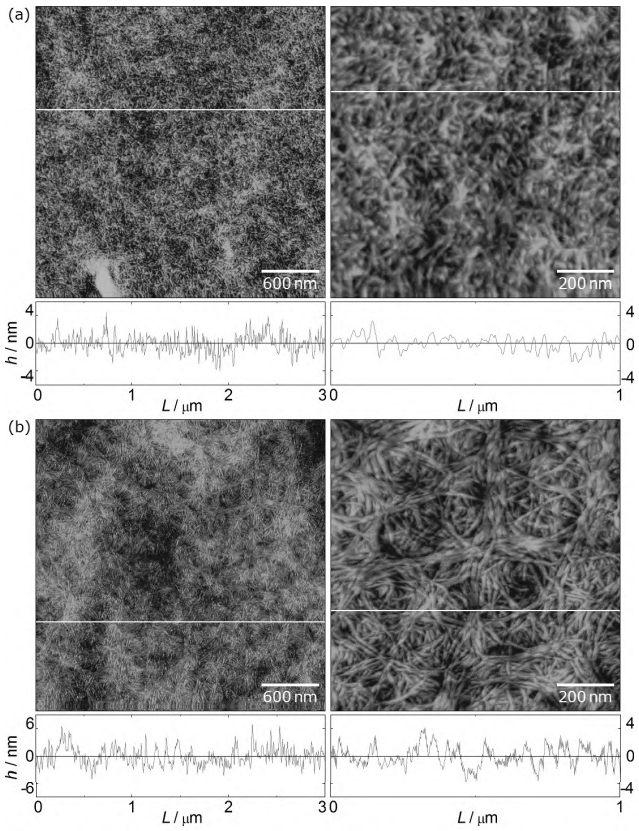

Figure 3. AFM morphology of PIAA brushes grown on a silicon wafer from Ni-SAM with film thicknesses of (a) 56 nm and (b) 387 nm.

The polyisocyanide brush growth is not restricted to silicon wafers, but can also be realised on gold and quartz substrates. To grow brushes on Au-coated silicon wafers, we first formed a 2-aminoethanethiol SAM and immobilised the Ni-catalyst onto the surface. This procedure yielded very thin films on silicon wafers, but on gold 40 nm thick brushes were obtained after two hours polymerisation time. These brushes showed morphologies similar to the ones grown on silicon wafers and quartz substrates.

We investigated the influence of different solvents on brush growth and morphology. First, substrates were prepared by forming an initiator SAM through the immersion of clean Si wafers in a 4mM solution of **1** in dichloromethane (DCM).

Subsequently, the polymerisation reaction was carried out in DCM, ethyl acetate (EtOAc), toluene or isopropyl alcohol (IPA) for a period of three hours. The thicknesses of the resulting brushes are listed in Table 2 and representative AFM images showing the variation in morphology are shown in Figure 4. From these results it is clear that toluene and IPA are less than ideal solvents for the PIAA brush growth, with only 6 nm and 60 nm thick brushes, respectively, and, more importantly, the AFM images show incomplete films with the penetration of many micron-sized holes. The monomers are only sparingly soluble in these solvents and alcohols (protic solvents) can destroy the nickel initiator complex, which might

well explain these results. DCM and EtOAc resulted in robust film growth, but again holes were observed in the case of EtOAc, although these are only approximately 40 nm deep and do not extend to the substrate.

Table 2 Film thickness of PIAA brushes prepared from various solvents[a]

Initiation[b]	Polymerisation[c]	Thickness (nm)
DCM	DCM	161
DCM	EtOAC	220
DCM	toluene	6
DCM	IPA	60
EtOH	DCM	40
EtOH	IPA	3

[a]Polymerised according the procedure B shown in Scheme 1 (DCM: dichloromethane; EtOH: ethanol; EtOAC ethyl acetate; IPA: isopropyl alcohol). [b]From a solution containing 4 mM of complex **1** for 30 min. [c]From a solution containing 48 mM of LL-IAA for three hours.

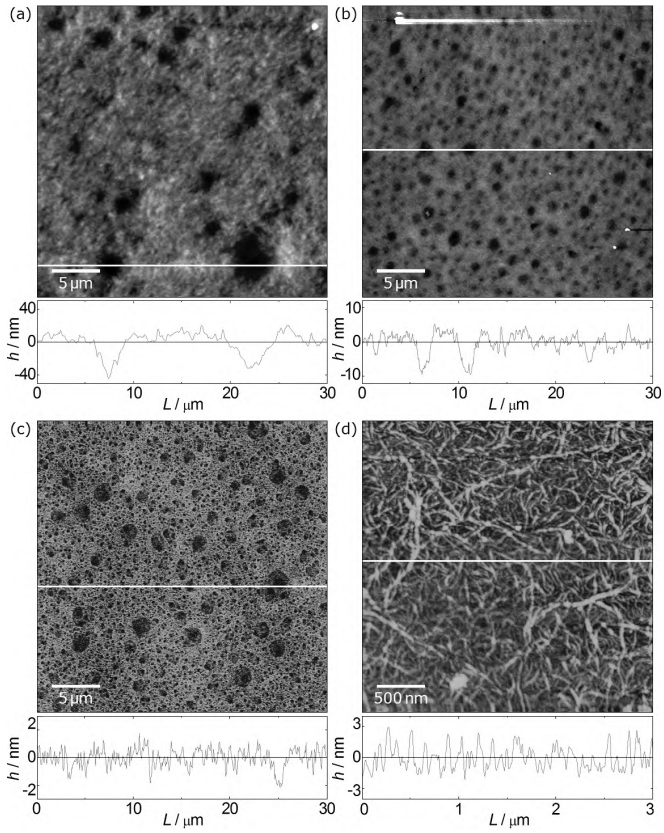

Figure 4. AFM images showing the morphology of LL-PIAA brushes on gold polymerised in (a) EtOAc, (b) toluene and (c) IPA. (d) AFM morphology of LL-PIAA brushes with low-grafting density.

The role of the solvent on the SAM formation was studied when the solvent was changed, i.e. ethyl alcohol was used instead of DCM (Table 2). Clearly, a significant decrease in brush thickness was observed for both polymerisation reactions in DCM and IPA. The decrease in

the thickness of the brushes hints at a much lower initiator density for EtOH deposited SAMs. The IPA-grown brushes were very thin (3 nm), but the AFM images of these surfaces showed some very interesting structures, see Figure 4d. The ellipsometry data revealed that very little polymer was present and hence the fibrillar structures seen in Figure 4d must be of monolayer thickness.

A powerful tool to characterize the helical structure of the polyisocyanides is circular dichroism (CD) spectroscopy. When the polypeptides are built from optically pure monomers, an excess of either left- or right-handed helices is expected; this phenomenon should be visible in the CD spectra in the wavelength range of 250–350 nm where the n-π* transition of the backbone imine functions reside.[18] As shown in Figure 5, the CD spectra of our PIAA brushes showed a strong positive single Cotton effect centred at 315 nm, which indicates that the brushes possess right-handed helical structures on the substrate. These helical structures are supported by hydrogen-bonding arrays between the side chains. Strong hydrogen bonding signals were also present in the IR spectrum as shown in Figure 5. The peaks at 3260 and 1650 cm^{-1} for the bulk PIAA polymer and the PIAA brush film are attributed to the N-H stretching vibration and amide I vibration, respectively. These peaks have shifted from 3276 and 1667 cm^{-1} for the IAA monomer, which implies that the polymer brushes have a structure in which the side chains have an ordered hydrogen-bonding arrangement. A similar investigation was reported in the solid-state IR spectrum of single crystals of the isocyanide monomer in which the β-sheet-like hydrogen-bonding array between stacked peptide strands was present.[9]

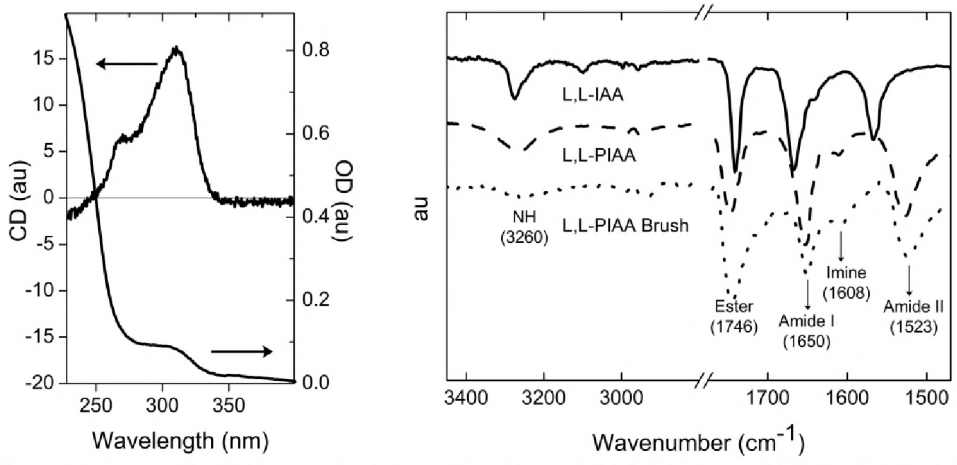

Figure 5. CD and UV-Vis spectra of LL-PIAA brushes and FT-IR spectra of the monomer LL-IAA (solid line), LL-PIAA (dashed line) and the LL-PIAA brush (dotted line).

Based on the successful synthesis of the helical polyisocyanide brushes, we aimed at the preparation of functionalised brushes. To this end, we incorporated carbazole groups into the polymer, since carbazole is cheap, easily functionalised at the nitrogen atom and has

favourable thermal, electrical and photophysical properties.[19] Carbazole based materials are well known for their favourable hole-transportation and electroluminescent properties and have therefore been investigated for many years.[19,20] In this paragraph a characterisation by IR and solid state NMR spectroscopies of the polymer is given and, by using a surface covered with Ni catalysts, the preparation of polymer brushes up to 150 nm is demonstrated by CD and IR spectroscopy and by AFM.

The synthetic route to the carbazole functionalised polyisocyanide is outlined in Scheme 2. Firstly, *N*-(2-aminoethyl)carbazole[21] **2** was coupled to Boc-L-ala-OH using 1-(3-dimethylaminopropyl)-3-ethyl carbodiimide hydrochloride (EDC) and 1-hydroxybenzatriazole (HOBt) to give **3**. The formamide **5** was obtained by cleavage of the Boc-protecting group of **3** with an HCl-saturated solution of ethyl acetate, followed by refluxing of the resulting amine salt (**4**) in ethylformate in the presence of sodium formate. Dehydration of formamide **5** with diphosgene and *N*-methylmorpholine (NMM) resulted in the formation of isocyanide monomer **6**. The isocyanide monomer was purified by column chromatography and recrystallised from tetrahydrofuran–heptane/petroleum ether, offering light yellow-brown crystals suitable for X-ray analysis (Figure 6). The X-ray structure has allowed us to establish the conformation and relative stereochemistry of the isocyanide. Monomer **6** crystallises in the orthorhombic system, space group $P2_12_12_1$, with four molecules in the unit cell. Analogous to related isocyanides,[22,23] a hydrogen bonding array was found between stacked molecules of **6**. Molecules of **6** are linked by N–H···O hydrogen bonds in the *b*-direction, with an N···O distance of 3.414(3) Å and an N–H···O angle of 155°.

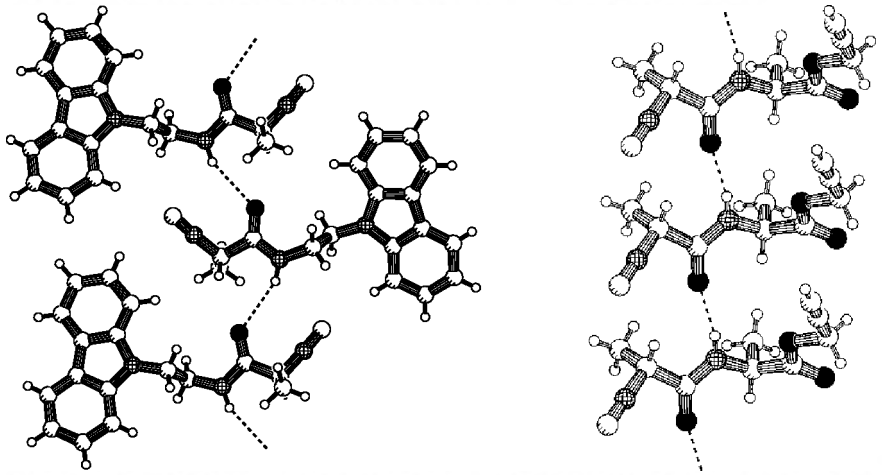

Figure 6. Molecular structure of two isocyanide monomers: **6** (left) and D-isocyanoalanyl-L-alanine prop-2-ynol ester(right).[23] In **6** the N···O distance is 3.414(3) Å and the N–H···O angle 155°; for D-isocyanoalanyl-L-alanine prop-2-ynol ester these values amount to 2.843 (7) Å and 167°, respectively.

The hydrogen bonding interactions are, however, weaker than for related isocyanides. Furthermore, no periodicity in the isocyanide groups in the stacked molecules is visible, as is the case for the isocyanide molecules of D-isocyanoalanyl-L-alanine prop-2-ynol ester (Figure

6, right). Most likely, the carbazole moiety introduces sufficient steric bulk and prevents a similar ordering.

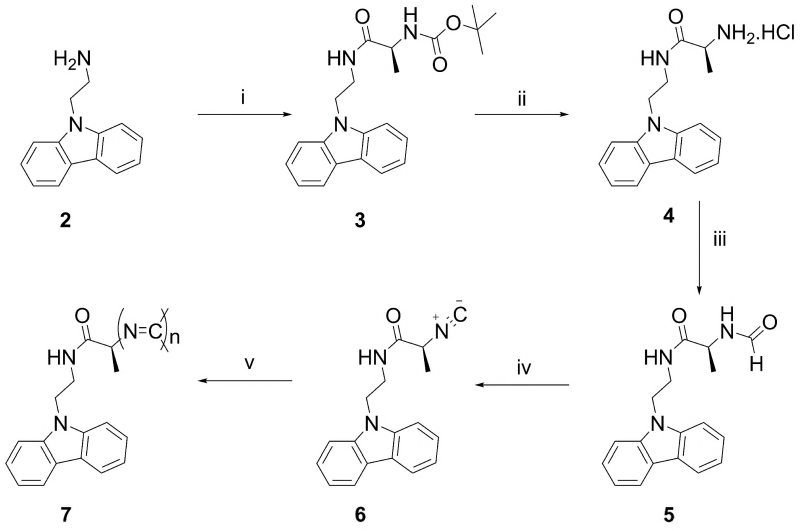

Scheme 2. Synthesis of polymer **6**; Reagents and reaction conditions: (i) Boc-L-Ala-OH, EDC, HOBt, CH_2Cl_2 (80%); (ii) EtOAc·HCl/^{t}BuOH; (iii) ethyl formate, $NaHCO_2$,reflux (46%); (iv) diphosgene, N-Methylmorpholine, CH_2Cl_2, –30°C (43%); (v) 0.01 equiv. $Ni(ClO_4)_2.6H_2O$, CH_2Cl_2 (86%).

The absorption spectrum of **6** in chloroform shows vibronic bands at 264, 294, 329 and 343 nm (Figure 7). The last two peaks are attributed to the π→ π* and the n→ π* transitions of the carbazole ring, respectively. Upon excitation at the absorption maximum of λ = 294 nm, the isocyanide monomer shows an emission profile with a weak band at λ = 351 nm and a more pronounced band at λ = 366 nm (Figure 7).

Isocyanide **6** was polymerised with 1 mol% $Ni(ClO_4)_2{\cdot}6H_2O$ in dichloromethane; the originally colourless solution rapidly turning yellow-orange. After stirring for five minutes polymer **7** precipitated from the solution. The off-white precipitate was filtered off and washed extensively with methanol and subsequently dried, offering a cream solid with satisfactory purity according to elemental analysis. The polymer was found to be insoluble in organic solvents, however, the polymerisation of isocyanopeptide **6** into polymer **7** could be monitored, at relatively low dilution, with infrared spectroscopy. Upon polymerisation of isocyanopeptides the NH-stretching vibration and the amide I vibration shift to lower wavenumbers, as is expected when hydrogen bonds are formed between the amide groups in the side chain. Therefore, the polymerisation of **6** in dichloromethane was followed over time, with IR spectroscopy (Figure 7) by the disappearance of the CN stretching vibration at ν = 2142 cm^{-1}, the shift of the N-H stretching vibration from ν = 3446 to ν = 3265 cm^{-1} and the shift of the amide I vibrations from ν = 1688 to ν = 1652 cm^{-1}; the last two shifts are comparable with the polymerisation of L-isocyanoalanyl-L-alanine methyl ester[9] and D-isocyanoalanyl-L-alanine prop-2-ynol ester[23] and indicate the formation of a hydrogen bonding network in the side chain of the polymer. The polymerisation was found to occur

rapidly in dichloromethane, chloroform, tetrachloroethane and tetrachlorethane/1,2-dichlorobenzene (1:1 v/v); the monomer was consumed within 10 minutes and the polymer could be seen as a precipitate in the cuvette.

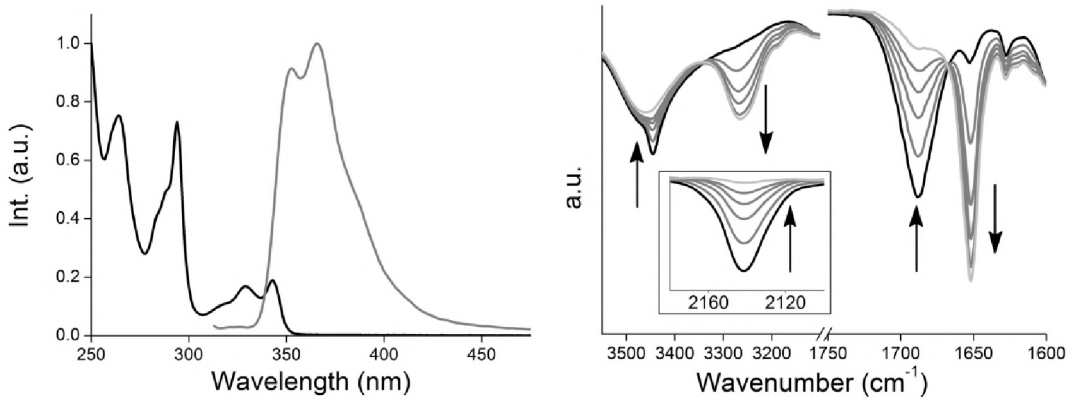

Figure 7. UV-Vis (black line) and Fluorescence (grey line) spectrum of **6** (λ_{exc} = 294 nm) in $CHCl_3$ (left). Polymerisation of **6** monitored with IR spectroscopy (right). Arrows indicate the increasing or decreasing signals.

In each of these solvents the differences observed in the N-H stretching and Amide I vibrational shifts of the spectrum are similar. Only tetrahydrofuran showed a significantly slower rate of polymerisation of **6** (> two hours) and less pronounced shifts of the N-H stretching and amide I vibrations were observed in the IR spectrum of the polymer. This observation can be rationalised by the higher polarity of solvents such as tetrahydrofuran, which will hamper the formation of the hydrogen bonding network.[24]

Due to the insolubility of **7**, characterisation was carried out using IR and Solid-state NMR spectroscopies and Differential Scanning Calorimetry (DSC). The solid-state IR spectrum of **6** (Figure 8) revealed the complete disappearance of the CN stretching vibration at ν = 2164 and 2148 cm^{-1} and the shift of the N-H stretching and Amide I vibrational characteristic of hydrogen bonding between the amides. DSC analysis of **6** did not show any melting or glass transition in the range from 20 to 250 °C, reflecting the stable and rigid nature of this polymer.

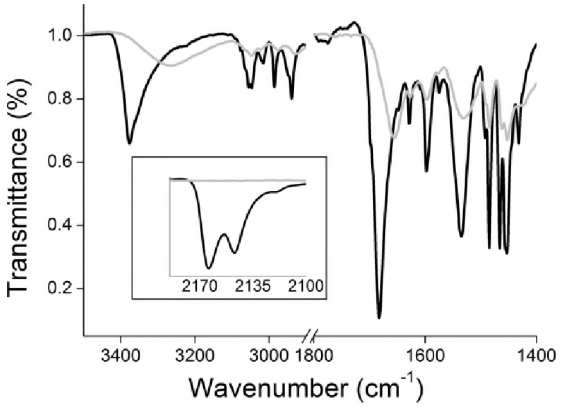

Figure 8. Solid State IR spectrum of monomer **6** (black line) and polymer **7** (grey line).

Hartman-Hahn cross-polarization (CP) solid state NMR spectroscopy in combination with Magic angle spinning (MAS) and dipolar decoupling with RF pulse irradiation techniques were used to obtain high-resolution solid state ^{13}C NMR spectra of monomer **6** and polymer **7**.[25]

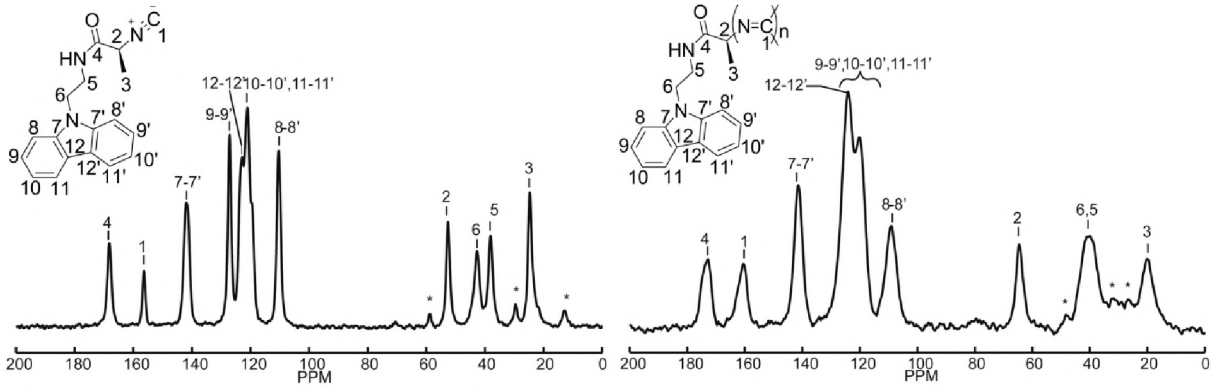

Figure 9. Cross Polarisation-Magic Angle Spinning solid state ^{13}C NMR spectra of monomer **6** (left) and polymer **7** (right) shown along with the assignments. The inset shows the numbering used for the assignment of the chemical shifts in the ^{13}C NMR spectra. The asterisks denote the spinning sidebands.

^{13}C NMR Spectroscopy. Figure 9 shows the one dimensional ^{13}C CPMAS spectra of the monomer **6** and the polymer **7**. The spectra are referenced to the CH_2 carbon peak of adamantane at δ = 38.48 ppm. The carbon resonances in the monomer are narrower than those of the polymer. The resonance at δ = 24.4 ppm (C_3) in the monomer has a width at half height of 105 Hz and the corresponding resonance at δ = 20 ppm in the polymer has a line width of 760 Hz; both these resonances correspond to the CH_3 group. The monomer is crystalline in nature and exhibits sharp lines, whereas the polymer apparently lacks long-range order and as a result shows dispersion in shifts. The aliphatic carbons appear between δ = 10–70 ppm, the aromatic carbons appear between δ = 100–145 ppm, the carbonyl (4),

the isocyano (1, C≡N) and the imine (1, C=N) carbons are more downfield shifted and appear above δ=150 ppm in the monomer and the polymer. The total number of carbon lines of the monomer spectrum in Figure 9 does not exceed the number of carbon sites in the molecule, which indicates that the monomer has one molecule per asymmetric unit cell, as also confirmed by X-ray crystallography. The wider line widths of the carbon resonances in the region between δ = 100–132 ppm results in considerable overlap for the polymer, hence it displays fewer lines than the monomer.

In summary, the assignment of polymer was obtained using ^{13}C CPMAS solid state NMR techniques. The ^{13}C resonances in the carbazole ring of the polymer **6** are limited in resolution, which hamper easy analysis; nevertheless small changes in the shifts are evident. Furthermore, the alanine moiety changes due to the hydrogen bonding network formed upon polymerisation and chemical change. The assignments obtained for polymer **7** are tabulated in Table 3.

Table 3 ^{13}C chemical shifts of the monomer **5** and the polymer **6** in the solid state

	Chemical shifts (ppm)	
Carbon site	**Monomer**	**Polymer**
1C, CN	115.8	160
2C, CH	52.3	64.5
3C, CH_3	24.4	20
4C, C=O	167.7	172.6
5C, CH_2	37.7	40.1
6C, CH_2	42.4	41.4
7C-7'C, ring	141.0, 141.8	140.8
8C-8'C, ring	109.9	108.6
9C-9'C, ring	126.8	123.6, 119.8[b]
10C-10'C, ring	121.0, 119.0[a]	123.6, 119.8[b]
11C-11'C, ring	121.0, 120.2[a]	123.6, 119.8[b]
12C-12'C, ring	123.2, 122.5	123.8

[a]These shifts correspond to the unprimed and primed positions in these cases, respectively. [b]unresolved.

To obtain brush layers of polymer **7**, we utilised a similar approach as previously demonstrated for the LL-PIAA brushes (see above).[13] A triethoxysilane carbene-like Ni(II) catalyst was used to create Ni-functionalised SAMs on Si/SiO_2 surfaces offering an activated platform for the efficient initiation and growth of the polyisocyanide brushes (Scheme 3) Within two hours brushes up to 150 nm could be obtained. The water contact angles for the brush were found to be around 90°, slightly higher than for the LL-PIAA brush (72°), which is attributed to the more hydrophobic carbazole moiety.

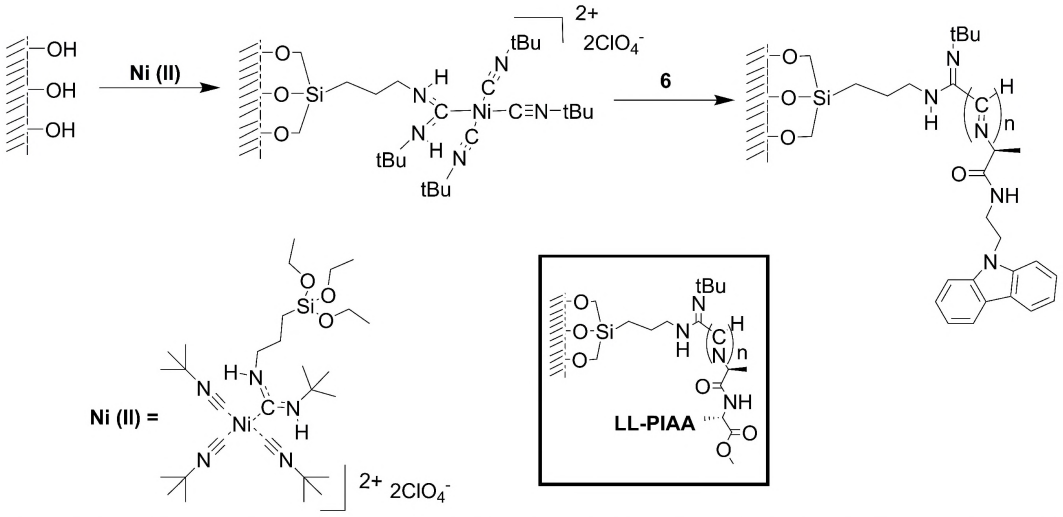

Scheme 3. Procedure for the surface-initiated polymerisation of **6**. The inset shows the LL-PIAA brush for comparison.[13]

The surface-initiated polymerisation of **6** could be controlled by changing the monomer concentration, the solvent and the polymerisation reaction time (Table 4 and Figure 10). The first hour of the polymerisation shows a nearly linear relationship between polymer growth versus time. At later stages of the polymerisation, the growth is no longer linear (see above). The influence of different solvents on the brush growth is clearly visible from Figure 10.

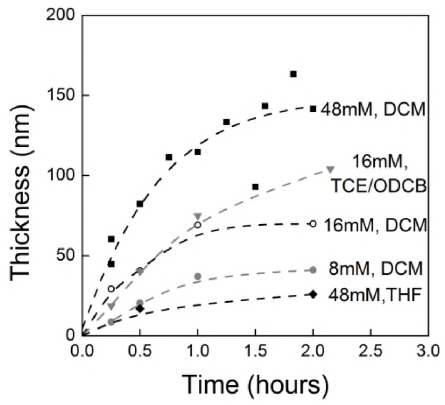

Figure 10. Film thicknesses as a function of polymerisation time for different concentrations of the monomer and various solvents. TCE: Trichloroethane; ODCB: *ortho*-dichlorobenzene.

In CH_2Cl_2 the polymerisation of **6** proceeds rapidly with a thickness of 150 nm for a 48 mM solution are obtained in two hours. In agreement with polymerisation studies of the monomer **6** in solution (see above), THF seemed to be a less ideal solvent for the polymerisation of **6**. By using higher monomer concentrations, thicker brushes for the same reaction time and solvent (48 mM vs. 16 mM yields 150 vs. 50 nm, respectively) could be obtained.

Table 4 Film thickness of PIAA brushes from various reaction times and monomer concentrations[a]

	Thickness (nm)[b]				
	DCM			TCE/ODCB[c]	THF
Polymerization time (minutes)[d]	**8 mM[e]**	**16mM[e]**	**48 mM[e]**	**16mM[e]**	**48 mM[e]**
15	9	29	62	18	
30	21	41	82	40	17
60	37	69	115	75	
120	41	70	142	104	26

[a]Polymerised according the procedure shown in Scheme 3. [b]Average values for separate brush samples prepared using the same conditions and from at least three spots on each sample. [c]TCE:ODCB =1:1 (v/v). [d] Polymerisation time after the immobilisation of the Nickel catalyst complex (Scheme 3).[e]Monomer concentration.

The AFM morphology of the polycarbazole brushes (on Si) are shown in Figure 11. The film morphologies varied by film thickness; thin (~9 nm) brushes show a moss-like appearance with a rms value of 1.8 nm, whereas in thicker brushes a more fibre-like architecture with rms value of around 4 nm is observed. The thicker films have, in general, rougher surfaces and in some cases bulk polymers could be found on top of the brush films. The specific fibre-like structure can result in large interfacial areas, which can be beneficial for organo electronic devices.

The UV-Vis spectrum of the polymer brush shows similar vibronic bands between 250–350 nm as for the monomer. The spectrum is broader, which is general for solid state spectra as compared to solution spectra. In addition, the maxima of all vibronic bands were red shifted by 2–6 nm, which indicates an interaction between the carbazole moieties. Similar observations were reported for polyacetylenes with carbazole side groups.[26] Examination of the surfaces with CD revealed a positive Cotton effect centred around 310 nm (Figure 12). This indicates the formation of right-handed helical structures on the brush.[18] The additional CD signals around 300 and 350 nm might originate from the carbazole moieties. A comparison with the bulk polymer **7** was, however, not possible due to a lack of solubility of **7**.

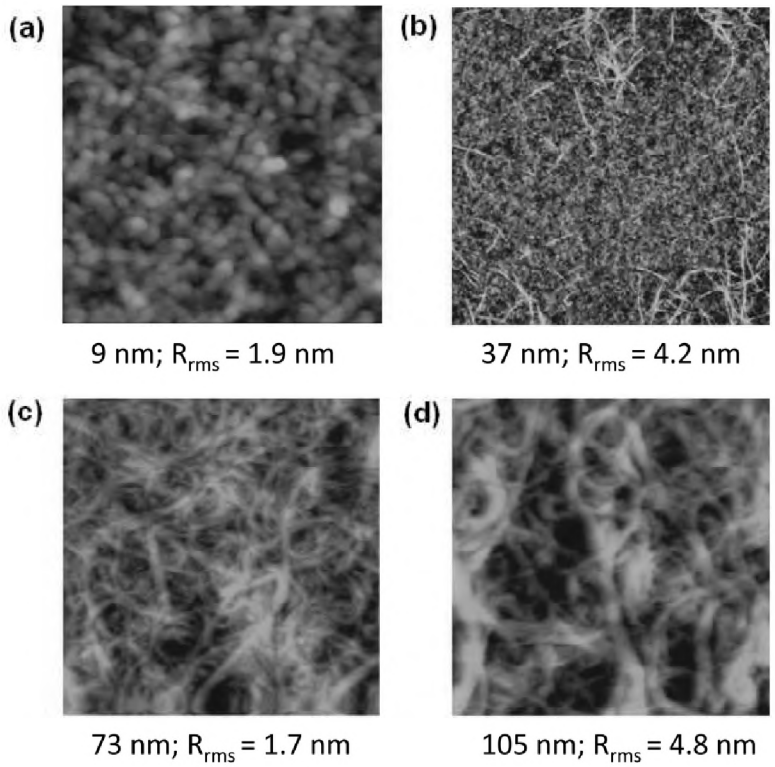

Figure 11. AFM morphology of carbazole polymer brushes grown on a silicon wafer with film thicknesses of (a) 9, (b) 37, (c) 73 and (d) 105 nm. (scan size; 1 x 1 μm^2 for (a), (c), (d) and 2 x 2 μm^2 for (b).

To obtain a final indication that the polymer brushes of **7** have similar properties to those of the bulk polymer, (solid state) IR spectroscopic measurements were carried out (Figure 12). Identical shifts (from ν = 3377 and 1683 cm^{-1} to ν = 3265 and 1655cm^{-1}, for the NH and amide I vibrations, respectively) compared to monomer **6** were found for both the bulk polymer as well as the brush of **7**. This result confirms that the hydrogen bonding arrays exist between the side chains of the polymer brush occurs both in the solid state of the bulk polymer and in the polymer brush.

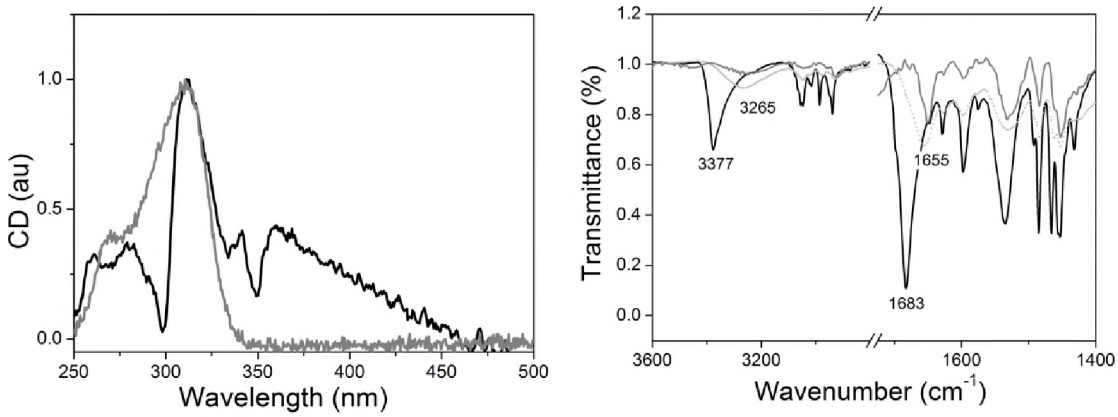

Figure 12. CD spectrum of the carbazole polymer brush (red line) and the PIAA brush (black line) (left). Solid IR spectra of the monomer (black line), polymer **7** (light grey dotted) and the carbazole polymer brush (dark grey) (right).

8.3 Conclusion

The controlled surface-initiated growth of helical polyisocyanopeptide brushes using catalytically active monolayers can be readily achieved. The synthetic strategy is different from most 'grafting from'-approaches in which the catalyst remains in solution, and only Ring Opening Metathesis Polymerisation employs a similar route. The main challenge in these polymerisations is the connection/interaction between catalyst and growing polymer chain, and we have shown here how self-assembled monolayer preparation, monomer concentration and solvents all influence the brush growth. This is the first time that such stiff polymers have been grown from the surface and we observed very unusual, feather-like morphologies in the brush films. An additional feature of polyisocyanopeptides is the helical nature of the polymer chains. We confirmed that the brushes retain this helical conformation by using CD and FT-IR spectroscopies and also observed helical aggregates in very low grafting density brushes with AFM. These polyisocyanide brushes could serve as a new rigid and well-aligned backbone for functional polymer thin films. The unusual, more open, morphologies of these brushes could be exploited by perhaps filling those voids with a second component or could lead to more pronounced surface wetting effects due to increased roughness.

We have shown that carbazole functionalised polyisocyanides can be prepared on the surface. Although these polymers suffer from a low solubility, characterisation by IR and solid state NMR spectroscopy confirmed the successful synthesis of **7**. Currently, Kelvin Probe measurements performed on both the macroscopic (KP) and sub-microscopic (KPFM) scale and electroabsorption measurements are being conducted in the groups of Prof. Franco Ciacialli at the UCL (University College London) and Prof. Paolo Samorì at the CNR (Consiglio Nazionale delle Ricerche) in Bologna to obtain more information on the electronic properties of these brushes.

8.4 Experimental

General

All solvents were distilled prior to use. All other chemicals were commercial products and used as received. Column chromatography was performed using silica gel (40–60 μm) purchased from Merck. TLC-analyses were carried out on silica 60 F_{254} coated glass from Merck and the compounds were visualised using Ninhydrine or $Ni(ClO_4)_2 \cdot 6H_2O$ in EtOH. ^1H NMR and ^{13}C NMR spectra were recorded on a Bruker AC-300 MHz instrument operating at 300 MHz and 75 MHz, respectively, unless otherwise stated. Film thicknesses and refractive indices (at λ = 632.8 or 532 nm) were measured using a J. A. Woollam alpha SE ellipsometer using a Cauchy model. Height-mode atomic force microscopy (AFM) images were obtained using a Digital Instruments Nanoscope III, in tapping mode. The root-mean-square (rms) surface roughness of brushes was obtained from AFM images of an area of $3 \times 3\ \mu m^2$. Contact angle measurements were performed using a homemade stage with a computer-controlled microsyringe and a digital camera. An infusion rate of 2 L min^{-1} was used, and images for advancing

angles were recorded. Circular Dichroism (CD) spectra were recorded on an Applied Photophysics Chirascan Circular Dichroism Spectrophotometer at 25°C. UV-Vis absorption spectra were obtained with a Varian 4000 UV-vis Spectrophotometer or a Varian Cary 50 spectrometer and fluorescence spectra on a Perkin Elmer Luminescence spectrometer LS50B. The PIAA brush film used in these CD and UV-Visible measurements were prepared on quartz using dichloromethane as solvent for both initiation and polymerisation at the same condition which resulted in the 125 nm-thick brush on Si wafer. ^{1}H NMR and ^{13}C NMR spectra were recorded on an Inova 400 MHz or a Bruker AC-300 MHz instrument (operating 75 MHz), respectively. FT-infrared spectra were recorded on a ThermoMattson IR300 spectrometer equipped with a Harrick ATR unit; the LL-PIAA brush film (126 nm) used for the IR measurement was prepared on Si wafer using dichloromethane as solvent for both initiation and polymerisation. The Ni(II) catalyst **1** and the isocyanide monomer and polymer were measured as solids. The solution infrared spectra were measured on a Bruker Tensor 27 in a fluid cell of KBr. Melting points were measured on a Buchi B-545 and are reported uncorrected. FAB mass spectra were recorded on a VG-7070E mass spectrometer with 3-nitrobenzylalcohol as matrix. ESI Mass spectrometry measurements were performed on a JEOL Accutof instrument. Elemental analyses were obtained by using a Carlo Erba 1180 instrument. Optical rotations were measured on a Perkin Elmer 241 Polarimeter at room temperature and are reported in 10^{-1} deg cm^2 g^{-1}. Differential Scanning Calorimetry (DSC) was carried out on a Perkin-Elmer DSC-7. The isocyanide monomer **6** could be recrystallised from tetrahydrofuran–heptanes/petroleum ether offering crystals suitable for X-ray analysis. A single crystal was mounted in air on a glass fibre. Intensity data were collected at –65 °C. A Nonius KappaCCD single-crystal diffractometer was used (ϕ and ω scan mode) using graphite monochromated Mo-Kalpha radiation. Unit cell dimensions were determined from the angular setting of 50 reflections. Intensity data were corrected for Lorentz and polarisation effects. SADABS multiscan correction was applied.[27] The structure was solved by the program CRUNCH[28] and was refined with standard methods using SHELXL97[29] with anisotropic parameters for the nonhydrogen atoms. All hydrogens were placed at calculated positions and were refined riding on the parent atoms. A PLUTON[30] drawing is shown in Figure 6. Cross Polarisation-Magic Angle Spinning (CPMAS) spectra of monomer **6** were obtained on a Chemagnetics Infinity 300 MHz spectrometer with a Bruker 4mm double resonance probe using a MAS speed of 7.3 kHz and 2 ms cross polarisation contact time. During CP the proton spin lock field is ramped for efficient CP transfer. Continuous phase modulation decoupling[31] of 78 kHz was applied during acquisition. CPMAS spectra of polymer **7** were obtained on a Varian VNMRS 600 MHz spectrometer using a MAS speed of 14 kHz with a CP contact time of 1.5 ms and two pulse phase modulation (TPPM)[32] of 78 kHz rf field strength was applied during acquisition.

Formation of self-assembled monolayers (SAMs). Silicon wafers and quartz substrates were cleaned in an O_2 plasma for 20 min and subsequently exposed to an APTS vapour. After this time the substrates were cured by a baking process. The amino terminated thiol monolayer was obtained by immersing Au (200 nm, 2 nm Cr adhesion layer) coated Si wafers into a solution of 0.1 M 2-aminoethanethiol in ethyl alcohol for 2 hrs, after which the substrate was rinsed with ethanol.[33]

Immobilisation of Ni(II) catalyst and preparation of polyisocyanide layer on substrates. The substrates with amine monolayers were added to a solution of $(t\text{BuNC})_4\text{Ni}(\text{ClO}_4)_2$ (5 mM) in dichloromethane (2 mL) and shaken for 15 min (Scheme 1a). Alternatively, the plasma-cleaned silicon wafer was immersed into a solution of 4 mM Ni(II) catalyst (**1**) (6 mg, 0.008 mmol) in dichloromethane (2 mL) (Scheme 1b). The substrates were rinsed thoroughly with chloroform to remove any non-bound catalyst, and dried with a stream of nitrogen. Subsequently, the polyisocyanide layer was prepared by placing the catalyst-modified substrates in a solution

of 48 mM LL-IAA (14 mg, 0.08 mmol) in dichloromethane (1.5 mL). Finally, the substrate was washed with chloroform and methanol and dried with a stream of nitrogen. Carbazole brushes were prepared in a similar manner.

Crystal data for **6**: translucent very light yellow-brown, $C_{18}H_{17}N_3O$, M = 291.35, orthorhombic, space group P212121, a = 9.0264(8), b = 9.9060(4), c = 16.8195(10) Å, α = 90, β = 90, γ = 90°, U = 1503.92 (17) $Å^3$, T = 208(2) K, Z = 4, μ(Mo-Kα) = 0.082 mm^{-1}, 26933 reflections measured, 2640 unique (R_{int} = 0.0679), final R1 0.0586, wR2 0.0828 (I › 2σ(I)).

Synthesis

Tetrakis(*tert*-butylisocyanide)nickel(II) perchlorate ((*t*BuNC)$_4$Ni(ClO$_4$)$_2$),[34] LL-IAA,[35] and *N*-(2-amino ethyl)carbazole **2**[21] were synthesised according to literature methods.

Ni(II) catalyst 1

To a suspension of tetrakis(*tert*-butylisocyanide)nickel(II) perchlorate (152 mg, 0.26 mmol) in CH_2Cl_2 (5 mL) was added 60 μL (0.26 mmol, 1 equiv.) of 3-(triethoxysilyl)-propan-1-amine. The solution immediately turned red and after a few minutes returned to yellow-orange and the solvent was evaporated, resulting in a sticky yellow-orange powder in quantitative yield. Four conformations for this complex are possible, two are in majority and reported here, one minor conformation was also detected, but not reported.

Mp 37 °C. ^{1}H NMR (δ ppm, $CDCl_3$, 400 MHz): 8.05 (t, 1H, N*H*CH$_2$, $^3J_{HH}$ = 8.0 Hz), 6.90 (m, 1H, N*H*CH$_2$), 7.90, 6.90 (br, 1H, N*H*C(CH$_3$)$_3$), 4.01, 3.37 (m, 2H, NHC*H*$_2$), 3.79, 3.22 (m, 6H, SiOC*H*$_2$CH$_3$), 1.88 (br, 2H, NCH$_2$C*H*$_2$CH$_2$Si), 1.70, 1.65 (s, 9H, NHC(C*H*$_3$)$_3$), 1.53, 1.40 (s, 27, NC(C*H*$_3$)$_3$), 1.18 (m, 9H, SiOCH$_2$C*H*$_3$), 0.69 (m, 2H, NCH$_2$CH$_2$C*H*$_2$Si). ^{13}C NMR (δ ppm, $CDCl_3$, 75 MHz): 178.2, 176.1 (N=C-N), 123.9 (Ni-C=N), 61.0, 60.6 (CN*C*(CH$_3$)$_3$), 58.6, 58.5 (SiO*C*H$_2$CH$_3$), 56.2, 55.7 (NH*C*(CH$_3$)$_3$), 53.0, 46.6 (NH*C*H$_2$), 31.1, 28.7 (CNHC(*C*H$_3$)$_3$), 29.6, 29.4 (CNC(*C*H$_3$)$_3$), 23.9, 22.0 (NCH$_2$*C*H$_2$CH$_2$Si), 18.4, 18.3 (SiOCH$_2$*C*H$_3$), 7.4, 7.3 (NCH$_2$CH$_2$*C*H$_2$Si). FT-IR (cm^{-1}, ATR): 3297 (NH), 2975, 2924, 2881 (CH), 2226, 2190 (C=N), 1589, 1546 (NCN), 1191 (SiOCH$_2$), 1073, 622 (ClO$_4^-$). MS (FAB) m/z: 710 (M-ClO$_4$)$^+$.

The numbering scheme used for the assignment of the chemical shifts in the NMR spectra of the carbazole compounds is shown in the figure below.

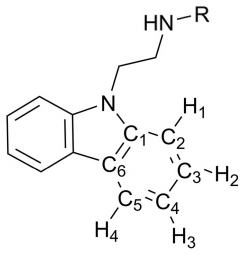

Boc-L-alanine 2-(9*H*-carbazole-9-yl) ethyl amide 3

N-(2-amino ethyl)carbazole **2** (2.00 g, 9.5 mmol) and Boc-L-alanine-OH (1.98 g, 10.5 mmol) were dissolved in CH_2Cl_2 (300 mL). To this solution diisopropylethylamine (DIPEA; 1.79 mL, 10.4 mmol, 1.1 equiv.), 1-hydroxybenzatriazole (HOBt; 1.60 g, 10.4 mmol, 1.1 equiv.) and 1-(3-dimethylaminopropyl)-3-ethylcarbodiimide hydrochloride (EDC; 2.00 g, 10.4 mmol, 1.1 equiv.) were subsequently added. After stirring for 3 hours the CH_2Cl_2 solution was washed, first with an aqueous 10% (w/w) citric acid solution (2 × 300 mL), followed by H_2O (300 mL), an aqueous 10 % (w/w) sodium carbonate solution (2 × 300 mL) and again by H_2O (300 mL). The organic layer was dried (Na_2SO_4), concentrated and subjected to column chromatography (1% MeOH in $CHCl_3$), yielding 80% of **3** as a white powder. Mp 195 °C. $[\alpha]_D$ = –6 (*c* 1.1, THF). ^{1}H NMR (δ ppm, $CDCl_3$, 300 MHz): 8.10

(d, *J* = 7.8 Hz, 2H, $H_{4,}$), 7.45 (m, 2H, H_1), 7.24 (m, 4H, H_2 + H_3), 6.14 (br s, 1H, NH), 4.51 (m, 2H, NCH_2), 4.01 (qn, *J* = 6.9 Hz, 1H, CH Ala,), 3.71 (m, 2H, CH_2NH), 1.36 (s, 9H, $C(CH_3)_3$), 1.24 (d, *J* = 6.9 Hz, 3H, CH_3 Ala,). ^{13}C NMR (δ ppm, $CDCl_3$, 75 MHz): 173.3, 154.8 (C=O), 140.3 (C_1), 126.0 (C_3), 123.1 (C_6), 120.6 (C_5), 119.4 (C_4), 108.8 (C_2), 80.2 ($C(CH_3)_3$), 68.1 (CH Ala), 41.9 (NCH_2), 38.8 (CH_2NH), 28.4 ($C(CH_3)_3$), 18.1 (CH_3 Ala). FT-IR (cm^{-1}, ATR): 3346, 3330 (NH), 1697 (Amide I), 1655 (C=C), 1545 (amide II). MS-ESI: m/z = 404 $[M+Na]^+$. HRMS for C_{22} $H_{27}N_3O_3Na$: Calcd 404.1950, Found: 404.1951.

N-formyl-L-alanine 2-(9*H*-carbazole-9-yl) ethyl amide 5

The Boc-protecting group of **3** (2.0 g, 5.2 mmol) was removed by dissolving the dipeptide in HCl-saturated ethyl acetate (150 mL). The mixture was stirred for 12 hours after which time the solvent was evaporated *in vacuo* and the excess HCl was removed by addition of *t*-BuOH/CH_2Cl_2 and subsequent evaporation. The resulting HCl salt **4** was taken up in ethyl formate (300 mL) and sodium formate (2.3 g, 33.8 mmol, 6.5 equiv.) was added. The mixture was stirred under reflux for 21 hours before the solid was filtered off and washed thoroughly with $CHCl_3$. The solvent was removed from the filtrate and the crude product was recrystallised twice from THF/diisopropyl ether to give 1.1 g (48%) of white solid. Mp 221 °C. $[\alpha]_D$ = –32 (*c* 1.1, DMSO). ^{1}H NMR (δ ppm, DMSO-D_6, 300 MHz): 8.16 (br, 1H, NH), 8.13 (d, *J* = 7.8 Hz, 2H, $H_{4,}$), 7.93 (s, 1H, HCO), 7.57 (d, *J* = 8.1 Hz, 2H, $H_{1,}$), 7.43 (t, *J* = 7.2 Hz, 2H, $H_{3,}$), 7.19 (t, *J* = 7.2 Hz, 2H, $H_{2,}$), 4.43 (t, *J* = 6.3 Hz, 1H, NCH_2,), 4.17 (qn, *J* = 6.9 Hz, 1H, CH Ala), 3.57 (m, 2H, CH_2NH), 0.99 (d, 3H, CH_3 Ala, *J* = 6.9 Hz). ^{13}C NMR (δ ppm, DMSO-D_6, 75 MHz): 172.3 (C=O), 160.8 (HCO), 140.2 (C_1), 125.8 (C_3), 122.2 (C_6), 120.3 (C_5), 119.0 (C_4), 109.2 (C_2), 46.9 (CH Ala), 41.6 (NCH_2), 38.0 (CH_2NH), 18.2 (CH_3 Ala). FT-IR (cm^{-1}, ATR): 3285 (NH), 1658 (Amide I), 1631 (C=C), 1562 (amide II). MS-ESI: m/z = 332 $[M+Na]^+$. HRMS for $C_{18}H_{19}N_3O_2Na$: Calcd 332.1375. Found: 332.1371. Anal. Calcd for $C_{18}H_{19}N_3O_2$: C, 69.88; H, 6.19; N, 13.58. Found: C, 69.85; H, 6.19; N, 13.19.

L-isocyanoalanine 2-(9*H*-carbazole-9-yl) ethyl amide 6

Compound **5** (0.94 g, 3.0 mmol) was dissolved in THF/$CHCl_3$ (400 mL 3:1 v/v) under an N_2 atmosphere and N-methyl morpholine (1.5 mL, 13.6 mmol, 4.5 equiv.) was added. The resulting solution was cooled to –30 °C (acetone/CO_2) and diphosgene (0.3 mL, 2.5 mmol, 0.8 equiv.) in $CHCl_3$ (20 mL) was added dropwise to over a period of 15 minutes, while the temperature was maintained at –30 °C. After complete addition of diphosgene, the orange solution was allowed to warm to 0 °C and an ice-cold saturated aqueous sodium bicarbonate solution (50 mL) was added and stirred vigorously for 10 minutes. The product was extracted with $CHCl_3$ (100 mL) and subsequently washed with an aqueous 10% (w/w) sodium bicarbonate solution and water (50 mL). The organic layer was dried (Na_2SO_4) and evaporated *in vacuo* resulting in a yellow-orange solid. The product was purified by using column chromatography (THF/Heptane 9: 1 v/v) and subsequently recrystallised twice from THF/heptanes/petroleum ether to yield **5** as yellow crystals (380 mg, 43%). Mp 166 °C. $[\alpha]_D$ = 23 (*c* 1.1, THF). ^{1}H NMR (δ ppm, DMSO-D_6, 300 MHz): 8.37 (t, *J* = 6.3 Hz,1H, NH,), 8.14 (d, *J* = 7.5 Hz, 2H, $H_{4,}$), 7.58 (d, *J* = 8.1 Hz, 2H, $H_{1,}$), 7.44 (t, *J* = 6.9 Hz, 2H, $H_{3,}$), 7.20 (t, *J* = 7.8 Hz, 2H, $H_{2,}$), 4.49 (t, *J* = 6.3 Hz, 1H, $NCH_{2,}$), 4.25 (q, *J* = 6.9 Hz, 1H, CH Ala,), 3.54 (m, 2H, CH_2NH), 1.21 (d, *J* = 6.9 Hz, 3H, CH_3 Ala,). ^{13}C NMR (δ ppm, DMSO-D_6, 75 MHz): 166.6 (C=O), 159.8 (CN), 140.1 (C_1), 125.7 (C_3), 122.1 (C_6), 120.2 (C_5), 118.8 (C_4), 109.0 (C_2), 52.2 (CH Ala), 41.2 (NCH_2), 38.3 (CH_2NH), 19.1 (CH_3 Ala). FT-IR (cm^{-1}, ATR): 3311 (NH), 2164 + 2148 (CN), 1681, 1669 (Amide I, C=C), 1557 (amide II). MS-ESI: m/z = 314 $[M+Na]^+$. HRMS for $C_{18}H_{17}N_3O_1Na$: Calcd 314.1269. Found: 314.1269. Anal. Calcd for $C_{18}H_{17}N_3O_1$: C, 74.20; H, 5.88; N, 14.42. Found: C, 74.11; H, 5.79; N, 14.12. UV-Vis ($CHCl_3$) λ_{max}, nm (ε) : 264 (20146), 294 (19060), 329 (4978), 343 (5368, mol^{-1} L cm^{-1}). Fluorescence ($CHCl_3$, λ_{exc} = 294 nm) λ_{max}, nm: 351 and 366.

Poly (L-isocyanoalanine 2-(9*H*-carbazole-9-yl) ethyl amide) 7

To a stirred solution of **6** (115mg, 0.41 mmol) in $CHCl_3$ (25 mL) was added $Ni(ClO_4)_2 \cdot 6H_2O$ (0.01 equiv.; 8 µL of a 0.53 M MeOH solution). The solution immediately turned yellow/orange and was stirred for five minutes before the polymer precipitated. The off-white polymer was filtered off and washed extensively with MeOH. Drying *in vacuo* gave the polymer as an off-white solid in 86% yield. FT-IR (cm^{-1}, KBr): 3265 (NH), 1654 (Amide I), 1532 (amide II). Anal. Calcd. for $C_{18}H_{17}N_3O$: C, 74.20; H, 5.88; N, 14.42. Found: C, 73.89; H, 6.06; N, 14.11.

8.5 References & Notes

(1) Edmondson, S.; Osborne, V. L.; Huck, W. T. S. *Chem. Soc. Rev.* **2004**, *33*, 14-22.

(2) Whiting, G. L.; Snaith, H. J.; Khodabakhsh, S.; Andreasen, J. W.; Breiby, D.; Nielsen, M. M.; Greenham, N. C.; Friend, P. H.; Huck, W. T. S. *Nano Letters* **2006**, *6*, 573-578.

(3) Ruhe, J.; Ballauff, M.; Biesalski, M.; Dziezok, P.; Grohn, F.; Johannsmann, D.; Houbenov, N.; Hugenberg, N.; Konradi, R.; Minko, S.; Motornov, M.; Netz, R. R.; Schmidt, M.; Seidel, C.; Stamm, M.; Stephan, T.; Usov, D.; Zhang, H. N. *Adv Polym Sci* **2004**, *165*, 79-150; Israels, R.; Leermakers, F. A. M.; Fleer, G. J.; Zhulina, E. B. *Macromolecules* **1994**, *27*, 3249-3261; Raviv, U.; Giasson, S.; Kampf, N.; Gohy, J. F.; Jerome, R.; Klein, J. *Nature* **2003**, *425*, 163-165; Zhou, F.; Huck, W. T. S. *Phys. Chem. Chem. Phys.* **2006**, *8*, 3815-3823.

(4) Zhou, F.; Shu, W. M.; Welland, M. E.; Huck, W. T. S. *J. Am. Chem. Soc.* **2006**, *128*, 5326-5327.

(5) Wieringa, R. H.; Siesling, E. A.; Geurts, P. F. M.; Werkman, P. J.; Vorenkamp, E. J.; Erb, V.; Stamm, M.; Schouten, A. J. *Langmuir* **2001**, *17*, 6477-6484; Wieringa, R. H.; Siesling, E. A.; Werkman, P. J.; Angerman, H. J.; Vorenkamp, E. J.; Schouten, A. J. *Langmuir* **2001**, *17*, 6485-6490; Wieringa, R. H.; Siesling, E. A.; Werkman, P. J.; Vorenkamp, E. J.; Schouten, A. J. *Langmuir* **2001**, *17*, 6491-6495.

(6) Jaworek, T.; Neher, D.; Wegner, G.; Wieringa, R. H.; Schouten, A. J. *Science* **1998**, *279*, 57-60.

(7) Cornelissen, J.; Rowan, A. E.; Nolte, R. J. M.; Sommerdijk, N. *Chem. Rev.* **2001**, *101*, 4039-4070.

(8) Kajitani, T.; Okoshi, K.; Sakurai, S. I.; Kumaki, J.; Yashima, E. *J. Am. Chem. Soc.* **2006**, *128*, 708-709.

(9) Cornelissen, J. J. L. M.; Donners, J. J. J. M.; de Gelder, R.; Graswinckel, W. S.; Metselaar, G. A.; Rowan, A. E.; Sommerdijk, N. A.; Nolte, R. J. M. *Science* **2001**, *293*, 676-80.

(10) Cornelissen, J. J. L. M.; Fischer, M.; Sommerdijk, N. A. J. M.; Nolte, R. J. M. *Science* **1998**, *280*, 1427-1430.

(11) Gomar-Nadal, E.; Mugica, L.; Vidal-Gancedo, J.; Casado, J.; Navarrete, J. T. L.; Veciana, J.; Rovira, C.; Amabilino, D. B. *Macromolecules* **2007**, *40*, 7521-7531; Hernando, J.; de Witte, P. A. J.; van Dijk, E. M. H. P.; Korterik, J.; Nolte, R. J. M.; Rowan, A. E.; Garcia-Parajo, M. F.; van Hulst, N. F. *Angew. Chem., Int. Ed.* **2004**, *43*, 4045-4049; Nishimura, T.; Maeda, K.; Ohsawa, S.; Yashima, E. *Chem. Eur. J.* **2005**, *11*, 1181-1190.

(12) Hida, N.; Takei, F.; Onitsuka, K.; Shiga, K.; Asaoka, S.; Iyoda, T.; Takahashi, S. *Angew. Chem., Int. Ed.* **2003**, *42*, 4349-4352.

(13) Lim, E.; Tu, G.; Schwartz, E.; Cornelissen, J. J. L. M.; Rowan, A. E.; Nolte, R. J. M.; Huck, W. T. S. *Macromolecules* **2008**, *41*, 1945-1951.

(14) Zhao, B.; Brittain, W. J.; Zhou, W. S.; Cheng, S. Z. D. *J. Am. Chem. Soc.* **2000**, *122*, 2407-2408.

(15) Samori, P.; Ecker, C.; Goessl, I.; de Witte, P. A. J.; Cornelissen, J. J. L. M.; Metselaar, G. A.; Otten, M. B. J.; Rowan, A. E.; Nolte, R. J. M.; Rabe, J. P. *Macromolecules* **2002**, *35*, 5290-5294; Zhuang, W.; Ecker, C.; Metselaar, G. A.; Rowan, A. E.; Nolte, R. J. M.; Samori, P.; Rabe, J. P. *Macromolecules* **2005**, *38*, 473-480.

(16) Wang, Y. L.; Chang, Y. C. *J. Am. Chem. Soc.* **2003**, *125*, 6376-6377.

(17) Jones, D. M.; Huck, W. T. S. *Adv. Mater.* **2001**, *13*, 1256-1259.

(18) Cornelissen, J. J. L. M.; Graswinckel, W. S.; Rowan, A. E.; Sommerdijk, N. A. J. M.; Nolte, R. J. M. *J. Polym. Sci., Part A: Polym. Chem.* **2003**, *41*, 1725-1736.

(19) Blouin, N.; Leclerc, M. *Acc. Chem. Res.* **2008**, *41*, 1110-1119.

(20) Grazulevicius, J. V.; Strohriegl, P.; Pielichowski, J.; Pielichowski, K. *Progress in Polymer Science* **2003**, *28*, 1297-1353.
(21) Conn, M. M.; Deslongchamps, G.; de Mendoza, J.; Rebek, J. *J. Am. Chem. Soc.* **1993**, *115*, 3548-3557.
(22) Cornelissen, J. J. L. M.; Donners, J. J. J. M.; de Gelder, R.; Graswinckel, W. S.; Metselaar, G. A.; Rowan, A. E.; Sommerdijk, N. A. J. M.; Nolte, R. J. M. *Science* **2001**, *293*, 676-680.
(23) Schwartz, E.; Kitto, H. J.; de Gelder, R.; Nolte, R. J. M.; Rowan, A. E.; Cornelissen, J. J. L. M. *J. Mater. Chem.* **2007**, *17*, 1876-1884.
(24) Kajitani, T.; Okoshi, K.; Yashima, E. *Macromolecules* **2008**, *41*, 1601-1611.
(25) Hartmann, S. R.; Hahn, E. L. *Physical Review* **1962**, *128*, 2042-2053.
(26) Qu, J. Q.; Suzuki, Y.; Shiotsuki, M.; Sanda, F.; Masuda, T. *Polymer* **2007**, *48*, 4628-4636.
(27) Sheldrick, G. M. (1996) *SADABS. Program for Emperical Absorption Correction*.
(28) de Gelder, R.; de Graaff, R. A. G.; Schenk, H. *Acta Crystallogr., Sect. A* **1993**, *49*, 287-293.
(29) Sheldrick, G.M. *SHELXL-97. Program for the refinement of crystal structures*, University of Gottingen: Germany, 1997.
(30) Spek, A.L. *PLATON, A Multipurpose Crystallographic Tool*, Utrecht University, Utrecht, The Netherlands, 2004.
(31) De Paepe, G.; Elena, B.; Emsley, L. *J. Chem. Phys.* **2004**, *121*, 3165-3180.
(32) Bennett, A. E.; Rienstra, C. M.; Auger, M.; Lakshmi, K. V.; Griffin, R. G. *J. Chem. Phys.* **1995**, *103*, 6951-6958.
(33) Hsia, T. H.; Liao, K. T.; Huang, H. J. *Analytica Chimica Acta* **2005**, *537*, 315-319.
(34) Cornelissen, J. J. L. M.; Fischer, M.; van Waes, R.; van Heerbeek, R.; Kamer, P. C. J.; Reek, J. N. H.; Sommerdijk, N. A. J. M.; Nolte, R. J. M. *Polymer* **2004**, *45*, 7417-7430; Stephany, R. W.; Nolte, R. J. M.; Drenth, W. *Recl. Trav. Chim. Pay. B.* **1973**, *92*, 275-280.
(35) Cornelissen, J. J. L. M.; Graswinckel, W. S.; Adams, P. J. H. M.; Nachtegaal, G. H.; Kentgens, A. P. M.; Sommerdijk, N. A. J. M.; Nolte, R. J. M. *J. Polym. Sci., Part A: Polym. Chem.* **2001**, *39*, 4255-4264.

Appendix

Preliminary studies on the use of chromophoric polyisocyanides as safety marker in banknote paper

A.1 Ink Experiments

In collaboration with *Joh. Enschedé Security Print*, experiments were carried out to investigate the implementation of the perylene functionalised polymer **9** (Chart 1) as a security marker in ink. To this end, the polymer was ground, with the help of a mortar, and subsequently mixed with a colourless base ink. The particles sizes of the pigments were between 5–15 µm. Although these values are slightly larger than those commonly applied in the graphics industry, it did not hamper the testing. A maximum of 20 weight% of pigment in the binding ink was used, since it was not possible to obtain a good blend at higher concentrations.

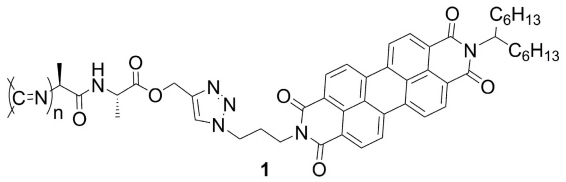

Chart 1. Molecular structure of the perylene 'clicked' polymer used for the ink studies.

The paper used in the ink experiments was 100% cotton and is comparable to the paper of official bank notes. The printing of the offset- and plate printing ink was carried out using an IGT Reprotest and a Barcoater.

Offset. *A*fter mixing of the perylene polymer with the basic ink, 0.25 cc (corresponding to 1.5 grams of ink per square meter) of this mixed ink was used for the IGT Reportest. To test the influence of the chromophore loading, batches with increasing percentages of the perylene were prepared, i.e., 1, 2.5, 5, 10 and 20 weight%. The results of this test are shown in Figure 1 (left). Using this technique ink thicknesses of 2 µm are obtained. It can be seen that only a vague pink stripe is visible on the banknote paper, which can be interpreted as being the result of the bigger pigment parts remaining attached to the rolls. In contrast to solution

studies of **1**, very limited fluorescence was observed from ink on the paper. Initial studies could not distinguish between the printed and original (non-printed) banknote paper.

Plate Printing. The best way to mimic the plate technique is with the help of a Barcoater. In this way a thick layer of ink is applied to the paper, which can approach the ink thicknesses obtained in industrial plate printing processes. Since the transparent basic ink, which is different from the basic ink used for the offset printing, is viscous and does not allow good mixing with our pigment, the basic ink had to be heated to 85 °C. At this temperature, the pigment is mixed and the resulting ink is spread out on the paper by using the Barcoater. This resulted in a thick layer of ink, of about 50 µm, on the paper.

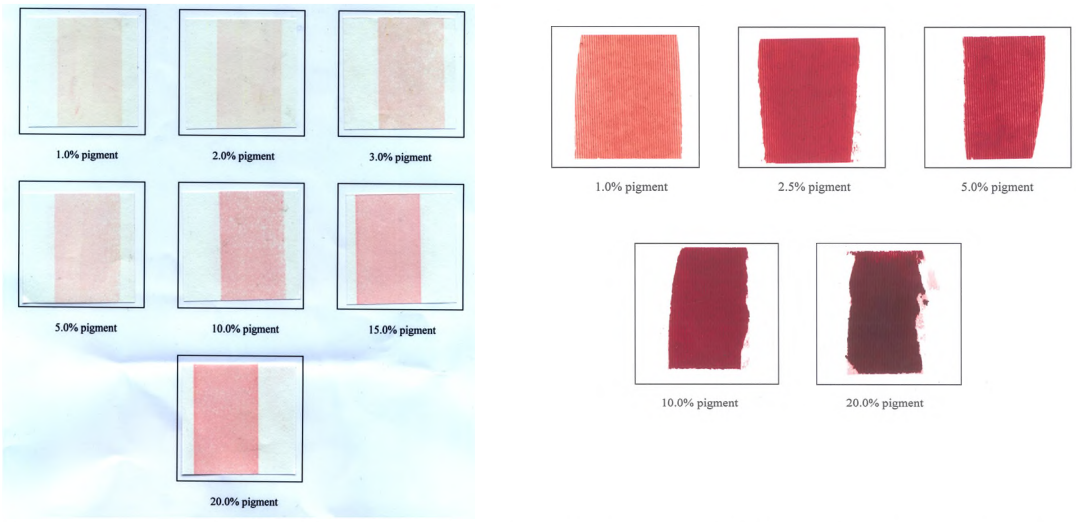

Figure 1. The results obtained with the IGT Reportest, which highlight that this test is not an effective method for printing chromophoric polyisocyanides (left) and the results obtained with the Barcoater, which show a clear fluorescence from the ink on the paper (right)

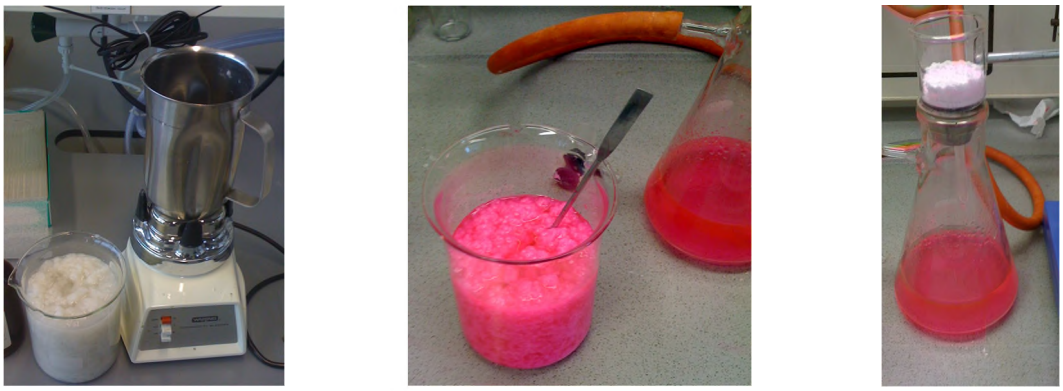

Figure 2. Affinity studies with polymer **2**. Preparation of the pulp (left), the polymer-pulp mixture (middle) and the slightly coloured cotton after filtration of the pulp mixture (right).

As for the offset, various ratios of perylene were incorporated in the polymer (Figure 1, right). In contrast to above, a clear fluorescence can now be seen from the paper, which can be easily rationalised by the difference in ink thickness obtained from both techniques.

Furthermore, an increase in fluorescence is observed with increasing percentages of perylene. The amount of pigment required to give a clear contrast is, however, too high to be easily processed in the ink and further studies are ongoing.

A.2 Paper Experiments

To test the affinity of the chromophoric polyisocyanides we also incorporated the water soluble polymers **2**–**4** in the paper pulp. Polymer **2** was synthesised by co-clicking the perylene azide (up to 3 weight%) and tetraethylene glycol azide to the acetylene polymer scaffold as described in Chapter 5. Polymer **3** was prepared by clicking a rhodamine dye to a polyisocyanide bearing ethylene glycol units and, finally polymer **4**, described in Chapter 6, was synthesised by deprotection of a random copolymer and subsequent reaction with a rhodamine dye. At first, the 'pulp' was prepared by mixing 30 g of cotton with 1 L of water for 5 min (Figure 2, left). The polymers were then added to a small portion of the pulp and left standing for 1 d (Figure 2, middle). Finally, the cotton was filtered and washed with water (Figure 3, right). It can be seen that after washing with water the cotton is only slightly coloured, which indicates that the affinity of our polymers for the cotton is low. In order to enhance this absorption cellulose functionalised polyisocyanides are being constructed.

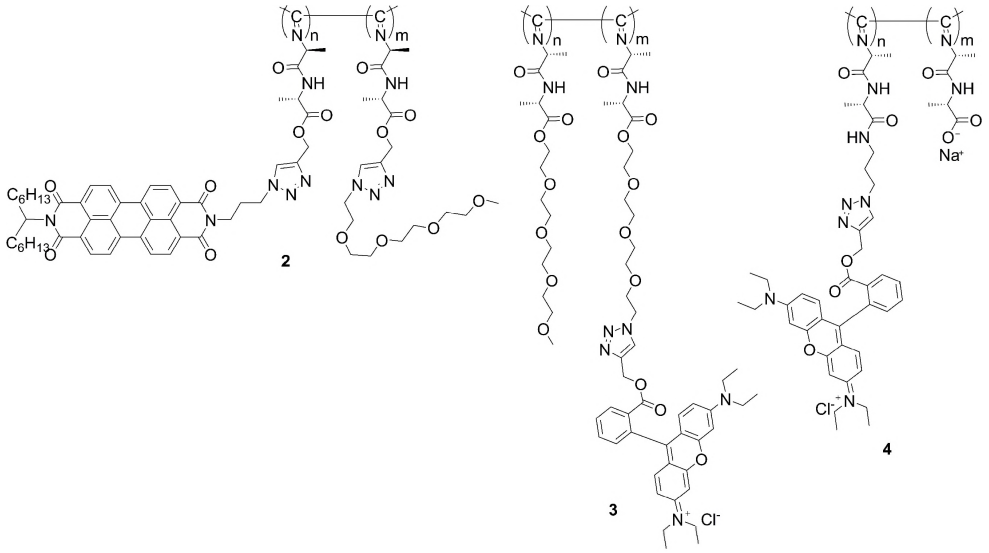

Chart 2. Molecular structures of polymers **2**–**4**.

A.3 Conclusion

The goal to synthesise long chromophoric 'nanowires' possessing unique chiroptical properties has been achieved. The initial incorporation of these materials in banknote paper reveals several design aspects, such as affinity for the cotton pulp and compatibility with printing ink. These issues need to be further explored and optimised. The initial studies do, however, suggest that future studies can be promising.

Summary

The helix is one of the key central motifs in many biological compounds, such as DNA and proteins, and often has a profound influence on their biologically activity. Shortly after the discovery of the helical nature of DNA by Pauling and Watson, Crick and Franklin in 1953, Natta found that highly isotactic polypropylene possessed a helical conformation in the crystalline state. Since that time, many chemists faced the challenge to develop stable helical polymers with a preferred handedness to study their unique properties and their potential application in materials science. The investigations presented in this thesis deal with a well-known helical polymer, namely, a polyisocyanide. Polyisocyanides have a well-defined conformation and are easily accessible, also in an optically active form by performing a nickel catalysed polymerisation reaction. The 4_1 (4 repeat units per helical turn) helical polymer backbone is only stable when additional stabilising interactions are present in the side chains. In recent years, it has been shown that polyisocyanides derived from peptides offer an improved stability and stiffness because hydrogen bonding interactions are introduced between the peptide side chains of the polymer. This thesis describes the synthesis of derivatised isocyanopeptides and the studies of the properties of the resulting polymers.

The determination of the screw sense of the polyisocyanides has been the subject of intense research efforts in the past and could, so far, only be determined by "indirect" methods, such as Circular Dichroism (CD). We therefore applied Vibrational Circular Dichroism (VCD), the extension of CD spectroscopy into the infrared regions of the spectrum, which allowed us to directly correlate the signal of the VCD spectra to the screw sense of the helix. It was found that the VCD spectra of poly(*R*)-2-methylheptylisocyanide and poly(*S*)-2-methylheptylisocyanide correspond to the VCD spectra predicted for a left- (*M*) and right- (*P*) handed helix, respectively.

The well-defined structural properties of polyisocyanopeptides make them attractive scaffolds onto which chromophores can be ordered. Decoration of the polymeric scaffold with perylenes offered a helical architecture in which perylene molecules form four 'helter-skelter-like pathways, as was revealed from various spectroscopic studies. Incorporation of two different types of chromophores (i.e., perylenes and platinum-porphyrins) into the polyisocyanopeptides allowed us to gain more insight into the complex photophysical processes that occur in these materials.

The synthesis of chromophoric isocyanopeptide monomers is tedious and not always straightforward; we therefore focused on a more modular approach to obtain polymers of these compounds and selected the cooper-catalysed click reaction between an acetylene and an azide for this purpose. Polyisocyanopeptides were synthesised containing acetylene groups in their side arms, which can be post-modified with a variety of azides. After

successful initial 'clicking' experiments with dodecyl azide, multifunctional derivatisation was achieved by using ethylene glycol azide and perylene azide as reagents, which allowed the synthesis of chromophoric water-soluble polymeric nanowires. The potential to incorporate a variety of chromophores was also demonstrated by the reaction of the acetylene-containing polymers with perylene azide and
azidocoumarin dyes. In the latter case, a blue-shifted emission of the coumarin was observed due to the interaction with the attached perylene molecules. In particular, the ability to form water-soluble, dye-containing polymers, which can be further modified by the addition of biomolecules, such as antibodies, proteins and peptides, offers the possibility to generate materials that are very promising as novel biomarkers.

The approach described above was also inverted, i.e. by introducing of azide groups into the polymer backbone and carrying out the post-modification with acetylene-containing compounds. To enhance the water-solubility, polyisocyanides were prepared by the statistical copolymerisation of azido functionalised isocyanopeptides with non-functionalised methyl ester isocyanides derived from alanine. Upon saponification of the latter function, a rigid rod water-soluble polymer with an accessible azide for post-functionalisation was obtained. The potential of these polymers was successfully demonstrated by using the click chemistry reaction to decorate them a rhodamine dye.

The hydrogen bonding array that is present in polyisocyanopeptides offers the possibility, at least in principle, to transport vibrational energy along the polymer chain. It was suggested by Davydov in 1973, and 31 years later directly observed by Hamm and co-workers, that in an α-helix, coupling between the amide I mode of the amide units and the hydrogen bonds can lead to self-trapping of vibrational energy. Our investigations revealed that in β-sheet-like polyisocyanides, which possess well-defined hydrogen bonding arrays in their side chains, NH-stretch vibrational self-trapping occurs. Disturbance of the hydrogen-bonding structure was achieved by the incorporation of a non-hydrogen bonding isocyanide monomer into the polymer. This statistical copolymer showed a completely regular NH-stretch vibrational response and hence showed no evidence of self-trapping. This first result implies that vibrational energy can, in principle, be transported through these polymer molecules. In the last part of this thesis, the surface-initiated polymerisation of two isocyanide monomers in a controlled manner is described. Polymer brushes up to 200 nm in length could be easily obtained within a time span of three hours of polymerisation. The growth of the polymer brushes was studied as a function of reaction time, monomer concentration and growth conditions, with atomic force microscopy (AFM) and ellipsometry. CD and infrared measurements confirmed that the well-defined helical conformation with hydrogen bonds along the polymer chains was retained in the polyisocyanide brushes.

Samenvatting

De helix is een belangrijke sleutelstructuur in veel biologische moleculen zoals DNA en eitwitten en heeft vaak een grote impact op de biologische activiteit. Na de ontdekking van de helixvormige structuur van DNA door Pauling en Watson, Crick en Franklin in 1953, ontdekte Natta dat polypropeen met een hoog isotactisch gehalte in de kristallijnen staat, een helixvormige conformatie heeft. Sinds die tijd zijn veel chemici de uitdaging aangegaan stabiele helixvormige polymeren te maken met een voorkeur voor een bepaalde schroefrichting, om zo de unieke eigenschappen van deze moleculen te bestuderen. Het onderzoek in dit proefschrift behandelt een bekend helixvormig molecuul, namelijk een polyisocyanide. Polymeren van isocyanides hebben een goed gedefinieerde helixvormige structuur en zijn toegankelijk in optisch actieve vorm door gebruik te maken van een door nikkel gekatalyseerde polymerisatiereactie. De ruggengraat bestaat uit vier repeterende eenheden per winding (4_1-helix) en is alleen stabiel wanneer de zijketens extra stabiliserende interacties bevatten. De afgelopen jaren heeft onderzoek laten zien, dat polyisocyanides afgeleid van peptiden een significante toename van stabiliteit en stijfheid geven door de aanwezigheid van onderlinge waterstofbruggen tussen de amide zijketens van het polymeer. Deze waterstofbruggen lopen parallel aan de polymere ruggengraat. Meer specifiek behandelt dit proefschrift de synthese van peptiden afgeleide gefunctionaliseerde isocyanides. Daarnaast zijn de eigenschappen van de resulterende polymeren bestudeerd.

De bepaling van de schroefrichting van polyisocyanides is een onderwerp dat reeds jaren veel interesse wekt van chemici. Tot nu toe kon dit alleen bepaald worden door indirecte methoden, zoals 'Circular Dichroism' (CD). Om de schroefrichting direct vast te stellen zijn 'Vibrational Circular Dichroism' (VCD) studies uitgevoerd. VCD is een uitbreiding van CD spectroscopie in het infrarode gebied en daar dit gebied veel meer conformationele informatie kan verschaffen, was het mogelijk het signaal van de VCD spectra direct te koppelen aan de schroefrichting van de helix. Uit deze studie bleek, dat de VCD spectra van poly(*R*)-2-methylheptylisocyanide en poly(*S*)-2-methylheptylisocyanide overeenkomen met de voorspelde VCD spectra voor een links- (*M*) en rechts- (*P*) draaiende helix.

Het goed gedefinieerde conformationele karakter van polyisocyanopeptides maakt ze zeer geschikt om als dragermaterieel te dienen voor de verankering en ordering van functionele groepen. Het decoreren van de polymere drager met perylenen geeft een helixvormig structuur waarin de peryleen moleculen vier 'spiraalvormige roetsjbanen' vormen, zoals is gebleken uit een verscheidenheid aan spectroscopische metingen. Het incorporeren van twee verschillende chromoforen, perylenen en platinum-porfyrines bood ons de

mogelijkheid beter inzicht te krijgen in de complexe fotofysische processen die zich afspelen in de polymere materialen.

De synthese van chromofore isocyanopeptide materialen is echter bewerkelijk en niet altijd even simpel. Daarom werd de aandacht gericht op een meer modulaire aanpak en gekozen voor de koper gekatalyseerde 'klikreactie' als werkpaard. Voor dit doel zijn polyisocyanopeptides met een eindstandige acetyleengroep gesynthetiseerd. De gefunctionaliseerde polyisocyanides kunnen dienen als dragermaterieel voor de postmodificatie met een scala aan azides. Deze methode werd succesvol getest met behulp van dodecaanazide. Vervolgens werden multifunctionele wateroplosbare materialen gecreëerd door zowel ethyleen glycol als peryleengroepen aan het polymeer te verankeren. Tevens werd aangetoond met behulp van fluorescentie spectroscopie dat het incorporeren van twee verschillende chromoforen tot een interactie tussen deze twee chromoforen leidt. De mogelijkheid chromofore wateroplosbare polymeren, die gemodificeerd kunnen worden met bijvoorbeeld antilichamen of eiwitten, te creëren, genereert materialen die als biomarker gebruikt kunnen worden.

De methode zoals hierboven beschreven, werd ook omgekeerd, namelijk door azidegroepen in het polymere dragermaterieel aan te brengen. Deze azidegroepen kunnen vervolgens met acetyleen gefunctionaliseerde moleculen aan elkaar worden geklikt. Om de wateroplosbaarheid te verhogen werd een co-polymeer gesynthetiseerd, en wel door een statistische co-polymerisatie reactie tussen een azide-gefunctionaliseerd isocyanopeptide en een niet-gefunctionaliseerde isocyanide met een methylester eindgroep uit te voeren. Het co-polymeer werd vervolgens in reactie gebracht met een base, waarbij de methylester-groepen werden omgezet in carboxylaatgroepen en de azidegroepen intact bleven. Het resulterende wateroplosbare polymeer kon nu succesvol worden gefunctionaliseerd met een rhodamine-chromofoor.

De geordende strengen van waterstoffenbruggen in polyisocyanopetides bieden de mogelijkheid het transport van vibrationeel energie te bestuderen met behulp van femtoseconde vibrationele pomp-probe-spectroscopie. Davydov suggereerde in 1973 dat in een α-helix de koppeling tussen de amide I mode van de amidegroepen en de waterstofbruggen kan leiden tot 'self-trapping' van de vibrationele groepen. Dit werd 31 jaar later in een α-helix voor het eerst aangetoond door Hamm en collegae. Onze studies laten zien dat in polyisocyanides met een β-sheet-conformatie deze self-trapping ook kan plaatsvinden. Tevens werd door het inbouwen van een isocyanide monomeer dat geen waterstofbruggen kan vormen, een polymeer gesynthetiseerd dat een regulier vibrationeel pomp-probe-spectrum gaf en waarin derhalve geen 'self-trapping' werd waargenomen. Dit impliceert dat vibrationele energie in principe door polyisocyanopeptides getransporteerd kan worden.

In het laatste deel van dit proefschrift wordt beschreven hoe twee verschillende isocyanide monomeren vanaf een grote variëteit aan oppervlaktes gegroeid kunnen worden op een gecontroleerde manier. Door een geactiveerde oppervlakte onder te dompelen in een oplossing van isocyanide monomeren, werd in drie uur een polymere borstel verkregen. De aanwas van polymeren op het oppervlakte werd bestudeerd als een functie van reactietijd, monomeerconcentratie en bestudeerd met behulp van 'atomic force microscopy' (AFM) en 'ellipsometry'. CD- en infrarood-studies bevestigden dat de goed gedefinieerde architectuur van de polyisocyanides behouden blijft in de polymere borstels.

Dankwoord

Toen ik, na mijn vwo-studie tropisch landgebruik ging studeren aan de Wageningen Universiteit, had ik (uiteraard) niet gedacht dat ik dit dankwoord zou schrijven na een studie en promotie in de chemie. Destijds had ik een droom later 'in het buitenland' te wonen en te werken... een droom die nu, ongeveer tien jaar later, gelukkig alsnog werkelijkheid wordt. In deze tien jaar is er veel gebeurd. Veel mensen zijn op enigerwijze van invloed geweest op mijn leven en de keuzes die ik gemaakt heb. In dit dankwoord wil ik diegenen bedanken die mij hebben geholpen en ondersteund en die hebben bijgedragen aan de fijne periode.

Als ik terugkijk, zijn het eigenlijk mijn drie stages geweest die een grote rol hebben gespeeld in mijn keuze te promoveren. Tijdens mijn eerste stage in de vakgroep anorganische chemie, bracht Quinten mij de basisbeginselen van gedegen onderzoek bij. Quinten, bedankt voor alle steun en je kritische kijk. Ik zal onze roze polymeren nooit vergeten. Vervolgens werd ik door Matthijs overladen met enthousiasme. Matthijs, je enorme drive was een belangrijke stimulans. Ik zal onze rode polymeren nooit vergeten. Enzo and Paolo, grazie mille for giving me the opportunity to work at the ISOF-CNR in Bologna and for showing me that there is more to life than synthetic chemistry.

In april 2005 begon ik met mijn promotie in de groep van Prof. Nolte en Prof. Rowan, die zojuist tot professor was benoemd. Roeland, bedankt voor alle vertrouwen en steun. Ons eerste gesprek gaf mij onmiddellijk een zeer goed gevoel, omdat u herhaaldelijk uw vertrouwen uitsprak in mijn capaciteiten. Ook in de jaren die volgden, stond uw deur altijd open. Als ik weer eens kwam vragen of u 'wellicht al tijd had gehad om naar een eerste versie van het artikel te kijken' of u op de hoogte wilde brengen van de voortgang van mijn polyisocyanide onderzoek, overtuigde u mij dat alles goed zou komen.

Alan, het lijkt me onwaarschijnlijk dat ik in de toekomst opnieuw iemand tegenkom, die in een uur zo veel (*crazy*) ideeën verzint als jij. Je bent een bron van inspiratie. Maar om met je te werken is lang niet altijd even eenvoudig. Je chaos is onovertroffen. En hoewel ik je wel eens heb... verwenst, wil ik je toch hartelijk bedanken voor de mooie jaren!

En dan is er natuurlijk mijn 'copromotor', die inmiddels ook professor is en nu dus ook promotor. Jeroen, bedankt voor je vertrouwen in mij en het onderzoek. En hoewel ons contact in de afgelopen jaren is verminderd en ik het soms oneens was met je aanpak, heb ik je inbreng altijd gewaardeerd. Succes in Twente.

De toekenning van de postdoctorale beurs van NWO en de bijbehorende aanstelling bij het Scripps Research Institute, hebben me genoopt vaart te maken met mijn promotie. Daarom wil ik de leden van de manuscriptcommissie (Dr. Richard Hoogenboom, Prof. Jan van Hest en Prof. Dick Broer) hartelijk danken voor hun flexibele inzet. Daarnaast ben ik de gebruikerscommissie van het STW-project zeer erkentelijk voor haar inbreng tijdens de

halfjaarlijkse vergaderingen. Die boden mij een kans kennis te nemen van het reilen en zeilen van een (veiligheids-)papierfabriek (VHP), een technologisch ingenieursbureau (Optel) en een drukker van waardepapieren (Koninklijke Joh. Enschedé). Verder wil ik ook de program officers van STW, Gert-Jan Bögels en Monique Wiegel (die het stokje overnam), bedanken voor het in goede banen leiden van de vergaderingen.

Een promotie op de afdelingen van organische chemie is schier onmogelijk zonder de ondersteuning van Désirée, Jacky, Paula en Peter (van Dijk). Bedankt voor jullie tomeloze inzet! Ook wil ik René en Jan bedanken voor het meten van alle kristalstructuren en Peter, Heleen, Ad, Paul en Theo voor de talloze analyses.

Samenwerking vormt de basis voor wetenschappelijk onderzoek. Gedurende mijn promotieonderzoek heb ik het genoegen mogen hebben om met velerlei mensen een project te starten en te ontwikkelen. Mijn dank gaat dan ook uit naar Dr. Eunhee Lim (thank you for introducing me to the world of polymer brushes) en Prof. Wilhelm Huck (bedankt voor de mooie tijd in Cambridge. Ik wens u veel succes in Nijmegen). Verder dank ik Prof. Johan Hofkens (voor alle prachtige reptation video's), Chandra Gowda (for performing the solid state NMR studies of the carbazole polymer), Dr. Chris Finlayson en Dr. Carol Huang (for the extensive photo-physical measurements on our perylene and platinum-porphyrin polymers), Dr. Oliver Fenwick en Prof. Franco Cacialli (for all the physical studies on the carbazole brushes), Pavol Bodis (for the complicated laser experiments and teaching me how to use the VCD apparatus) en Dr. Sander Woutersen (voor het inwijden en voor het uitleggen van zeer ingewikkelde formules en fysische processen) en tot slot Prof. Paolo Samori (for all the AFM and KPFM studies on our perylene based materials and for the incredibly and admirably fast responses).

Gelukkig heb ik ook binnen onze eigen gelederen met talloze mensen mogen samenwerken. Heather, thank you very much for the years we worked together. I think you and I were a good team (remember the porphyrin synthesis, luckily I won that bet) and I apologise for having brought you to Lunteren (of all places), just some days after you arrived from New-Zealand. Thank you also for correcting my many reports and manuscripts, including this one! Matthieu, the men who could perform three columns and five reactions simultaneously, I admire how you always kept on going with the many challenging projects you were working on. I would also like to make an apology to you: I'm truly sorry for my singing capabilities (and I will not call myself 'the voice' anymore). I hope we will be living in the same country in 2010! Stephane (Monsieur La Chouffe) you were the last post-doc to arrive and to work on the security paper project. I think you did a great job in developing the cysteine project nearly on your own. I'm sure it will go splendidly in Rennes and I hope our extensive review on chromophoric scaffolding will result in a nice publication. I would also like to thank Tomeu and Ismael for our (small) collaboration projects.

Verder heb ik de dankbare taak gehad om enkele studenten te mogen begeleiden. Vanuit het zonnige Spanje arriveerden in Nijmegen achtereenvolgens Vicent (Villareal!) Nebot Carda (send me your report ;o)), Irene (bulky) González Valls (it was always a lot of fun to work with you. Good luck with the last years of your PhD project), Luis (sorry Erik, can you repeat?) García Bonal (although communication was sometimes difficult, we always managed at the end!) en Mónica (the queen of Langmuir-Blodgett) Espelt Ripoll (you managed to work very independent and I'm sure you will do great in your PhD).

Verder hebben Marlies (bewonderenswaardig hoe je je in de nieuwe wereld van synthetische chemie hebt gestort, en sorry voor mijn niet altijd even duidelijke taalgebruik), Liping (I admire your exceptionally drive and for sure you will make your PhD project a succes in Cambridge) en tenslotte Maarten (het was niet makkelijk werken met een begeleider die op het punt staat te promoveren) een grote bijdrage gehad in de totstandkoming van dit proefschrift. Hoewel Matthieu het leeuwendeel van de begeleiding op zich nam, vond ik het leuk om jullie, Jelle en Petra, ook af en toe van enige hulp te zijn.

Aangezien het lab de bakermat van de organische chemie is, wil ik hier ook zeker mijn labgenoten bedanken (in willekeurige volgorde): Matthijs, Mark (ik bewonder je boekenkast), Irene, Nico (koning der Pov-rays), Linda (biochemische buurvrouw), Richard, Paul T., Paul van G., Joost, Inge, Alexander, Friso, Onno, Femke (twee keer), Roy, Gerald, het Encapson Team (Lee, Dennis (twee keer)), Arend, Erik K, Victor, Hans Peter, Johan (courtesy flush), Hans, Ruud, Rosalie, Stijn, Aurelie, Sander, Ton, Joris, Michal, Johny, Suzanne (Gabberuh), Marco, Pili, Andrés, Dani (el rey del NMR), Mauri, Christine, Stephane, Matthieu, Heather, Marta, Nikos H., Jorge, Bas, Rosalyne, Nikos M (the blue party in Strasbourg!), Guillaume (aka Guillom), Alexandra, Paul K, Bram, Tim, Jasper (waar de overname van de Rutjes-groep begon), Roserie en Lieke (waar de overname is gerealiseerd).

Gelukkig was er naast het werk op het lab af en toe ruimte voor een heerlijke pot voetbal (bedankt heren voetballers van de Pingel voor de dinsdagavonden). Natuurlijk verdienen de heren van het Huukske aka Cornerito hier een prominente plek: Krul, de D, Bartverh (de Joker), Jos, de Pool, Q, Reno, de Geus, Flo en meneer Kaal. Op onze talloze uitstapjes - van Centerparcs tot het Jamaicaanse weekendkamp, van de Fiets tot een feest in een verlaten gymzaal in Groningen - hebben we menigmaal, na een niet exact te noemen dosis alcohol, de boel bijeen geschreeuwd. En hoewel de wilde jaren (helaas) voorbij zijn, is het nog altijd lekker gezellig als we bij elkaar zijn.

In het bijzonder wil ik ook Geert (bedankt dat je in altijd present was en dat er nog vele fietstochten in Limburg mogen volgen), Harm aka Arie (altijd in voor een gezellige pint), Tommie (de marathonman!, bedankt voor de goede en diepe gesprekken in Tilburg of Nijmegen) en Maartje noemen. Verder wil ik de familie in Lent (Laura, Maarten, Dzenita, Alexandra en Maria), Henar and Ozan, de heren van Señor Hernandez, Quim en Cinta,

Baldiri, Jordi en Elena, en Dr Houssein (voor de prachtige fietstocht door het indrukwekkende Luxor (Egypte)) bedanken voor alle leuke en gezellige momenten.
Hoewel ik de essentie van hardlopen niet kan beschrijven, heb ik geprobeerd het gevoel te vangen op de omslag. Het pad staat voor de lange weg die ik heb afgelegd en de meters die ik nog wil volbrengen. Het hardlopen heeft mij altijd veel geholpen. De talloze trainingen door Heumensoord, op de atletiekbaan, de 1400 meter baan (rondje bos) of op het zevenheuvelenparcous gaven mij de scherpte die ik soms nodig had in de middag. Greet, bedankt voor de hardloopschema's.
Poezie is een kunst van de korte afstand. Ik ben blij met de medewerking van de dichter des vaderlands, die een prachtige verbinding heeft gemaakt tussen wetenschap en dichtkunst. Beste Ramsey, bedankt voor het complot. Hetzelfde geldt voor Margreet Ruardi van Stichting Schrijvers School Samenlevingen en Hayo Deinum van uitgeverij De Bezige Bij (W.F. Hermans!).
Leonie en Renoud, bedankt dat jullie mijn paranimf zijn. Leonie, je mocht dan wel in het 'verre' München verblijven - tegenwoordig woon je een stuk dichterbij :-) - ons contact was altijd speciaal. Ik bewaar heel goede herinneringen aan mijn tripjes naar München! Renoud, kerel, ik bewonder je doorzettingsvermogen enorm. Het was niet altijd even eenvoudig afspraken te maken met mij (en je zult menigmaal gebaald hebben), maar onze vriendschap staat buiten kijf. Bedankt ook voor je luisterend oor al deze jaren en ik weet zeker dat ook jouw promotie een succes wordt.
Teresa, Antonio i Laia, i Xavier, Maribel, Andreu i David, moltes gràcies pels bons moments passats a Barcelona, on sempre m'heu fet sentir benvingut. Desitjo que n'hi hagi molts més en el futur! Laura, moltíssimes gràcies pel disseny de la coberta de la tesi.
Lieve Marta, het was niet altijd even eenvoudig om beiden aan een promotieonderzoek te werken, maar ik denk dat we het er prima van af hebben gebracht. Moltes gràcies voor je steun, onuitputtelijke energie en zorgzaamheid... Ik kijk ernaar uit om samen met jou naar San Diego te gaan en aan een nieuw leven te beginnen.
Pa en ma, bedankt voor jullie onvoorwaardelijke steun, liefde en enthousiasme. Jullie stonden altijd klaar om mij te helpen en waren nimmer te beroerd om naar Nijmegen te komen. De tuin ziet er picobello uit. Hoewel dit proefschrift qua inhoud wellicht hocus-pocus is voor jullie, heb ik het aan jullie te danken dat ik dit alles kon realiseren. Bedankt! Sanne, ook jij bedankt voor al het goeds (chef de torte!) de afgelopen jaren.
De laatste woorden zijn voor mijn lieve broer, Jeroen. Een paar woorden tussen wetenschapper en journalist. Jeroen, bedankt dat we op velerlei gebieden (literatuur, hardlopen, toneel, ~~muziek~~, tot een goede espresso...) zoveel kunnen delen. Je mening en inbreng waardeer ik enorm en ik hoop dat onze band in de toekomst niet verandert.

List of Publications

Macromolecular scaffolding: The relationship between nanoscale architecture and function in multichromophoric arrays for organic electronics.
Palermo, V; Schwartz, E.; Finlayson, C. E.; Liscio, A.; Otten, M.B.J.; Trapani, S.; Müllen, K.; Beljonne, D.; Friend, R. H.; Nolte, R. J. M.; Rowan, A. E.; Samorì, P.
Adv. Mat ***2009****, DOI: 10.1002/adma.200903672.*

Vibrational self-trapping in β -sheet structures observed with femtosecond nonlinear infrared spectroscopy.
Bodis, P.; Schwartz, E. Koepf, M.; Cornelissen, J. J. L. M.; Rowan, A. E.; Nolte, R. J. M.; Woutersen, S.
Journal of Chemical Physics, **2009**, *131*, 124503.

Influence of π-π stacking on the self-assembly and coiling of multi-chromophoric polymers based on perylenebis(dicarboximides): an AFM study
Palermo, V.; Schwartz, E.; Liscio, A.; Otten, M. B. J.; Müllen, K.; Nolte, R. J. M.; Rowan, A. E.; Samorì, P.
Soft Matter, **2009**, *5*, 4680–4686.

Self-trapped vibrational states in synthetic β-sheet helices
Schwartz, E.; Bodis, P.; Koepf, M.; Cornelissen, J. J. L. M.; Rowan, A. E.; Woutersen, S.; Nolte, R. J. M.
Chemical Communications, **2009**, 4675–4677.

The relationship between nanoscale architecture and charge transport in conjugated nanocrystals bridged by multi-chromophoric polymers
Dabirian, R.; Palermo, V.; Liscio, A.; Schwartz, E.; Otten, M. B. J.; Finlayson, C. E.; Treossi, E.; Friend, R. H.; Calestani, G.; Mullen, K.; Nolte, R. J. M.; Rowan, A. E.; Samori, P
Journal of the American Chemical Society **2009**, 131, 7055–7063.

Water soluble azido polyisocyanopeptides as functional β-sheet mimics
Schwartz, E.; Koepf, M.; Kitto, H. J.; Espelt-Ripoll, M.; Nebot-Carda, V.J.; de Gelder, R.; Nolte, R. J. M.; Cornelissen, J. J. L. M.; Rowan, A. E.
Journal of Polymer Chemistry: Part A: Polymer Science **2009**, *16*, 4150–4163

'Helter skelter-like' perylene polyisocyanopeptides
Schwartz, E.; Palermo, V.; Finlayson, C. E.; Huang, Y.-S.; Otten, M. B. J.; Liscio, A.; Trapani, S.; González-Valls, I.; Brocorens, P.; Cornelissen, J. J. L. M.; Peneva, K.; Müllen, K.; Spano, F.; Yartsev, A.; Westenhoff, S.; Friend, R. H.; Beljonne, D.; Nolte, R. J. M.; Samori, P.; Rowan, A. E.
Chemistry- A European Journal **2009**, *11*, 2536–2547.

Method for the preparation of high molecular weight oligo(alkylene glycol) functionalized polyisocyanopeptides.
Rowan, A. E.; Nolte, R. J. M; Cornelissen, J. J. L. M.; Kitto, H. J. Schwartz, E.; Koepf, M.
EP 09165705, **2009**

Improved performance of perylene-based photovoltaic cells using polyisocyanopeptide arrays
Foster, S.; Finlayson, C. E.; Keivanidis, P. E.; Huang, Y.-S.; Hwang, I.; Otten, M. B. J.; Lu, L. L.; Schwartz, E.; Nolte, R. J. M.; Rowan, A. E.
Macromolecules **2009**, *42,* 2023–2030.

The relationship between nanoscale architecture and function in photovoltaic multi-chromophoric arrays as visualized by Kelvin Probe force microscopy
Palermo, V.; Otten, M. B. J.; Liscio, A.; Schwartz, E.; de Witte, P. A. J.; Castriciano, M. A.; Wienk, M. M.; Nolde, F.; De Luca, G.; Cornelissen, J.; Janssen, R. A. J.; Mullen, K.; Rowan, A. E.; Nolte, R. J. M.; Samori, P.
Journal of the American Chemical Society **2008**, 130, 14605–14614.

Synthesis and characterization of surface-initiated helical polyisocyanopeptide brushes
Lim, E.; Tu, G.; Schwartz, E.; Cornelissen, J. J. L. M.; Rowan, A. E.; Nolte, R. J. M.; Huck, W. T. S.
Macromolecules **2008**, 41, 1945–1951.

Post-modification of helical dipeptido polyisocyanides using the click reaction
Kitto, H. J.; Schwartz, E.; Nijemeisland, M.; Koepf, M.; Cornelissen, J. J. L. M.; Rowan, A. E.; Nolte, R. J. M.
Journal of Materials Chemistry **2008**, 18, 5615–5624.

Electronic transport properties of ensembles of perylene-substituted poly-isocyanopeptide arrays
Finlayson, C. E.; Friend Richard, H.; Otten, M. B. J.; Schwartz, E.; Cornelissen, J. J. L. M.; Rowan, A. E.; Samori, P.; Palermo, V.; Liscio, A.; Peneva, K.; Mullen, K.; Trapani, S.; Beljonne, D.
Advanced Functional Materials **2008**, 18, 3947–3955.

X-ray spectroscopic and diffraction study of the structure of the active species in the Ni-II-catalyzed polymerization of isocyanides
Metselaar, G. A.; Schwartz, E.; de Gelder, R.; Feiters, M. C.; Nikitenko, S.; Smolentsev, G.; Yalovega, G. E.; Soldatov, A. V.; Cornelissen, J.; Rowan, A. E.; Nolte, R. J. M.
ChemPhysChem **2007**, 8, 1850–1856.

Synthesis, characterisation and chiroptical properties of 'click'able polyisocyanopeptides
Schwartz, E.; Kitto, H. J.; de Gelder, R.; Nolte, R. J. M.; Rowan, A. E.; Cornelissen, J. J. L. M.
Journal of Materials Chemistry **2007**, 17, 1876–1884.

Chemical ligand non-innocence in pyridine diimine Rh complexes
Kooistra, T. M.; Hetterscheid, D. G. H.; Schwartz, E.; Knijnenburg, Q.; Budzelaar, P. H. M.; Gal, A. W.
Inorganica Chimica Acta **2004**, 357, 2945–2952.

Synthesis, characterisation and surface initiated polymerisation of carbazole functionalised isocyanides
Schwartz, E.; Lim, E.; Gowda, C. M.; Liscio, A.; Fenwick, O.; Tu, G.; Palermo, V.; de Gelder, R.; Cornelissen, J. J. L. M.; van Eck, E. R. H.; Kentgens, A. P. M.; Cacialli, F.; Nolte, R. J. M.; Samorì, S.; Huck, W. T. S.; Rowan, A. E.
Submitted

Macromolecular multi-chromophoric scaffolding
Schwartz, E.; Le Gac, S.; Cornelissen, J. J. L. M.; Nolte, R. J. M; Rowan, A. E.
Submitted

Sequential energy and electron transfer in polyisocyanopeptide-based multi-chromophoric arrays
Huang, Y-S.; Yang, X.; Schwartz, E.; Lu, L.; Albert-Seifried, S.; Ulgut, B.; Koepf, M.; Kitto, H. J.; Otten, M. B. J. Cornelissen, J. J. L. M.; Nolte, R. J. M.; Rowan, A. E.; Friend, R. H.
In preparation

Cysteine containing polyisocyanides as versatile nano-platforms for chromophoric and bio-scaffolding
Le Gac, S.; Schwartz, E.; Koepf, M.; Cornelissen, J. J. L. M.; Rowan, A. E.; Nolte, R. J. M.
In preparation

Vibrational circular dichroism as a direct probe of screw sense in polyisocyanides
Schwartz, E.; Koepf, M.; Cornelissen, J. J. L. M.; Buma, W. J.; Rowan, A. E. ; Nolte, R. J. M.; Woutersen, S.
In preparation

Structural study of carbazole functionalised polyisocyanides using solid state NMR
Gowda, C. M.; Schwartz, E.; van Eck, E. R. H.; Brinkmann, A.; de Wijs, G.; Kresse, G.; Marsman, M.; De Gelder, R.; Cornelissen, J. J. L. M.; Nolte, R. J. M.; Rowan, A. E.; Kentgens, A. P. M.
In preparation.

Oligo(ethylene glycol) decorated polyisocyanopeptides: expanding the class of non linear poly(ethylene glycol) analogues
Koepf, M.; Kitto, H. J.; Schwartz, E.; Cornelissen, J. J. L. M.; Nolte, R. J. M.; Rowan, A. E.
In preparation

Curriculum Vitae

Erik Schwartz werd op 14 augustus 1980 geboren in Silvolde, gelegen in de Achterhoek. Daar behaalde hij in 1998 zijn vwo-diploma aan het Isala College. Na een universitair studiejaar in Wageningen, begon hij in september 1999 met de studie scheikunde aan de Radboud Universiteit Nijmegen. Deze studie werd in 2005 *cum laude* afgerond, na stages in de vakgroepen Anorganische chemie, onder leiding van Prof. Ton Gal en Dr. Peter Budzelaar, en Fysisch-organische en Supramoleculaire chemie, onder leiding van Prof. Roeland Nolte en indertijd nog Dr. Alan Rowan. Als onderdeel van de laatst genoemde stage was hij drie maanden verbonden aan het *Instituto per la Sintesi Organica e la Fottoreativitá, Consiglio Nationale della Richerche* (ISOF-CNR) in het Italiaanse Bologna. Van april 2005 tot en met maart 2009 was de auteur werkzaam als Junior Onderzoeker op de afdelingen Fysisch-organische en Supramoleculaire chemie en Moleculaire materialen op een project van de Stichting Tecnnologische Wetenschappen (STW) (project nummer NBC 6992), getiteld 'Helical polymer fibres as safety marker in security paper'. De resultaten van het onderzoek uitgevoerd in dit STW-project, onder leiding van Prof. Roeland Nolte, Prof. Alan Rowan en Dr. Jeroen Cornelissen, sinds kort Prof. Jeroen Cornelissen, staan beschreven in dit proefschrift. Vanaf februari 2010 is Erik Schwartz als postdoctoraal onderzoeker verbonden aan het Amerikaanse Scripps Research Institute te La Jolla (San Diego). Daar gaat hij onder leiding van Prof. Valery Fokin werken aan het ontwerpen van synthetische antilichamen. Voor dit project kreeg hij in 2009 zowel een RUBICON-beurs van NWO als een beurs van Schering-Plough. Het was voor het eerst dat Schering-Plough deze beurs toekende aan een Nederlandse promovendus, ter ondersteuning van een postdoctoraal onderzoek aan een Amerikaanse universiteit.

Erik Schwartz was born on 14 August 1980, in Silvolde, situated in the Achterhoek, The Netherlands. He attended the Isala College secondary school, which he finished in 1998. After studying one year at the University of Wageningen, Erik started his chemistry study at the Radboud University Nijmegen, where he obtained his master degree in 2005, graduating *cum laude*. Erik did his major in Inorganic Chemistry under the supervision of Prof. Ton Gal and Dr. Peter Budzelaar and his minor in the Physical Organic and Supramolecular Chemistry group of Prof. Roeland Nolte and (at that time) Dr. Alan Rowan, during which time he spent three months at the *Instituto per la Sintesi Organica e la Fottoreativitá, Consiglio Nationale della Richerche* (ISOF-CNR) in Bologna, Italy. From April 2005 until March 2009, Erik was working as a Junior Researcher in the Physical Organic and Supramolecular Chemistry and Molecular Materials group under supervision of Prof. Roeland Nolte, Prof. Alan Rowan and Dr. (now Prof.) Jeroen Cornelissen on a project financed by the Dutch Technology Foundation (STW) (project number NBC 6992), entitled 'Helical polymer fibres as safety marker in security paper'. The results of this STW-project are presented in this thesis. As of February 2010 Erik will be affiliated with the Scripps Research Institute in La Jolla, San Diego, where he will be working on the development of stable synthetic antibodies, for which he received both a RUBICON fellowship and a postdoctoral fellowship from Schering-Plough. Erik Schwartz is the first recipient of this Schering-Plough award, recently established to support a PhD student from The Netherlands as post-doctoral researcher at a university within the United States.